The Transcriptional Basis of Seasonal Life-history Transitions in the Siberian Hamster

Calum Stewart

MSc Biomolecular Sciences

BSc Applied Biomedical Science

Submitted in fulfilment of the requirements for the Degree of Doctor of Philosophy

School of Biodiversity, One Health and Veterinary Medicine

College of Medical, Veterinary & Life Sciences

University of Glasgow

August 2023

Abstract

Seasonal changes in physiology and behaviour are widespread in plants and animals. Changes in external photoperiod provide an initial predictive cue which animals used to drives changes in physiology. These long-term regulated changes in physiological stability are referred to as programmed rheostasis. Rheostasis controls changes in the set-point of homeostatically defended physiological variables. The aim of this thesis was to investigate the neuroendocrine mechanisms which regulate programmed regulation of energy rheostasis in the Siberian hamsters (*Phodopus sungorus*). Next-generation sequencing was used to examine the expression of transcripts within the hypothalamus during the photoperiod-induced involution and regrowth in body mass. Despite large changes in body mass and food intake, neuroendocrine markers showed limited changes in expression with only somatostatin (*sst*) showing large seasonal changes. Expression of many transcripts is upregulated exclusively when the set-point in body mass is decreasing. One such transcript Myocyte enhancer factor 2c (*mef2c*), is a transcription factor which may be involved in effecting transciption changes to control the set-point. Then, two separate studies using common manipulations of negative and positive energy balance were conducted to identify molecular markers associated with rheostatic and homeostatic regulation of energy balance. Short term food restriction was shown to increase neuropeptide-y (*npy*) expression. Conversely, *Sst* expression increased significantly in short photoperiod hamsters but remained stable despite food restriction. Next, by a manipulation of positive energy balance using a high-fat diet paradigm it was found that neither homeostatic, nor rheostatic programs in energy balance were impacted. Overall, the studies describe here provide evidence for two separate neuroendocrine systems that independently regulate short-term homeostatic, versus long-term rheostatic changes in energy balance.

Table of Contents

List of Tables

List of Figures

Acknowledgements

First, I would like to acknowledge and thank my primary supervisory, Dr Tyler Stevenson, for his guidance and support. Over the last three years his guidance and support has been essential to develop the skill and expertise necessary to both carry out the research described within this thesis, and which I will carry with me throughout my academic career.

I would like to thank various staff members at the university of Glasgow. Firstly, Ana Monteiro and, the now retired, Lynne Fleming. Both of whom have provided invaluable assistance with ordering items and keeping the laboratory running. Special thanks also go to the biological services department here at the uni, who have been critically helpful in the maintenance of the Siberian hamster colony.

I would also like to thank those that worked with me during the production of this thesis. Dr Jo Edward Lewis from the university of Cambridge very kindly carried out some of the hormonal analyses on samples from Siberian hamsters in this study. Ms Fallon Cuthill at the university of Glasgow kindly volunteered to rate behavioural videos of Siberian hamsters. Both of their contributions are highly valued, and both were a pleasure to work with.

I would like to thank members of the lab group, past and present both for their advice and friendship throughout the course of my PhD. Special thanks go to past members of the lab Dr Christopher Marshall and Dr Gaurav Majumdar. Both of whom provided critical advice in the early years of my PhD. As well as the current members of the lab, Adam Liddle, Irem Denizli and Sayantan Sur.

Finally, I would like to thank my family and friends who have supported me throughout the entire process of my PhD, and without whom I would not have been able to successfully carry out this PhD programme.

Author's Declaration

I declare that, except where explicit reference is made to the contribution of others, this dissertation is the result of my own work and has not been submitted for any other degree at the University of Glasgow or any other institution.

Printed name: Calum Stewart

Signed:

Abbreviations

2-Arachidonoylglycerol – 2-AG

Ad libitum – AL

adrenocorticotropic hormone – ACTH

agouti-related peptide – AgRP

alpha-Melanocyte-stimulating hormone - α-MSH

Arginine vasopressin – AVP

basic helix-loop-helix ARNT like 2 – bmal2

brown adipose tissue – BAT

cellular retinol binding protein-1 - crbp1

Cerebrospinal fluid – CSF

ChIP-X Enrichment analysis 3 – ChEA3

ciliary neurotrophic factor – CNTF

Cryptochrome 1 – cry1

Cryptochrome 2 – cry2

cyclic adenosine monophosphate – cAMP

dehydroepiandrosterone – DHEA

DNA methyltransferase 1 – dnmt1

DNA methyltransferase 3b – dnmt3b

dorsomedial nucleus of the hypothalamus – DMH

eWAT – epididymal white adipose tissue

Eyes-absent 3 - eya3

False discovery rate – FDR

fat mass and obesity associated – fto

fluorescent in situ hybridisation – FISH

Follicle stimulating hormone – FSH

Food restriction – FR

fucosyltransferase-8 – Fut8

g protein-coupled receptor 50 - GPR50

Gamma aminobutyric acid – GABA

Glycoprotein Hormones, Alpha Polypeptide – cga

gonadotropin hormone-releasing hormone – GnRH

Growth hormone – Gh

heat shock protein b7 – Hspb7

high density lipoprotein – HDL

high fat diet – HFD

High Fat High Sugar – HFHS

Hydroxyindole-O-methyltransferase – HIOMT

In-situ hybridisation – ISH

insulin-like growth factor 1 - IGF-1

intraclass correlation coefficient – ICC

Jonckheere-Terpstra-Kendall – JTK

kilocalories – kcal

kisspeptin, neurokinin b, and dynorphin – KNDy

Lipoprotein lipase – lpl

long day - LD

low density lipoprotein – LDL

Low Fat High Sugar – LFHS

Low Fat Low Sugar – LFLS

Luteinising hormone – LH

Medio-basal hypothalamus – MBH

Melanocortin 1 receptor – MC1R

Melanocortin 2 receptor – MC2R

Melanocortin 3 receptor – MC3R

Melanocortin 4 receptor – MC4R

Melanocortin 5 receptor – MC5R

mucolipin TRP cation channel 1 – Mcoln1

Myocyte enhancer factor 2c – Mef2c

N-acetyltransferase – AANAT

neuronal cell adhesion molecule – NrCAM

Neuropeptide-y – npy

nitric oxide – NO

open field test – OFT

opsin-3 – Opn3

Paraventricular nucleus – PVN

pars distalis – PD

pars tuberalis – PT

Period 1 – per1

Period 2 – per2

peroxisome proliferator-activated receptors – PPAR

Principle component analysis – PCA

Prohormone convertase – PC

Prolactin – PRL

pro-opiomelanocortin – pomc

Quantitative polymerase chain reaction - qPCR

Reactive oxygen species – ROS

retinoic acid receptor alpha – rara

RFamide-related peptide-3 - RFRP3

short day – SD

Solute carrier, family 1, member - Slc1a2

Somatostatin – sst

somatotropin-release inhibiting factor – SRIF

suppressor of cytokine signaling-3 - Socs3

suprachiasmatic nucleus – SCN

tachykinin precursor 1 – tac1

Thyroid hormone – T3

thyroid hormone receptor beta – Thrb

thyroid hormone response element – TRE

thyroid stimulating hormone – TSH

thyroid stimulating hormone beta – tshb

Thyrotoph embryonic factor – Tef

thyrotropin releasing hormone – TRH

total cholesterol – TC

total triglycerides – TG

Type 2 deiodinase – dio2

Type 3 deiodinase – dio3

uncoupling protein-1 - UCP-1

Vasoactive intestinal polypeptide – VIP

Vascular Endothelial Frowth Factor- VEGF

Vimentin – vim

white adipose tissue – WAT

Chapter 1 - Introduction

1.1 Opening statements

The axial tilt of the planet produces abiotic cyclical changes in environmental conditions. The tilt produces seasonal conditions which have facilitated the evolution of endogenous seasonal timers in plants and animals. These annual endogenous timers function to facilitate survival and growth of an organism (Lincoln, 2019). It is now understood that seasonal biology has important consequences on human health, ecology and commercially (Stevenson et al., 2015). Consequently, seasonal biology is a growing area of research. In this thesis the molecular programme involved in the neuroendocrine timing of seasonal changes in mammalian physiology will be investigated, with a focus on energy balance within the Siberian hamster (*Phodopus sungorus*). This chapter will first introduce seasonal biology and then place the current work into a historical perspective. Next, the concepts of homeostasis and rheostasis will be described and proposed to consist of distinct physiological mechanisms. Then, the chapter will describe the physiological basis of seasonal interval timers and the neuroendocrine control. And finally, the cellular and molecular basis of seasonal interval timers will be described. The chapter will include the overall aims and hypotheses of the thesis.

1.2 Brief History of Seasonal Biology

In 1915 the first evidence of an endogenous program of seasonality was identified when the mass of pituitary glands in woodchucks were found to decrease in hibernating animals and spontaneously increase as animals exit hibernation (Cushing and Goetsch, 1915). The first evidence that external photoperiod was responsible for seasonal change was found after plants were found to depend upon certain photoperiod to inform flowering (Garner and Allard, 1920). It had been assumed that temperature was the primary mechanism informing seasonal breeding in animals, however it was soon demonstrated that short days were responsible for driving reproduction in aphids (*Aphis forbesi*), the first animal to be shown to be photoperiod responsive (Marcovitch, 1923). In one major early publication Erwin Bünning proposed that photoperiod changes are dependent upon changes to the timing of light administration to plants relative to an endogenous circadian timer (Buenning,

1940; Buning, 1936). This idea would form the basis of the much later proposed "external coincidence timer" model for the molecular decoding of photoperiod information. Around the same time, prolactin was first identified as a lactogenic hormone released from the anterior pituitary (Riddle et al., 1933). By the end of the 1930s, the necessity of light in driving seasonal prolactin release was well understood (Mayo Fiske, 1941). However, the mechanisms communicating external light levels remained unknown.

In 1958, melatonin was initially isolated from bovine pineal glands, after an investigation seeking to identify a hormone responsible for lightening skin tone (Lerner et al., 1958). The role of melatonin in driving sleep was initially of much interest to the study of the acute effects of melatonin on physiology. Much of this focused on the hypnotic effects of melatonin, for which it became apparent that the timing of melatonin administration was crucial (Marczynski et al., 1964). However, much of this work focused on the immediate physiological and behavioural analyses of melatonin functions. An early study exposed female rats to daily melatonin injections and found a progressive, long term decrease in ovarian mass (Wurtman et al., 1963). This was the earliest evidence that melatonin may drive long term changes in physiology. It was not until much later however, that light dependant melatonin secretion in humans was first demonstrated (Lewy et al., 1980).

Light exposure was found to drive an increase in thyroid hormone synthesis in the MBH of Japanese quail, dependent upon type 2 deiodinase (*dio2*) (Yoshimura et al., 2003). Subsequent investigations in Japanese quail identified reciprocal switching in dio2 and dio3 within the MBH when animals were transferred from short to long days (Yasuo et al., 2005). They found that thyroid stimulating hormone (TSH) signalling drove an increase in Dio2 expression (Nakao et al., 2008). However, in Siberian hamsters, the expression of dio2 does not appear to be under photoperiod control. Instead, changes in local thyroid hormone availability in Siberian hamsters appears exclusively driven by type 3 deiodinase (dio3), with short photoperiod driving an increase in expression (Barrett et al., 2007). Curiously, in Syrian hamsters (*Mesocricetus auratus*) the opposite pattern was noted, and local thyroid hormone conversion appears to be exclusively mediated by *dio2* expression (Revel et al., 2006). More recently the advent of next-generation sequencing (NGS) has allowed for higher throughput analyses of

the seasonal waveform. Whereas traditional methods focused on analysing known seasonal genes NGS allows for a ‘wide net’ approach which may unveil a more complete molecular picture of seasonality. The Siberian hamster genome, and seasonal transcriptome has recently been published, which allowed for the identification of a number of transcripts associated with photoperiodism (Bao et al., 2019). Further, they investigated select transcripts using quantitative polymerase chain reaction (qPCR) to identify that homeostatic and rheostatic neuroendocrine mechanism may be fully distinct.

1.3 Seasonality in Living Organisms

1.3.1 Seasonality Across Diverse Taxa

Innate seasonal timing is an evolutionarily ancient trait, likely predating multicellular life, it is widespread in eukaryotic organisms. Due to the ancient nature of this strategy, there are many shared mechanisms in modern species to deal with seasonal challenge. Unicellular eukaryotes such as *Alexandrium minutum* display an endogenous seasonal clock in transitioning from cysts to mature cells (Andersen and Keafer, 1987). Most families of multicellular eukaryotes display seasonal rhythms. In plants, *Arabidopsis* is a highly studied model of seasonality, with many molecular correlates of seasonality having been identified to date (Yanovsky and Kay, 2002). Seasonality in the plant kingdom is widespread, with most plants at temperate latitudes displaying significant seasonal changes.

In bacteria, innate seasonal timing has not been demonstrated. However, the environmental changes which accompany seasonality are known to coincide with large changes in microbial mass (Nikitin et al., 2019). However, rather than being driven by photoperiod or by an endogenous program, this change likely stems from the annual change in temperature. Similarly, prokaryotes which exist in some form of commensal relationship with a multicellular eukaryote may be affected by the seasonal rhythm of its host. This is, once again, a change driven by environmental cues, in this case, the host organisms own seasonal biology. The lack of innate seasonal timing in prokaryotes allows for an approximate estimation of the evolutionary timescale at which photoperiod driven seasonality first arose. While not universal, photoperiodism has been demonstrated in various fungal species. Photoperiodism in fungi is very poorly understood, as

most research has historically focused on animals and plants. Photoperiod appears to affect, along with temperature, the formation and release of spores from multiple fungal species, and shares many similarities with photoperiodism in other kingdoms, such as being interrupted by short light pulses during the dark phase. One of the more studied of these is *Neurospora crassa,* in which some of the underlying molecular mechanisms may have been elucidated, the *frq* system which plays a role in fungal circadian clock is necessary for *neurospora* photoperiodism (Roenneberg et al., 2009).

In animals, there are examples of seasonality in all major classes. As early as the 70s fish were being utilised as model organisms in the investigation of seasonal biology. Circadian rhythms in locomotor activity and heart rate in carp depend upon the season, with a light phase increase in activity during summer and winter, but an inverse relationship in spring and autumn (Kneis and Siegmund, 1976). Many species of fish display long term free running circannual rhythms. rainbow trout (*Oncorhynchus mykiss*), held under constant photoperiod, trout show a circannual rhythm in spawning, which persists for multiple years (Duston and Bromage, 1991). As ectotherms fish are highly sensitive to changes in ambient temperature. In zebrafish, photoperiod does not appear to drive changes in seasonal thermogenesis, instead depending upon ambient temperature (Condon et al., 2010).

Seasonal changes in mammals are widespread and diverse, both in timing and response. The Soay sheep, a common animal model in seasonal research breeds under short day (SD) conditions (Lincoln and Baker, 1995). Inhibition of breeding is driven by SD in animals such as horses (Thompson and Oberhaus, 2015), polar bears (Howell-Skalla et al., 2002) and California ground squirrels (Holekamp et al., 1988). However, many mammals are SD breeders, such as Soay sheep (Hazlerigg et al., 2004) and Syrian hamsters (Maywood et al., 1990). Seasonality in mammals is conserved even in marsupials, with Bushtail possums (*Richosurus vulpecula*) and wallabies (*Macropus rufogriseus*) showing a short-day driven decrease in prolactin and significant seasonal breeding (Crawford et al., 2006; Curlewis, 1991). In mammals, there are many conserved elements of seasonality. For example, prolactin is generally downregulated in mammals under short photoperiod, regardless of the reproductive or energetic state of an animal under that condition (Stewart and Marshall, 2022).

Humans too display seasonality, birth rate in humans has been widely reported to display variation over the course of a year (Rojansky et al., 1992). However, the pattern of births in humans has been reported both as bimodal or unimodal (Roenneberg and Aschof, 1990), and this may preclude photoperiod as the sole orchestrator of this phenomenon. Evidence for human seasonal reproduction has been found in a number of communities and appears to be associated with latitude, with higher latitudes leading to an earlier peak of births (Martinez-Bakker et al., 2014). Evidence such as this implies that photoperiodism is involved in the timing of human seasonality, however, the changes in human reproduction seem to show some degree of cultural variability. Additionally, human reproduction has shown biannual peaks in some conditions, though interestingly this biannual pattern appears to be diminishing over time (Martinez-Bakker et al., 2014).

There are also potential energetic effects of photoperiod on human physiology. A recent meta review of medical records unveiling significant human seasonality in blood hormone levels (Tendler et al., 2021). Body mass has been reported to fall by approximately 0.5kg in autumn months in humans (Ma et al., 2006; Yoshimura et al., 2020). BAT was once thought to predominantly exist in infants, however more recently it has been discovered to exist seasonally in adults and has been associated closely with photoperiod (Au-Yong et al., 2009). It is difficult to determine from these the role of photoperiod in human seasonality due to the possible influence of cultural factors. Some studies have attempted to overcome this by maintaining humans in controlled photoperiod conditions, such studies have delivered conflicting results. For example, human sleep has been suggested to be biphasic under short photoperiods (Wehr, 1992). However, robust research into human photoperiodism is difficult to study in a controlled experiment, due to ethical considerations pertaining to the development of severe adverse psychological affects in some individuals.

1.4.2 Siberian Hamster

The Siberian hamster (*Phodopus sungorus*) is a small seasonal rodent native to the steppes of Siberia. The Siberian hamster belongs to a genus (*Phodopus*) of closely related species which live in geographic proximity to each other. This has led to some historic confusion over the naming and taxonomical classification of

species within this genus. The Siberian hamster was historically referred to as the Djungarian hamster, however some have also used this term to refer to the closely related *Phodopus campbelli*. The Siberian hamster has played a major role in the development of our understanding of seasonality in mammals. In Siberian hamsters exposure to SD will drive a decrease in body mass and basal metabolic rate, leading to a large winter decrease in energy requirements (Heldmaier and Steinlechner, 1981). Behavioural changes also act to minimise energy requirements, in summer hamsters have well defined patterns of wheel running, in winter activity levels drop and become arrhythmic (Wollnik et al., 1991). A seasonally inappropriate loss in body mass can be established in Siberian hamsters by food restriction, however, when food is returned they will regain weight only to a seasonally appropriate level (Mercer et al., 2001). This demonstrates the endogenous rheostatic component of seasonal timing, a sliding set point of body mass rather than a simple homeostatic regulation given available resources.

1.5 Maintenance of physiological conditions across time

1.4.1 Homeostasis

The first published evidence that organisms defend internal conditions or "internal milieu") was published as early as 1865 by Claude Bernard (Bernard, 1865; Gross, 1998). This would be later developed into the concept of homeostasis by Walter Cannon, who would identify that various systems act together to "defend" the physiological condition of an organism (Cannon, 1939, 1929). Homeostasis is the process by which the condition of an organism is defended around a set point to maintain physiological stability. Homeostasis typically operates using error-correction based on feedback from peripheral hormonal signalling, for example negative feedback control (Cannon, 1939). Homeostasis acts when feedback from peripheral signalling indicates a deviation from the homeostatic set point. A general model of homeostatic systems involves a sensor which detects the regulated variable, an error detector which compares the reported variable to the set-point, a controller which determines the degree of physiological response required to control the error and an effector which drives the correction of the error (Modell et al., 2015). Homeostasis likely evolutionary origins is as an adaptive system to maintain physiological conditions

in a manner compatible with life. With homeostasis providing early organisms a competitive advantage during periods of disruption (Giordano, 2013). However, some have integrated information theory into analyses of the evolution of homeostasis to propose that homeostasis evolved as a means to minimise noise across physiology (Woods and Wilson, 2013).

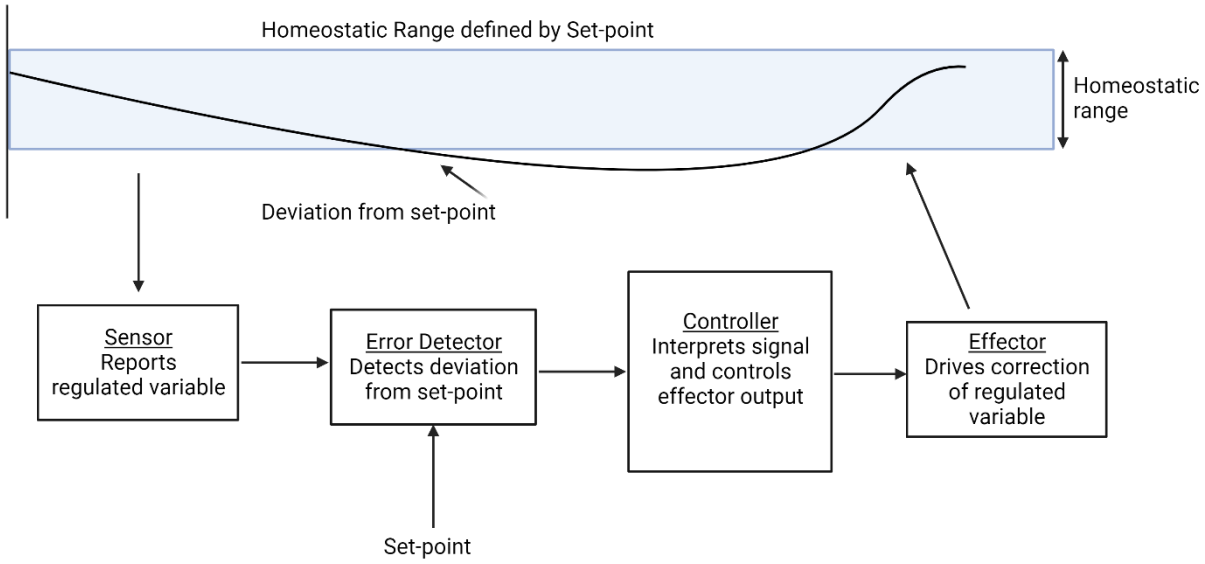

Figure 1-1: A model of a homeostatic systems containing; a sensor, an error detector, a controlled and an effector. The sensor detects the regulated variable. The error detector detects deviation from the establish set-point of the regulated variable. The controlled interoperates the error and determines the degree of response. The effector drives the physiological response of the regulated variable back towards homeostasis. Created with BioRender.com.

1.4.2 Allostasis

There are a number of ways in which this simple model of homeostasis fails to account for the changes which occur in living organisms. In 1988, Sterling & Eyer proposed allostasis as a concept. In allostasis an organisms internal milieu varies to meet physiological demands the organism is placed under (Sterling and Eyer,

1988). A major concept in allostasis is that of “allostatic state” and “allostatic load”. Allostatic state refers to a deviation of the homeostatic set-point of any given physiological factor and is driven by chronic stress to the homeostatic response mechanism (Koob, 2001). Allostatic load refers to the cumulative stresses on the organism and the adjustments to homeostasis which accommodate these changes (McEwen and Wingfield, 2003). Allostasis as a concept is somewhat controversial with various criticisms having been levied. Many of these criticisms focus on the lack of distinctions between homeostasis and allostasis. Some have suggested that responses to stress on the homeostatic response does not require allostasis and can be best explained simply by prolonged deviation from homeostasis driven by external conditions (Day, 2005). An alternative proposal to allostasis, attempting to remedy some of these criticisms, is that of adaptive homeostasis in which the homeostatic range is expanded in response to deleterious conditions (Davies, 2016). More pertinently, allostasis cannot be used to explain seasonal changes in physiology and behaviour, despite some authors attempts to do so. For example, McEwen & Wingfield suggest that seasonal changes which facilitate and drive migration in birds as examples of allostasis (McEwen and Wingfield, 2003). But this is a misunderstanding of the programmed and endogenous nature of the seasonal changes which drive migration, that is changes in photoperiod driving endogenous programmed changes, and for which “stress” to homeostatic systems is not required (Kumar et al., 2001).

1.5.3 Programmed Rheostasis Accounts for Seasonal Changes in Physiology

Perhaps the best model to explain the changes in homeostatic set-point that occur seasonally is that of programmed rheostasis. Rheostasis was initially proposed in 1990 by Nicholas Mrosovsky, and envisioned as a method by which the defended set-point of a regulated variable would change over time in a manner appropriate to the life-history and environmental conditions of an animal (Mrosovsky, 1990). Mrosovsky envisioned two main types of rheostasis, programmed and reactive rheostasis. In reactive rheostasis, the defended set-point shifts in response to environmental stresses. An example suggested by Mrosovsky is the increase of cardiac output at higher altitudes. Programmed rheostasis, describes changes which occur at given stages of the life-history of organisms and is a more relevant process in the study of seasonal biology

(Mrosovsky, 1990; Stevenson, 2023). Examples of rheostatic changes driven by biological rhythms can be seen in the circadian rhythm of blood glucose. Blood glucose levels are highly rhythmic across the circadian rhythm. Animals challenged with insulin at different points in the circadian waveform showed altered response, with animals challenged late in the day (ZT19) responding with an initial decrease and subsequent large increase in blood glucose (Rudic et al., 2004). In this experiment the set-point of blood glucose was challenged, and homeostatic mechanisms were rapidly induced to defend the set-point. In Siberian hamsters, short photoperiod driven loss of body mass can be disrupted by food restricting animals, when food is returned, animals will refeed to the appropriate phase of the seasonal cycle in body mass (Steinlechner et al., 1983). Thus, the seasonal rheostat must contain an initiator (or in some species an entrainer), this sets in motion an endogenous timer. Signalling form this timing mechanism must be integrated, alongside photoperiod and physiological signals within the rheostat. The output from this must then be output as hormonal or nervous control to drive the set point of a regulated physiological variable. A generalised version of this can be seen in figure 1-2.

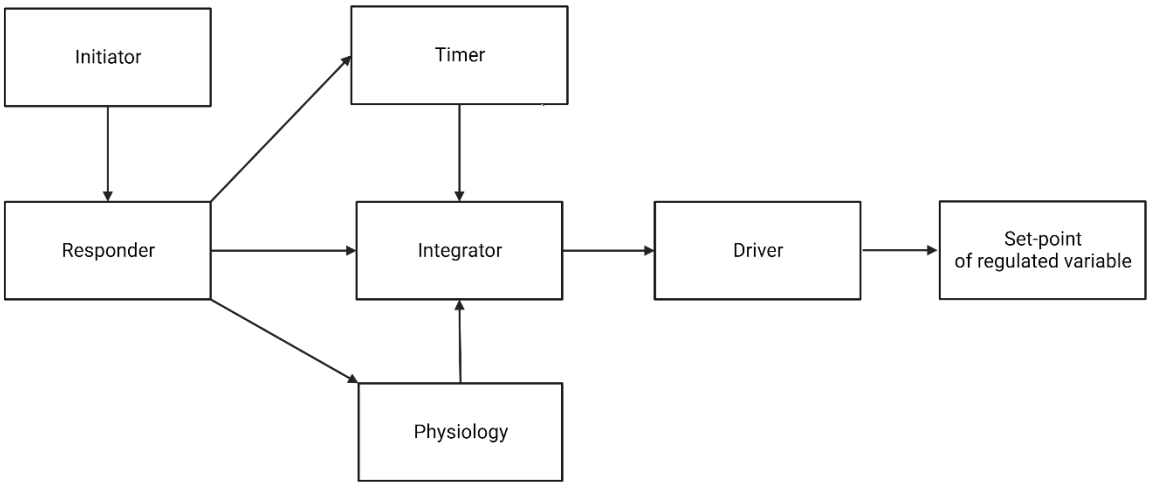

Figure 1-2: A generalised working model of an endogenous rheostatic timer. An initial signal (initiator) drives an initial responder to external signalling. This initiates an endogenous timer and drives changes in physiology. Signalling from the endogenous timer, the responder (photoperiod) and physiology are then integrated to drive rheostatic changes. Created with BioRender.com.

1.4.4 Properties of Seasonal Rhythms

To understand how rheostatic changes affect life-history transitions, the properties of seasonal rhythms must be considered. Seasonal rhythms are composed of distinct phases. Animals are said to be photoreactive when exposure to a short photoperiod drives the associated changes in physiology for that species. After a period of time the seasonal response will spontaneously cease, and animals will no longer respond to the external photoperiod. This is said to be the photorefractory phase of the seasonal cycle (Goldman, 2001). A simplified diagram of these phases of a seasonal rhythm can be seen in figure 1-3. Another important consideration for the properties of a seasonal rhythm is the photoperiod history of an individual organism. Siberian hamsters exposed to intermediate photoperiod lengths, will either show gonadal regression or recrudescence, depending on recent photoperiod exposure (Prendergast et al., 2000).

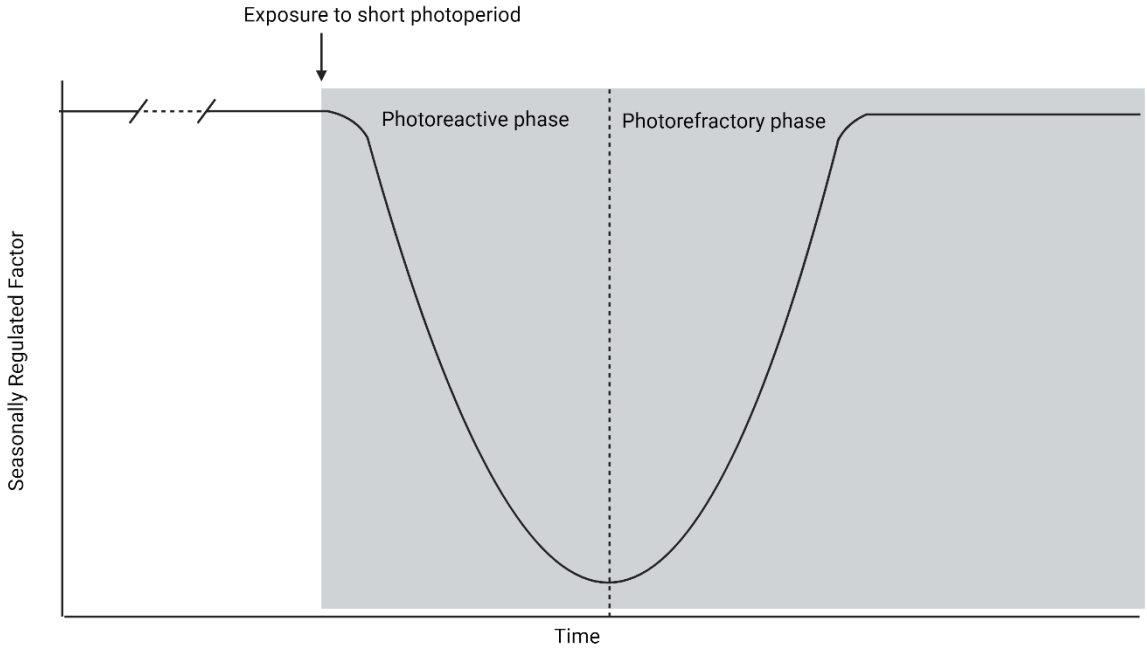

Figure 1-3: A representative diagram of the seasonal waveform in Siberian hamsters. Hamsters exposed to long photoperiods are photoreactive, when exposed to short photoperiod they will initiate the seasonal response. After a period of time, the endogenous timer will drive animals to become photorefractory and subsequent spontaneous reversion of physiology. Created with BioRender.com.

1.5.5 Circannual Timing and Seasonal Interval Timing

One major factor in considering seasonality is the difference between genuine circannual rhythmicity and seasonal interval timing. Circannual rhythms are long term rhythms which are entrained by external photoperiod. In sheep, rhythms of body mass and reproductive fitness will persist over multiple years in the absence of any change in photoperiod conditions (Lincoln et al., 1996), and this is referred to as circannual rhythmicity. The Siberian hamster will become photorefractory to short photoperiods and will no longer respond to short photoperiods until it is expose to long photoperiod for a time (Kauffman et al., 2003). This is not genuine circannual rhythmicity but rather an annual interval timer which orchestrates the development of photorefractoriness and must be 'reset' by a long day (LD) signal. The molecular basis underlying the distinction between the two is not understood. In aged Siberian hamsters, a reduced proportion of animals display the seasonal response (Horton and Yellon, 2001). It is possible that the lack of recurrent cycles may result from aging. Hamsters

which undergo a full seasonal cycle and sufficient time such that the seasonal response may be re-initiated would be of advanced age. However, it is notable that hamsters maintained on LD will never undertake the seasonal response, implying a lack of innate seasonal rhythmicity. In sheep, innate circannual rhythmicity persists under conditions of either constant SD or LD (Lincoln et al., 1996). Ecologically, the distinction between circannual rhythms and seasonal interval timers may not be significant, as Siberian hamsters exposed to realistic photoperiods will always show the seasonally response appropriate for the photoperiod that they exist within (Butler et al., 2010).

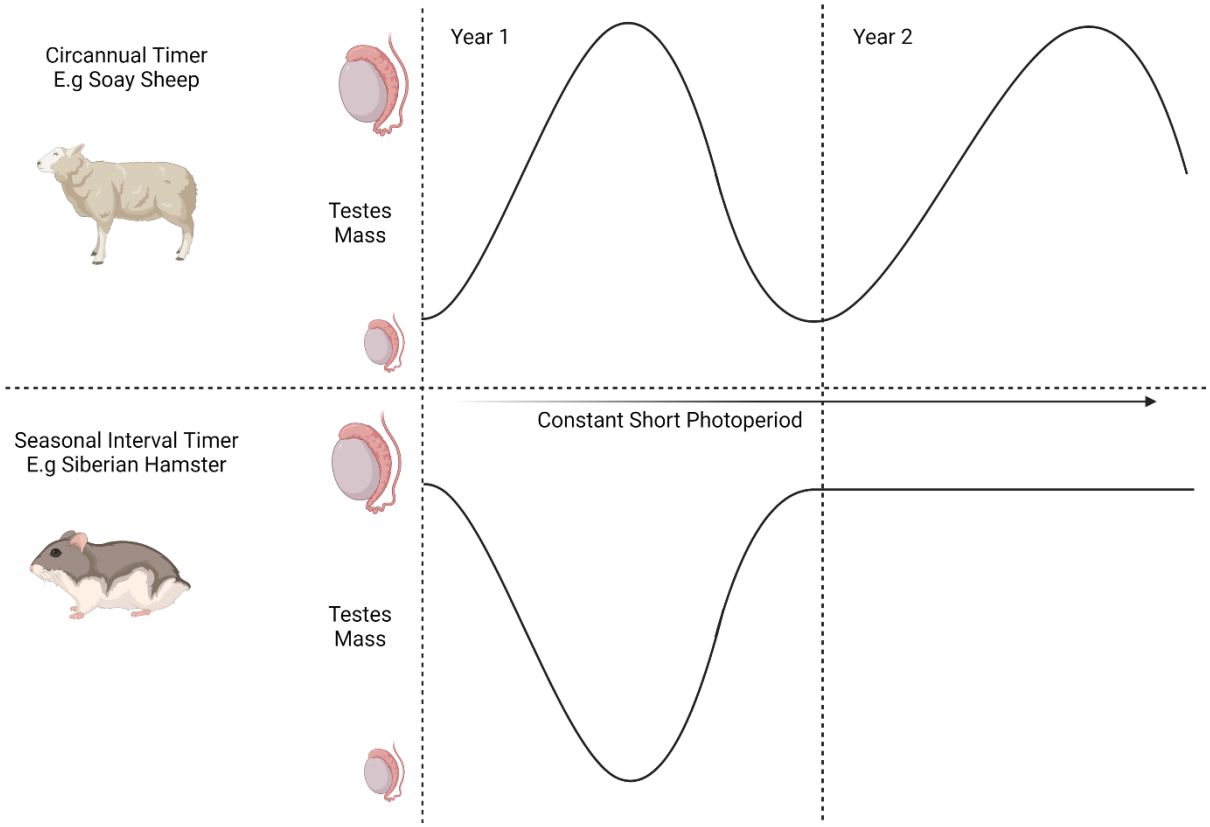

Figure 1-4: Comparison of circannual timing (top) and seasonal interval timing (bottom) in reproductive traits. Data presented is representative. In Soay sheep (top) constant short photoperiods drive gonadal growth and subsequent regression, this pattern persists over multiple years (Lincoln et al., 1996). This is typically considered a true circannual rhythm and is typical in long-lived species such as sheep. The Siberian hamster (bottom) responds to short photoperiods with gonadal regression and subsequent recrudescence, this will occur only once. This is not considered a true circannual rhythm, instead this pattern is representative of a seasonal interval timer. Created with BioRender.com.

1.5 Molecular Decoding of the Circadian Melatonin Rhythm

The decoding of the melatonin signal is critical in establishing seasonality and multiple models have been proposed as a mechanism for this. The first model proposed was an “internal coincidence” timer model of clock gene expression. In short, the *period* genes, period 1 (*per1*) and period 2 (*per2*), peak at the onset of the light phase while the cryptochrome genes, cryptochrome 1 (*cry1*) and cryptochrome 2 (*cry2*), peak early in the dark phase. Consequently, interactions between per and cry depend upon a short dark period (long days) when the two proteins will co-exist and form per-cry complexes. These complexes subsequently bind e-box elements and drive transcriptional changes ultimately giving rise to the appropriate seasonal response. In contrast a long dark phase leads to the degradation of per in advance of cry expression, preventing complex formation (Hazlerigg and Wagner, 2006). Lincoln et al. carried out an analysis of several clock genes within the suprachiasmatic nucleus (SCN) and pars tuberalis (PT) of the Soay Sheep. They identified that within the SCN *per1* and *per2* were cyclic throughout the day and identified an interaction with photoperiod. In the PT, most investigated genes were cyclic, and photoperiod affected the relative timing of cry and per genes within the PT. From this, they came to argue that the internal coincidence model was suitable for explaining the cycling of genes within the PT, and the development of innate seasonal rhythmicity. While the external coincidence model was sufficient to explain the photoperiod responsiveness of genetic expression within the SCN. They later developed a mathematical model of *per/cry* interactions within the pars tuberalis (MacGregor and Lincoln, 2008). However, the internal coincidence model has not been experimentally demonstrated. The relative phasing of *per1* expression within the PT does not appear altered as animals become photorefractory (Johnston et al., 2003).

An alternative to the “internal” model is the “external” coincidence timer model. This model was first proposed from a study investigating the role of D-box elements in driving thyroid stimulating hormone beta (*tshb)* expression in Soay sheep. Expression of eyes-absent 3 (*Eya3*) is induced under long day conditions, specifically *eya3* expression is induced 12 hours after darkness onset. However, nocturnal melatonin supresses eya3 expression. In short days the 12-hour peak of *eya3* will coincide with external darkness, and melatonin signalling,

and will be supressed, while LP allows for *eya3* expression. *Eya3* is a transcriptional co-activator which facilitates *Tshb* expression via the thyrotoph embryonic factor (Tef) (Dardente et al., 2010). *Eya3* was first identified as a seasonal response gene in Japanese quail, where it is immediately upregulated in response to a single long photoperiod signal (Nakao et al., 2008). This increased *Eya3* expression coincides with increased *TshΒ* expression in the PT of the Japanese quail (Nakao et al., 2008). It was later demonstrated that eya3 is under photoperiod driven regulation in mammals (Dardente et al., 2010). However, some studies in mammals have failed to find a clear relationship between *eya3* and *tshΒ* expression. A study in Soay sheep found that *eya3* and *tshΒ* appear to possess different critical photoperiods, with *tshΒ* downregulation occurring with a critical photoperiod of 12.5 hours of light, but eya3 not responding until 8 hours of light (Hazlerigg et al., 2018).

There have been several proposed models to account for the cycling of seasonal timing. Circadian rhythms are tissue autonomous timers which are entrained by central melatonin signalling (Huang et al., 2011; Koronowski et al., 2019). Similarly, there have been proposals that circannual rhythms arise from tissue autonomous timers. Lincoln and Hazlerigg proposed a model of tissue autonomous cycles of remodelling and differentiation. To support their argument, they highlight various elements of seasonal timing. Such as, many of the key hormones involved in seasonality, such as thyroid hormone, are involved in driving remodelling. Further many of the key seasonal regions are known stem cell niches, such as the epithelial layer of the 3rd ventricle. Finally, hormone feedback models do not sufficiently explain seasonal timing. They suggested putative stem cell niches which could be responsible for the generation of circannual rhythms, wherein sequential cycles of amplification, differentiation, and apoptosis drive rhythmicity. On an organism wide model, they propose a system wherein photoperiod acts at the level of the pars tuberalis to entrain, via the pars distalis and the hypothalamus, a number of peripheral rhythms driven by local remodelling (Hazlerigg and Lincoln, 2011).

1.6 Retinohypothalamic track/ Melatonin as orchestrator of Seasonality

1.6.1 External Light Transmission to the SCN

Seasonality is driven by external photoperiod, in mammals this is detected by retinal ganglion cells which communicate photic information to the SCN of the hypothalamus (Berson, 2002). Retinal ganglion cells serve as the entraining mechanism for both the circadian as well as seasonal and circadian rhythms. Melanopsin containing retinal ganglion cells are photosensitive and axonal branches from these cells form the retinohypothalamic tract, ultimately projecting to the SCN (Berson, 2002; Perez-Leon et al., 2006). In addition, they project to other brain regions of the brain, such as the lateral geniculate nucleus and the amygdala (Schmidt et al., 2011). These cells respond to light stimulation by generating large membrane potentials via light stimulated TRP channels, this generates the signal which transduces to the SCN (Warren et al., 2006).

The SCN is the major pacemaker of the circadian rhythm and is necessary for the transduction of photoperiod signals in mammals. Ablation of the SCN eliminates circadian rhythmicity, and transplantation of exogenous SCN sufficient to restore it (Ralph et al., 1990). The SCN is subdivided into the dorsomedial SCN, expressing arginine vasopressin (AVP), and the ventrolateral SCN expressing vasoactive intestinal polypeptide (VIP) (Moore et al., 2002). The dorsomedial SCN has many projections to the ventrolateral SCN, but no the reverse, highlighting the potential for hierarchical organisation of circadian rhythmicity within the SCN (Leak et al., 1999). Within the ventrolateral SCN there exists cells with weak oscillations, they depend upon signalling from pacemaker cells (Hastings and Herzog, 2004). However, most individual SCN neurons generate autonomous circadian rhythms (Welsh et al., 1995). This internal coupling of SCN neurons allows for a coordinated singular circadian output from the SCN (Mohawk and Takahashi, 2011). However, different regions of the SCN may respond in a differential manner to changes in light phase. Nakamura et al. investigated period 1 expression using a luciferase, and found considerable desynchrony in the SCN under phase advanced conditions (Nakamura et al., 2005). This suggests that asynchrony in SCN circadian rhythms may explain behavioural changes under advanced light phase. The overall rhythmicity of the

SCN depends upon innervation from other regions. The dorsomedial SCN receives direct retinal innervation via the retino-hypothalamic tract (Abrahamson and Moore, 2001). One of the major outputs of the circadian rhythm in the SCN is the control of pineal melatonin release. SCN neurons innervate the paraventricular nucleus of the hypothalamus and onwards, to eventually arrive at the pineal gland (Moore, 1995).

Of major relevance to seasonal biology is the circadian melatonin rhythm which is entrained by external photoperiod (Lincoln et al., 2008). Melatonin is an evolutionarily ancient molecule, likely originating prior to the evolution of eukaryotic organisms. Melatonin likely arose as a reactive oxygen species (ROS) scavenger, a role which it retains to this day (Manchester et al., 2015; Tan et al., 2013). Synthesis of melatonin in the mitochondria was likely an essential evolutionary step for eukaryotes to tolerate high atmospheric oxygen levels (Manchester et al., 2015). ROS scavenging is driven by melatonin indirectly by acting through its receptors MT1 and MT2, G-protein coupled receptors which drive cyclic adenosine monophosphate (cAMP) mediated signalling (Pandi-Perumal et al., 2008). Melatonin receptors are widespread, expressed within the reproductive system, the pancreas, skin, bones kidneys and within the brain (Slominski et al., 2012). Melatonin can also directly scavenge ROS (Zang et al., 1998). It is readily able to transfer across cellular membranes and may function as an electron donor to ROS, in order to deactivate them (Reiter et al., 2007). Other roles of melatonin include; promoting immune function (Carrillo-Vico et al., 2013), regulating metabolic factors such as insulin tolerance (Cipolla-Neto et al., 2014), promoting neuronal and glial cell survival (Borlongan et al., 2000), and even protecting against some cancers (Hill et al., 2015). Melatonin is expressed by endosymbiotic cellular components such as mitochondria (Acuña-Castroviejo et al., 2001).

Pineal expression of melatonin is regulated by the enzyme N-acetyltransferase (AANAT), which shows higher activity at night, and the SCN is necessary for this activity rhythm (Klein and Moore, 1979). Inhibition of gamma aminobutyric acid (GABA) signalling within the PVN leads to time increase in melatonin, probably by an increase in rate limiting AANAT expression, suggesting that GABAergic SCN signalling inhibits pineal melatonin expression (Kalsbeek et al., 2000). In mammals, melatonin is produced in a variety of tissues, most significantly within

the pineal gland (Tan et al., 2010). Melatonin synthesis is two-step process, first serotonin is synthesised to N-Acetylserotonin, by AANAT, and then into melatonin by hydroxyindole-O-methyltransferase (HIOMT) (Klein and Moore, 1979). Melatonin also displays very diverse effects across multiple species (Tan et al., 2010). It plays a role as an antioxidant, upregulating superoxide dismutase, as well as scavenging some ROS directly, such as the hydroxyl radical (Reiter et al., 2000).Its direct interactions with ROS are chemical in nature and not dependent upon species and, in evolutionary terms, was likely its earliest role (Tan et al., 2010). It also plays a hypnotic role, driving the onset of sleep in the early dark phase (Lavie, 1997).

Pinealectomy is sufficient to abolish the response to external photoperiod in Siberian (Dennis S. Carter and Goldman, 1983; D. S. Carter and Goldman, 1983) and Syrian (Maywood et al., 1990) hamsters. Infusions of melatonin are capable of driving gonadal regression similar to that observed in short day animals, but only if the infusion persist over a sufficient time scale. Siberian hamsters infused with 6 hours melatonin do not display gonadal regression, however 12 hours of infusion is sufficient to initiate testicular regression (Dennis S. Carter and Goldman, 1983). This phenomenon, of timing dependant melatonin infusions driving seasonal changes, can also be observed with body mass, as well as plasma Follicle stimulating hormone (FSH) and prolactin (D. S. Carter and Goldman, 1983). In addition to duration of melatonin administration, frequency is also critical in establishing seasonal responsiveness. Pinealectomised Syrian hamsters which receive 10 hour daily melatonin infusion demonstrate gonadal regression, however 48 hour administrations of melatonin failed to establish this response (Maywood et al., 1990). Thus, development of appropriate seasonal responses depends upon the duration of daily pineal melatonin signalling.

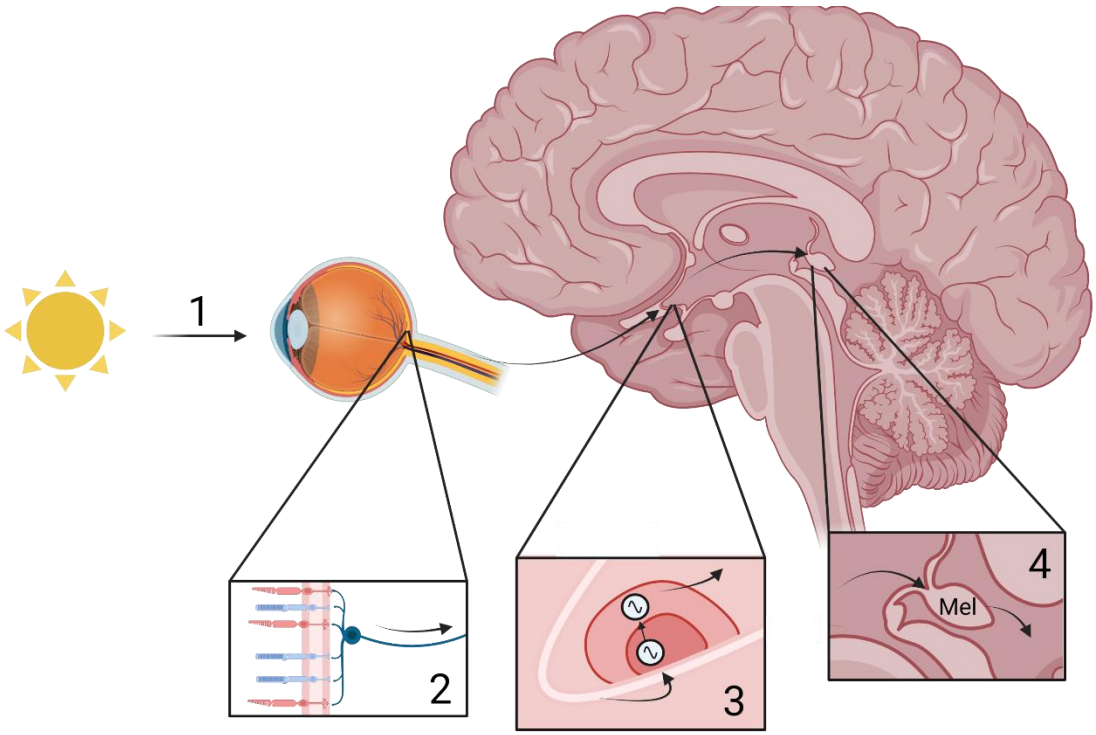

Figure 1-5: A simplified overview of the transduction of photic information into circadian melatonin signalling. In this simplified figure; 1; Photic information enters the eye. 2; Retinal ganglion cells are activated by the light and depolarise initiating signalling through the rentinohypothalamic tract. 3; Rentinohypothalamic tract depolarises neurons with the dorsomedial SCN, entraining the circadian rhythm. Internal SCN innervation ensures synchronous rhythmicity. 4; Melatonin is released from the SCN in a circadian manner. Created with BioRender.com.

1.7 Melatonin Signalling as an entrainer of seasonal biology.

1.7.1 Pars Tuberalis

In sheep, thyroid hormones are critical mediators of seasonal reproduction. Ewes thyroidectomised during the peak of their summer anoestrus resume normal breeding as they move into their short-day breeding period, however, do not successful re-enter that summer anoestrus, unless supplemented with active thyroid hormone. This evidence implied that thyroid synthesis was critical for seasonality and began a search for the tissue responsible for thyroid mediated seasonal response. The pars tuberalis possesses the highest proportion of melatonin receptors in mammals and thus was a key target for investigating the transduction of the seasonal melatonin signal (Dardente, 2012).

The PT of the pituitary gland is a site of high MT1 expression, colocalised with TSH producing thyrotropes (Klosen et al., 2002). In culture, PT MT1 positive cells respond to melatonin by driving cAMP production. Interestingly, the action of melatonin in these cells is time-dependent, exposure to 16-hours of melatonin treatment drives higher cAMP accumulation than treatment with 8-hours. Further, the binding of melatonin to MT1 positive PT cells begins to decrease after 16-hours (Hazlerigg et al., 1993). In the PT melatonin nightly onset induces *cry1* expression (Dardente et al., 2003). The offset of melatonin signalling at the onset of the next light phase drives *per1* expression. This led to the development of an “internal coincidence” model of the decoding of the seasonal melatonin signal within the PT (Lincoln et al., 2002). The cycling of core clock proteins in the PT is dependent on MT1, as $MT1^{-/-}$ rodents lack rhythmicity within the PT (Jilg et al., 2005). Changes to circadian clock proteins have been proposed to drive a molecular switch governing *tshb* expression within the PT. This proposal suggests that short photoperiod melatonin signalling suppresses *Eya*3 via e-box dependant mechanisms. As a co-activator involved in *tshb* transcription, this leads to a short photoperiod inhibition of *tshb* (Dardente et al., 2010).

1.7.2 Pars Distalis

The pituitary is also the site of prolactin synthesis, a hormone which is highly seasonal in a wide variety of seasonal species. In mammals, seasonal prolactin release is highly conserved and remarkably consistent Circulating prolactin levels are inhibited by short photoperiod in the vast majority of seasonal

mammals, regardless of the breeding phase of that species (Stewart and Marshall, 2022). For example, short day breeding Soay sheep decrease prolactin levels under short days, while long day breeding Siberian hamsters show the same prolactin response (Stewart and Marshall, 2022). This suggests a conserved mechanism of prolactin seasonality that is distinct from seasonal breeding.

Prolactin is known to affect multiple physiological systems, including but not limited to reproduction. In female mammals, prolactin acts to maintain the corpus luteum following ovulation by driving an increase in LH receptor expression (Bachelot et al., 2009; Morishige and Rothchild, 1974). Similarly, in male mammals, prolactin drives fertility in multiple ways, such as driving an increase of androgen production and increasing LH sensitivity in Leydig cells (Purvis et al., 1979). However, the timing of seasonal reproduction and prolactin secretion is often misaligned and experimental data supports this dissociation (Stewart and Marshall, 2022). Prolactin also plays a role in metabolic regulation, there is some evidence that prolactin drives changes in hypothalamic neuropeptides which regulate energy balance. Hypothalamic pro-opiomelanocortin (*pomc*) expression is downregulated by prolactin (Tong and Pelletier, 2008), and there is some evidence that *npy* expression within the dorsomedial hypothalamus is regulated by prolactin (Chen and Smith, 2004).

1.7.3 Seasonal Pars distalis Output Controlled by Pars Tuberalis

Notably, in a seasonal context, the pars distalis does not possesses melatonin receptors and has been shown to lack melatonin binding capacity in seasonal species (Bittman and Weaver, 1990). This implies that control of seasonal prolactin release is a downstream effect of direct melatonin action elsewhere. Homeostatic control of prolactin release is normally under dopaminergic release from the hypothalamus (Moore, 1987). However, in studies of hypothalamic pituitary disconnected sheep, wherein the connection between the hypothalamus and the pituitary is disrupted, normal seasonal release of prolactin signalling persists (Lincoln and Clarke, 1994). This implicates the pars tuberalis in the control of seasonal prolactin release. The identity of a potential seasonal signal from the pars tuberalis to the pars distalis remains elusive. Morgans *et al.* (1996) identified that pars tuberalis medium regulated gene expression and prolactin release in pars distalis (PD) cells. They identified both a low molecular

mass (<10kDa) and a high molecular mass (>10kDa) protein fragment within this media which were individually capable of driving gene regulation (Morgan et al., 1996). This protein was putatively named tuberalin, and its identity has not yet been uncovered. Multiple factors have been proposed as identities for tuberalin, though none have been conclusively demonstrated. After the tachykinin precursor 1 (*tac1*) was found to be photoperiodically regulated in the pars tuberalis by exposure to LP (Dupré et al., 2010). Peptides derived from tachykinin are capable of modulating prolactin release within the pars distalis. *Tac1* product substance p is capable of modulating prolactin release via directly inducing prolactin expression (Vijayan and McCann, 1979) and regulating tuberoinfundibular neurons which provide dopaminergic mediated negative feedback of prolactin release (Isovich et al., 1994). However, lactotrophs do not appear to possess tachykinin receptors (Dupré et al., 2010), however it remains possible that tachykinins act on lactotrophs through intermediary steps. Another potential candidate, the endocannabinoid 2-Arachidonoylglycerol (2-AG), shows a similar increase in the PT under LP (Yasuo et al., 2010). Based on studies of tissue culture extracts 2-AG is capable of driving prolactin expression (Yasuo et al., 2014). Promisingly, the primary receptor for 2-AG, CB1, has been detected within the pars distalis, however localisation studies of the CB1 receptor have placed it on ACTH producing corticotrophs and on folliculostellate cells, rather than on lactotrophs (Yasuo and Korf, 2011). It remains possible that 2-AG acts on lactotrophs through a paracrine mechanism within the pars distalis itself, however such a mechanism has not been uncovered. Administration of cb-1 agonists appears to drive the development of a SP like phenotype of decreased food intake and body mass in Siberian hamsters signalling (Ho et al., 2012). This is contrary to the anticipated effect 2-AG would drive were it the sole molecule responsible for pars tuberalis signal transduction to the pars distalis. It is notable that multiple molecular weight fractions were originally identified in PD medium (Morgan et al., 1996), and this could suggest that multiple factors are released to control prolactin release. Gerald Lincoln mathematically modelled a proposed negative feedback model controlling prolactin's seasonal oscillation. By including two positive feedback stages before final negative feedback into tuberalin secretion, they were able to model the seasonal waveform of prolactin release in a manner similar to that which is observed in hypothalamo-pituitary disconnected sheep (MacGregor and Lincoln, 2008). This "delayed feedback"

model of prolactin secretion allows for a free running endogenous rhythm of prolactin secretion such as that which exists in sheep, wherein high levels of prolactin under LP eventually undergo an endogenous rhythm. It does not adequately explain a system in which an endogenous prolactin rhythm occurs only under SP and in which high levels of prolactin secretion persist under LP.

1.8 Hypothalamus

1.8.1 Tanycytes

1.8.1 Tanycytes in Physiology

One major cellular population involved in seasonality are the tanycytes, glial like cells which line the ependymal layer of the third ventricle of the hypothalamus. Tanycytes can be further broke down into α1, α2, ß1 and ß2 tanycytes, each of which have different functions. The ß1 and ß2 tanycytes contact the cerebrospinal fluid (CSF) within the third ventricle but have processes which span across the median eminence, where they contact portal capillary vessels. While α1 and α2 tanycytes project to hypothalamic regions, specifically; the dorsomedial and ventromedial nuclei for α1, and the arcuate nucleus for α2 tanycytes (Bolborea and Dale, 2013). Tanycytes share many similarities with radial glial cells, however tanycytes arise late during development from the same neural precursor cells which give rise to hypothalamic neurons (Goodman and Hajihosseini, 2015). In the adult brain, tanycyte neurogenesis leads to the development of neurons within the arcuate nucleus, a region closely involved in energy balance. Indeed, tanycyte neurogenesis is both responsive to energy state and regulates energy balance. Tanycyte neurogenesis is increased in response to a high fat diet and prevention of neurogenesis by radiological elimination of the tanycyte niche ameliorates body weight gain in response (Lee et al., 2012). Tanycyte neurogenic potential remains even in aged animals and remains responsive to metabolic insulin-like growth factor 1 (IGF-1) signalling (Chaker et al., 2016).

Tanycytes play a major role in transport of molecules from the bloodstream into the CSF and subsequently into central signalling. Tanycytes act as barriers for the entry of molecules such as leptin into the CSF. Leptin receptor mediated

transport of leptin by tanycytes regulates food intake, lipogenesis and glucose tolerance (Duquenne et al., 2021). Similarly, tanycytes regulate the shuttling of insulin and ghrelin into the CSF via similar receptor driven shuttling across the median eminence (Porniece Kumar et al., 2021). Once across the blood brain barrier, leptin and insulin act upon POMC and agouti-related peptide (AgRP) neurons within the arcuate nucleus to up- and down-regulated expression respectively (Varela and Horvath, 2012). In addition to reacting to metabolic hormones, tanycytes are also capable of directly sensing the energy state of an organism. Tanycytes are glucosensitive and have multiple mechanisms of detecting glucose. Tanycytes possess taste receptors, Tas1r2 and Tas1r3, in addition to GLUT1 and GLUT2 (Benford et al., 2017). Glucose induces tanycyte barrier plasticity by inhibiting VEGF-A expression in tanycyte, minimising transport across the median eminence (Langlet et al., 2013).

1.8.1.2 Tanycytes in Seasonal Biology

The tanycytes are currently thought to be key in the transduction of the seasonal signal from the pituitary to the hypothalamus. Tanycytes possess TSH receptors and respond to the release of TSH from the pars tuberalis, and respond by altering the expression of the iodothyrine deiodinases, *dio2* and *dio3* (Barrett et al., 2007). In most seasonal mammals, *dio2* is upregulated in response to long photoperiods, and facilitates the increase of thyroid hormone signalling to the hypothalamus (Murphy and Ebling, 2011). In the Siberian hamsters, short photoperiods induce expression of DNA methyltransferases 1 and 3b (*dnmt1* and *dnmt3b*), coinciding with greatly reduced global methylation in SD Siberian hamsters (Stevenson and Prendergast, 2013).

Changes in iodothyrine deiodinases within tanycytes drive changes in local thyroid hormone (T3) availability (Lechan and Fekete, 2005). Siberian hamsters respond only by decreasing Dio3 expression, limiting the deactivation of active thyroid hormone (Barrett et al., 2007). Chronic replacement of T3 in short photoperiod Siberian hamsters is sufficient to prevent the development of short-day physiology (Barrett et al., 2007). Administration of exogenous TSH is sufficient to drive the reactivation of the reproductive axis in short-day exposed animals (Klosen et al., 2013). In most photoperiodic species, including Siberian hamsters, a single long photoperiod is sufficient to drive reproductive changes

associated with seasonality (Finley et al., 1995; Nicholls et al., 1983; Spears et al., 1990). A summary of the role that hypothalamic thyroid hormone signalling plays within the third ventricle in Siberian hamster seasonality can be seen in figure 1-6. There also exists peripheral rhythms of *dio3* expression, with circulating lymphocytes downregulating dio3 expression in short-day exposed Siberian hamsters (Stevenson et al., 2014). Suggesting, the potential for tissue-autonomous seasonal regulation of thyroid hormone availability.

A recent study demonstrated that tanycytes express neuronal cell adhesion molecule (NrCAM), a gene closely associated with neurogenesis. They demonstrated that tanycytes from NrCAM deficient mice possess reduced neurogenic capacity and that the arcuate nucleus of these animals show reduced TH positive neurons. In addition, they demonstrated a repression in NrCAM deficient animals, with reduced food intake and body mass (Moore et al., 2022). This finding is particularly interesting within the context of seasonal biology given that NrCAM expression is supressed in the tanycytes under short photoperiod in the Siberian hamster, and this reduction appears to be melatonin driven (Bolborea et al., 2011). It seems likely that tanycyte neurogenesis and remodelling are critical components of seasonal changes, and this is in line with proposed mechanisms of tissue independent proliferation timers.

Of interest from a seasonal perspective is the expression of the orphaned melatonin receptor g protein-coupled receptor 50 (GPR50), the functional deletion of which drives torpor and reduces body temperature in mice (Bechtold et al., 2012). Work by Barrett *et al*. utilised fluorescent in situ hybridisation (FISH) to identify the location and relative expression of GPR50 in the hypothalamus of Siberian hamsters under long and short photoperiods. They identified that *gpr50* expression is lower under short photoperiod, and further demonstrated the location of the GPR50 protein by generating mice with LacZ spliced into the GPR50 gene and visualised its expression with x-gal staining. In addition, they also demonstrated that nestin and cellular retinol binding protein-1 (crbp1) are under photoperiodic control in a similar manner. Of note, expression of these genes is region specific, for example Gpr50 is most responsive to short photoperiod in the medial region of the 3rd ventricle, implying a differential response to photoperiod in different regions of the hypothalamus (Barrett et al., 2006). This study, utilised animals that were

exposed to short photoperiod for 13 weeks, and it could be possible that the temporal dynamics of these genes are more complex than reported. *Gpr50* also appears to be downregulated in tanycytes that are NrCAM deficient (Moore et al., 2022), painting a potential role of GPR50 in driving seasonal proliferation and development of tanycytes. Hypothalamic tanycytes project to regions critical for the control of energy balance such as the arcuate nucleus. Tanycytes are a likely candidate for being closely involved in integrating multiple signals for rheostatic control.

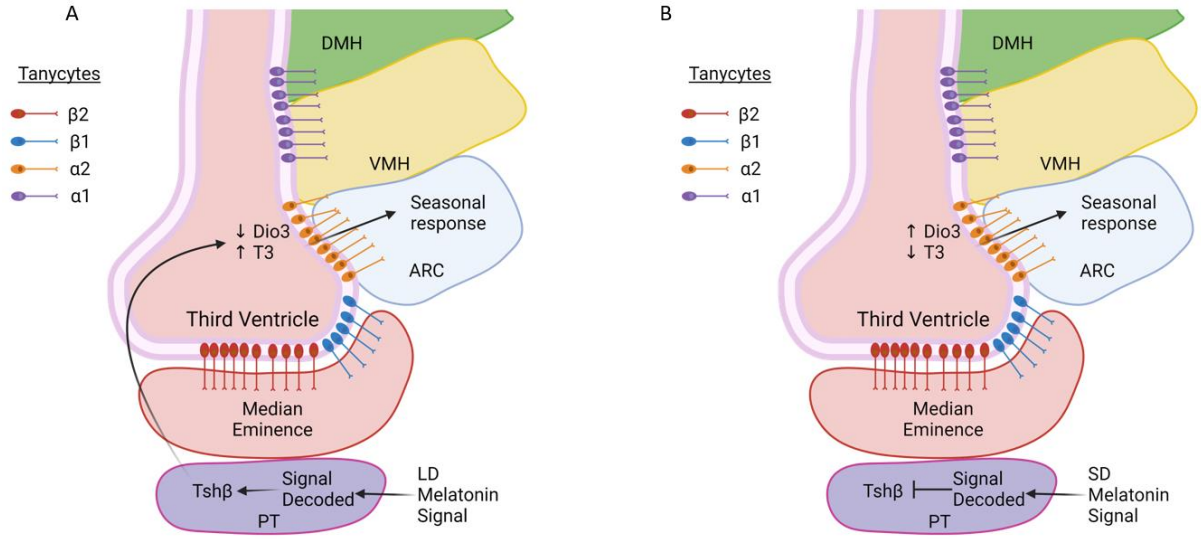

Figure 1-6: The role of pituitary TSH signalling in driving seasonal responsiveness in the Siberian hamster. Under Long photoperiods (A) the long photoperiod signal is decoded within the pars tuberalis (PT) and TSH is released into the median eminence. B2 tanycytes transport TSH into the third ventricle, wherein Dio3 expression is inhibited in α1 and α2 tanycytes. This drives a local increase in thyroid hormone (T3) availability. Under short photoperiods (B) the short-day melatonin signal is decoded. This inhibits the release of thyroid hormone signalling to the hypothalamus. Expression of Dio3 in the tanycytes leads to suppressed local levels of T3. The decoding of the photoperiod signal within the pars tuberalis represents a key response mechanism for the rheostat. Within the tanycytes, this response drives an endogenous timer. The integration of this timer, and the signalling from pars tuberalis acts to set the seasonal rheostat. Created with BioRender.com.

1.8.2 Arcuate

Hypothalamic tanycytes project to regions critical for the control of energy balance such as the arcuate nucleus. Ablation of the arcuate nucleus does not inhibit the changes in body mass shown by Siberian hamster exposed to short photoperiods (Ebling et al., 1998). However, later reanalyses of arcuate ablation studies would identify that the dorsomedial part of the arcuate nucleus is not ablated in such studies (Barrett et al., 2005). Later ablations of the dorsomedial part of the arcuate would find that it too was not necessary for seasonal response in reproduction, body mass or thermogenesis (Leitner and Bartness, 2011). However, the arcuate nucleus contains multiple photoperiodically regulated transcripts related to body mass such as VGF (non-acronymic) (Helfer and Stevenson, 2020) and POMC (Bao et al., 2019). This may suggest the arcuate nucleus as a responsive tissue to rheostatic timing, but not in setting the rheostat.

1.8.3 Dorsomedial Hypothalamus

Sitting anterior to the arcuate nucleus and directly contacted by tanycyte end-feet is the dorsomedial nucleus of the hypothalamus (DMH). The DMH is critical to the transmission and maintenance of circadian rhythms, with the DMH directly innervated from the SCN. DMH neurons have several projections to regions of the brain involved in the regulation of circadian systems. For example, DMH projections to the locus coeruleus and the ventrolateral preoptic area are thought to be important in the mediation of sleep (Chou et al., 2003). The DMH was initially identified as a key region for seasonality in studies in the Syrian hamster. An early study identified melatonin binding sites within the DMH and used electrolytic lesioning to generate lesions of these the regions. They identified that lesions of the DMH prevent a melatonin induced decrease in plasma luteinising hormone (LH) levels and prevent the associated decrease in testes weight (Maywood et al., 1996). Further investigations were later carried out in Siberian hamsters and revealed very similar data. Bartness and Leitner (2011) identified that lesions of the Siberian hamster DMH, prevented a melatonin driven decrease in white adipose tissue (WAT) mass and food intake, but interestingly did not ameliorate the decrease in total body mass. Further, the authors link this DMH mediation of the photoperiod response, to previous

work identifying melatonin responsive neurons that control sympathetic outflow from the DMH. Subsequently, they argue for a photoperiod driven modulation of WAT via sympathetic innervation originating within the DMH (Bartness and Song, 2007; Leitner and Bartness, 2011). These studies cannot, conclusively demonstrate that the seasonal response in the DMH results from melatonin acting directly on the DMH rather than via an intermediary, such as tanycyte T3 signalling.

Neurons within the DMH play key roles in the regulation of reproductive fitness. RFamide-related peptide-3 (RFRP3) neurons work in concert with kisspeptin neurons to regulate the release of gonadotropin releasing hormone. RFRP3 acts on its receptor GPR147, a G-protein coupled receptor expressed in the gonadotropes of the pituitary, to inhibit the release of GnRH (Ubuka et al., 2009). Evidence from naked mole rats, suggests that RFRP3 neurons play major roles in supressing puberty, indicating that they may play a role in the timing of puberty in mammals (Peragine et al., 2017). In mice, a decrease in RFRP3-ir neurons within the DMH has been associated with testicular development during puberty and subsequently an increase appears associated with decrease in reproductive fitness later in life (Sethi et al., 2010). RFRP3 neurons are critical in control of the oestrus cycle in mammals, with higher activity in RFRp3 neurons in proestrous. Similarly, a circadian pattern of RFPR3 neuron c-fos expression is closely aligned with the transition from dark to light phase (Angelopoulou et al., 2021). RFRP3 neurons project into regions of the hypothalamus associated with energy balance such as the arcuate nucleus. Leptin binding to its receptor on RFRP3 neurons likely drive a decrease in gonadotropin hormone-releasing hormone (GnRH) release (Anjum et al., 2021). Together, these findings highlight the key role that RFRP3 plays in integrating multiple signals to regulate reproduction. Siberian hamsters downregulate expression of RFRP3 under short photoperiod and this response is abolished following pinealectomy and is recovered following melatonin injection. This downregulation occurs during a time in which the reproductive system is inhibited, highlighting the differential effects RFRP3 could have on the reproductive system (Revel et al., 2008). It is interesting that RFRP3 expression is upregulated under LP conditions, even in species which are long day breeders (Angelopoulou et al., 2019).

1.9 Molecular Correlates of Programmed Seasonal Rheostasis

1.9.1 The Melanocortin System

The melanocortins are a family of peptide hormones, derived from a common single precursor peptide POMC, which have diverse roles in the control of homoeostasis. The melanocortin family includes ß-endorphin, lipotropin and alpha-Melanocyte-stimulating hormone (α-MSH), and which act on a family of trans membrane receptors known as melanocortin receptors (Hadley and Haskell-Luevano, 1999). POMC posttranslational cleavage is thought to be tissue specific and may depend upon concentrations of prohormone convertase (PC) 1/3, giving rise to adrenocorticotropic hormone (ACTH) and lipotropin, and PC2, which gives rise to ß-endorphin and α-MSH (Seidah et al., 1999). Human patients with dysfunctional pomc genes suffer from severe early-onset obesity (Krude et al., 1998).

It is now understood that the *pomc* neuron population is composed of multiple distinct neuronal subtypes (Quarta et al., 2021). *Pomc* express either glutamate decarboxylase, responsible for GABA production, or glutamate transporters, indicating that they may be wither GABAergic or glutamatergic in nature (Hentges et al., 2009). GABAergic and glutamatergic *pomc* neurons may have different functions in regulating physiology, with each group being spatially distinct and appear to respond differently to administration of mTORC1 (Saucisse et al., 2021). Similar findings in AGrP neurons, of distinct neuronal sub populations with unique projections (Betley et al., 2013). Further a single cell sequencing experiment of *pomc* neurons surveyed the distinct sub-types. It identified four distinct clusters of *pomc* neuron, with diverse expression of transcripts and response to leptin administration. Interestingly, a number of cells in this experiment expressed *npy* and *agrp* alongside *pomc* (Lam et al., 2017).

Pomc expression is responsive to energetic conditions. Genetically obese *ob*/*ob* mice have lower arcuate *pomc* expression, that is restored with exogenous leptin administration (Schwartz et al., 1997). Leptin drives an increased in *pomc* neuron depolarisation, both via direct action of leptin on *pomc* neurons, but also

by driving reduced inhibitory γ-aminobutyric acid signalling from NPY neurons (Cowley et al., 2001). Indeed, targeted deletion of leptin receptors in *pomc* neurons are obese and hyperlectinaemic (Balthasar et al., 2004). Insulin is another major regulator of *pomc* neuron activity. Some reports have suggested that insulin and leptin are opposing forces in driving *pomc* neuron depolarisation (Al-Qassab et al., 2009). However, insulin and leptin appear to act on distinct sets of *pomc* neurons, providing further evidence of the importance of pomc subpopulations (Williams et al., 2010).

Melanocortin hormones act on one of five melanocortin receptors; MC1R, MC2R, MC3R, MC4R and MC5R, each of which possess a different potency for binding the aforementioned POMC product proteins (Gantz and Fong, 2003). MC3R deficiency in mice appears to inhibit a food restricted delay in pubertal timing (Lam et al., 2021). Further, deleterious mutations of MC3r are overrepresented in human patients displaying delayed onset of puberty (Duckett et al., 2023). MC3R is expressed on kisspeptin, neurokinin b, and dynorphin (KNDy) neurons, alongside MC4R (Merkley et al., 2020). On POMC neurons, MC3R may act in autocrine manner, wherein POMC neuron derived melanocortins act on MC3R on those neurons to inhibit POMC signalling, thus having a orexigenic effect (Cowley et al., 2001). Deletion of MC4R in mice leads to profound hyperphagia, hyperinsulinemia and obesity providing a key link between MC4R signalling and control of energy balance (Huszar et al., 1997).

Pomc mRNA has been reported as a seasonal transcript. Mercer et al. investigated the role of various neuropeptides in the control of seasonal and identified a significant decrease of *pomc* expression in the arcuate nucleus of Siberian hamsters exposed to SD (Mercer et al., 2000b). This change in expression was paradoxical, as lower *pomc* expression in the arcuate nucleus is classically associated with a decrease in body mass (Millington, 2007). They similarly found a paradoxical increase in *Agrp* expression (Mercer et al., 2000b). AgRP drives obesity by acting as an antagonist of melanocortin receptors (Ollmann et al., 1997). A study in gonadectomised Syrian hamsters found that seasonal changes in *pomc* expression depend upon intact gonads (Bittman et al., 1999), suggesting that androgen signalling is the critical mechanism driving *pomc* seasonality.

B-endorphin signalling is critical for the development of puberty (Prasad et al., 2008). A study investigating testicular expression of *pomc* noted a decrease in expression preceding testicular regression under SD (Morgan et al., 2003). Indeed, some studies have suggested that a kisspeptin-pomc pathway is necessary to drive nutritional acceleration of pubertal onset, via α-MSH signalling (Cardoso et al., 2015). Further studies attempted to characterise this putative pathway. Leptin signalling is per. Thus *pomc* neurons appear to play a major role in translating the peripheral leptin signal to kisspeptin neurons and ultimately GnRH release (Manfredi-Lozano et al., 2016). It is possible that this mechanism may be relevant for seasonal biology.

1.9.2 Somatostatin

In 1968, purified hypothalamic extracts were found to inhibit the release of growth hormone from cultured rat pituitary cells (Krulich et al., 1968). Several years later, the peptide component of hypothalamic extracts which inhibit growth hormone release was identified and named somatotropin-release inhibiting factor (SRIF) (Brazeau et al., 1973). This hormone was subsequently named somatostatin (SST) given its role in inhibiting growth hormone release. It became apparent early, that SST also inhibits prolactin release from cultured lactotrophs in vitro (Vale et al., 1974). Somatostatin is initially synthesised as prepro-somatostatin, and subsequently cleaved into one of two active peptides, somatostatin-14 or somatostatin-28 (Olias et al., 2004). Somatostatin, and related peptides, are ubiquitous in vertebrates, suggesting an ancient evolutionary origin (Koch et al., 2022). Somatostatin expression is known to increase within the hypothalamus of short-day acclimatised Siberian hamsters (B. J. Prendergast et al., 2002). Treatment of Siberian hamsters with somatostatin agonists drives a response like that of a short day response (Dumbell et al., 2015). Further to seasonal control of body mass, activation of somatostatin receptors may be critical in the development of seasonal torpor in Siberian hamsters (Scherbarth et al., 2015). Leaving somatostatin as a key neuroendocrine target for rheostatic control.

1.9.3 Prolactin

One of the key outputs of the key seasonal responses in most animals is marked seasonal variation in prolactin secretion (Stewart and Marshall, 2022). Prior to

the discovery of prolactin, the existence of a pituitary hormone driving lactation in mammals had been proposed. Prolactin was discovered in birds after efforts to identify this putative hormone and its name was given to describe this purpose (Riddle et al., 1933). Prolactin is an evolutionarily ancient hormone, likely arising in early chordate evolution and present in all extant chordates (Dobolyi et al., 2020). Prolactin is a large (23kDA) hormone REF.Prolactin levels in mammals spike during pregnancy in mammals, though its actions are opposed by progesterone. Following parturition, progesterone levels drop and prolactin drives lactation (Ostrom, 1990). A 16kDA isoform of prolactin also exists, arising from cleavage of the full isoform, and acts in an antitumorigenic and antiangiogenic capacity (Bernard et al., 2015). Prolactin is produced by the lactotrophs of the pituitary gland. It is classically under dopaminergic regulation, hypothalamic dopamine acts on lactotroph D2 receptors to inhibit prolactin release (Fitzgerald and Dinan, 2008). However, several peripheral tissues are also known to express prolactin. Adipocytes express prolactin beginning early in adipogenesis and is regulated by cyclic AMP activators (Brandebourg et al., 2007). Prolactin may play roles in the regulation of adipocyte signalling, suppressing the release of adiponectin and leptin (Brandebourg et al., 2007). Interestingly, extra-pituitary expression of prolactin appears far more prevalent in humans, and closely related species, than in most mammals such as rodents (Bernichtein et al., 2010). Extra-pituitary sources produce prolactin in far lower quantities than lactotrophs, and may only acct to drive increased local prolactin concentrations (Bernichtein et al., 2010). Prolactin acts through prolactin receptors, which are widespread in Siberian hamsters (Stewart et al., 2022). Four prolactin receptor isoforms are known, long, intermediate, short and a soluble prolactin binding molecule. The long prolactin receptor is a transmembrane receptor which dimerises to present the ligand site. Prolactin binding drives jak-stat mediated signal transduction and subsequent biological effect (Bole-Feysot et al., 1998). Various reports have found that prolactin receptor isoforms can drive different physiological effects (Abramicheva and Smirnova, 2019) and this may have implications for the seasonal response. The expression of prolactin receptors is differential, both spatially and temporally. Prolactin receptor isoforms vary over the oestrous cycle (Nagano and Kelly, 1994). Though prolactin was discovered as a lactogenic hormone, it is now understood to have pleiotropic effects on physiology (Bernard et al., 2019; Bole-

Feysot et al., 1998). The prolactin receptor is widely expressed within the hypothalamus, in regions associated with energy balance such as the arcuate nucleus (Chiu and Wise, 1994). Treatment with prolactin also drives a number of changes to energy balance regulation in the hypothalamus such as up-regulation of NPY expression (Lopez-Vicchi et al., 2020) and down-regulation of POMC expression (Tong and Pelletier, 2008). Notably, hyperprolactinaemia is positively associated with obesity in patients with pituitary adenomas (Greenman et al., 1998). Additionally, prolactin administration drives increased food intake in a dose dependant manner (Gerardo-Gettens et al., 1989). Together these studies suggest that prolactin drives major central changes in neuropeptide expression which drive changes in food intake and body mass.

1.10 Thesis objectives

The molecular program driving the endogenous timing of seasonal change in mammalian physiology is poorly understood. This thesis investigated the neuroendocrine and molecular program controlling seasonal rheostasis. The first objective was to characterise the molecular changes which occur over the endogenous annual interval timer in Siberian hamsters. This will include an examination of the photoperiod driven change in transcripts using next-generation sequencing at the resolution of hypothalamic nuclei. Secondly, the distinction between molecular mechanisms regulating rheostatic and homeostatic changes in body mass was investigated using a commonly applied paradigm of negative energy balance. And then, the rheostatic control of seasonal physiology was examined by applying a manipulation of positive energy balance. It was hypothesised that the molecular programme controlling rheostatic change will be diverse and distinct from that of homeostasis, which will act in defence of the rheostatic set-point in body mass.

Chapter 2: Temporal Dynamics of Neuroendocrine Transcriptomes Underlie Seasonal Interval Timing

2.1 Introduction

2.1.1 The Advent of Next Generation Sequencing

In 1953, James Watson and Francis Crick famously postulated their model for the structure of DNA (Watson and Crick, 1953). This sparked the beginning of a long effort, through the 20th century, by the biological community to develop and implement technologies to sequence the genetic code. The first major efforts, hydrolysed RNA fragments and performed two dimensional gel electrophoresis, to determine nucleotide sequences (Adams et al., 1969). This early form of sequencing would eventually unveil the nucleotide sequence of the first gene to have its entire nucleotide sequence mapped, the bacteriophage MS2 coat protein, by a combination of partial sequencing of RNA fragments and extrapolation from the known amino acid sequence (Jou et al., 1972). It was not until 1977, that the first practical method of nucleotide sequencing was unveiled, a method which utilises terminal chain inhibition to measure each successive base in sequence, now known as sanger sequencing (Sanger et al., 1977). This was the first practical and somewhat affordable method of sequencing and quickly became the primary method by which sequencing was performed. This early sequencing method could unveil the sequence of a transcript but offered nothing in terms of quantification. Sequencing would soon be supplanted in quantitative genetic analyses by the development of qPCR, which quickly became, and to an extent remains, the primary method for quantification of nucleic acids (Mullis et al., 1986). This new sequencing method did, however, allow for the transcripts of genes and organisms to begin being published. By the 1990s full genome transcripts were beginning to be assembled. Full genomic transcript sequences were published for the first bacterium (*H. Influenzae*) and the first animal (*C. Elegans*) (Fleischmann et al., 1995; The C. elegans Sequencing Consortium*, 1998). The most famous of these was the human genome project which spanned from 1990 to 2003 and successfully sequenced a single human genome (Collins et al., 2003). These achievements were completed at extraordinary cost, by 1998 the annual budget of the human genome project was as high as $250 million (Venter et al., 1998). Naturally,

these extreme costs, coupled with the amount of time it would take for a single laboratory to complete a genome, left sequencing out of the hands of the majority of researchers.

After the discovery that the staphylococcus aureus toxin α-hemolysin, when embedded in an membrane, can act as a voltage mediated biosensor (Menestrina, 1986). Interest began to develop for the application of biosensor for distinguishing nucleotide sequences. Later experiments demonstrated that this protein was able to facilitate the electrophoresis of ssDNA or RNA across a membrane and differentiate homopolymers formed by RNA bases and that it was capable of identifying 30 base pair segments of one base embedded within a larger segment (Akeson et al., 1999). A major breakthrough occurred when it was demonstrated that individual adenine bases could be resolved in an otherwise polycytosine segment (Ashkenasy et al., 2005). Some initial limitations of this method were first identified at this stage, specifically that nucleotides up and downstream of the detected point an affect the charge, highlighted the need for complex algorithms to basecall the reads. Later, all 4 DNA bases were shown to be individually identifiable using this method, and with immobilising the DNA strand using a biotin-streptavidin complex (Stoddart et al., 2009). These experiments demonstrated that nucleotide sequencing using protein nanopores was feasible. The next major step was the development of a synthetic pore, a mutant of the MspA porin from *Mycobacterium smegmatis,* which eliminated a problem wherein multiple nucleotides could be present within the sensing region of the pore (Butler et al., 2008). By this stage the basis of nanopore sequencing had been established and would later become commercially available.

This method of next generation sequencing is readily applicable to seasonal biology. The bulk of molecular investigations in the field of seasonal biology utilise low dimensionality methods such as qPCR. Such investigations, while crucial, do not capture the entire picture of molecular changes occurring across the seasonal waveform.

2.1.2 Molecular Control of the Timing of Seasonality

As detailed in chapter 1, seasonal and circannual timers are pervasive and highly conserved. They are conserved across diverse taxa, ranging from unicellular eukaryotes (Andersen and Keafer, 1987), mammals (Ebling and Lincoln, 1987),

birds (Nicholls et al., 1983), and fish (Duston and Bromage, 1991). Key features of these timers are that they are capable of driving rheostatic changes in physiology and behaviour in a transient manner (Brian J. Prendergast et al., 2002). While the photo-transduction of the external photoperiod is well understood (Berson, 2002; Lincoln et al., 2008), the molecular mechanisms driving the timing of subsequent seasonal waveforms remain to be elucidated. Siberian hamsters display, an initial response to short photoperiod by losing body mass and displaying gonadal regression. After a period of time, the seasonal interval timer will drive a photorefractory recrudescence of reproductive and energetic seasonal changes (Milesi et al., 2017). Some have proposed models of photoperiod decoding which could allow for this refractory response. For example, the internal coincidence model of photoperiod transduction. In this model the phasing of core clock proteins *per1*, which tracks light onset, and *cry1* which tracks dark onset is altered by exposure to short photoperiods (Lincoln et al., 2002). Per and Cry heterodimers inhibit the action of core clock proteins, CLOCK and BMAL1, thus the coincidence of per and cry expression is a necessary component of the circadian clock (Ye et al., 2014). However, subsequent studies have failed to identify the necessary changes occurring in core clock proteins to facilitate the development of a refractory state with these proteins. For example the relative phasing of *Per1* expression in the PT of the Siberian hamster does not appear altered when the animals become photorefractory (Johnston et al., 2003). Further, hormonal output from the PT does not appear to change as animals become photorefractory. Seasonal changes in TSH output from the PT appears to remain supressed even after animals have fully recrudesced body mass and gonadal function. Thus, the major molecular mechanisms which drive the seasonal interval timer remain elusive.

A major recent paper utilising in-situ hybridisation (ISH) identified a large number of rhythmic genes across the seasonal waveform (Milesi et al., 2017). This paper attempted to identify the molecular mechanisms regulating the development of photorefractoriness in the Siberian hamster. The authors identify that downregulation of *dio3* is the earliest molecular event in the development of photorefractoriness. *Dio3* in this paper appears to be upregulated in the early photoinducible phase of the seasonal waveform. It begins to be downregulated after 8 weeks of SP exposure, returning to LD like levels by 20 weeks. However,

as this paper utilised ISH, only genes of interest which the authors specifically investigated may be detected, therefor it remains possible that other genes may be orchestrating the seasonal molecular architecture. By applying a the “wide-net” strategy of next generation sequencing, previously unknown seasonal transcripts may be elucidated.

A recent experiment characterised both the genome of the Siberian hamster, though not to significant depth, and the transcriptome of the whole hypothalamus (Bao et al., 2019). This experiment featured long and short photoperiod exposed hamsters and utilised them to generate transcriptomic data. The authors identified a number of genes involved in the seasonal response that had not previously been identified. The authors further demonstrate that hypothalamic thyroid hormone availability, mediated by *Dio3*, is critical in mediating seasonal physiology (Bao et al., 2019). This study aims to expand upon the work presented in Bao *et al.*; first, as shown by vitelli *et al.* many of the genes which are seasonal regulated are not simple switches but rather possess rhythmic expression across the entire seasonal waveform. Second, the hypothalamus is composed of multiple distinct nuclei each of which may pose different relevance for seasonality. A nuclei-scale resolution of the seasonal changes occurring across the entire waveform has not yet been established.

It has long been establish that refractoriness to melatonin signalling occurs independently at different nuclei of the hypothalamus in Siberian hamsters (Freeman and Zucker, 2001). However, this study utilised melatonin implants in individual nuclei, which may not fully replicate the entirety of seasonal signalling in short day exposed animals. Additionally, studies which have utilised ablation of individual hypothalamic nuclei have revealed diverse effects on seasonal systems. Ablation of the DMH in Syrian hamsters prevents photoperiod driven testicular regression, while other seasonal indicators, such as blood prolactin and FSH concentrations remain unaffected (Jarjisian et al., 2013). In contrast, lesions of the arcuate nucleus maintain normal short photoperiod driven response in body weight and reproductive recrudescence, however that response was blunted in comparison to sham operated control animals (Ebling et al., 1998). Additionally, ablation of the paraventricular nucleus (PVN) abolishes seasonal torpor in Siberian hamsters, without affecting the energetic seasonal response (Ruby, 1995). Surgical interventions within the hypothalamus can give

us much information on the role and necessity of different hypothalamic regions. Similarly, an approach of individual nuclear sequencing will allow for the dissection of the molecular changes occurring within the hypothalamus at a resolution that has not previously been achieved.

2.1.3 Analysis of Biological Rhythms

Biological rhythms, such as the circadian rhythms, are often analysed using statistical methods developed for the specific purpose of analysing rhythms. Standard analyses of large-scale data sets may not capture transcripts which may subtly oscillate, however such transcripts may be detect by statistical methods designed to detect rhythmicity within a data set. The key issue is that standard models of null-hypothesis significance testing generally gives information of the statistical difference between groups, however, gives no information on the rhythmicity of data sets. Many statistical methods have been developed to identify rhythmicity in biological datasets. One of the earliest designed methods was the cosinor method. Designed initially for limited data sets, cosinor based analysed are now commonly utilised in studies investigating biological rhythms (Cornelissen, 2014). The Jonckheere-Terpstra-Kendall (JTK) cycle analysis was developed as a non-parametric test of rhythmicity within biological data sets, and is the method which will be utilised in this study (Hughes et al., 2010). The method utilises the Jonckheere-Terpstra-Kendall algorithm, which organises data based on the order of independent groups and calculates Kendall's tau value based on the distribution of a hypothetical random variate. The JTK cycle takes given biological data and compares this to a set of user defined waveforms, and Bonferroni corrects p values to adjust for multiple comparisons. This method was further improved upon on the empirical JTK cycle algorithm which allows for better estimation of significance in noisy datasets (Hutchison et al., 2015). This analysis method was later incorporated into the online tool Biodare, alongside sets of waveforms to utilise in rhythmicity analysis (Zielinski et al., 2014).

2.1.4 The Relationship Between Expression of Hypothalamic Neuropeptides and Behaviour in the Siberian hamster

Understanding the spatial and temporal expression within the hypothalamus may be key to understanding the behavioural changes that occur in seasonal animals.

Rheostatic changes in body mass are thought to be orchestrated within the hypothalamus. Seasonality drives significant behavioural changes in Siberian hamsters. The action of melatonin on MT1 in the adrenal leads to higher plasma concentrations of the adrenal androgen dehydroepiandrosterone (DHEA) (Munley et al., 2020). DHEA subsequently is transported into the brain where it is transformed into testosterone and oestrogen locally within substrates in the brain (Munley et al., 2018). However, others work has identified that changes in gut microbiota may drive seasonal aggression, as faecal transplants from LD exposed Siberian hamsters appears to ameliorate the increased aggression of SD exposed animals (Shor et al., 2022). SD exposed Siberian hamsters lose rhythmicity of, and decrease total output of, locomotor activity which may contribute to the reduced energy expenditure of Siberian hamsters under short photoperiod (Warner et al., 2010).

2.1.5 Aims

The aim of this chapter was to identify the seasonal rhythmicity of transcripts within individual hypothalamic regions in adult Siberian hamsters. This was achieved by monitoring the physiological and behavioural characteristics of Siberian hamsters across a 32-week exposure to SD. Measurements occurred at 4-week intervals to capture the entirety of the waveform during this period. To characterise the molecular changes within the hypothalamus, individual hypothalamic nuclei were dissected. This included the medio-basal hypothalamus (consisting primarily of the arcuate nucleus, pars tuberalis, median eminence and the ependymal layer of the third ventricle), dorsomedial hypothalamus, the paraventricular nucleus of the hypothalamus and the pituitary. This strategy provides a high temporal and high spatial resolution of the molecular architecture of the seasonal waveform within the hypothalamus. This will generate a complete transcriptome expression within distinct nuclei and provides a comprehensive picture of the seasonal interval timer.

2.2 Hypothesis

Transient alterations in gene expression will be unique to hypothalamic nuclei. Previously identified Seasonal transcripts such as *tshb* will show strong seasonal alterations in gene expression. Hypothalamic nuclei will possess unique patterns of expression which will grant further insight in Photorefractory Siberian hamster will display molecular distinction from long photoperiod Siberian hamsters.

2.4 Methods

2.4.1 Ethics

All procedures were in accordance with the National Centre for the Replacement, Refinement and Reduction of Animals in Research ARRIVE guidelines (https://www.nc3rs.org.uk/revision-arrive-guidelines). All procedures were approved by the Animal Welfare and Ethics Review Board at the University of Glasgow and conducted under the Home Office Project Licence PP5701950.

2.4.2 Study Design

Adult male Siberian hamsters (n = 99) were held in LD (16h light:8h darkness) (n = 6) or SD (8h light:16h darkness) for up to 32 weeks. Animals were age matched to minimise effects of aging upon the data set. A subset of animals (n = 54) was selected for molecular testing. Food (RPM1) and water were provided *ad libitum* throughout the course of the experiment. At 4-week interval groups of animals (n = 6) were sacrificed by cervical dislocation. This generated a 32-week period over which analyses may be performed, sufficient to cover the seasonal waveform in the Siberian hamster (Milesi et al., 2017). Brain, pituitary, brown adipose tissue (BAT), WAT, liver, kidney, spleen, and testes were immediately extracted, weighed, and stored at -70°C until further analysis. The brains were dissected into 200µm sections using a Leica CM1520 cryostat. Anatomical structures (optic tract to the infundibular stem; Bregma -2.12mm to -3.80mm) were used to isolate the medio-basal hypothalamus (MBH), DMH and PVN. Bilateral tissue punches were performed using an integra Miltex 1mm disposable biopsy punch. Tissue punches were stored at -80°C until further analysis.

2.4.3 Open Field Test

Animals were subject to an open field test (OFT). The open field test consisted of a $1m^2$ box subdivided into 25 $20cm^2$ sections. Siberian hamsters were placed in the centre of the box and their activity was recorded over a 5-minute period. After 5 minutes the animals were removed from the box. Videos of each animal were then reviewed, and the following was recorded; line crossings, rearing, grooming events, time sent in the central region of the box. Scoring of videos was very kindly carried out by Ms Fallon Cuthill from the University of Glasgow.

2.4.4 Blood Chemistry Analyses

Terminal trunk blood was collected in tubes containing 30µl heparin and assessed for blood glucose. Blood glucose was assessed using an Accu-check performa nan0 blood glucose meter. Plasma was separated from blood by spinning at 7000 RPM at 4°C in a fresco 21 microcentrifuge (thermofisher). Analysis of plasma insulin as very kindly carried out by an external collaborator Dr Jo Edward Lewis at the University of Cambridge.

2.4.5 RNA Extraction

RNA was extracted from Siberian hamster tissues using the RNeasy Plus Mini Kit (Qiagen). Punched tissue samples were submerged in 600µl buffer RLT plus (Qiagen) and homogenised using a Polytron PT 1200 E. Lysate centrifuged for 3 minutes at 12,000 RPM, eluate removed and transferred to a gDNA eliminator column. DNA elimination was achieved by spinning the column for 30 seconds at 10,000 RPM, column flow through retained. 70% molecular grade ethanol prepared and 600µl added to each sample. 700µl of sample added to a RNEasy spin column and spun for 15 seconds at 10,000 RPM. 700µl of buffer RW1 added to the column and spun for 15 seconds at 10,000 RPM. 500µl of buffer RPE added to the column and spun for 15 seconds at 10,000 RPM. A further 500µl of buffer RPE added to the column and spun for 2 minutes at 10,000 RPM. The Spin column was placed in a collection tube and 30µl nuclease free water (Millipore) added to the column. Column spun for 1 minute at 10,000 RPM to eluate RNA. RNA quantity and quality was determined using an ND-1000 Nandorop spectrophotometer (Thermofisher Scientific).

2.4.6 Seasonal Transcriptome Sequencing

Pituitary RNA was then transformed into cDNA using either the direct cDNA sequencing kit (SQK-DCS109; Oxford Nanopore) and then sequenced following the manufacturer's instructions (SQK-DCS109 with EXP-NBD104; Oxford Nanopore). Briefly, 100ng of extracted RNA was made up to 7.5µl using nuclease free water (millipore) and added to 2.5µl VNP (Oxford Nanopore) and 1µl dNTP mix (NEBnext technologies). The tube was mixed, spun and incubated at 65°C for 5 minutes in a SimpliAMP thermal cycler (Applied Biosystems) and then snap cooled in a cold block. A strand switching mixture consisting of 4µl 5X RT Buffer (from Maxima H Minus Reverse Transcriptase Kit), 1µl RNaseOUT (Invitorgen), 2µl

Strand Switching Primer (Oxford Nanopore) and 1µl RNAse free water (Millipore). The sample was incubated at 42°C for 2 minutes. 1µl of Maxima H Reverse Transcriptase was added (Invitrogen). The tube was mixed and spun briefly then incubated in sequence at 42°C for 90 minutes, 85°C for 5 minutes and finally held at 4°C until further processing. 1µl of RNAse cocktail mix (Thermofisher) was added to the sample and it was incubated at 37°C for 10 minutes. 17µl of AMPure XP beads was added to the reaction and it was incubated for 5 minutes at room temperature on a roller mixer (Stuart SRT6D). Fresh 70% Ethanol (Fisher Bioreagents) was prepared, and samples were spun down. The samples were placed on a magnetic particle concentrator (Dynal MPC-M (120.09)), until magnetic beads had pelleted. Supernatant was removed and the beads were washed twice with 70% ethanol. The pellet was spun, and remaining ethanol was removed. The pellet was resuspended in 20µl nuclease free water (Millipore) and incubated for 10 minutes at room temperature on the roller mixer. The beads were pelleted on the magnetic particle concentrator and the eluate was removed and retained. The eluate was added to with 25µl LongAmp Taq Mastermix (NEBnext), 2µl PR2 Primer (Oxford Nanopore) and 3µl nuclease free water (Millipore). The samples were incubated in sequence; 94°C for 1 minute, 50°C for 1 minute, 65°C for 15 minutes and held at 4°C until further processing. 40µl of resuspended AMPure XP beads were added to the reaction and incubated at room temperature for 5 minutes on a roller mixer. Fresh 70% Ethanol (Fisher Bioreagents) was prepared, and samples were spun down. The samples were placed on a magnetic particle concentrator (Dynal MPC-M (120.09)), until magnetic beads had pelleted. Supernatant was removed and the beads were washed twice with 70% ethanol. The pellet was spun, and remaining ethanol was removed. The pellet was resuspended in 21µl nuclease free water (Millipore) and incubated for 10 minutes at room temperature on the roller mixer. The beads were pelleted on the magnetic particle concentrator and the eluate was removed and retained. 1µl of eluate was analysed for quality and quantity on a ND-1000 Nandorop spectrophotometer (Thermofisher Scientific). An end-prep reaction mixture was prepared as follows; 20µl of prepped cDNA, 30µl of nuclease free water (Milipore), 7µl Ultra II end prep reaction buffer (NEBnext) and 3µl Ultra II End-prep enzyme mix (NEBnext). The reaction was incubated at 20°C for 5 minutes and at 65°C for 5 minutes. 60µl of AMPure XP beads were added to the mixture and it was incubated for 5 minutes at room temperature

on a roller mixer (Stuart SRT6D). Supernatant was removed and the beads were washed twice with 70% ethanol. The pellet was spun and remaining ethanol was removed. The pellet was resuspended in 22.5µl nuclease free water (Millipore). The reaction was incubated for 2 minutes at room temperature and then pelleted on the magnetic particle concentrator and the eluate was removed and retained. A reaction mixture was prepared as follows; 22.5µl cDNA, 2.5µl appropriate barcode (Oxford Nanopore) and 25µl blunt/ta ligase master mix (NEBnext) and incubated at room temperature for 10 minutes. 50µl AMPure XP beads were added to the mixture and incubated at room temperature for 5 minutes on a roller mixer (Stuart SRT6D). Sample was spun and supernatant was removed, and the beads were washed twice with 70% ethanol. The pellet was spun, and remaining ethanol was removed. The pellet was resuspended in 26µl nuclease free water (Millipore). Barcoded samples from each run were pooled at this stage to a total of 65µl such that each barcoded sample has equal concentration. For adapter ligation a reaction mixture was prepared; 65µl pooled barcoded cDNA, 5µl Adapter mix II (Oxford Nanopore), 20µl quick ligation reaction buffer (NEBnext) and 10µl quick T4 DNA ligase (NEBnext). The reaction was incubated for 10 minutes at room temperature. 50ul of AMPure XP beads were added to the reaction and incubated for 5 minutes on a roller mixer. Beads were pelleted on a magnetic concentrator and washed twice with 140µl wash buffer (Oxford Nanopore). Pellet resuspended in 13µl elution buffer (Oxford Nanopore) and incubated for 10 minutes at room temperature. Beads pelleted on a magnetic concentrator and eluate removed and retained. Eluate contained the prepared sequencing library and was loaded on an oxford nanopore SpotON flow cell.

MBH, VMH and DMH RNA was transformed into cDNA using the PCR-cDNA Barcoding kit (SQK-PCB109; Oxford Nanopore) and then sequenced following the manufacturer's instructions. Briefly, A total of 50ng RNA was added to 1µl VN primer (2 µM) (Oxford Nanopore) and 1µl dNTP mix (NEBnext technologies) and made up to 11µl with RNAse free water (Millipore). The tube was mixed, spun, and incubated at 65°C for 5 minutes in a SimpliAMP thermal cycler (Applied Biosystems) and then snap cooled in a cold block (Eppendorf). A strand switching mixture consisting of 4µl 5X RT Buffer (from Maxima H Minus Reverse Transcriptase Kit), 1µl RNaseOUT (Invitorgen), 2µl Strand Switching Primer (Oxford Nanopore)

and 1µl RNAse free water (Millipore). The sample was incubated at 42°C for 2 minutes. 1µl of Maxima H Reverse Transcriptase was added (Invitrogen). The tube was mixed and spun briefly then incubated in sequence at 42°C for 90 minutes, 85°C for 5 minutes and finally held at 4°C until further processing. A reaction containing 5µl of sample, 1.5µ of the appropriate barcode primer (Oxford Nanopore), 18.5µl of Nucleus Free water (Millipore) and 25µl 2X LongAMP Taq Mastermix (NebNext). The sample was amplified by incubating in sequence; at 95°C for 30 seconds, 14 cycles of (95°C for 15 seconds, 62°C for 15 seconds, 65°C for 10 minutes), at 65°C for 6 mins, held at 4°C until further processing. 1µl of Exonuclease 1 (NEBnext) was added and mixed by pipetting. The sample was incubated in sequence at 37°C for 15 minutes followed by 80°C for 15 minutes. 40µl of resuspended AMPure XP beads were added to the sample and it was incubated for 5 minutes at room temperature on a roller mixer (Stuart SRT6D). Fresh 70% Ethanol (Fisher Bioreagents) was prepared, and samples were spun down. The samples were placed on a magnetic particle concentrator (Dynal MPC-M (120.09)), until magnetic beads had pelleted. Supernatant was removed and the beads were washed twice with 70% ethanol. The pellet was spun, and remaining ethanol was removed. The pellet was resuspended in 12µl of elution buffer (Oxford Nanopore) and incubated at room temperature for 10 minutes on a roller mixer. The beads were pelleted on the magnetic particle concentrator and the eluate was removed and retained. The eluate was analysed for quality and quantity on a ND-1000 Nandorop spectrophotometer (Thermofisher Scientific). 100ng of this made up to 11µl using elution buffer (Oxford Nanopore), this contained the prepared sequencing library and was loaded on an oxford nanopore SpotON flow cell.

Multiplexed sequencing libraries were run on SpotON flow cells. Briefly, a priming mix was prepared by adding 30µl flush tether to a flush buffer tube. A SpotON flow cell was primed by adding 200µl priming mix, incubating for 5 minutes and then adding 800µl priming mix. A running mixture was prepared containing; 37.5µl Sequencing Buffer, 25.5µl loading beads and 12µl sequencing library. The running mixture was added to the SpotON flow cell. All sequencing was carried out onboard a Minion Mk1B sequencing device (Oxford Nanopore) at -180mV using the Minknow software (Oxford Nanopore Technologies).

2.4.7 cDNA Synthesis and qPCR

RNA was transformed into cDNA for qPCR analysis using superscript III (Invitrogen). A mastermix was prepared containing, per sample; 2µl 5X first strand buffer (Invitrogen), 1µl DTT (Invitrogen), 0.2µl Random Primers (Promega), 0.2µl dNTP mix (as prepared), 0.26µl RNase block (Agilent), 0.26µl reverse transcriptase enzyme (Invitrogen), 2.08µl nuclease free water (Millipore). 6µl of this mastermix was combined with 4µl RNA (total 200ng). Quantification of transformed cDNA was achieved using Brilliant II SYBR Mastermix (Agilent). Stock forward and reverse primers (100pmol/µl) were mixed and diluted in nuclease free water to 20pmol/µl. A working SYBR mixture was prepared by mixing 1-part primer mixture per 24-part SYBR mastermix. Reaction mixtures were prepared in wells on a 96-well plate by mixing 4.8µl of normalised sample and 4.8µl of SYBR working mix. All reactions were performed in duplicate. qPCR reactions were carried out in a Stratagene Mx3000P thermal cycler. Cycling conditions utilised were in sequence; at 95°C for 5 minutes (denaturing), 40 cycles at (95°C for 30 seconds, X°C for 1 minute – see table 2-1, 72°C for 30 seconds with fluorescent measurement at end), 95°C for 1 minute, 55°C for 30 seconds increasing to 95°C (Melt curve analysis). Melt cure analysis was used to determine specificity of amplification. Data was analysed for meanCT, efficiency and variability using PCR Miner (Zhao and Fernald, 2005).

Gene	Forward Primer	Reverse Primer	Temp (°C)
Prl	TCCGGAAGTCCTTCTGAACC	CGCAGGCAGCGAATCTTATTG	60
Gh	ACCTACAAAGAGTTTGAGCGTG	ATGAGCAGCAGCGAGAATCG	58
bactin	CTGGAACGGTGAAGGTGACA	AAGGGACTTCCTGTAACAATGCA	60

Table 2-1: Primer sets used in qPCR.

2.4.8 Analysis of Sequencing Reads

Raw reads (Fast5) were demultiplexed and basecalled using guppy basecaller. Porechop was used to remove adapters from reads and Filtlong was used to filter for long reads (>25 base pairs). Transcripts were aligned to *Mus musculus* genome (GRCm39) using Minimap2. Previously, rodent genomes have been

demonstrated to show significant similarity, such that cross-species transcriptomic analysis appears feasible (Ernst et al., 2006). Transcript expression levels were generated using Salmon and EdgeR was used to normalise and detect differential expression. To identify seasonal rhythmic expression of transcripts, we selected differentially expressed genes identified by EdgeR ($P<0.05$). Data were analysed using non-linear regression for rhythmicity using the online resource BioDare 2.0 (Zielinski et al., 2014) (biodare2.ed.ac.uk). The empirical JTK_CYCLE method was used for detection of rhythmicity and the classic BD2 waveform set was used for comparison testing. Rhythmicity was determined by a Benjamini-Hochberg controlled false discovery rate (BH corrected FDR < 0.1). Data for heatmaps were clustered using PAM clustering from the cluster package (Maechler, 2019). The number of clusters present within the data was identified using gap statistic-analysis. Heatmaps were created using the Complexheatmaps package (Gu et al., 2016). GeneMANIA was used for predicting interactions between differentially expressed transcripts (Warde-Farley et al., 2010). Gene ontology analysis was carried out using ShinyGO v0.77 (Ge et al., 2020).

2.4.9 Transcription Factor Enrichment

To identify changes in transcription factor activity which could explain the observed changes in gene expression data, the online tool ChIP-X Enrichment analysis 3 (ChEA3) was used. ChEA3 collates many experimental data, such as transcription factor-gene co-expression studies and chip-seq experiments to generate a comprehensive tool for comparing user submitted gene lists and generating transcription factor enrichment lists. The tool is also capable of identifying known interactions between transcripts within this list (Keenan et al., 2019). Significantly rhythmic gene lists from each of the regions sequenced were submitted to this online tool and was used to generate enriched transcription factor lists and transcription factor interaction networks for each region.

2.4.10 Statistics

Physiological and qPCR data sets was tested for normality using the Shapiro test and transformed by log transformation is normality was violated. Statistical significance was determined using a two-way ANOVA. Post hoc analysis of

significant data was achieved by t-test. Type 1 error was minimised by utilising the Bonferroni adjustment on post-hoc analyses. The empirical JTK cycle used to determine and characterise rhythmicity in genome scale data sets. Initially the JTK cycle was developed as a method to study the oscillations in large circadian data sets. It is based off the Jonckheere-terpstra non-parametric test and the Kendall's tau, which computes the Kendall rank between a data set provided and a range of reference data sets. By utilising a set of known reference waveforms with known periods, phases and amplitudes, JTK cycle can compute the rhythmicity and phases of an experimental data set (Hughes et al., 2010). The false discovery rate of this data set was controlled by applying the benjamini-hochberg method (Benjamini and Hochberg, 1995). Clusters within the data set were identified using the gap-statistic and clustered using k-means clustering. Quantification of behavioural was completed in-part by one rater and in-whole by another. To minimise observer biases and demonstrate a high inter-rater reliability, a two-way random effects intraclass correlation coefficient (ICC) was performed. The ICC is a widely utilised rater reliability index (Koo and Li, 2016). Guidelines for ICC interpretation indicate that scores may be grouped into bands of <40 (poor), .41-.59 (fair), .60-.74 (good) and .75 -1.00 (excellent) (Cicchetti, 1994). All tested measurements in this data scored either good or excellent for consistency. The results of ICC testing can be seen in table 2-2.

Open Field Test	**ICC**	**Interpretation**
Grooming	1	Excellent
Total lines crossed	0.79	Excellent

Table 2-2: ICC results from open field test.

2.5 Results

2.5.1 Rheostatic Change in Physiology is Dynamic Through the Seasonal Waveform

Over the seasonal waveform, body mass was significantly decreased by exposure to short photoperiod ($F = 7.481_{1, 8}$; $p < 0.05$) (fig. 2-1a). Exposure to short photoperiod significantly decreased epididymal white adipose tissue mass ($F = 25.266_{1, 8}$; $p < 0.001$) (fig. 2-1b), kidney mass ($F = 4.487_{1, 8}$; $p < 0.001$) (fig. 2-1c) and testes mass ($F = 25.955_{1, 8}$; $p < 0.001$) (fig. 2-1d) However, spleen mass was not affected by exposure to short photoperiod ($F = 0.42_{1, 8}$; $p > 0.05$) (fig. 2-1e). Exposure to short photoperiod reduced testis width ($F = 13.388_{1, 8}$; $p < 0.001$) (fig. 2-1f) and length ($F = 25.976_{1, 8}$; $p < 0.001$) (fig. 2-1g). Body temperature was significantly decreased across the seasonal waveform at the sweat gland ($F = 7.292_{1, 8}$; $p < 0.001$) (fig. 2-1h) and at the paw ($F = 3.751_{1, 8}$; $p < 0.001$) (fig. 2-1i). Bonferroni adjusted post hoc analyses of these revealed that of the physiological factors affected by photoperiod, followed a pattern of immediate reduction followed by spontaneous reversal. Body mass significantly decreased by 4 weeks and recovered by 24 weeks. eWAT mass decreased significantly by 8 weeks and recovered by 28 weeks. Kidney mass decreased by 4 weeks and recovered by 28 weeks. Testes mass significantly decreased by 4 weeks and recovered to long day levels by 28 weeks. Testes width decreased by 4 weeks and recovered by 28 weeks of exposure, however showed a further significance from LD by 32 weeks. Testes length decreased by 4 weeks and recovered by 28 weeks. Sweat gland temperature significantly decreased by 12 weeks and recovered by 32 weeks of exposure. Paw temperature was significantly decreased only at 16 weeks of short photoperiod exposure.

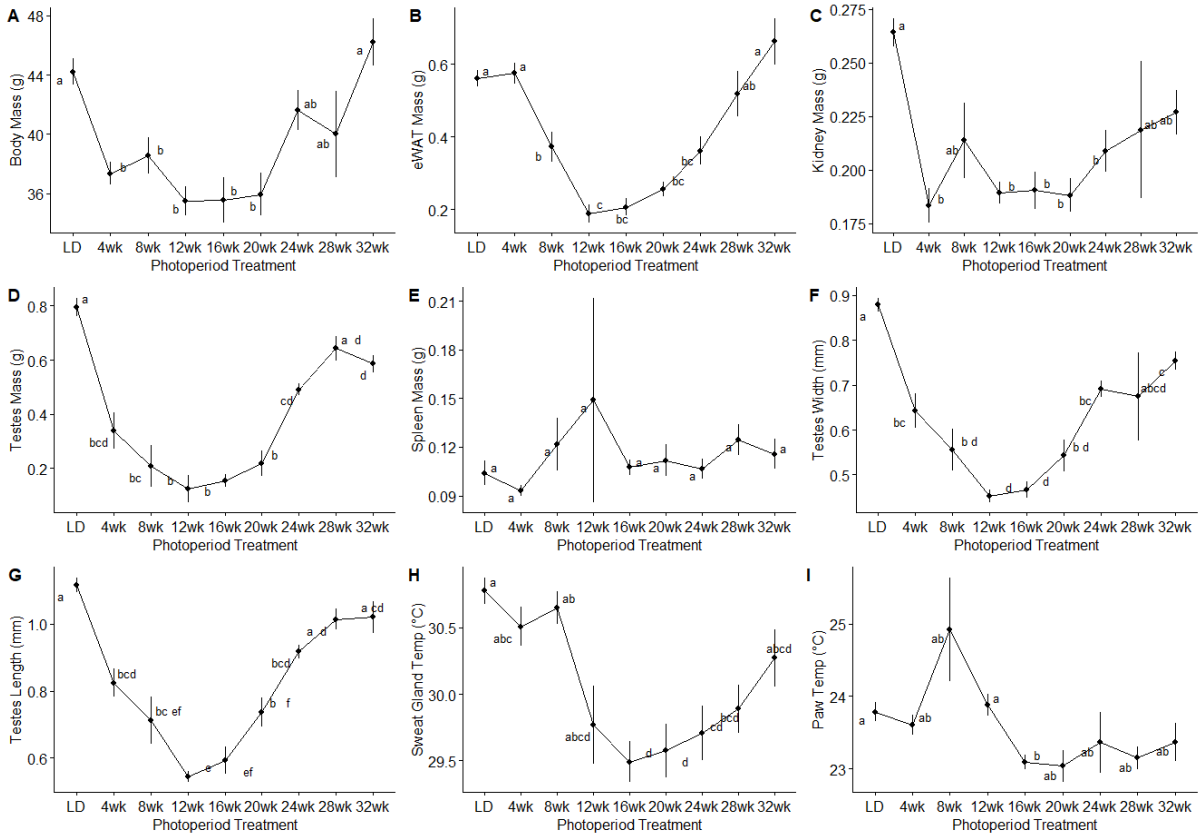

Figure 2-1: Physiological indicators of Siberian hamsters (n = 99) across the seasonal waveform. Hamster were measured from a long photoperiod (LD) condition (n = 14) or from short photoperiod after 4 weeks (n = 10), 8 weeks (n = 10), 12 weeks (n = 11), 16 weeks (n = 11), 20 weeks (n = 12), 24 weeks (n = 10) 28 weeks (n = 10) or 32 weeks (n = 11). Hamster body mass (A), eWAT mass (B), Kidney mass (C), Testes mass (D), Spleen mass (E), Testes Width (F), testes length (G), Sweat gland temperature (H) and paw temperature (I). Data shown is mean ± SEM. Lettering indicates significance groupings by Bonferroni adjusted t-test ($P < 0.05$).

2.5.2 Short photoperiod Exposure Drives a Transient and Biphasic increase in Locomotor Activity

In the open field test, there was no significant effect of photoperiod on total number of grooming events($F = 1.904_{8, 90}$; $p = 0.069$) (fig. 2-2a). This does represent a trend to increased grooming activity in SD exposed hamsters. Short photoperiod drove a significant waveform in total line crossings ($F = 2.465_{8, 90}$; $p < 0.05$) (fig. 2-2b). Post hoc analysis of total line crossings revealed a biphasic pattern of significance within the data set, with significant increases in line crossings occurring at 24 weeks relative to LD control animals ($P = 0.032$).

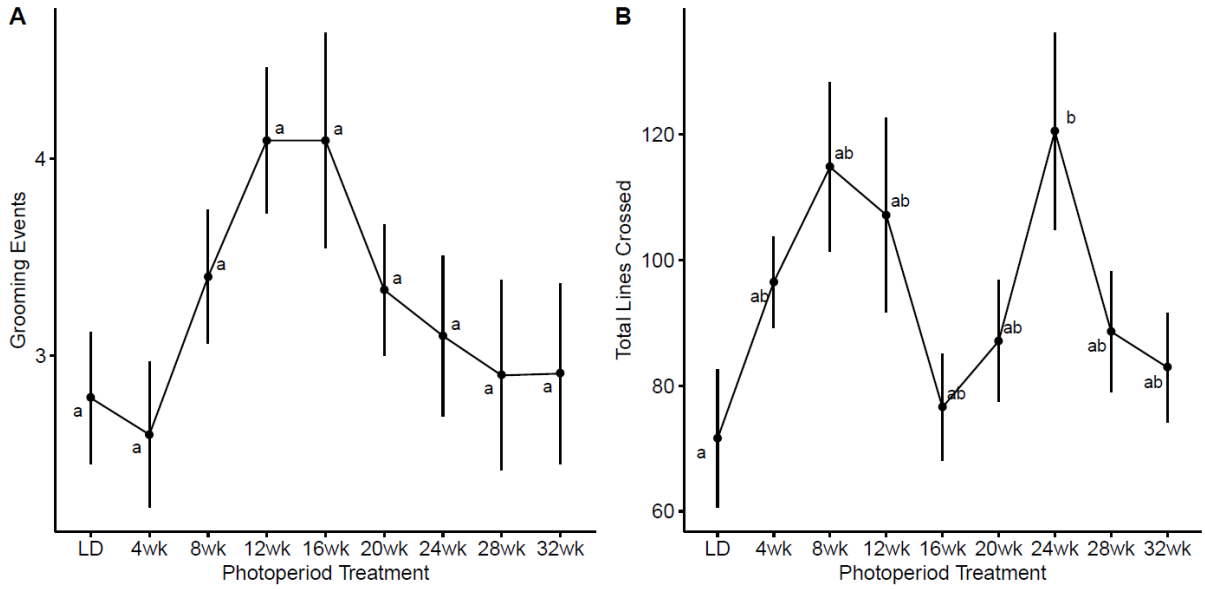

Figure 2-2: Behavioural data of Siberian hamsters (n = 99) across the seasonal waveform. Hamster were measured from a long photoperiod (LD) condition (n = 14) or from short photoperiod after 4 weeks (n = 10), 8 weeks (n = 10), 12 weeks (n = 11), 16 weeks (n = 11), 20 weeks (n = 12), 24 weeks (n = 10) 28 weeks (n = 10) or 32 weeks (n = 11). (A) Grooming events and (B) total line crossings were assessed using an open field test. Data shown is mean ± SEM. Lettering indicates significance groupings assessed by Bonferroni adjusted t-test.

2.5.3 Blood Chemistry

Blood glucose was not significantly affected by exposure to short photoperiod ($F = 1.704_{8, 45}$; $p > 0.05$) (fig. 2-3a). Plasma insulin decreased upon exposure to short days ($F = 8.37_{8, 19}$; $p < 0.001$) (fig. 2-3b). Bonferroni post-hoc analysis was not able to detect significant differences between individual groups (fig. 2-3b).

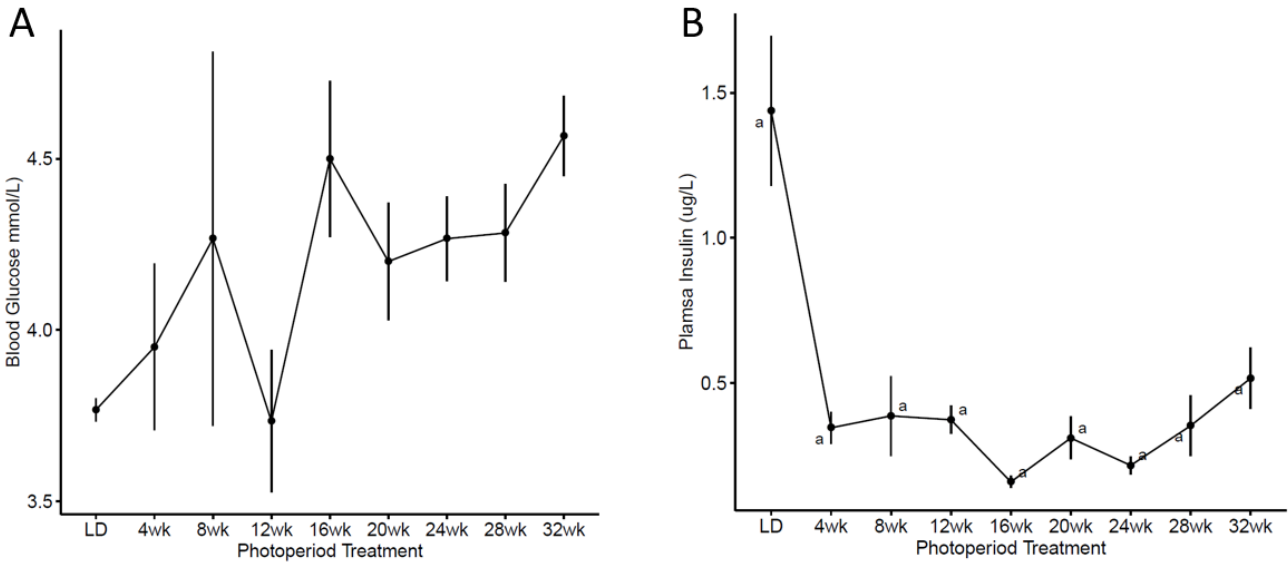

Figure 2-3: Blood chemistry data of Siberian hamsters (n = 99) across the seasonal waveform. Blood glucose (A) and plasma insulin (B) were assessed from terminal trunk blood. Data shown is mean ± SEM. Lettering indicates significance groupings, assessed by Bonferroni adjusted t-test ($P < 0.05$).

2.5.4 Quality Control Information of Sequencing Reads

In the medio-basal hypothalamus, the average number of transcript reads per sample was 779,045. The mean quality value per sample was 20. The mean n50 of sequencing length was 1,256. In the pituitary sequencing, the average number of reads per sample was 108,877. The mean quality value per sample was 19. The mean n50 of sequencing length was 1,733. In the dorsomedial nucleus, the average number of transcript reads per sample was 596,894. The mean quality value of dorsomedial sequencing reads was 20. The mean n50 of dorsomedial sequencing read lengths was 671. In the paraventricular nucleus, the average

number of transcript reads per sample was 499,322. The mean quality value of paraventricular sequencing reads was 21. The mean n50 of paraventricular sequencing read lengths was 1,111.

2.5.5 Validation of Sequencing Results by qPCR

A select number of transcripts identified from the sequencing data were analysed using qPCR to provide a cross-technique validation of sequencing using more traditional methods. Transcripts investigated were *gh* and *prl*. *Prl* was expression was significantly decreased by exposure to short photoperiod (fig. 2-4a). *Prl* expression was initially decreased after exposure to short photoperiod but recovered to initial levels after 24 weeks of short photoperiod exposure. *Gh* exposure was not significantly altered by exposure to short photoperiod (fig. 2--4b).

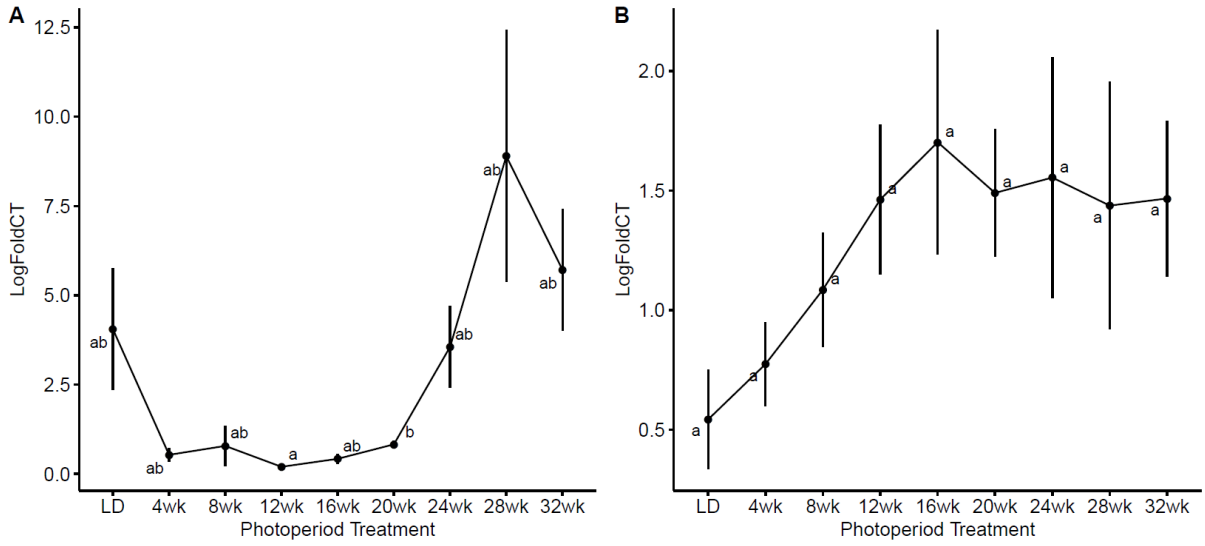

Figure 2-4: qPCR from Siberian hamsters (n = 54) collected after 0 (= 6), 4 (n = 6), 8 (n = 6), 12 (n = 6), 16 (n = 6), 20 (n = 6), 24 (n = 6), 28 (n = 6) or 32 (n = 6) weeks of short photoperiod exposure. *Prl* (A) and *Gh*(B) logfold expression was assessed by qPCR and normalised against bactin expression. Data shown is mean ± SEM. Lettering indicates significance groupings, determined by Bonferroni adjusted t-test (P< 0.05)

2.5.6 Pituitary Transcriptome Sequencing

A total of 250 genes were detected as significantly rhythmic within the pituitary sequencing data set. Analysis of the top 100 significantly rhythmic genes by gap-statistic analysis indicated the existence of 14 clusters (K-means) within the data set. The top 100 clustered z-scores were then plotted on a heatmap (fig. 2-5a), revealing a very diverse range of expression patterns from the pituitary. Principal component analysis (PCA) of this data set reveals that, of the groups many clusters closely together indicating very similar expression across the waveform (fig. 2-5b). Gene ontology analysis revealed a number of enriched GO terms associated with rhythmic transcripts (fig. 2-6a-c). Analysis of the position of rhythmic genes on the reference genome (*Mus musculus*) did not reveal any spatial significance, with significant genes distributed across chromosomes (fig. 2-6d). Within this sequencing was a number of genes which were anticipated to change with photoperiod exposure. The strongly seasonal gene prolactin was the most significant rhythmic gene and possesses the anticipated waveform (fig. 2-7a). Other pars distalis transcripts were detected in this sequencing run but were not significantly rhythmic, such as growth hormone (fig. 2-7b) and pro-opiomelanocortin (fig. 2-7c). In addition to this several novel genes were rhythmic throughout the seasonal waveform. The mucolipin TRP cation channel 1, *mcoln1*, shows a very similar pattern of expression to that of prolactin (fig. 2-7d). Many of the other rhythmic transcripts, however, display a pattern of expression very different to that of prolactin, such as fucosyltransfer-8 (*fut8),* which rises over the seasonal waveform (fig. 2-7e). Another major example of a gene with this pattern of expression is *cwc15* (fig. 2-7f).

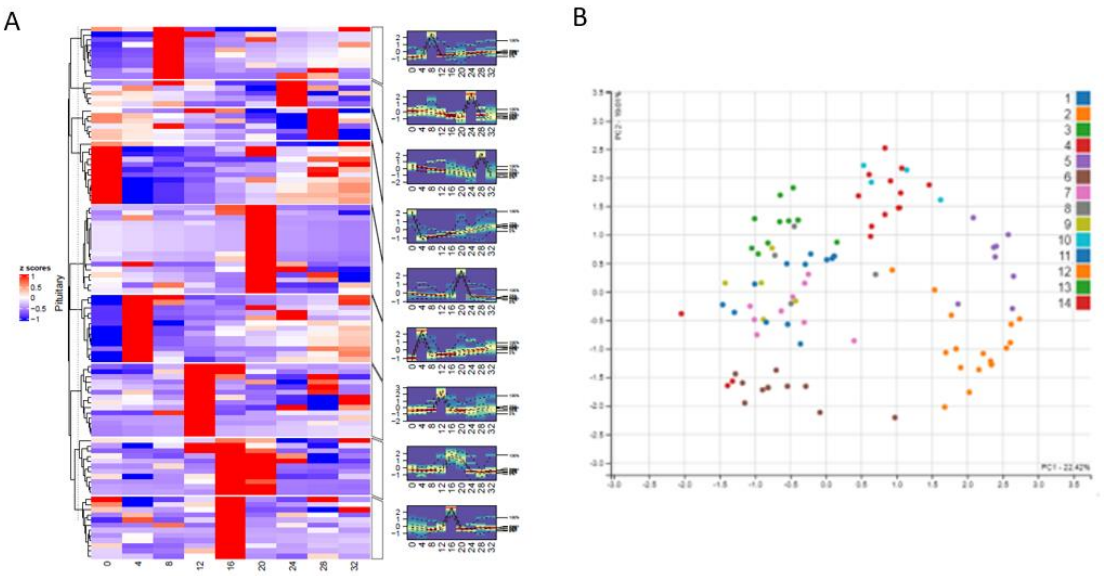

Figure 2-5: The grouping of sequencing data from seasonal Siberian hamster pituitaries. (A) heatmap of the top 100 seasonal transcripts clustered by k-means clustering and associated density heatmaps. (B) Grouped PCA plot of significantly rhythmic genes from Siberian hamster pituitary sequencing.

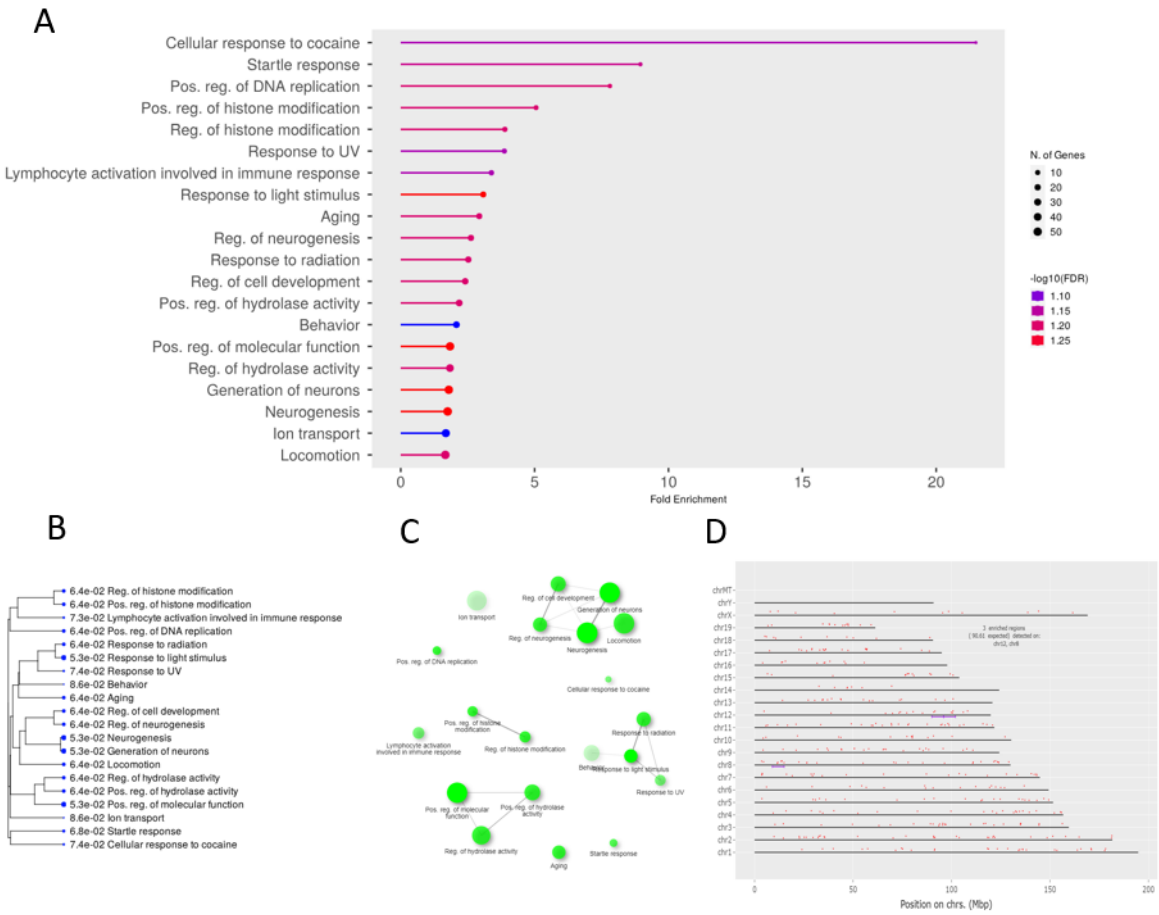

Figure 2-6: Gene ontology analysis of Siberian hamster pituitary sequencing. (A) Enriched terms detected using significantly rhythmic transcripts. (B) A hierarchical clustering tree displaying correlation between enriched pathways. (C) A node plot showing relationship between enriched terms, terms are joined if they share >20% transcripts. (D) Genomic location of significantly enriched transcripts based on *mus musculus* genome. Plot was produced using ShinyGO 0.77.

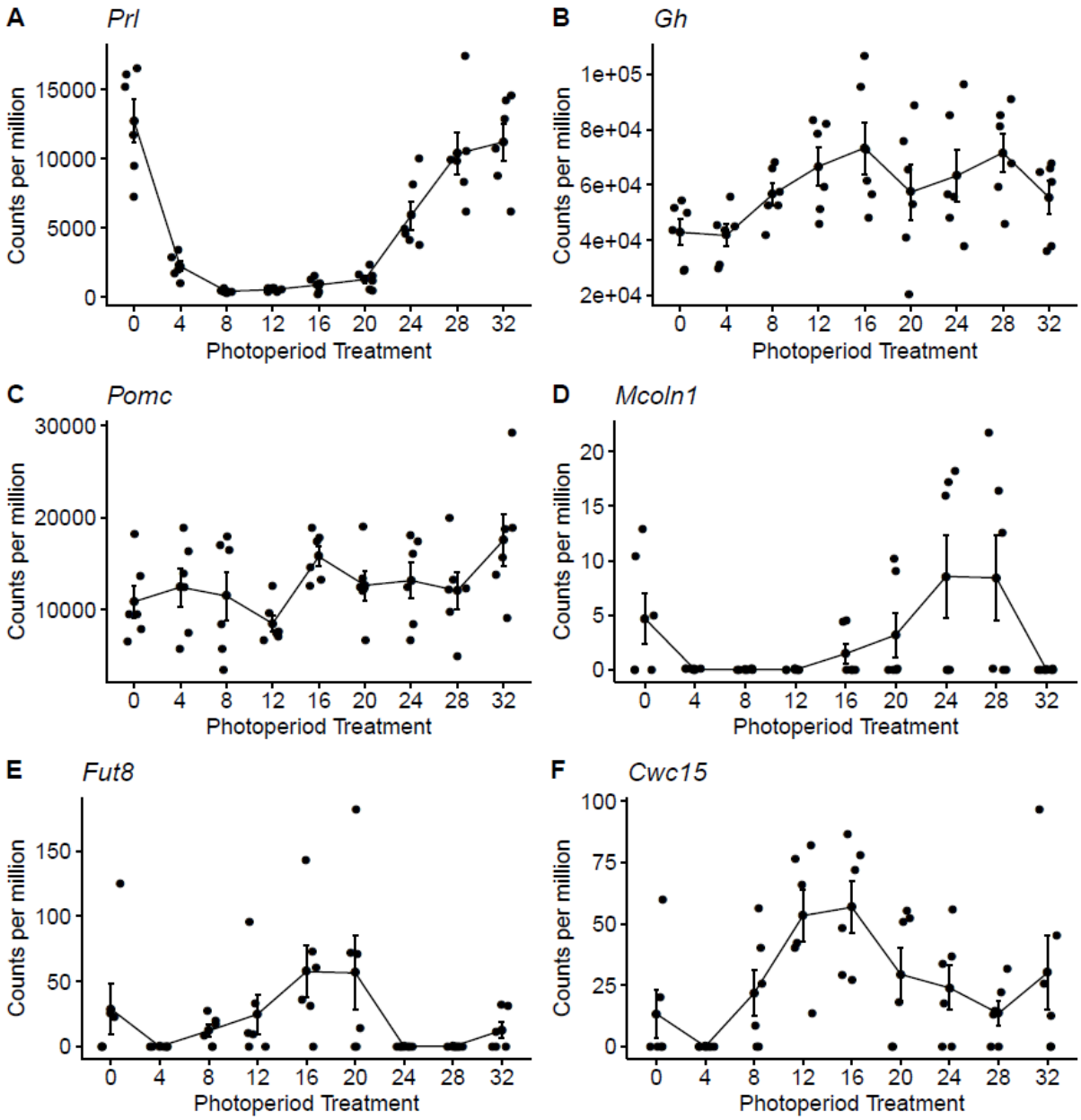

Figure 2-7: Seasonally rhythmic genes from pituitary sequencing from Siberian hamsters (n = 54) collected after 0 (n = 6), 4 (n = 6), 8 (n = 6), 12 (n = 6), 16 (n = 6), 20 (n = 6), 24 (n = 6), 28 (n = 6) or 32 (n = 6) weeks of short photoperiod exposure. Transcripts shown are *Prl* (A), *Gh* (B), *Pomc* (C), *Mcoln1* (D), *Fut8* (E) and *Cwc15* (F). Data shown is mean ± SEM. Points represent individual data points. Star indicates transcript is significant by empirical JTK test (FDR < 0.1)

2.5.7 Medio-basal Hypothalamus Sequencing

In the MBH a total of 290 transcripts were identified to be rhythmic throughout the seasonal waveform. Gap-statistic analysis of the rhythmic gene set from the arcuate revealed the presence of 10 clusters within the data. A heatmap of the z scores of the expression of rhythmic genes reveals the diversity in expression patterns observed across the seasonal waveform (fig. 2-8a). Several clusters display peaks at certain time points in the seasonal waveform, while others display rhythmic changes in expression across the entire waveform. A clustered PCA plot of the transcripts from the seasonal waveform reveals that many of the seasonal genes of interest (e.g., *tshb* and *dio3*) are present in very different clusters (fig. 2-8b). Further it reveals that many of the groups identified are very closely clustered, suggesting very similar seasonal expression. Gene ontology analysis of these transcripts revealed several enriched terms (FDR < 0.1) (fig. 2-9a-c). Analysis of the position of rhythmic genes on the reference genome (*Mus musculus*) did not reveal any spatial significance, with significant genes distributed across chromosomes (fig. 2-9d). Of the genes which were detected several known seasonal genes were identified which granted confidence over the specificity of the punches and of the photoperiod manipulation, such as *tshb* (fig. 2-10a), Glycoprotein Hormones, Alpha Polypeptide (*cga)* (fig. 2-10b) and *dio3* (fig. 2-10c). The pattern of expression these genes demonstrated was similar to data that has previously been reported for these genes (Milesi et al., 2017). The sequencing also unveiled novel seasonal genes such as *mef2c* (fig. 2-10d), which demonstrated a similar pattern of expression as *dio3*. The only significant energy balance related transcript was somatostatin (fig. 2-10e). A major structural component of tanycyte projections, vimentin, was downregulated under short photoperiod (fig. 2-10f) and did not recover to long-day like levels. The melatonin receptive orphaned g-protein coupled receptor *gpr50* also showed seasonal regulation (fig. 2-10g). Heat shock proteins and retinol-binding proteins were among the enriched terms (fig. 2-10a) and the genes heat shock protein b7 (*hspb7)* (fig. 2-10h) and retinol binding protein 1 (*rbp1*) (fig. 2-10i) are representatives of these groups.

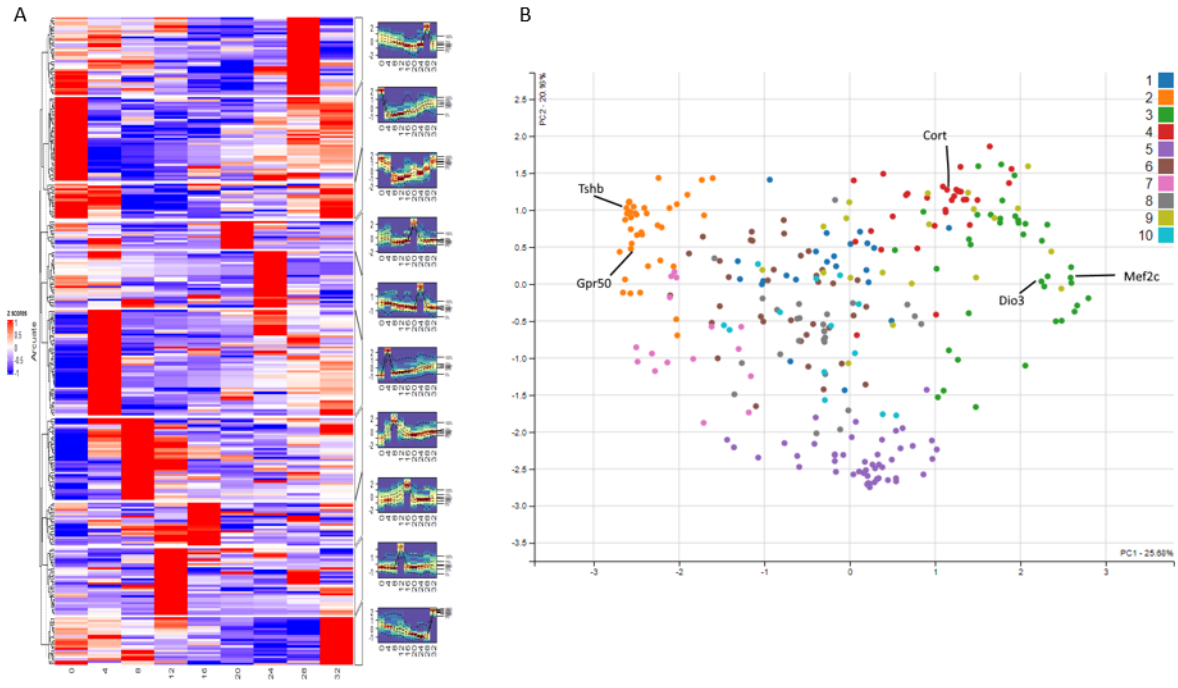

Figure 2-8: Overview of sequencing from the MBH of Siberian hamsters. (A) clustered heatmap of transcripts from the arcuate nucleus, corresponding density heatmaps for each cluster are shown to the left. (B) Clustered PCA plot of rhythmic transcripts.

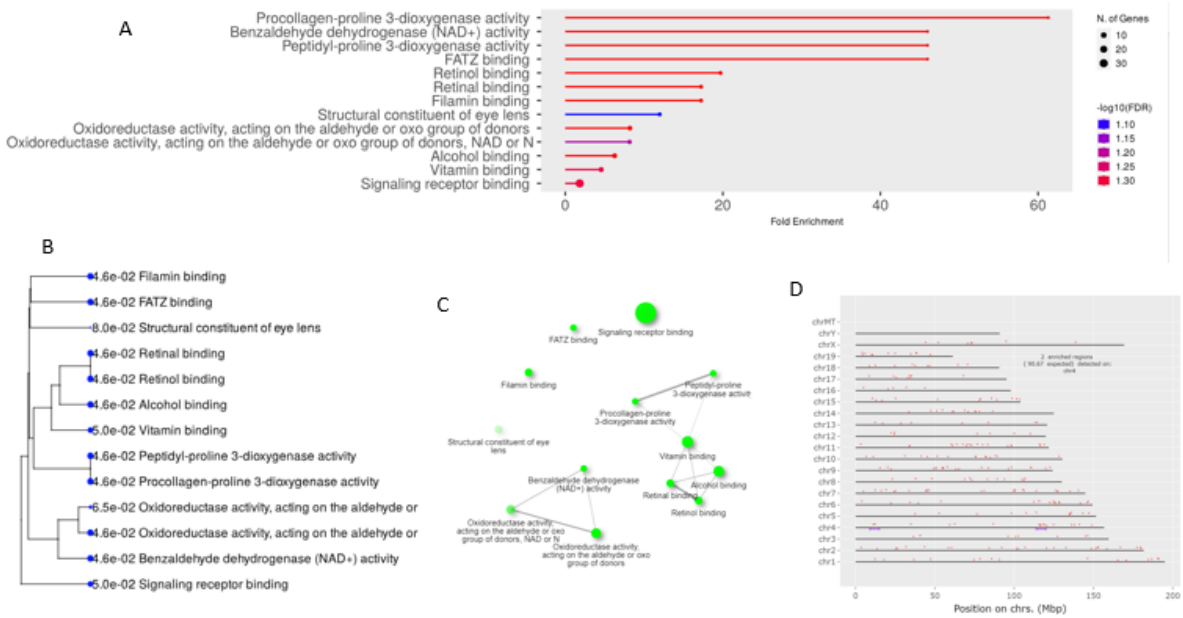

Figure 2-9: Gene ontology analysis of Siberian hamster medio-basal hypothalamus nucleus sequencing. (A) Enriched terms detected using significantly rhythmic transcripts. (B) A hierarchical clustering tree displaying correlation between enriched pathways. (C) A node plot showing relationship between enriched terms, terms are joined if they share >20% transcripts. (D) Genomic location of significantly enriched transcripts based on *Mus musculus* genome. Plot was produced using ShinyGO 0.77.

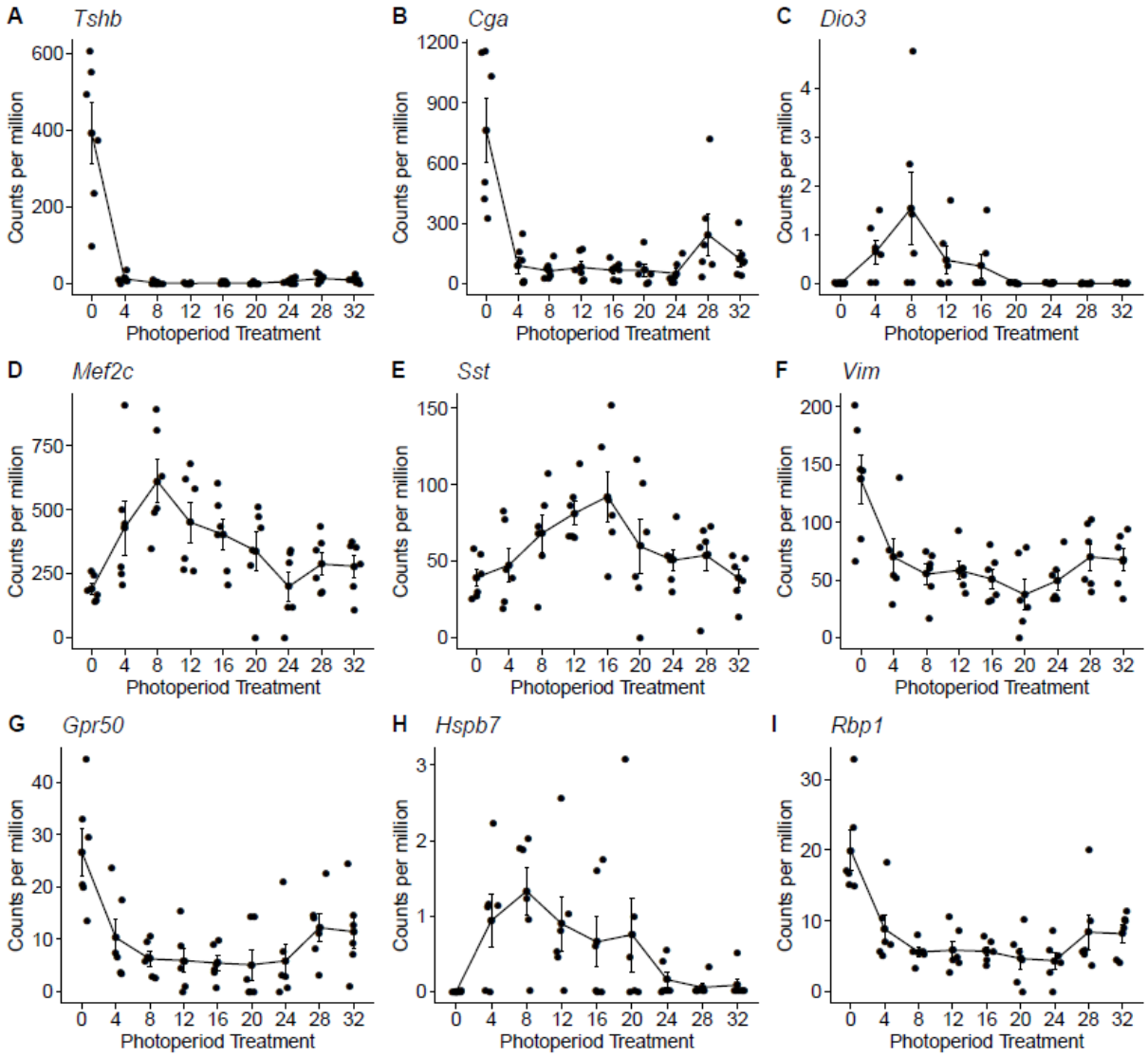

Figure 2-10: Seasonally rhythmic genes from medio basal hypothalamic sequencing from Siberian hamsters (n = 54) collected after 0 (n = 6), 4 (n = 6), 8 (n = 6), 12 (n = 6), 16 (n = 6), 20 (n = 6), 24 (n = 6), 28 (n = 6) or 32 (n = 6) weeks of short photoperiod exposure. Transcripts included are *Tshb*(A), *Cga*(B), *Dio3*(C), *Mef2c* (D), *Sst*(E), *Vim*(F), *Gpr50*(G), *Hspb7*(H) and *Rbp1*(I). Data shown is mean ± SEM. Points represent individual data points. All transcripts shown are significant by empirical JTK test (FDR < 0.1)

2.5.8 Paraventricular Nucleus Sequencing

In the PVN, a total of 374 genes were identified to be rhythmic throughout the seasonal waveform. Gap-statistic analysis revealed that there were 12 unique clusters within the data. A heatmap of this clustered data reveals that the majority of these are genes which are upregulated at specific time points, however clear rhythmicity exists in several groups. This includes a group showing upregulation during the photoreactive phase of the seasonal waveform, and a group which appears to show photoperiodic regulation (fig. 2-11a). A clustered principal component plot of this data reveals that a small number of these groups are more closely clustered than others (fig. 2-11b). Gene ontology analysis of these transcripts revealed several enriched terms (FDR < 0.1) (fig. 2-12a-b). Analysis of the position of rhythmic genes on the reference genome (M*us musculus*) did not reveal any spatial significance, with significant genes distributed across chromosomes (fig. 2-12d). One of the top reported seasonal genes, and one which shows photoreactive upregulation, is *fam214a*, which produces a protein of unknown function (fig. 2-13a). Other genes include *decr1* (fig. 2-13b), which catabolises the oxidation of fatty acids and opsin-3 (*opn3)* an opsin widespread within the brain (fig. 2-13c). Of note, the thyroid hormone receptor beta (*Thrb*) was significantly rhythmic within the PVN (fig. 2-13d).

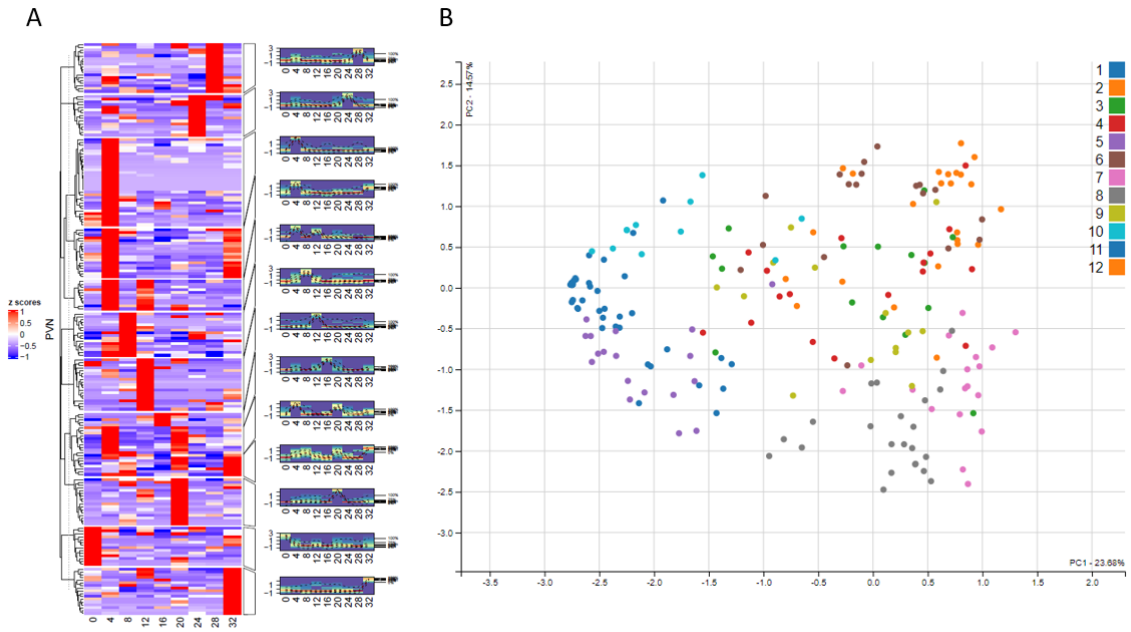

Figure 2-11: Overview of sequencing from the paraventricular nucleus of the hypothalamus. (A) grouped heatmap of transcripts form the PVN sequencing, corresponding density heatmaps for each cluster are shown to the left. (B) Grouped PCA plot of significant transcripts from the paraventricular nucleus sequencing.

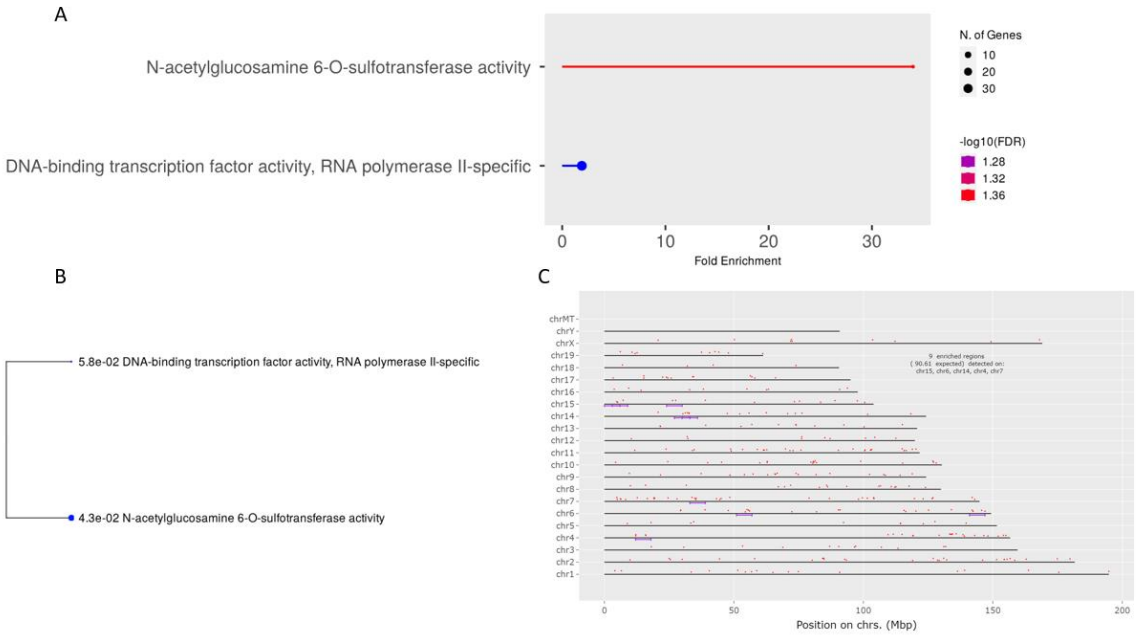

Figure 2-12: Gene ontology analysis of Siberian hamster paraventricular hypothalamus nucleus sequencing. (A) Enriched terms detected using significantly rhythmic transcripts. (B) A hierarchical clustering tree displaying correlation between enriched pathways. (C) Genomic location of significantly enriched transcripts based on *Mus musculus* genome. Plot was produced using ShinyGO 0.77.

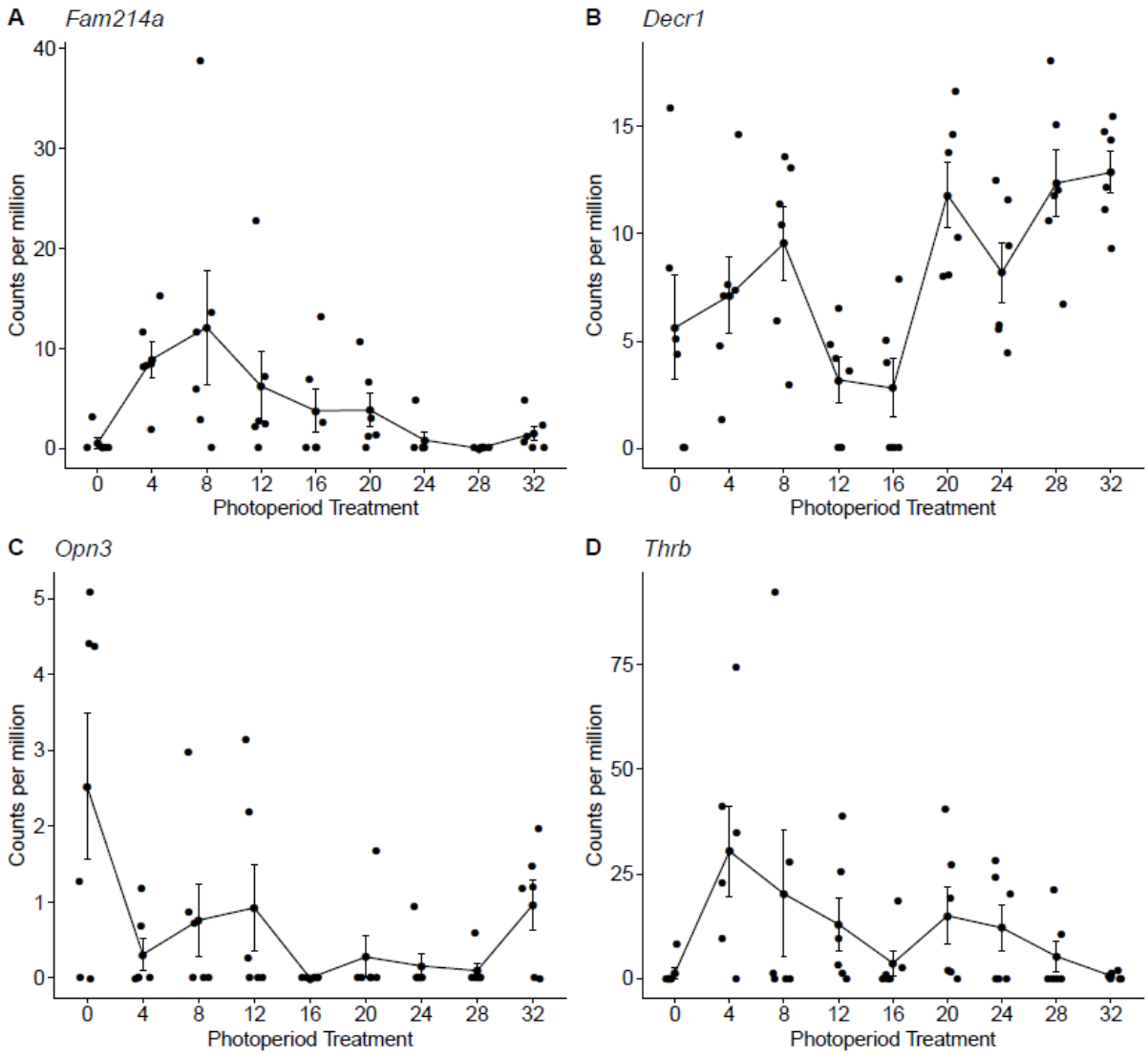

Figure 2-13: Seasonally rhythmic genes from paraventricular hypothalamic sequencing from Siberian hamsters (n = 54) collected after 0 (n = 6), 4 (n = 6), 8 (n = 6), 12 (n = 6), 16 (n = 6), 20 (n = 6), 24 (n = 6), 28 (n = 6) or 32 (n = 6) weeks of short photoperiod exposure. Transcripts included are *Fam214a* (A), *Decr1* (B), *Opn3* (C), and *Thrb* (D). Data shown is mean ± SEM. Points represent individual data points. All transcripts shown are significant by empirical JTK test (FDR < 0.1)

2.5.9 Dorsomedial Nucleus Sequencing

A total of 518 genes were significantly rhythmic across the seasonal waveform within the dorsomedial nucleus sequencing. Gap-statistic analysis revealed that there were 15 unique clusters within the data sets. A clustered heatmap reveals multiple unique patterns, including several genes with a clear rhythmic pattern (fig. 2-14a). A clustered principal component plot of this data reveals that a small number of these groups are more closely clustered than others (fig. 2-14b). Gene ontology analysis of these transcripts revealed several enriched terms (FDR < 0.1) (fig. 2-15a-c). Analysis of the position of rhythmic genes on the reference genome (*Mus musculus*) did not reveal any spatial significance, with significant genes distributed across chromosomes (fig. 2-15d). Among these genes, there were many expected photoperiodic genes, such as retinoic acid receptor alpha (*rara*) (fig. 2-16a), lipoprotein lipase (*lpl*) (fig. 2-16b), RFRP3 (*nvpf*) (fig. 2-16c), and the novel gene *Gucy1a2* (fig. 2-16d).

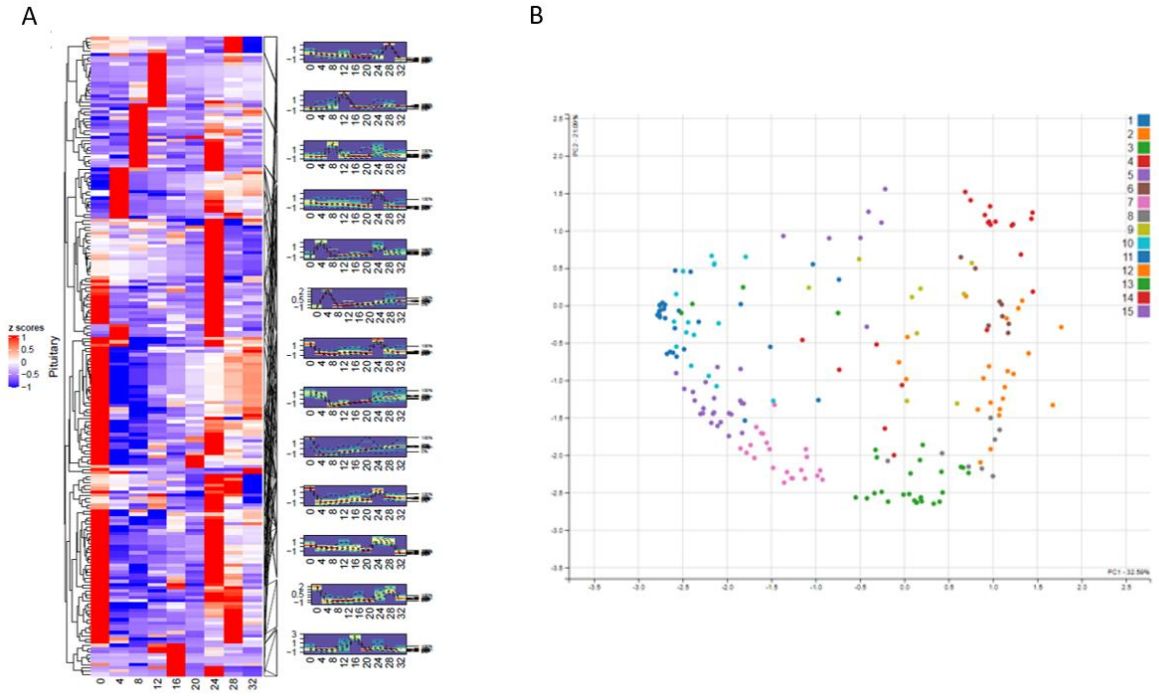

Figure 2-14: Overview of sequencing from the DMH. (A) grouped heatmap of transcripts form the DMH sequencing, corresponding density heatmaps for each cluster are shown to the left. (B) Grouped PCA plot of significant transcripts from the paraventricular nucleus sequencing.

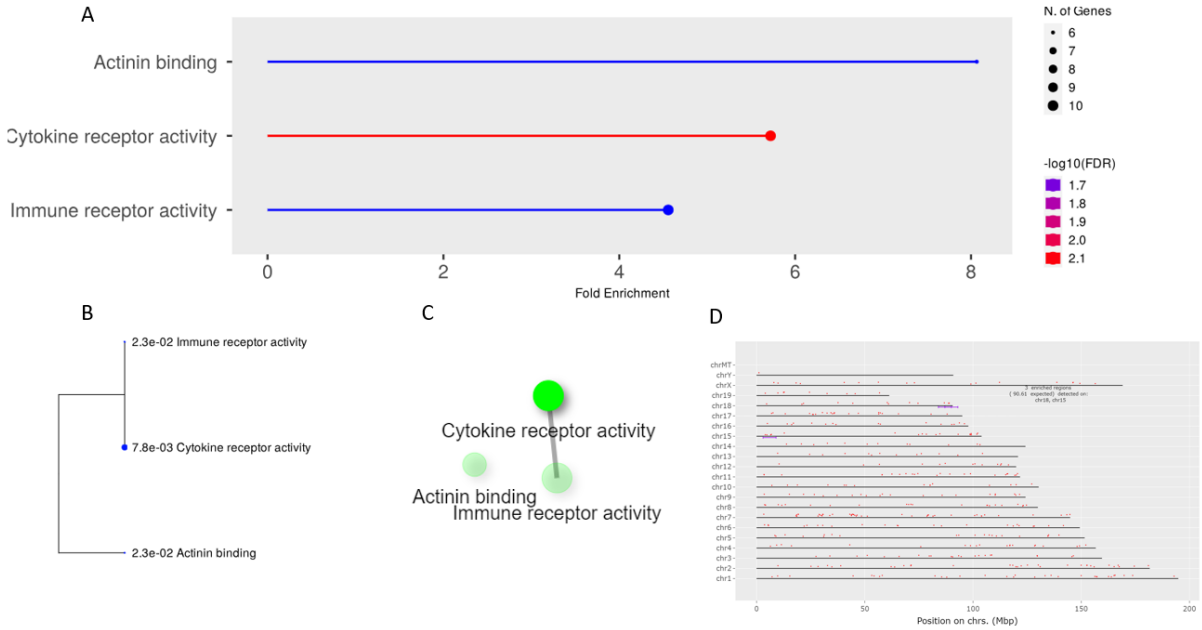

Figure 2-15: Gene ontology analysis of Siberian hamster dorsomedial hypothalamus nucleus sequencing. (A) Enriched terms detected using significantly rhythmic transcripts. (B) A hierarchical clustering tree displaying correlation between enriched pathways. (C) A node plot showing relationship between enriched terms, terms are joined if they share >20% transcripts. (D) Genomic location of significantly enriched transcripts based on *Mus musculus* genome. Plot was produced using ShinyGO 0.77.

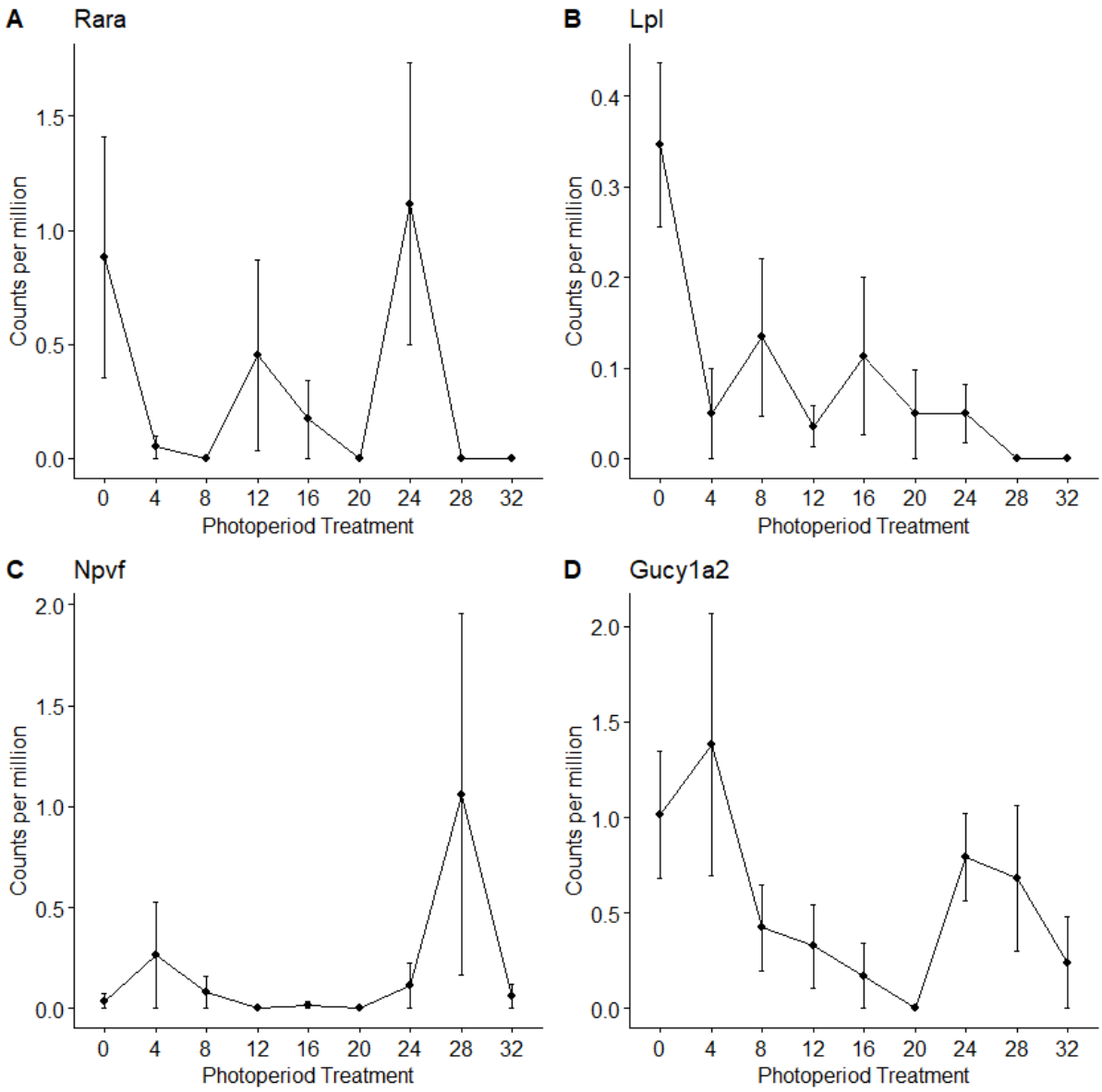

Figure 2-16: Seasonally rhythmic genes from dorsomedial hypothalamic sequencing from Siberian hamsters (n = 54) collected after 0 (= 6), 4 (n = 6), 8 (n = 6), 12 (n = 6), 16 (n = 6), 20 (n = 6), 24 (n = 6), 28 (n = 6) or 32 (n = 6) weeks of short photoperiod exposure. Transcripts included are *Rara* (A), *Lpl* (B), *Nvpf* (C) and *Gucy1a2* (D). Data shown is mean ± SEM. Points represent individual data points. All transcripts shown are significant by empirical JTK test (FDR < 0.1)

2.5.10 Transcription Factor Enrichment Analysis

Rhythmic gene sets were investigated for transcription factor enrichment. Within the pituitary, the highest scoring enriched transcription factor was Borcs8Mef2b, which did not have known co-expression with the remaining top factors (fig. 2-17a). The top enriched transcription factor from the MBH was EHF, the majority of top enriched factors share co-expression networks (fig. 2-17b). Within the PVN the top enriched transcription factor was E2F2, the majority of enriched factors shared co-expression with each other (fig. 2-17c). Within the DMH the top enriched transcription factor was Znf831, with all of the top enriched transcription factors sharing known co-expression (fig. 2-17d).

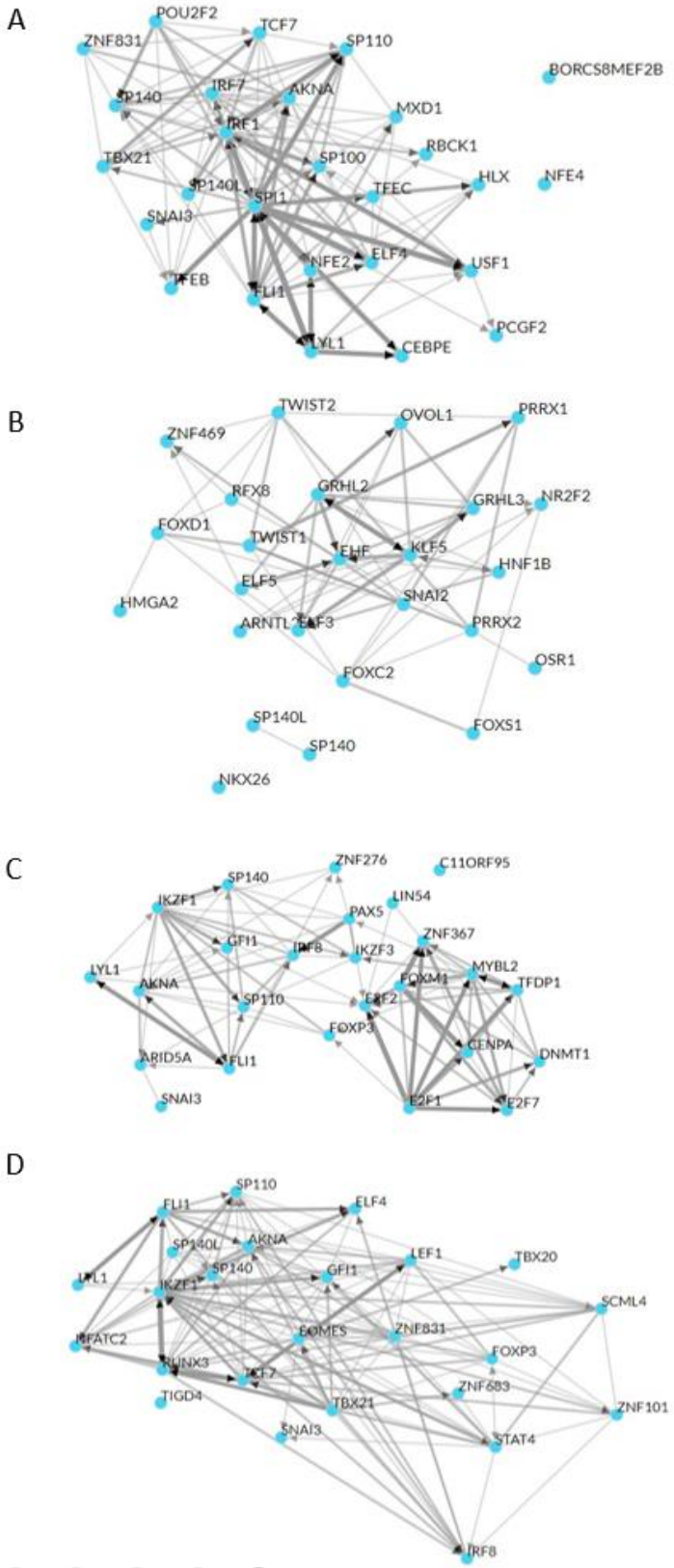

Figure 2-17: Interaction networks of the top 25 scoring enriched transcription factors from Pituitary (A), MBH (B), PVN(C) and DMH(D).

2.6 Discussion

In this chapter the dynamics of change in molecular expression within individual hypothalamic nuclei was investigated. Currently, the molecular mechanisms governing the timing of the seasonal interval timer are not known. It was previously believed that Dio3 was unique in that it was the first gene to downregulate prior to the development of photorefractoriness (Milesi et al., 2017). In this study a host of transcripts were identified which behave in a similar way. This suggests that a programmed change in gene expression is occurring, notably during the photoreactive phase of the seasonal waveform.

2.6.1 Seasonal Rhythms in Behaviour and Physiology are Diverse and Widespread

Hamster physiology follows the well-known seasonal interval timing with initial photoperiod driven reduction followed by spontaneous reversal. This is easily observed in body mass (fig. 2-1a), eWAT mass (fig. 2-1b), Kidney mass (fig. 2-1c) and testes mass (fig. 2-1d). Changes in kidney mass are interesting and could perhaps indicate changes to water balance. It is possible that changes in kidney mass represent physiological adaptations to possible reduced water availability without behavioural adaptations. These changes in kidney mass are simple reflection of the change in body mass, as with reduced body mass the energetic resources for a large kidney do not exist. Blood glucose levels were maintained throughout the seasonal waveform (fig. 2-3a). Low body mass has been shown to drive a decrease in blood glucose in Siberian hamster, under normal homeostatic conditions (Bae et al., 2003). Under seasonal driven body mass loss however, blood glucose levels are defended throughout the seasonal waveform, only increasing as the animals begin to regain body weight (fig 2-3a). Plasma insulin follows the seasonal waveform with a large decrease driven by short photoperiod exposure (fig. 2-3b).

In Siberian hamsters, various immune functions have been shown to be enhanced by exposure to short photoperiod, this includes spleen mass and splenocyte proliferation (Yellon et al., 1999). Spleen mass was maintained while the mass of other organs was decreased (fig. 2-1e). When considering the spleen mass as a proportion of total body mass, this represents a considerable increase. The maintenance of immune function throughout the annual waveform is necessary

for survival, and this likely insulates the immune system from the energetic depression which affects the organism. Seasonal immune changes have previously been reported in various species, and have been proposed to arise from changes in adrenocortical steroids (Nelson and Demas, 1996). These changes affect different elements of immune function, potentially leading to enhanced function and survival in winter months (Nelson, 2004). Sweat gland temperature showed the seasonal pattern, initially decreasing and then recovering (fig. 2-1b), however paw temperature showed no seasonal variation (fig. 2-1i). This suggests that changes in temperature are central and not being driven by increase peripheral loss via vasodilation. Metabolic suppression is well established as a key element of the seasonal response, and this decrease in central body temperature results.

Body mass shows a significant decrease after only 4 weeks of short photoperiod exposure (fig. 2-1a), while body temperature was not significantly decreased until 16 weeks (fig. 2-1h). Both body mass and body temperature are largely under hypothalamic control, though under the control of different regions and neuron populations. The DMH and PVN play key roles in thermoregulation (Arancibia et al., 2008; DiMicco and Zaretsky, 2007; Rezai-Zadeh and Münzberg, 2013), while body mass is typically thought of as under arcuate control (Yu et al., 2009). The differential regulation of seasonal characteristics would allow for a highly precise response to specific annual environmental conditions.

Siberian hamsters display a biphasic increase in locomotor activity throughout the seasonal waveform (fig. 2-2b). The decrease in locomotor activity which occurs at 16 weeks, the peak of the seasonal waveform and the time during which energy utilisation is at its most suppressed (Warner et al., 2010). . Siberian hamsters typically display highly rhythmic patterns of locomotion, however they lose this rhythmicity when exposed to short photoperiod (Warner et al., 2010). However, during the peak of the seasonal response locomotor activity is highly supressed as the animal conserves energy. Locomotor activity then recovers and subsequently decreases again as circadian rhythmicity returns.

2.6.2 Pituitary Sequencing

The pituitary sequencing revealed 250 rhythmic genes many of which are novel discoveries. The pituitary possessed several expression patterns of transcripts

throughout the seasonal waveform (fig. 2-5a). Most patterns are not strongly rhythmic, peaking at individual points throughout the seasonal waveform, however some patterns do possess rhythmicity. One pattern represents genes which appear to peak near the apex of the seasonal response. An example of a transcript matching this pattern of expression would be *cwc15* (fig. 2-7f). *Cwc15* is a spliceosome component which binds to core proteins within the complex and seems to be necessary for normal spliceosome function. The rhythmicity of this gene suggests seasonal changes in spliceosome functioning within the pituitary. Another gene peaking slightly later is *fut8* (fig. 2-7e), a fucosyltransferase necessary for growth factor receptor activity (Wang et al., 2006). This may further suggest changes in post transcriptional modification, like potential changes in spliceosome activity.

Of the classic pituitary genes only *prl* showed a significant seasonal effect. Prolactin followed its well-known seasonal pattern of decreasing upon SD exposure before a photorefractory recovery, driven by the endogenous seasonal interval timer (fig. 2-7a). Prolactin is a good indicator of the seasonal response, it serves as a major output of seasonality, however, tells us little about the regulation of seasonality within the pituitary itself. Other pituitary transcripts such as *gh* (fig. 2-7b) and *pomc* (fig. 2-7c) were not significantly rhythmic throughout the waveform. It should be noted however, that the release and, in the case of *pomc*, post-translational modification of these transcripts is the relevant aspect for communication of the seasonal state to peripheral tissues.

Some evidence exists pertaining to the release of hormones form the pituitary within this data set. *Mcoln1* mediates exocytosis by modulating the fusion of lysosomes to endosomes (Kim et al., 2019). *Mcoln1* mediated exocytosis regulates various systems, such as adipogenesis (Kim et al., 2019). While the actions of *mcoln1* in the pituitary specifically are not well investigated, it is likely playing a role in exocytotic release. The pattern of expression in the pituitary suggests an initial decrease in exocytotic release in response to short photoperiod followed by a recovery in the refractory phase (fig. 2-7d). A general reduction in pituitary output in the initial photoreactive phase of the waveform could explain the lack of change in certain transcripts such as *gh*.

2.6.3 Medio-basal Hypothalamus

Gene ontology analysis of this region was unsurprising given the regions involved (fig. 2-9). Changes in retinol and receptor binding are unsurprising given previously identified seasonal processes within the MBH. Additionally, two kegg pathways were enriched; “Neuroactive Ligand Receptor” highlights the key changes occurring in the regulation of homeostasis in regions such as the arcuate nucleus.. This is unsurprising given the role that regulation of cAMP signalling plays in the transduction of the melatonin signalling (Barrett and Bolborea, 2012), and likely represents changes in transcription occurring within the PT.

Many of the expected photoperiod driven transcripts are represented within this data set, such as *tshb* and *cga* (fig. 2-10a + b) this data is well-known but does highlight the photoperiod responsiveness of the PT as well as the lack of rhythmicity within this tissue (figure 2-10). The most significant of the ‘classic’ transcripts involved in energy balance was *Sst*, which peaks in the midst of the seasonal waveform and inverse to body weight (fig. 2-10e). Other known transcripts includeg*Gpr50,* the orphaned g-protein receptor with affinity for melatonin, and vimentin a well-known marker of tanycytes, both of which highlight the central role that the tanycytes play in coordinating the seasonal response (figure 2-10g).

Within the MBH sequencing data was a host of genes with transient increases in expression levels upon exposure to short photoperiod. Expression of these transcripts was driven by exposure to short photoperiod, but expression of these transcripts spontaneously dropped back to long day levels, often with a peak expression at 8 weeks. This pattern of expression is markedly similar to that of *dio3* which has previously been reported as the first switch in the transition into the photorefractory state (Milesi et al., 2017). *Dio3* forms a major element in the thyroid hormone driven hypothalamic response to short photoperiod, however this change in *dio3* expression apparently occurs without rhythmic *tshb* expression (fig 2-10c). The timing of these transcripts therefor, may represent an important element in the timing of the development of the photorefractory response. However, the exact mechanism driving this pattern is not known, a likely possibility could be that this represents a host of thyroid responsive transcripts within the MBH.

Among this class of transcripts, one of the more interesting is *mef2c* (fig. 2-10d). *Mef2c* belongs to the MADS-box binding family of transcription factors. It was initially characterised as a transcription factor responsible for driving cellular differentiation and tissue maturation in muscle and cardiac tissues. *Mef2c* is expressed in heart and muscle precursor cells and genetic ablation of *mef2c* prevents the correct development of heart and muscle tissues in mice (Lin et al., 1997). *Mef2c* is involved in thyroid hormone signalling, *mef2c* and thyroid hormone receptor are capable of binding and acting as co-activators for each other, jointly binding to regulatory elements in the genome (Lee et al., 1997). There is some evidence that *mef2c* regulates *npy* expression, siRNA-mediated manipulation of mef2c expression revealed that *mef2c* appears to play a role in positively regulating *npy*. Further investigation by this group using luciferase reported assay revealed that overexpression of *mef2c* drove an increase in *npy* promoter activity (Sakai et al., 2013). Though, it is worth noting that the *npy* expression levels within this data do not match the observed change in *mef2c* levels.

Mef2c is an interesting transcript from the perspective of a timed response to an initial stimulus, as it possesses the ability to negatively regulate its own expression, by upregulating the microRNA miR-92b which in turn accumulates to downregulate *mef2c* expression (Chen et al., 2012). If *mef2c* is regulating the expression of seasonal transcripts, but also regulating its own expression, then it could play a role in the timing of the seasonal response. Additionally, sequencing experiments identified a number of other seasonal transcripts with this pattern of expression as being regulated by *mef2* expression, such as *Dhrs7c* and *Hspb7*, and they identify Mef2 protein as highly enriching transcripts involved in nervous system development (Chan et al., 2015). The results of this sequencing experiment, taken in context with the existing literature, could imply that *mef2c* playing a role in the timing of the seasonal waveform, potentially via a neurogenic programme.

Genes with other functions also show this same pattern of expression, for example *sugct*, a poorly studied non-essential mitochondrial gene which catalyses the catabolism of glutarate into glutaryl-coenzyme a. One study generated *sugct* knockout mice and investigated the effect on metabolic state. Of note from this study, *sugct* knockout animals were significantly metabolically

altered, with a gradual increase in body weight, increased lipids and adipose dysregulation compared to wild type controls (Niska-Blakie et al., 2020). This bears some degree of similarity to the long-day state of the animals in this study (fig. 2-1), though notably the *sugct* knockout animals suffer from deleterious symptoms unlike long-day hamsters. Interestingly, this short term photoreactive response of *sugct* was unique to the MBH, which may suggest a localised effect of or on *sugct* within the MBH rather than a systemic effect as shown in previous work. A small number of studies carrying out sequencing experiments have identified *sugct* as playing a role in neurogenesis (Busskamp et al., 2014), though none of these studies highlight *sugct* as a main finding and only present this data in gene banks, most notably in the expression atlas (Search results < Expression Atlas < EMBL-EBI).

The recovery of animals out of the short photoperiod response and into the refractory response is poorly understood. Out data suggests that transient changes in the role of tanycytes in driving neurogenesis and remodelling may play an important role in the development of the photorefractory response. Questions remain surrounding the seasonal regulation of *mef2c*, it follows a similar pattern to *dio3* expression which has been previously identified as the earliest change in the development of the photorefractory response (Milesi et al., 2017). However, this work identifies a host of transcripts which follow a similar pattern, peaking at 8 weeks, before decreasing as the animal enters the photorefractory state. It also suggests a future course of work in functionally investigating the role of *mef2c* in driving the regulation and timing of the seasonal molecular architecture.

2.6.4 PVN

The PVN sequencing revealed several seasonal transcripts, with patterns of expression largely independent of the observed MBH sequencing. As before, many of these transcripts are novel seasonal transcripts. One of the top enriched transcripts from the PVN, *fam214a*, is an interesting transcript as it stands out as it matches many of the rhythmic changes occurring within the MBH sequencing data (fig. 2-13a). Its expression increases on exposure to short days and peaks at 8 weeks. The function of *fam214a*, and that of its protein product, are poorly understood though a few studies have investigated these to some degree. A

recent study identified that *fam214a* may play a role in urine metabolism and drive pathologies derived from the purine breakdown product uric acid (Hilsabeck et al., 2022). Interestingly, a study in adult humans identified a summer increase in plasma urate levels in the northern hemisphere. This has been suggested to account for a seasonal increase in the rate of gout, for which uric acid is a major driver, in humans in the northern hemisphere which occurs at the same time of year (Åkerblom et al., 2017). The function transcript as a seasonal marker within the PVN remains unknown, the PVN is not a major site of metabolism. It is possible that this gene is not a major driver of the seasonal response and has simply represents one part of the large metabolic changes which occur throughout the seasonal waveform. However, it is of note that it appears to match the expression of a number of MBH transcripts, perhaps acting as a downstream indicator of MBH signalling.

Another major transcript is *decr1*, which produces the 2,4 dienoyl-CoA reductase. This gene remains stable through most of the seasonal waveform but display a transient decrease in expression at 12 and 16 weeks of short-day exposure (fig. 2-13b). *Decr1* is most commonly investigated in an oncogenic capacity, however some of these studies have unveiled functional elements of this gene. A study investigating the role *decr1* plays in prostate cancer, identified that *decr1* expression is suppressed by androgens and regulates the fatty acid oxidation in the context of cancers, however this function of *decr1* likely exists in non-transformed tissues (Nassar et al., 2020). *Decr1* has been functionally linked to fat mass and obesity associated (*fto)* expression, a major driver of body mass change (Tóth et al., 2020). These studies could imply a mechanism by which *decr1* may play a role in the seasonal regulation of body mass. However, *fto* has not been demonstrated to be a seasonal transcript in any study, including this one and it is unclear why alterations in fatty acid oxidation within the hypothalamus would affect peripheral tissues.

A recent sequencing experiment investigated the seasonality of cold adaptations in Tibetan sheep, they utilised free-living sheep exposed to natural photoperiods. They identified *decr1* as a major seasonal gene within the rumen of Tibetan sheep. The authors link this to cold season survivability, however, their experimental design (i.e. free living animals) leaves many compounding factors, most obviously photoperiod, for such an absolute description of the

function of *decr1* (Liu et al., 2022). Nevertheless, the sharp decrease in *decr1* expression would be co-temporal with the period in which the animals are most likely to enter torpor, perhaps suggesting this gene play a role in thermoregulation. This explanation of the function of this gene within the PVN seems a more likely seasonal role given the functions of the PVN as pertains to thermoregulation (see introduction).

This sequencing experiment unveiled the seasonal cycling of *opn3* (fig. 2-13d), a photoreceptor highly expressed within the mammalian PVN (Blackshaw and Snyder, 1999). Within melanocytes *opn3* is highly expressed and modulates skin pigmentation by negatively regulating the cAMP response of the MC1R (Ozdeslik et al., 2019). In principle, this allows *opn3* to regulate the response to hormonal signalling based on existing environmental conditions. If this ability to regulate cAMP response to melanocortin signalling exists in other tissues, it is possible that *opn3* is playing a role in modulating the seasonal melanocortin system. *opn3* is expressed within adipose tissue and photon flux onto adipose tissue appears to be sufficient for *opn3* activation. *Opn3* appears to regulate energy metabolism and thermogenesis via a peroxisome proliferator-activated receptors (PPAR) mediated pathway. *Opn3* knockout mice possess decreased thermogenesis and energy usage (Nayak et al., 2020), a phenotype not entirely dissimilar from short-day exposed Siberian hamsters. The timing of the observed decrease in *opn3* is consistent with the decrease in thermoregulation and, ultimately, energy requirements.

Overall, many of the transcripts within the PVN appear to point towards a role in the seasonal regulation of thermoregulation. As previously mentioned, this is unsurprising given the role of the role of the PVN. Thyroid hormone receptors are known to be expressed within the PVN, specifically on TRH neurons which act as regulators of the HPT axis. *Thrb* plays a central role in the negative feedback control of circulating T3 on hypothalamic TRH release and, subsequently, TSH production. TRH neurons are important integrators of multiple signals pertaining to energy balance, being directly innervated by both POMC/CART and AGRP/NPY neurons from the arcuate nucleus. While *Thrb* expression, known to be involved in thyrotropin releasing hormone (TRH) signalling is seasonal, TRH does not appear to have any significant rhythmicity. Thyroid hormone signalling also mediates the expression of mc4r within the PVN,

classically this occurs via thyroid hormone driven AgRP signalling to the PVN, but some studies have shown direct effects of T3 on MC4R expression in the PVN via direct action on a thyroid hormone response element (TRE) within the MC4R promoter (Kouidhi and Clerget-Froidevaux, 2018). However, only the receptor *Thrb* appears to be changing and both of these transcripts remain stable in the sequencing data provided. It is possible that the increase in *Thrb* reflects the short-day driven decrease in T3 signalling, and increased sensitivity to T3 allows for the maintenance of normal homeostatic control of energy balance. Additionally, increase T3 sensitivity may primer the system for exposure to LD. Overall, many of the transcripts within the PVN appear to point towards a role in the seasonal regulation of energy balance and thermoregulation. The PVN is a likely integrator of multiple seasonal signals, such as thyroid hormone and arcuate nucleus.

2.6.5 DMH

Retinoic acid has recently been identified as a major element in regulation of the seasonal response, potentially being synthesised alongside T3 in the tanycytes (See chapter 1). This chapter has reported *rara* as a seasonally regulated transcript within the DMH. *Rara* expression has been identified within the DMH previously, though at very low levels (Meng et al., 2011). This is reflected in the very low levels of expression detected within this data set. *Rara* expression decreases in these animals after exposure to short days, though appears to have peaks at 12 and 24 weeks (fig. 2-16a). This may be caused by the sporadic nature of rara expression within the DMH in combination with the sequencing depth, leading to a masking of the actual pattern. It may also represent a response to decreased retinoic acid signalling, via decreases tanycyte synthesis. Loss of *lpl* expression in the MBH (fig. 2-16b) has been shown to drive an increase in body mass, development of hyperinsulinemia and a decrease in body temperature (Laperrousaz et al., 2018, 2017). This is contrary to the relationship between the physiology and timing of *lpl* expression within this data, however it is unclear the role that *lpl* plays within the DMH specifically. *Lpl* activity has been shown to be downregulated by both T3 and melatonin (Saffari et al., 1992; Wakatsuki et al., 2001), suggesting a sensitivity to molecules closely involved in seasonality. Most studies investigated the regulation of *lpl* focus on tissues other than the hypothalamus, which remains relatively poorly understood.

Npvf (more commonly known as *Rfrp3*) is a well-known seasonal transcript involved seasonal release of Gnrh and ultimately the control of reproductive state (see chapter 1). *Nvpf* expression was generally downregulated with the exception of a peak late in the waveform (fig. 2-16c). This is somewhat unusual given the expected pattern of expression of *Nvpf* but could represent the sequencing depth available in this region. Like in other regions, there were many novel transcripts such as *gucy1a2* (fig. 2-16d), a gene involved in nitric oxide (NO) reception (Engeli et al., 2004). In the DMH, NO drives high fat food intake via heightened glutamate signalling (Poole et al., 2020). Interestingly, there is some evidence of seasonality in NO within the bloodstream (McLaren et al., 2000), but is challenging to determine if this results from endogenous production of NO or variations in atmospheric NO concentrations. Nevertheless, the change in *gucy1a2* expression hints at the existence of NO mediation of the seasonal response in the DMH.

2.6.6 Transcription factor enrichment

Changes in gene expression are ultimately driven by changes in transcription factor activity, thus a tool like Chea3 can be used to predict which transcription factors are involved in driving observed differential transcripts. The predicted transcription factors generally all share co-expression (fig. 2-17). This could suggest a common initiating factor in each region leading to a cascade of transcription factor activity. Various genes of interest revealed themselves as being enriched transcription factors, such as basic helix-loop-helix ARNT like 2 (*bmal2)*, a circadian gene known to be *involved* in seasonality, being identified as a transcription factor in the MBH. *Bmal2* plays a key role in the proposed *eya3* model of seasonal *tshb* control (Wood et al., 2020) (See chapter 1).

2.7 Conclusions

Much of the data presented within is expected and allows for validation of the seasonal response to short photoperiod. There is some novel, or largely unreported, physiological data presented here, but the main strength is the breadth of physiological and molecular investigation across the waveform. Most notably the change in kidney mass, which could imply changes in water balance regulation across the seasonal. However, it could however reflect the widespread seasonal changes occurring, with smaller overall mass. It is notable that the timing of different seasonal factors is not aligned. For example, body weight mass drops significantly by 4 weeks and recovers by 24 weeks of short-photoperiod exposure (fig. 2-1a). While epididymal WAT mass decreases by 8 weeks and recovers by 20 weeks of short photoperiod exposure. Other factors have yet different patterns, most notably locomotor activity which possesses a biphasic pattern throughout the seasonal waveform (fig. 2.1b). These data imply either differential central regulation of seasonal physiological factors, or differential peripheral response to the central photoperiodic signal.

Similarly, the apparent independence of the timing of the expression of transcripts is indicative of differential response to the seasonal signal. These nuclei independent response may be the key mechanisms driving. There is certainly cross region regulation of transcript expression. It is well accepted that T3 synthesis within the tanycytes of the third ventricle drive downstream regulation of transcripts within the arcuate nucleus. The circadian rhythm has been implicated in the control of the photoperiod response and is a cell autonomous timer entrained by melatonin signalling. Similarly, it has previously been reported that seasonal rhythmicity within the pituitary persists in the absence of hypothalamic signalling and in certain species in the absence of photoperiodic information. And while the development of the photoperiod response depends upon external photoperiod information, the development of the photorefractory response is endogenous. It could be argued that the rhythmic refractory response is entrained by photoperiod information. Overall, this data indicates that separate hypothalamic nuclei may be acting independently to drive the seasonal output. This chapter further identifies the transcripts which may be involved in the regulation of changes in body mass, namely somatostatin.

A limitation to this work is that, while it captures the molecular architecture of the seasonal waveform there are other factors affecting seasonality it does not. As examples, the release of hormones into the bloodstream and the exact nature of cellular remodelling are not captured. Both of these are known to be relevant to seasonality and some data pertaining to them is present within this data. We can only infer from this data set, the timing of certain events, such as seasonal neurogenesis. In addition, this chapter has identified new transcription factors which may be modulating the timing of seasonal remodelling, such as *mef2c*. Overall, the work in this chapter identifies a large number of novel seasonal transcripts and suggests differential regulation of the seasonal response in hypothalamic nuclei.

A key limitation of the work presented in this study is the lack of functional manipulations of the physiological systems affected by seasonality. Thus, the rheostatic and homeostatic mechanisms guiding change in energy balance cannot be dissected from this study. In the next chapter a negative energy balance will be induced in short day Siberian hamsters. This will allow for molecular investigations to identify the specific molecular changes which drive programmed rheostasis compared to those which act in a homeostatic manner.

Chapter 3 – Discrete Hypothalamic Populations Regulate the Seasonal Rheostat and the Energy Balance Homeostat

3.1 Introduction

In the previous chapter, the molecular mechanisms underlying rheostatic changes were unveiled. In this chapter the distinction between short term homeostatic regulation in body mass and seasonal rheostatic regulation of body mass were investigated. There is significant evidence that the seasonal rheostat and the homeostat regulating energy balance are distinct. One of the key mechanisms by which homeostatic regulation of body mass is achieved is via leptin signalling from the periphery to the hypothalamus (Houseknecht et al., 1998). In Siberian hamsters, exposure to long photoperiods drives the development of leptin insensitivity. Though notably this appears to occur only with certain neuropeptides. For example, Rousseau *et al*. found that *npy* expression remains responsive to leptin administration under short photoperiods while pro-opiomelanocortin expression did not (Rousseau et al., 2002). NPY has widely been reported as non-responsive to photoperiod changes (Reddy et al., 1999). Additionally, NPY and agouti-related peptide, with which it is co-expressed, remain responsive to food restriction under short photoperiods while other neuropeptides, such as POMC does not (Mercer et al., 2001). Taken together these reports suggest that NPY/AgRP neurons acts as a homeostatic regulator of body mass. Thus, NPY presents a key mechanism by which homeostatic regulation of energy balance may persist even under considerable rheostat-driven alterations in body mass.

3.1.1 Rheostatic Tracking of Body Mass

Siberian hamsters maintained on short photoperiods lose body mass. Treatment of these animals with food restriction, drives an additional decrease in body mass. However, rheostatic tracking of body mass changes continues through the food restricted period, and when food is returned animals will regain body weight appropriate for their phase in the seasonal cycle (Steinlechner et al., 1983). A simplified example of this phenomenon can be seen in figure 3-1. Later studies would investigate the expression of select neuropeptides in conditions of food restriction in short photoperiod treatment. NPY remained responsive to short-term changes in body mass loss imposed by food restriction (Mercer et al.,

1995). Implying that NPY plays a role in homeostatic regulation of body mass under short photoperiod induces rheostatic loss in body mass. Further work would identify that food restriction increases the timing of torpor bouts (Ruf et al., 1993). These data show that rheostatic tracking of body mass is independent of energetic balance.

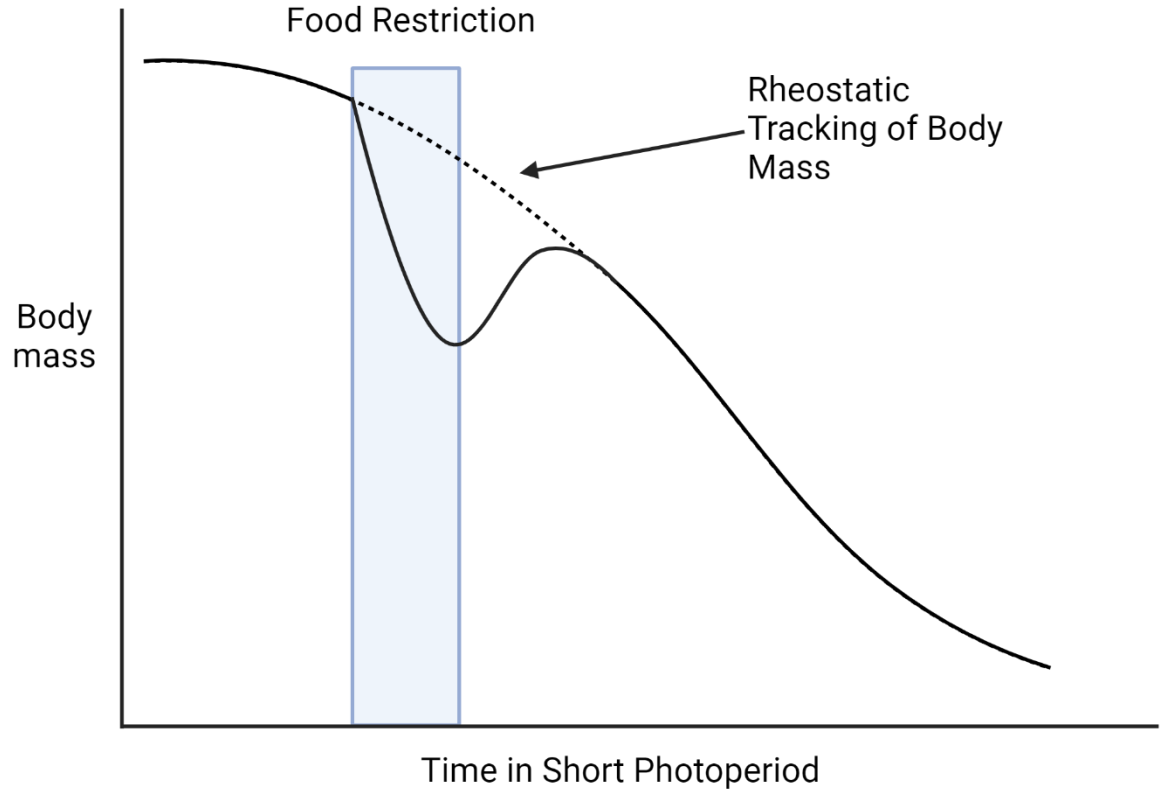

Figure 3-1: Changes in body mass of Siberian hamsters. Siberian hamsters gradually lose body mass on short photoperiod. Food restriction can induce seasonal inappropriate loss of body mass, however the rheostatic set point of body mass continues to be tracked. Figure created utilising data available from (Steinlechner et al., 1983). Created with BioRender.com.

3.1.2 Homeostatic and Rheostatic regulation within the hypothalamus

The hypothalamus appears to be a key region in regulating rheostatic changes in energy balance. In chapter 2, *sst* was identified as the primary transcript which could be responsible for rheostatic seasonal changes in energy balance. Somatostatin administered intra peritoneally is anorexigenic in rats and baboons, while administration to cerebrospinal fluid has no effect (Lotter et al., 1981). In the arcuate nucleus somatostatin acts upon receptors on growth hormone releasing hormones to inhibit it's release into hypophyseal portal blood (Tannenbaum et al., 1998). Somatostatin has diverse inhibitory effects which affect body mass. Classically, somatostatin drives a decrease in body mass by inhibiting growth hormone release from the pituitary gland (Siler et al., 1973). It also inhibits the release of TSH and prolactin (Vale et al., 1974). Somatostatin also drives several peripheral changes associated with energy balance, acting directly on beta cells in the pancreas to inhibit insulin release (Alberti et al., 1973).

Long term food restriction has been shown to inhibit *sst* expression in ovariectomised ewes (Belinda Henry et al., 2001). Somatostatin secretion appears to increase with age, and is associated with decreased GH mediated body mass (Sonntag et al., 1986). Indeed, in Siberian hamster treatment of a somatostatin agonist (pasireotide) drives changes in body mass which mimic changes which occur under short photoperiods. Similarly, administration of Growth hormone drives increases in body mass in short day Siberian hamsters, which resemble changes in animals transferred to long photoperiods (Dumbell et al., 2015). This agonist appears to inhibit wheel running, and to inhibit exercise-associated gain in body mass (Dumbell et al., 2017). Treatment of this agonist also appears to drive increased duration and frequency of torpor bouts (Scherbarth et al., 2015). Evidence from the previous chapter, and from published literature, strongly suggest that somatostatin acts as an effector output for rheostatic regulation of body mass in seasonal Siberian hamsters. Another hypothalamic neuropeptide implicated in the rheostatic control of energy balance is VGF (non-acronymic). VGF expression is upregulated in the dorsomedial part of the arcuate nucleus of Siberian hamster that are transferred into short photoperiod (Barrett et al., 2005). The VGF derived peptide TLQP-21 drives a decrease in food intake, and in uncoupling protein-1 (UCP-1) expression

within BAT (Jethwa et al., 2007). TQP-21 acts on the membrane bound complement C3a 1 receptor in rodents (Hannedouche et al., 2013). This receptor is expressed om Siberian hamster BAT, and in the hypothalamus (Lisci et al., 2019). Interestingly, short photoperiod appears to sensitise Siberian hamster to the energetic effects of TLQP-21 administration (Lisci et al., 2019). Leptin, released by adipose tissue, is critical for regulation of energy balance (Spiegelman and Flier, 2001).

The arcuate nucleus of the hypothalamus is a well-known centre in the control of energy balance homeostasis. The key neurone populations involved in controlling homeostasis within the arcuate nucleus are POMC/CART and NPY/AgRP neurons. These two neuron populations act antagonistically to one another to regulate homeostasis in energy balance (Vohra et al., 2022). NPY/AgRP neurons are thought to act in an orexigenic manner, driving increases in body mass and food intake (Morton and Schwartz, 2001). However, *npy* expression does not appear to be significantly affected by exposure to short photoperiods (Reddy et al., 1999). *Npy* shows considerable downregulation in the arcuate nucleus of the Siberian hamster in response to food restriction, regardless of the seasonal cycle (Mercer et al., 1995). Strongly implying NPY acts a homeostatic mediator of body mass even under considerable rheostatic alterations.

Leptin, released by adipose tissue, is critical for regulation of energy balance (Spiegelman and Flier, 2001). A number of factors associated with energy balance regulate leptin signalling (Ahima and Osei, 2004). Leptin concentrations are positively correlated with body fat percentage (Considine et al., 1996). Leptin concentrations are increase by short term overfeeding, demonstrating an immediate role in energy homeostasis in addition to longer term changes in adipose tissue mass (Kolaczynski et al., 1996). Both NPY/AgRP and POMC/CART neurons express leptin receptor, and respond to leptin by altering excitatory and inhibitory output (Pinto et al., 2004). Indeed, leptin signalling appears to be critical for the response of NPY/AgRP neurons to food restriction (Takahashi and Cone, 2005). Other peripheral hormones act to confer energetic state to the hypothalamus. Insulin has long been established to drive a decrease in food intake and body mass (Woods et al., 1979). Insulin receptor expression within the arcuate nucleus decreases under short photoperiods (Alexander Tups et al.,

2006). However, insulin administration does not appear to significantly affect seasonal cycles in body mass (Bartness et al., 1991).

3.1.3 The melanocortin system and Rheostasis

The melanocortin system (introduced in chapter 1) is a major regulator of body mass. However, some evidence exists that the melanocortin system may play critical roles in rheostatic changes in energy balance. POMC, a pre-propeptide which give rise to the melanocortins and has a classic satiety effect (See chapter 1). However, studies of seasonal expression of POMC in Siberian hamsters have revealed an apparently decrease in expression under short photoperiods (Mercer et al., 2000b). This decrease in POMC expression coincides with large decreases in body mass. This is paradoxical, as arcuate POMC neurons are generally thought of as driving anorexic changes in behaviour and physiology (Millington, 2007). However, recent findings suggest the presence of multiple distinct POMC sub-populations within the arcuate nucleus which may have distinct role on food intake (Quarta et al., 2021). Another proposed explanation for the apparent paradox of seasonal POMC expression is altered post-translational cleavage of POMC into its products. Indeed, seasonal changes in prohormone convertase expression have been noted in the Siberian hamster arcuate nucleus (Helwig et al., 2006). POMC has been reported to be downregulated by SD in Siberian hamsters, and to be non-responsive to food restriction (Reddy et al., 1999). A recent sequencing experiment identified that *pomc* was strongly downregulated by exposure to short photoperiod. It also identified that food restriction drove an increase in *pomc* expression in short day exposed hamsters (Bao et al., 2019). The reported expression of POMC is similar to that AgRP, which is also overexpressed within the arcuate nucleus of Siberian hamsters (Jethwa et al., 2010).

Ghamari-Langroudi *et al*. investigated the role of MC3R in rheostasis. They achieved this by generating MC3R knockout mice. When challenged with food restriction, MC3R knockout mice showed a normal loss n body mass, however when food was returned to these animals, they displayed a markedly reduced set point of body mass following refeeding. Interestingly, MC3R KO abolished fat mass changes in response to progesterone administration, providing a link between reproductive state and melanocortin signalling (Ghamari-Langroudi et

al., 2018). MC3R KO mice gain body weight and become hyperlectinaemic and hyperinsulinaemic without an increase in food intake (Chen et al., 2000). MC3R deficient mice display altered metabolism, with reduced utilisation of fats in metabolism (Butler et al., 2000). MC3R levels within the arcuate nucleus of Siberian hamster have been shown to be downregulated under short photoperiods, while decreased within the VMH (Ellis et al., 2008). Interestingly, one study using Siberian hamsters found than MC3R expression was reduced by both short photoperiod and food restriction, but that there was no further decrease when short photoperiod animals were food restricted (Mercer et al., 2001). These data suggest that MC3R may be playing a role in integrating energetic cues to allow for rheostatic changes in body mass. Indeed, MC3R expression within the arcuate nucleus of short photoperiod Siberian hamsters (Herwig et al., 2013)

3.1.4 Aims

The aim of this chapter is to investigate the role of neuropeptides in the seasonal rheostat and the energy balance related homeostat. This was achieved by treating Siberian Hamsters, under long and short photoperiods, to a short-term bout of food restriction or maintaining on *ad libitum* feeding. Physiology factors such as body mass, BAT mass and eWAT mass were investigated to confirm the effects of seasonal and food restriction protocols. Thermoregulatory behaviour was investigated using a tube utilisation test. Anxiogenic behaviour was investigated using a light-dark box test. Food investigatory behaviour was investigated using a novel tri-arm test. Blood chemistry was also investigated to determine hormonal signalling involved in both seasonality and food restriction. Expression of *gh*, lhb, *npy*, *pomc*, *prl* and *sst* were then investigated by qPCR to determine their role in rheostasis and homeostasis.

3.2 Hypothesis

Neuroendocrine markers of rheostatic and homeostatic regulation of body mass will be distinct. Somatostatin will act as rheostatic marker of energy balance regulation. It will be insensitive to changes in short term energy balance. Instead, it will show robust response to seasonal changes. In contrast neuropeptide y will display robust homeostatic regulations of body mass. It will respond to acute negative energy balance and will not respond to seasonal changes in body mass.

3.3 Methods

3.3.1 Ethics

All procedures carried out were conducted under home office license (PP5701950) and in accordance with ARRIVE guidelines at the veterinary research facility at the University of Glasgow. Male (n = 35) Siberian hamsters (*Phodopus Sungorus*) were used in this study.

3.3.2 Animals

Adult male Siberian hamsters, without prior short photoperiod (SD) exposure, were individually housed in polypropylene cages in either 16h light (LD) (n = 18) or 8h light (SD) (n = 17) for 12 weeks. Food (SDS [BK001]) and tap water were provided ad libitum. Body mass, food intake and body temperature were measured every 2 weeks. Animals were held at a room temperature of 21°C, and a humidity of 50%. In the final dark phase of the experiment, 50% of animals were placed on a food restriction regime (FR), wherein food was not available, and the other 50% maintained on ad libitum feed (AL). Animals were food restricted only across the final dark phase as per home office license PP5701950. Similar protocols of short term caloric restriction induce reliable negative energy balances which are capable of driving changes in neuropeptide expression associated with food intake and homeostatic control of body mass (Hanson and Dallman, 1995; Speakman and Mitchell, 2011). Siberian hamsters remain responsive to food restriction under short photoperiod induced rheostatic body mass loss (Mercer et al., 1995). Further, total food restriction, as described here, is effective at driving body mass loss in rodents (Speakman and Mitchell, 2011). Such that there were four groups in this experiment LDAL (n = 9), LDFR (n = 9), SDAL (n = 9) and SDFR (n = 8). Body mass and body temperature were recorded prior to and following food restriction. Animals were sacrificed by cervical dislocation followed by exsanguination. Interscapular Brown adipose tissue and epididymal white adipose tissue were dissected, weighed and frozen on dry ice. Terminal trunk blood sample was collected and heparinised with 50ul heparin (Workhardt, 1,000 I.U./ml, PL 29831/0109). Gonad mass was recorded to confirm seasonal response. Brains were stored at -80°C until sectioning. The brains were dissected into 200µm sections using a Leica CM1520 cryostat. Anatomical structures (optic tract to the infundibular stem; Bregma -2.12mm to

-3.80mm) were used to isolate the Arcuate nucleus. Bilateral tissue punches were performed using an integra Miltex 1mm disposable biopsy punch. Tissue punches were stored at -80°C until RNA extraction.

3.3.3 Behaviour

Hamster behaviour was assessed prior to the beginning of food restriction treatment. Food motivation was assessed using a novel investigatory test. This test involved a triangular central chamber with removable transparent walls containing air holes. Behind each removable arm are one of three extended arms containing either regular chow (SDS [BK001]), hamster treats (Tiny Friends Farm) or nothing. Hamsters were placed in the central chamber for 1 minute. Subsequently removable walls were removed, and hamsters were recorded for 5 minutes. Time in each chamber, and investigation behaviour of each object were noted. A schematic diagram of this test is available in figure 3-2. Anxiety behaviour was tested using a light-dark shuttlebox test. This consists of a $1m^3$ box, with one half of the box secluded by a dark covering. Hamsters were place in the box for 5-minute periods and recorded. Time spent in the dark box and light box, as well as entrance and exits from the box were counted across the 5-minute period. Scoring of behavioural videos was very kindly carried out by Ms Fallon Cuthill, University of Glasgow.

3.3.4 RNA Extraction

RNA was extracted from samples using the TRIzol method following the manufacturer's instructions. Briefly, 1ml of TRIzol reagent (Thermofisher, 15596026) was added to each sample in a 1.5ml Eppendorf tube. Tissue was homogenised using a Polytron PT 1200 E. Homogenised tissue was incubated for 5 minutes at room temperature. 0.2ml of chloroform (Sigma-Aldrich, 102175901) was then added to the mixture. Mixture was incubated for 3 minutes at room temperature. The mixture was then centrifuged for 15 minutes at 12,000 g. The upper aqueous layer was then pipetted into a separate 1.5mll Eppendorf tube. 0.5ml isopropanol (Sigma-aldrich) was added to the aqueous phase. The mixture was incubated for 10 minutes at room temperature. The mixture was centrifuged for 10 minutes at 12,000 g. Supernatant was removed from the subsequent pellet of RNA. The pellet was resuspended in 75% ethanol (Fisher Bioreagents, BP2818-500) and vortexed briefly. The solution was centrifuged for 5 minutes at

7,500 g. The supernatant was removed from the resultant pellet of RNA. The pellet was resuspended in 20µl nuclease free water (Millipore). RNA was tested for quality and quantity using an ND-1000 nanodrop.

3.3.5 cDNA Synthesis and qPCR

RNA was transformed into cDNA for qPCR analysis using superscript III (Invitrogen). A mastermix was prepared containing, per sample; 2µl 5X first strand buffer (Invitrogen), 1µl DTT (Invitrogen), 0.2µl Random Primers (Promega), 0.2µl dNTP mix (as prepared), 0.26µl RNase block (Agilent), 0.26µl reverse transcriptase enzyme (Invitrogen), 2.08µl nuclease free water (Millipore). 6µl of this mastermix was combined with 4µl RNA (total 200ng). Quantification of transformed cDNA was achieved using Brilliant II SYBR Mastermix (Agilent). Stock forward and reverse primers (100pmol/µl) were mixed and diluted in nuclease free water to 20pmol/µl. A working SYBR mixture was prepared by mixing 1-part primer mixture per 24-part SYBR mastermix. Reaction mixtures were prepared in wells on a 96-well plate by mixing 4.8µl of normalised sample and 4.8µl of SYBR working mix. All reactions were performed in duplicate. qPCR reactions were carried out in a Stratagene Mx3000P thermal cycler. Cycling conditions utilised were in sequence; at 95°C for 5 minutes (denaturing), 40 cycles at (95°C for 30 seconds, X°C for 1 minute – see table 2.2, 72°C for 30 seconds with fluorescent measurement at end), 95°C for 1 minute, 55°C for 30 seconds increasing to 95°C (Melt curve analysis). Melt cure analysis was used to determine specificity of amplification. Data was analysed for meanCT, efficiency and variability using PCR Miner (Zhao and Fernald, 2005). Logfold CT was calculated using the ΔΔCT method using the geometric mean of GAPDH and HRPT reference transcripts.

Gene	Forward Primer	Reverse Primer	Temp (°C)
Prl	TCCGGAAGTCCTTCTGAACC	CGCAGGCAGCGAATCTTATTG	60
Gh	ACCTACAAAGAGTTTGAGCGTG	ATGAGCAGCAGCGAGAATCG	58
Lhb	ATGGAGAGGCTCCAGGGGCT	CATTGGTTGAGTCCTGGGACC	60
Npy	CCAGGCAGAGATACGGCAAGAGATC	CCATCACCACATGGAAGGGTCC	60
Pomc	TGGAGAGCAGACAGTGTCAGGAC	TCTCGGTCAACGTCTGGTCGTC	60
Sst	GAAGTCTCTGGCGGCTGCTG	CAGCCTCATTTCATCCTGCTCCG	60
GAPDH	TTCTTGTGCAGTGCCAGCCTCG	CTGTGCCGTTGAACTTGCCGTG	60
HRPT	AGTCCCAGCGTCGTGATTAGTGATG	CGAGCAAGTCTTTCAGTCCTGTCCA	62

Table 3-1: Primer sequences and annealing temperatures of qPCR transcripts in chapter 3.

3.3.6 Hormones and Blood Chemistry

Hormones and blood chemistry were tested using heparinised terminal trunk blood. Blood glucose was investigated using an SD Biosensor CodeFree blood glucose monitor (01GC110) with SD CodeFree blood glucose test strips (01GS11). Blood was then spun for 15 minutes at 4°C in a Heraeus Fresco 21 (Thermofisher) to separate plasma. Plasma was stored at -20°C until analysis. Analysis of Plasma Insulin and GLP-1 were very kindly carried out by Dr Jo Edward Lewis at the University of Cambridge.

3.3.7 Statistics

Quantification of behavioural was completed in-part by one rater and in-whole by another. To minimise observer biases and demonstrate a high inter-rater reliability, a two-way random effects intraclass correlation coefficient (ICC) was performed. The ICC is a widely utilised rater reliability index (Koo and Li, 2016). Guidelines for ICC interpretation indicate that scores may be grouped into bands of <40 (poor), .41-.59 (fair), .60-.74 (good) and .75 -1.00 (excellent) (Cicchetti, n.d.). All tested measurements in this data scored either good or excellent for consistency. The results of ICC testing can be seen in table 3-1. Data was tested for normality using the Shapiro wilk test. Data which violated normality was log transformed. A repeated-measures (within-subject) ANOVA was utilised to detect significance of change in body mass, daily food intake and sweat gland temperature following transfer to short photoperiod. Post-hoc analysis of repeated measures was carried out using a Bonferroni post-hoc test with reference to baseline measurements made at week 0. Two-way ANOVA was carried out on PCR data and on all physiological factors following termination of the experiment; % change in body mass, BAT mass, eWAT mass, testes mass and body temperature. Post-hoc analysis of non-repeated measures was carried out using a Bonferroni post-hoc test between test conditions.

Tri-arm test	**ICC**	**Interpretation**
Time in Food Area (S)	1	excellent
Time in Treat Area (S)	0.99	excellent
Time in Control Area (S)	0.75	excellent
Time in Central Area (S)	0.97	excellent
Chow investigations	0.71	good
Treat Investigations	0.96	excellent
Light-dark box	**ICC**	**Interpretation**
Movement between regions	1	excellent
Time in light area (s)	1	excellent
Time in dark area (s)	1	excellent

Table 3-2: ICC scores of behavioural measurements in this study. ICC is a widely utilised index of inter-rater reliability.

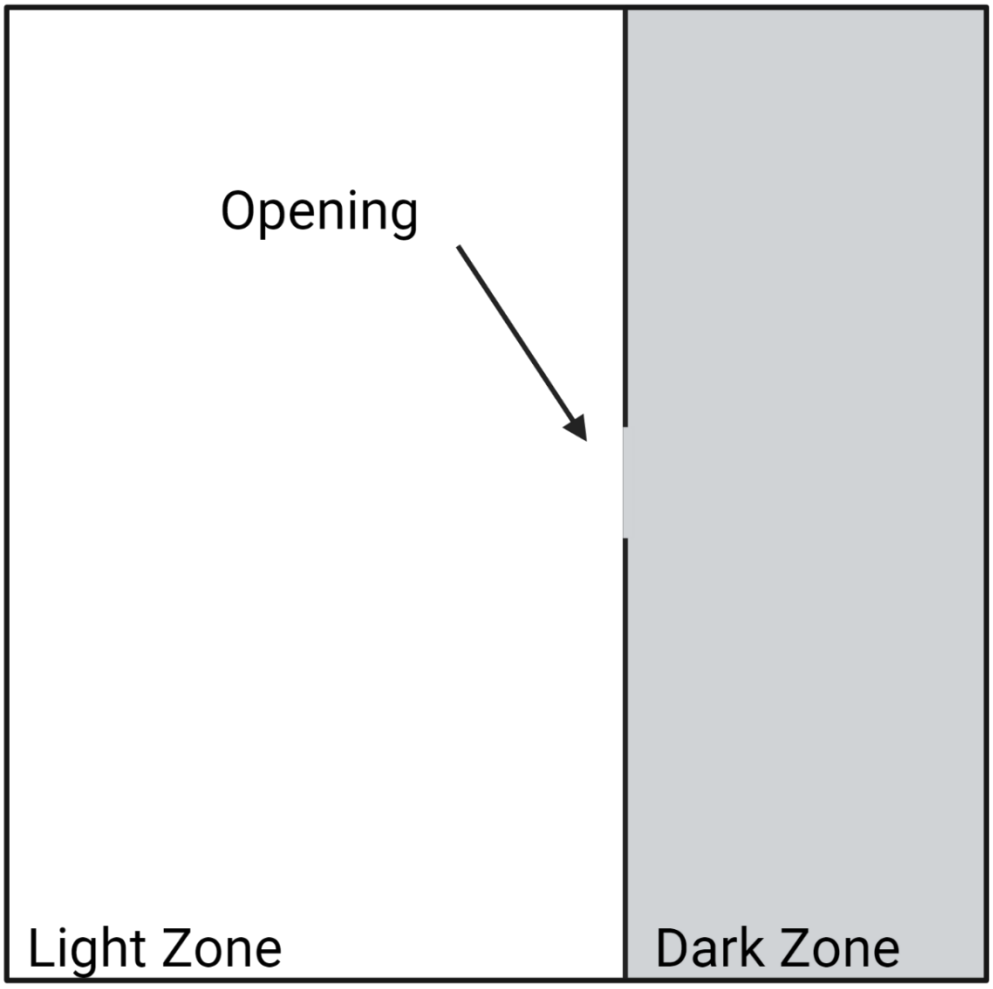

Figure 3-2: Schematic diagram of the light-dark shuttle box test. The test apparatus consists of a light area, in which ambient lighting can penetrate, and a dark zone, protected from ambient lighting. Siberian hamsters were released within the centre of the light zone. Hamsters were monitored for 5 minutes and time in light and dark zones were recorded.

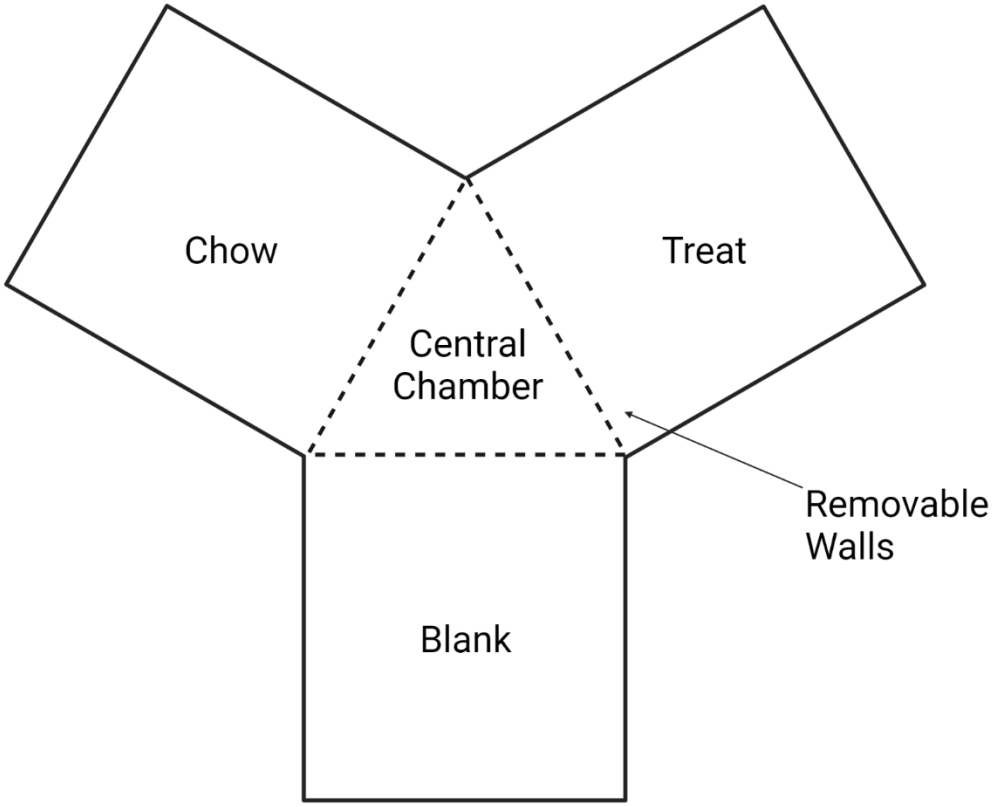

Figure 3-3: Schematic diagram of tri-arm food motivation test. The central chamber is surrounded by removable transparent walls. Three chambers containing either regular chow, hamster treats or nothing. Hamsters were placed in the central chamber and subsequently removable walls were removed.

3.4 Results

3.4.1 Photoperiod Drives Expected Energetic Changes in Siberian Hamsters

Body mass, food intake and sweat gland temperature were monitored in the 12 weeks preceding the food restriction treatment. There was a significant effect of photoperiod on body mass ($F = 56.901_{1, 243}$; $p < 0.00001$). There was a significant decrease in body mass at 6 ($p = 0.048$), 8 ($p = 0.00342$), 10 ($p = 0.0005$) and 12 ($p = 0.0012$) weeks of short photoperiod relative to baseline (Fig 3-4a). There was a significant effect of photoperiod on food intake ($F = 25.296_{1, 208}$; $p < 0.00001$). There was a significant increase in food intake at 2 ($p = 0.018$), 6 ($p < 0.0001$), 8 ($p < 0.001$), 10 ($p < 0.001$) and 12 ($p < 0.001$) weeks of long photoperiod treatment relative to baseline (fig 3-4b). There was no significant effect of photoperiod on sweat gland temperature ($F = 1.913_{1, 173}$; $p = 0.168$).

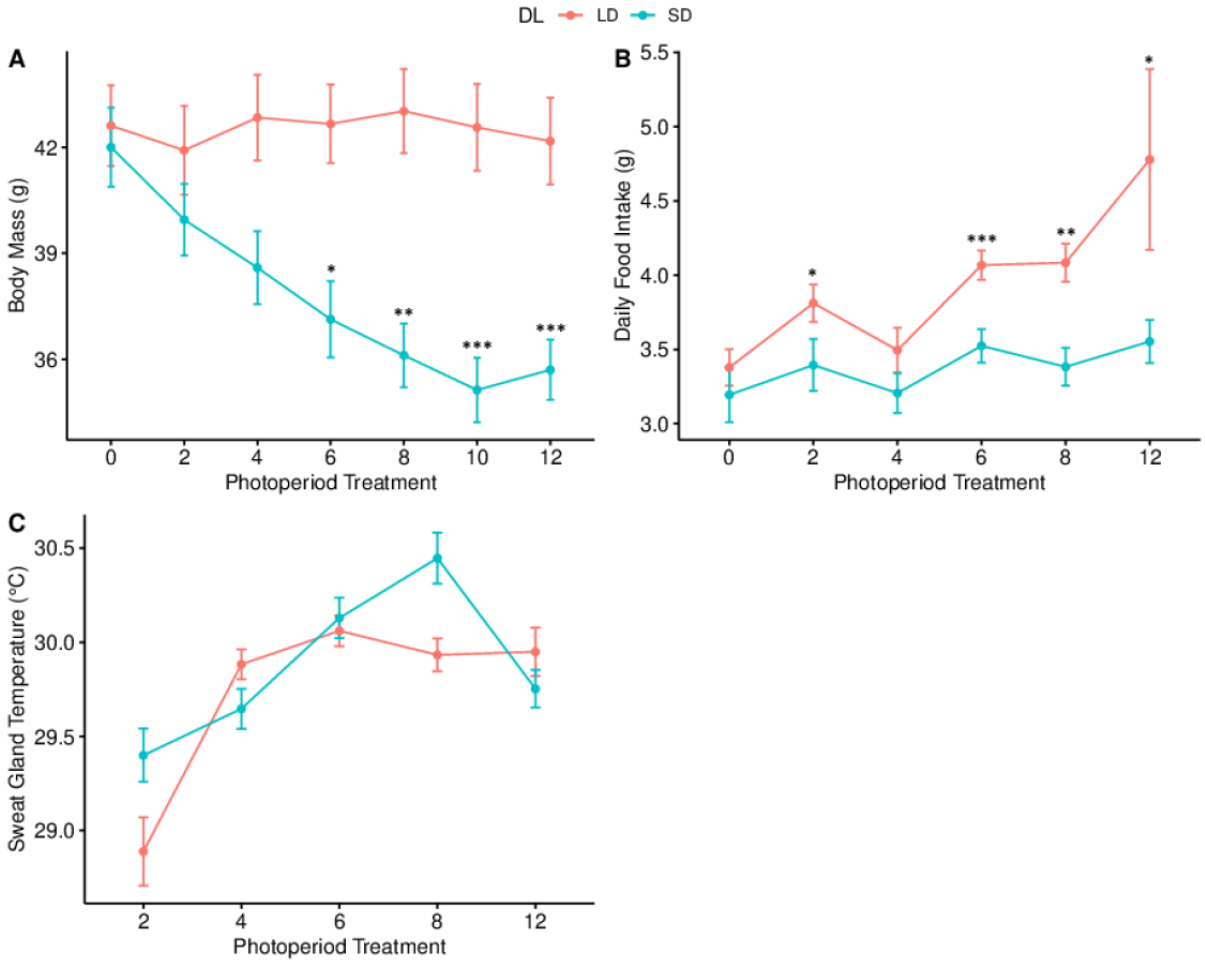

Figure 3-4: Programmed rheostatic changes in physiology prior to restricted feeding. (A) Body mass, (B) daily food intake and (C) sweat gland temperature in Siberian hamsters during the 12-week period preceding food restriction. Values are mean ± SEM. (* = P < 0.05, ** = P < 0.01, *** = P < 0.001, **** = P < 0.0001).

3.4.2 Photoperiod Drives Investigatory and Thermoregulatory Behaviours

Food investigatory behaviour was assessed using the novel tri-arm test apparatus (fig. 3-3). There was no significant effect of photoperiod on time spent in the food chamber ($F = 0.698_{1, 31}$; $p = 0.41$) (fig. 3-5a). There was no significant effect of photoperiod on time spent in the treat chamber ($F = 0.945_{1, 31}$; $p = 0.339$) (fig. 3-5b). There was no significant effect of photoperiod on the time spent in the control chamber ($F = 4.07_{1, 31}$; $p = 0.052$) (fig. 3-5c). There was no significant effect of photoperiod on time spent in the central chamber ($F = 3.653_{1, 31}$; $p = 0.065$) (fig. 3-5d). Short photoperiod significantly increased total investigations of chow ($F = 20.458_{1, 31}$; $p < 0.001$) (fig. 3-5e). Short photoperiod significantly increases treat investigations ($F = 27.146_{1, 31}$; $p < 0.001$) (fig. 3-5f). Anxiogenic behaviour was investigated using the light-dark shuttle box test. There was no significant effect of photoperiod on time spent in the light area ($F = 0.955_{1, 33}$; $p = 0.336$) (fig. 3-6a). There was no significant effect of photoperiod on time spent in the dark area ($F = 0.955_{1, 33}$; $p = 0.336$) (fig. 3-6b). There was no significant effect of photoperiod on movement between the regions ($F = 1.849_{1, 33}$; $p = 0.183$) (fig. 3-6c). These data suggest that there were no photoperiod driven anxiogenic behaviours in these animals (Bourin and Hascoët, 2003). Thermoregulatory behaviour was tested using the tube test. Short photoperiod significantly increased the utilisation of tubing material for nest construction ($F = 48.738_{1, 33}$; $p < 0.001$) (fig. 3-6d).

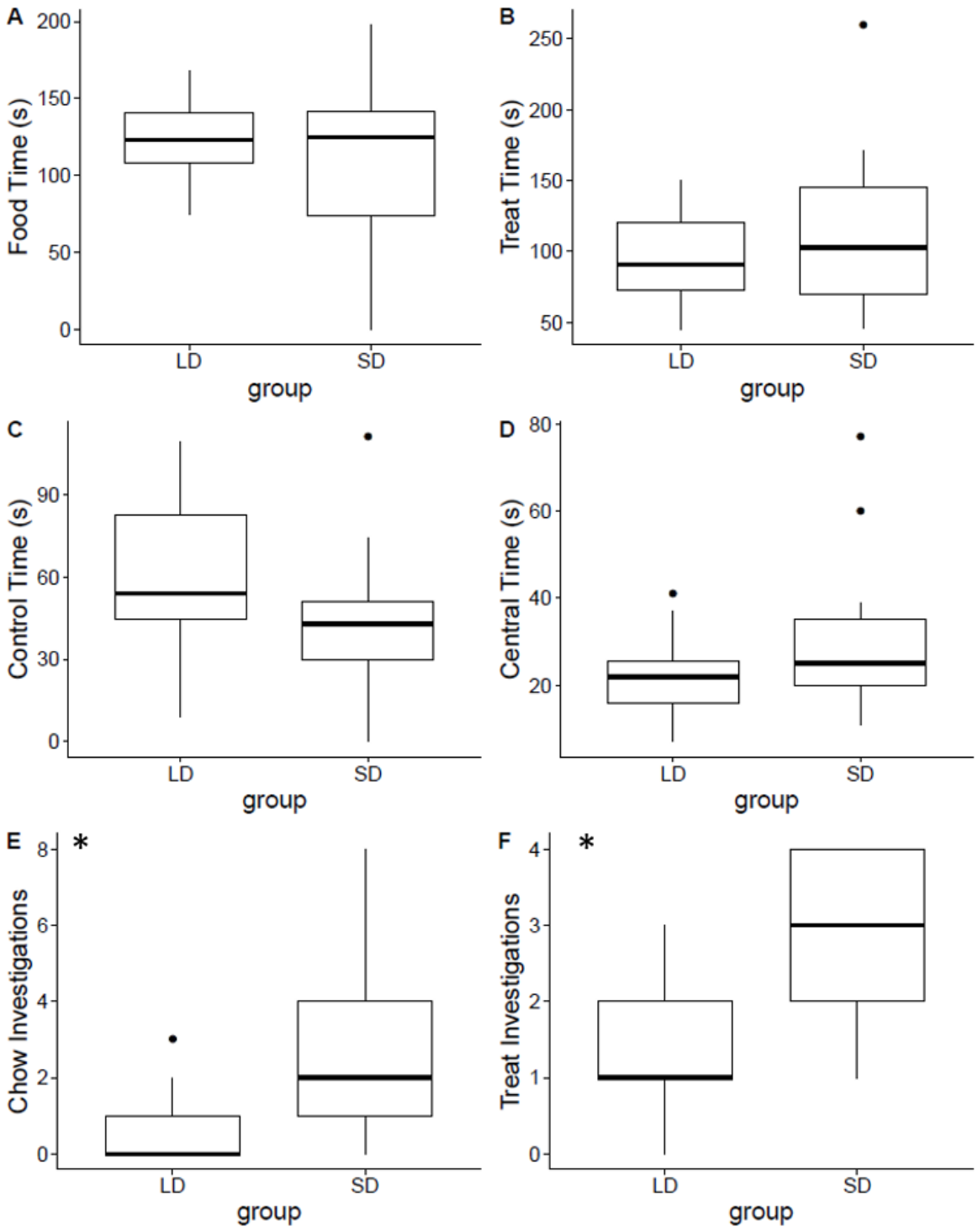

Figure 3-5: Investigatory behaviour and time spent in each chamber of the tri-arm test. (A) Time spent in the chamber containing chow. (B) Time spent in the chamber containing treats. (C) Time spent in the empty control chamber. (D) Time spent in the central chamber. (E) Total investigations of chow over the 5-minute period. (F) Total investigations of treats over the 5-minute period. Values are mean ± SEM. Asterix indicates significance by one-way ANOVA.

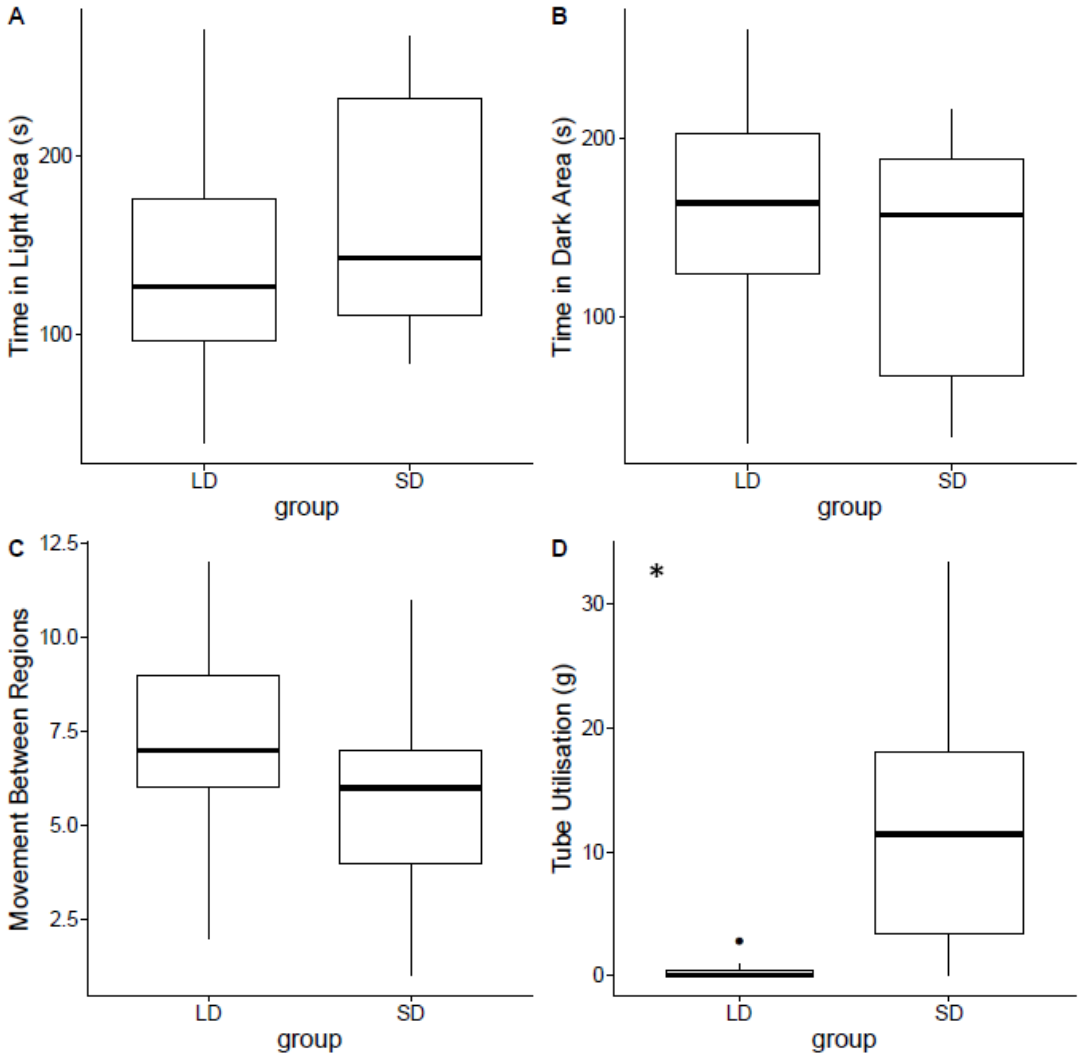

Figure 3-6: Anxiogenic and thermoregulatory behaviours tested using light-dark shuttle box and tube utilisation tests. (A) Time spent in the light area of the shuttle box. (B) Time spent in the dark area of the shuttle box. (C) Movement between the light and dark areas of the shuttle box test. (D) Percentage utilisation of tube for nesting material. Asterix indicates significance by one-way ANOVA.

3.4.3 Short Photoperiod Drives Daily Rhythmicity in Peripheral Body Temperature

Body temperature was measured across a 24-hr period in long and short-day Siberian hamsters. There was no significant effect of photoperiod on sweat gland temperature ($F = 0.056_{1, 278}$; $p = 0.814$) (Fig 3-7a). There was a significant effect of photoperiod on ear temperature ($F = 6.603_{1, 278}$; $p < 0.05$). Ear temperature was significantly increased at ZT +9 ($p = 0.028$), ZT +12 ($p = 0.0106$), ZT +15 ($p = 0.0036$) and ZT +18 ($p = 0.028$) vs ZT +0 in SD exposed Siberian hamsters (Fig 3-7b). These results suggest that rhythmicity in peripheral body temperature is dependent upon short photoperiod.

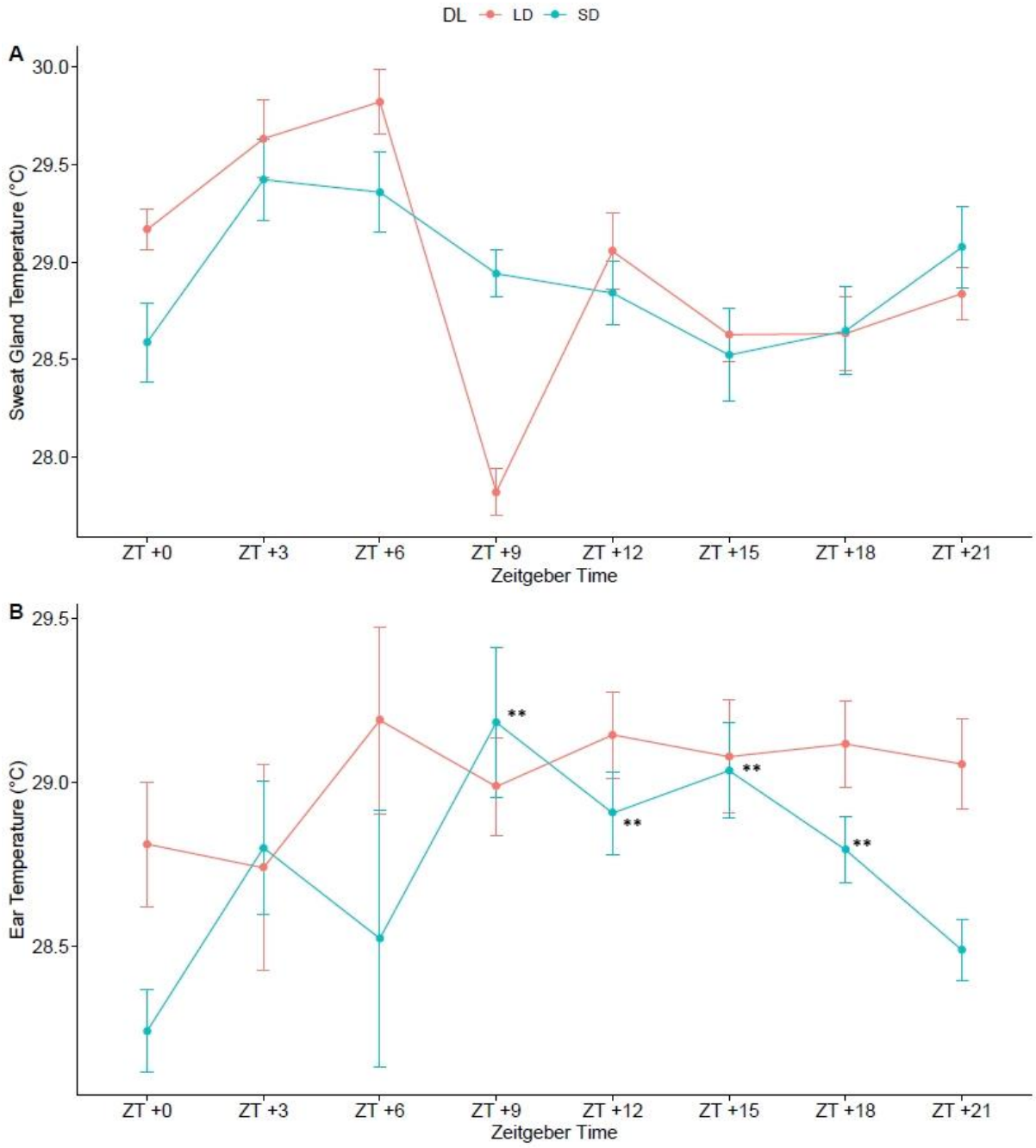

Figure 3-7: Daily body temperature of Siberian hamsters (n = 35) exposed to short photoperiods develops daily changes in peripheral body temperature. Sweat gland (A) and Ear (B) temperatures measured across a 24hr period in both long- and short-day Siberian hamsters. Values are mean ± SEM v ZT +0. (* = P < 0.05, ** = P < 0.01, *** = P < 0.001, **** = P < 0.0001).

3.4.4 Photoperiod Drives Greater Physiological Changes than Short-Term Food Restriction

To test the effectiveness of the food restriction protocol, change in body mass and body temperature over the restriction period was calculated. There was no significant effect of photoperiod on body mass change across the restriction period ($F = 0.156_{1, 31}$; $p = 0.696$). The food restriction protocol drove a significant decrease in body mass change ($F = 49.567_{1, 31}$; $p < 0.001$). There was no significant interaction between photoperiod and food restriction across the restriction period ($F = 0.031_{1, 31}$; $p = 0.861$).

Exposure to short photoperiod significantly reduced eWAT mass ($F = 112.346_{1, 31}$; $p < 0.001$). There was no significant effect of food restriction on eWAT mass ($F = 0.014_{1, 31}$; $p = 0.907$). There was no significant interaction of photoperiod and food restriction on eWAT mass ($F = 0.042_{1, 31}$; $p = 0.839$).

BAT mass was significantly lowered by exposure to short photoperiod ($F = 20.667_{1, 31}$; $p < 0.001$). There was no significant effect of food restriction on BAT mass ($F = 0.093_{1, 31}$; $p = 0.763$). There was no significant interaction between photoperiod and food restriction on BAT mass ($F = 0.07_{1, 31}$; $p = 0.793$).

Exposure to short photoperiod significantly reduced testes mass ($F = 409.891_{1, 31}$; $p < 0.001$). There was no significant effect of food restriction on testes mass ($F = 1.303_{1, 31}$; $p = 0.262$). There was no significant interaction between photoperiod and food restriction on testes mass ($F = 0.011_{1, 31}$; $p = 0.917$).

Short days drove a significant decreased in body temperature ($F = 6.26_{1, 31}$; $p < 0.05$). There was a significant effect of food restriction on body temperature ($F = 5.47_{1, 31}$; $p < 0.05$). There was no significant interaction between photoperiod and food restriction on body temperature ($F = 0.08_{1, 31}$; $p = 0.78$).

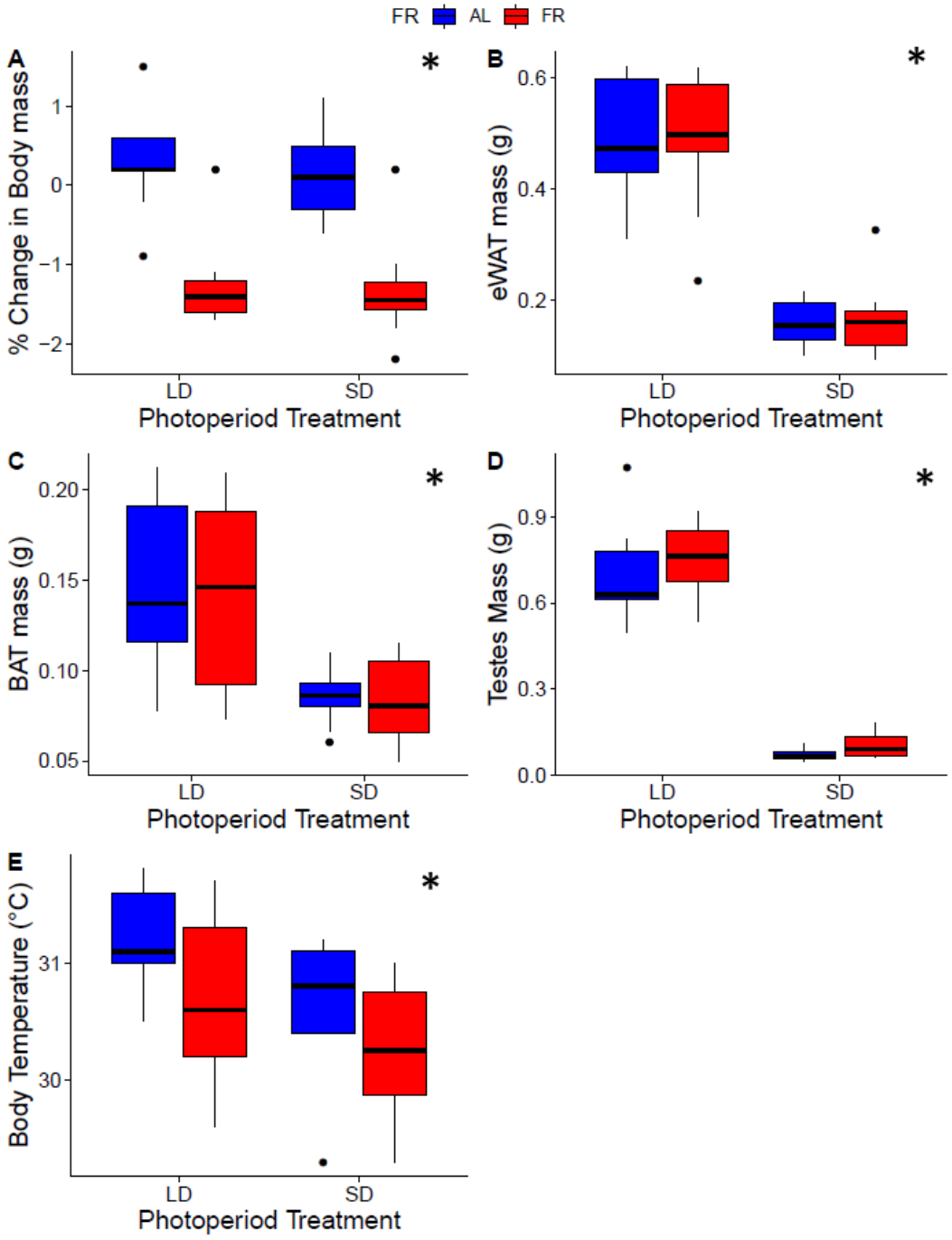

Figure 3-8: Physiological features of Siberian hamsters (n = 35) held under long (LD) or short (SD) photoperiods and treated with food restriction (FR) or maintained on ad libitum (AL) feeding. Such that there were four groups in this experiment LDAL (n = 9), LDFR (n = 9), SDAL (n = 9) and SDFR (n = 8). (A) Percentage change in body mass, (B) epididymal white adipose tissue mass, (C) interscapular brown adipose tissue mass, (D) Testes mass and (E) body temperature of Siberian hamsters under treatment conditions. Data shown is mean ± SEM. Asterix indicates significance by two-way ANOVA.

3.4.5 Photoperiod and Food Restriction Drive Unique Neuroendocrine Programmes

The expression of neuroendocrine markers of photoperiod and food restriction were measured using qPCR. There was no significant effect of photoperiod on *gh* expression ($F = 2.673_{1, 20}$; $p = 0.118$). There was no significant effect of food restriction on *gh* expression ($F = 0.411_{1, 20}$; $p = 0.529$). There was no significant interaction between photoperiod and food restriction on *gh* expression ($F = 0.006_{1, 20}$; $p = 0.939$) (fig. 3-9).

There was no significant effect of photoperiod on *lhb* expression ($F = 0.457_{1, 20}$; $p = 0.507$). Food restriction drove a significant increase in *lhb* expression ($F = 23.045_{1, 20}$; $p < 0.001$). There was no significant interaction between photoperiod and food restriction on *lhb* expression ($F = 0.039_{1, 20}$; $p = 0.845$).

There was no significant effect of photoperiod on *npy* expression ($F = 1.068_{1, 15}$; $p = 0.318$). Food restriction drove a significant increase in *npy* expression ($F = 6.441_{1, 15}$; $p < 0.05$). There was no significant interaction between photoperiod and food restriction on *npy* expression ($F = 0.337_{1, 15}$; $p = 0.57$) (fig. 3-9). This supports *npy* acting as a homeostatic marker in response to short term energy balance regulation.

There was no significant effect of photoperiod on *pomc* expression ($F = 0.005_{1, 15}$; $p = 0.946$). There was no significant effect of food restriction on *pomc* expression ($F = 1.907_{1, 15}$; $p = 0.188$). There was no significant interaction between photoperiod and food restriction on *pomc* expression ($F = 1.38_{1, 15}$; $p = 0.258$) (fig. 3-9).

Short photoperiod drove a significant decrease in prolactin expression ($F = 49.171_{1, 20}$; $p < 0.0001$). There was no significant effect of food restriction on prolactin expression ($F = 1.437_{1, 20}$; $p = 0.134$). There was no significant interaction between photoperiod and food restriction on prolactin expression ($F = 1.912_{1, 20}$; $p = 0.134$) (fig 3-9). Post-hoc analysis revealed significance between the LD FR and the SD FR ($p = 0.0369$) and SD AL ($p = 0.042$) groups, as well as between the LD AL and SD FR ($p = 0.012$) and SD AL ($p = 0.012$) groups.

Short photoperiod drove a significant increase in *sst* expression ($F = 5.587_{1, 14}$; $p < 0.05$). There was no significant effect of food restriction on *sst* expression ($F = 1.782_{1, 14}$; $p = 0.203$). There was no significant interaction between photoperiod and food restriction on *sst* expression ($F = 0.067_{1, 14}$; $p = 0.8$) (fig. 3-9). This supports *sst* acting as a rheostatic marker of energy balance regulation.

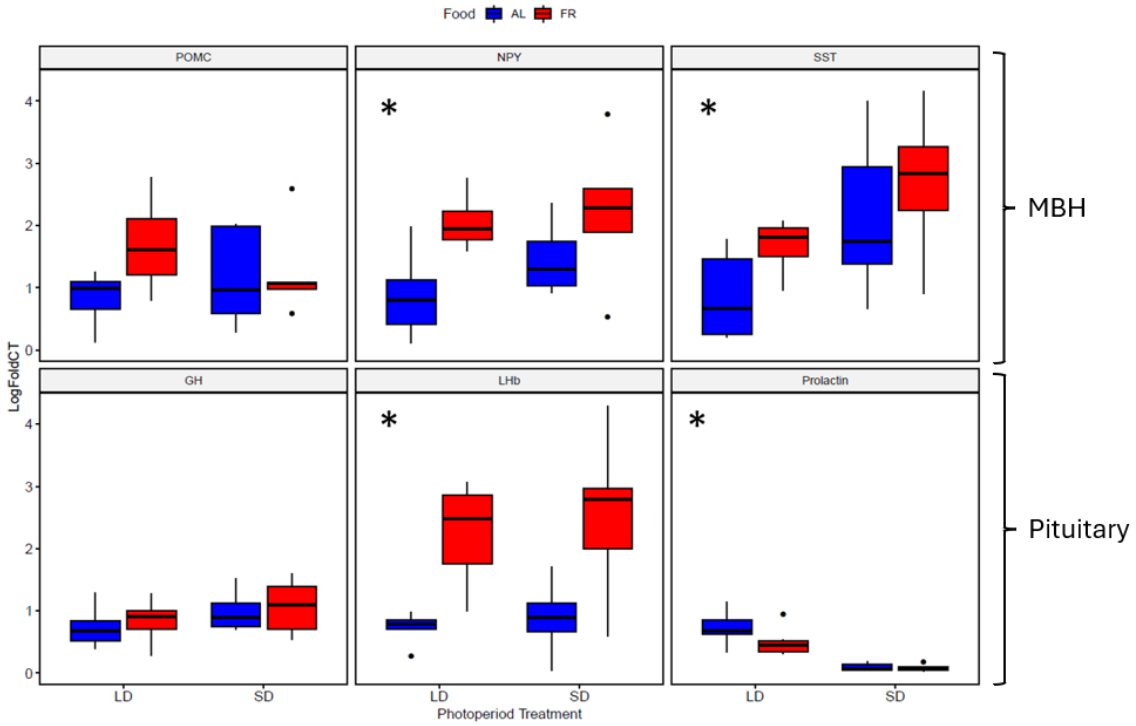

Figure 3-9: Logfold expression of neuroendocrine transcripts associated with seasonality and energy balance in Siberian hamster (n = 35) held under long (LD) or short (SD) photoperiods and treated with food restriction (FR) or maintained on ad libitum (AL) feeding. Transcripts were assessed by qPCR. Transcripts identified were GH, LHß, NPY, POMC, Prolactin and SST. Data shown is mean ± SEM. Asterix indicates significance by two-way ANOVA. POMC, NPY and SST qPCRs were performed on MBH cDNA. GH, LHß and Prolactin qPCRs were performed on pituitary cDNA.

3.4.6 Changes in Hormones Protect Seasonal and Energetic Blood Chemistry

Hormone and blood chemistry was investigated from terminal trunk blood. Plasma insulin levels were significantly decreased by exposure to short photoperiod ($F = 13.305_{1, 31}$; $p < 0.01$). There was no significant effect of food restriction on plasma insulin ($F = 3.45_{1, 31}$; $p = 0.073$). There was no significant interaction between photoperiod and food restriction on plasma insulin ($F = 0.468_{1, 31}$; $p = 0.499$). There was no significant effect of photoperiod on blood glucose ($F = 1.718_{1, 31}$; $p = 0.2$). There was no significant effect of food restriction on blood glucose ($F = 2.478_{1, 31}$; $p = 0.126$). There was no significant interaction between photoperiod and food restriction on blood glucose ($F = 1.009_{1, 31}$; $p = 0.323$). There was no significant effect of photoperiod on plasma GLP-1 ($F = 3.081_{1, 31}$; $p = 0.089$). Plasma GLP-1 levels were significantly reduced by food restriction ($F = 6.277_{1, 31}$; $p < 0.05$). There was no significant interaction between photoperiod and food restriction on plasma GLP-1 ($F = 3.392_{1, 31}$; $p = 0.075$). This data suggests that changes in blood chemistry are different during rheostatic and homeostatic changes in body mass.

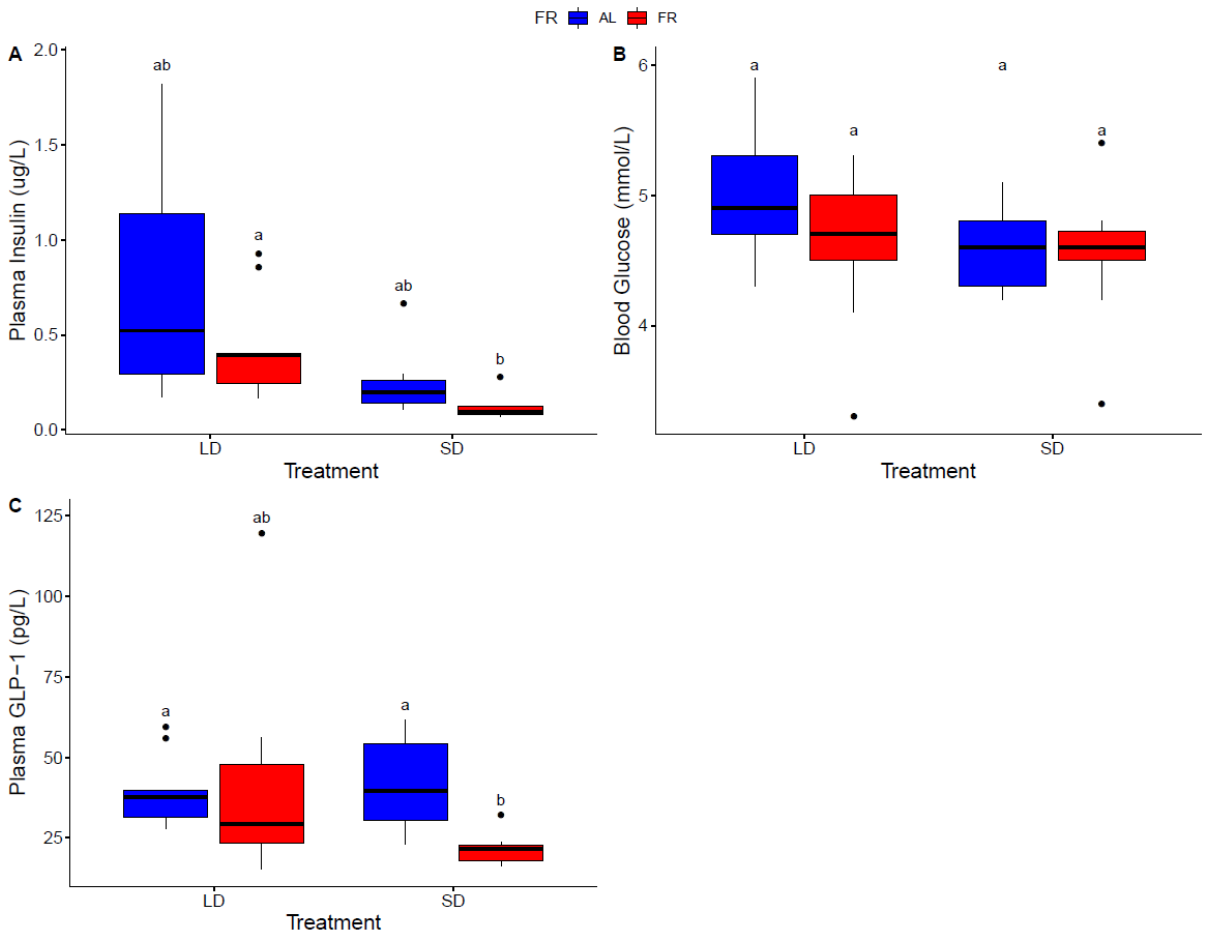

Figure 3-10: Chemistry of terminal trunk blood from Siberian hamsters under rheostatic (photoperiod) or homeostatic (food restricted) changes in body mass regulation. Animals in the AL condition were not fasted. (A) Plasma insulin, (B) blood glucose and (C) plasma GLP-1 levels assessed under the treatment conditions. Data shown is mean ± SEM. Lettering indicates significance groupings.

3.5 Discussion

In this study, it as hypothesised that, within a seasonal context, somatostatin would represent a neuroendocrine driver of rheostatic change in body mass. Further it was hypothesised that Neuropeptide y would act in a homeostatic manner under short photoperiod conditions. The data in this study showed that somatostatin is regulated exclusively by exposure to short photoperiod. Conversely, neuropeptide y showed upregulation in response to food restriction, but not to short photoperiod. These data support the hypothesis that somatostatin acts as a rheostatic output from the hypothalamus to drive body mass changes, while neuropeptide y acts in a homeostatic manner.

3.5.1 Rheostatic Changes in affective and thermoregulatory behaviour

Hamster behaviour showed some marked changes between the LD and SD conditions. There was no significant difference in time spent near the treat or chow pellets (fig. 3-5a-d). Siberian hamsters have been shown to alter dietary preference under short photoperiod conditions, with increased preference for carbohydrate intake under short photoperiods (Fine and Bartness, 1996). In this study no alterations in food preference were discovered, instead a general increase in investigatory behaviour of both food items was observed under SD (fig. 3-5e-f). It is notable that this increase occurred in both chow and treat pellets, indicating that there was no seasonal effect on food choice. However, this likely represents an SD driven increase in investigatory behaviour in Siberian hamsters, similar to data collected from novel object tests. Novel object exploration is a common method of assessing exploratory behaviour and has been used in seasonal contexts. Many studies have been carried out in birds have been carried out. In seasonal breeding rooks, willingness to approach a novel object appears stable throughout the year (Greggor et al., 2016). Though seasonally breeding warblers were found to possess a peak of novel object exploration in spring, with decreased exploration the rest of the year (Mettke-Hofmann, 2007). A study utilising female Siberian hamsters found that treatment with short photoperiods extended a pubertal decline in exploratory behaviour in ovariectomised animals (Kyne et al., 2019).Short photoperiods are known to drive anxiogenic and depressive affects in Siberian hamsters (Prendergast and

Nelson, 2005). Photoperiod driven changes in affective behaviour induced early in life appear capable of persisting into adulthood (Pyter and Nelson, 2006). Behavioural thermoregulation was investigated using the tube test and found a categorical increase in nest construction under short photoperiod conditions (fig. 3-6d). Increased availability of nesting materials does not appear to alter Siberian hamster metabolism under long or short photoperiods (Jefimow and Przybylska-Piech, 2022). Taken together with the data presented in this study, this implies that a short photoperiod increase in nest building is not a result of increased thermoregulatory requirements, rather a behavioural output of the seasonal program.

3.5.2 Food Restriction Drives Physiological Changes in Photoregressed Siberian Hamsters

Physiological factors associated with energy balance, such as eWAT mass (Fig 3-8b) and BAT (Fig 3-8c) mass did not show significant change across the food restricted period. It is notable that short term food restriction drove a decrease in body mass over the food restriction period (Fig 3-8a). This confirms the effectiveness of the food restricted feeding regimen. Changes in physiological factors such as eWAT and BAT mass may be being masked by the short-term nature of the food restricted protocol, however it was not possible to test this. Under natural photoperiods, energy requirements from thermoregulation drop by as much as 36% in the winter in Siberian hamsters (Heldmaier and Steinlechner, 1981). In this data set, body temperature was decreased only under food restricted conditions. Long term caloric restriction is well known to decrease core body temperature in rodents (Ferguson et al., 2007). Daily rhythmicity in peripheral (ear) body temperature exists only in the short day exposed Siberian hamsters (Fig 3-7). Notably, the food restricted decrease in body temperature is occurring without changes in BAT mass. Blood glucose levels were constant under both photoperiod and food restriction treatment (Fig 4-10b). It is likely that animals under both treatments will act to protect blood glucose levels in a homeostatic manner. This can be seen in plasma insulin and GLP-1 levels (Fig 3-10a, 3-10c), both of which require food restriction for significant changes in signal strength.

3.5.3 Hypothalamic Neuropeptides Track the Seasonal Rheostat or the Energy Balance Homeostat

Most neuropeptides appear to show either a response to photoperiod or, to food restriction. For example, NPY was significantly affect by food restriction, but not with photoperiod. This is in line with the expected pattern of this neuropeptide (Mercer et al., 2001). NPY acts by increasing motivation to eat, altering dietary and increasing meal size (Beck, 2006). It is known to be upregulated in the arcuate nucleus in response to acute food restriction (Bi et al., 2003). Its actions on behaviour are immediate and drives animals to large changes in food intake and body mass. In contrast, SST, acts by inhibiting the release of growth hormone from the pituitary gland (Siler et al., 1973). A short photoperiod increase in somatostatin gradually decreases growth hormone release and subsequently, total body mass (Scacchi et al., 1999). Similarly, SST, one of the strongest seasonal signals relating to energy balance (See chapter 2) shows a significant effect of photoperiod, but not from food restriction. Prolactin also showed the expected seasonal response and showed no effect of food restriction. GH did not show significant seasonal alterations, however it is likely that the short photoperiod driven limitation in SST is constraining GH release (Siler et al., 1973). Together, the observed changes in neuropeptide expression suggest that seasonal changes in body mass are driven by altered SST expression, while NPY remains responsive to energy balance.

This work was not able to replicate findings of reduced POMC intake under short photoperiod (Helfer and Stevenson, 2020; Mercer et al., 2000b). Which is consistent with the observed data presented in chapter 2. POMC has been reported to play a role in the rheostatic control of body mass (Helfer and Stevenson, 2020). This is further supported by the role that MC3R appears to play in rheostatic changes in body mass regulation (Butler et al., 2000; Chen et al., 2000; Ghamari-Langroudi et al., 2018). However, as discussed POMC expression is highly heterogeneous and not it is not fully understood exactly how hypothalamic POMC expression related to food intake. Some reports have noted that food restriction in Siberian hamsters drives a decrease in POMC neurons in the mid and rostral regions of the arcuate nucleus, but does not affect expression within the caudal region (Rousseau et al., 2002). Additionally, in intact golden hamsters, photoperiod drives an increase in POMC expression

within the middle and caudal parts of the arcuate nucleus, but not the rostral zone (Bittman et al., 1999). Thus, it is possible that unique populations of POMC are responsible for rheostatic and homeostatic change and that bulk processing of the MBH as a single tissue is masking these effects. Another possibility is that seasonal changes occur in post-translational modification of POMC. The prohormone convertases PC1/3 and PC2, which are responsible for POMC processing, appear to be vary under different photoperiods. In the Siberian hamster an SD driven increase in PC2 may lead to preferential processing of POMC into α-MSH (Helwig et al., 2006). Together, these results could explain the lack of effect of photoperiod on POMC expression within this study. It is possible that widely reported changes in MC3R expression that occur under short photoperiods in Siberian hamsters could be responsible for any rheostatic action of POMC.

It is also worth considering that, as reductions in body mass precede reductions in food intake, animals entering the seasonal waveform are in a persistent positive energy balance state relative to the “set-point” of body mass. In models of chronic dietary restriction, classically orexigenic peptides such as NPY and AgRP can be upregulated, playing an important role in refeeding when food is available (Yu et al., 2009). IT is possible that a similar mechanism may explain paradoxical findings of certain seasonal neuropeptides.

Perhaps the most surprising finding was that LHß showed a strong response to food restriction but not to photoperiod (Fig 3-9). NPY has significant inhibitory effects on LHß expression irrespective of season in sheep (Barker-Gibb et al., 1995). However, sheep and hamsters have markedly different seasonal cycles (see chapter 1). Food restriction is known to drive a loss of pulsatile LH secretion in mammals (Cameron and Nosbisch, 1991). Decreases in arcuate Kisspeptin expression is thought to drive this decrease. This loss of kisspeptin has been suggested to be driven by leptin, with leptin administration reversing LH loss (Ba Henry et al., 2001). Later studies found that only pharmacological levels of leptin had this effect, with administration of physiological leptin levels having no effect (True et al., 2011). It is also possible that ghrelin signalling drives changes in kisspeptin expression under food restricted conditions (Forbes et al., 2009). However, the noted increase in LH expression is difficult to explain.

3.8 Conclusions

This chapter has demonstrated the independence of homeostatic and rheostatic in energy balance. This can more specifically be described as the difference between rheostatic (seasonal) and homeostatic (food restricted) changes in energy balance. Somatostatin (SST)is upregulated by short photoperiod exposure, acting in a rheostatic manner to control body mass. Neuropeptide Y (NPY) is not affected by photoperiod, instead it responds to food restriction, acting to regulate body mass in a homeostatic manner. This separation of homeostatic and rheostatic is essential for optimising seasonal fitness. It permits a gradual decrease in energy intake without the risk of entering a starvation state. Further, if some neuropeptides associated with energy balance continue to act as in a strictly homeostatic manner, such as NPY. This would allow for the rheostat to change the “set point” of body mass, while regular homeostatic mechanisms remain functional. A simplified diagram of this can be seen in figure 3-11. Rheostatic lowering of body mass in Siberian hamsters by photoperiod is a temporary phenomenon. After a period, animals will become refractory to photoperiod and the rheostatic set point of body mass will revert. In the next chapter the distinction between this rheostatic increase in body mass and a seasonally inappropriate high body mass will be investigated.

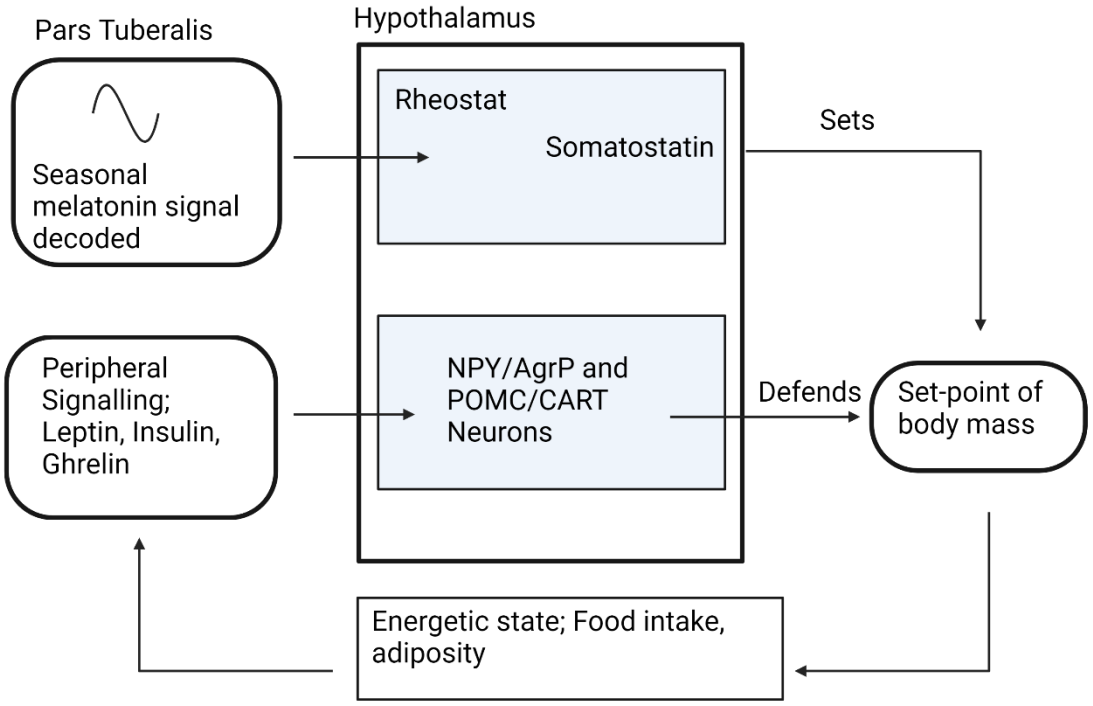

Figure 3-11: Simplified diagram of hypothalamic rheostatic and homeostatic regulation of body mass. A hypothalamic rheostat drives somatostatin output to regulate the set-point of body mass. The hypothalamic homeostat responds to peripheral signalling to defend the set-point of body mass. Figure made with Biorender.com.

Chapter 4: Homeostatic Mechanism Protect Blood Chemistry Despite Rheostat Driven Seasonal Changes in Energy Balance

4.1 Introduction

Previous chapters have investigated molecular change associated with the seasonal waveform and investigated the distinction between homeostatic and rheostatic changes in neuropeptide expression. In this chapter, a seasonally inappropriate body mass will be generated by treating Siberian hamster with obesogenic diets, to disrupt rheostatic regulation of body mass.

4.1.1 Rheostat Driven Seasonal Increase in Body Mass

The initial response of Siberian hamsters to short photoperiods appears distinct from the refractory responses which later predominates. Refractoriness to photoperiod signals in Siberian hamsters typically persists until “reset” by a long photoperiod signal (Goldman, 2001). Gorman and Zucker challenged Siberian hamster with an intermediate photoperiod (10L:14D) to investigate seasonal cycling under these conditions. They found that Siberian hamsters initially displayed initial regression of testes volume and body and subsequent recrudescence. However, they found that Siberian hamsters in 10L photoperiods showed further periods of regression in testes and body mass. This data indicates that the program driving refractoriness to short photoperiods may be a distinct timer from the initial seasonal response (Gorman and Zucker, 1995). In chapter 2, several neuropeptides were identified as being differentially expressed between obese long photoperiod animals and obese photorefractory animals.

4.1.2 Obesity and programmed rheostatic changes in body mass

Obesity is a major risk factor for conditions such as type 2 diabetes, coronary heart disease and hypertension. The wide range of consequences which arise from obesity leads to great healthcare and economic costs, some estimates suggest that an obese individual costs healthcare systems an increase of up to 40% compared to a non-obese individual, on average (Lehnert et al., 2013). Obesity generally coincides with a wide range of metabolic changes, including increased blood pressure, insulin resistance and high fasting glucose levels generally referred to as metabolic syndrome. Large changes in blood triglycerides and high density lipoproteins (HDL) are key elements of diagnosing

metabolic syndrome (Cornier et al., 2008). Higher blood triglyceride and lower HDL levels appear to drive higher incidences of ischaemic heart disease at rates higher than other elements of obesity such as high blood pressure (Jeppesen et al., 2000).

In humans, there is evidence of seasonal changes in energy balance and body mass. Significant seasonal variations in body mass have been discovered in human children, with decreased body weight in summer (Kobayashi and Kobayashi, 2006). Notably, this study also discovered that obese children showed an atypical summer increase in body weight, suggesting that disruption of seasonal body weight regulation may play a role in obesity. In addition, the presence of human BAT shows strong seasonal variation. Human BAT is more likely to be present in adults during winter months, and more likely to be present in females than males (Au-Yong et al., 2009). This could imply the presence of seasonal energy expenditure in humans. Some studies have also suggested the presence of seasonal food intake in humans. Humans appear to increase total caloric intake in fall, primarily driven by increased carbohydrate intake (de Castro, 1991). Interestingly, individuals in this study rated themselves as feeling hungrier after a meal during fall, suggesting that changes in body mass may be driven, in part, by behavioural changes.

The similarities between seasonal changes in body mass and obesity have led to suggestions that the Siberian hamster could be used as a model for studying obesity (Lewis and Ebling, 2018; Murphy et al., 2013; Schuhler and Ebling, 2006). For example, leptin resistance is a major feature of the metabolic changes which occur during obesity. Leptin, an adipose derived hormone, which acts via it’s receptor in a STAT3 dependant manner, in multiple hypothalamic regions including the arcuate nucleus, the dorsomedial hypothalamus and ventromedial hypothalamus to regulate energy balance (Myers et al., 2008). Central action of leptin on its receptor achieves this in multiple ways, leptin modulates the action of neurons in the hypothalamus to reduce food intake while simultaneously stimulating sympathetic nervous activity leading to increase energy utilisation by adipose tissue (Enriori et al., 2006). Leptin resistance and a loss of this regulatory system is a key feature of obesity, though the mechanisms driving this are not completely understood, some have suggested that alterations to transport of leptin across the blood brain barrier via decreased sensitivity of

leptin receptors within the median eminence. However, more recent studies have suggested that leptin maintains its ability to transfer across the blood brain barrier and that reduced binding efficiency in the arcuate nucleus may be the primary mechanism by which leptin insensitivity develops(Izquierdo et al., 2019). LD exposed Siberian hamsters are leptin resistant, notably this photoperiodic regulation of leptin resistance appears independent of body mass, as food restricted long day animals appear to maintain leptin insensitivity (Rousseau et al., 2002). This provides key evidence that the response to peripheral hormone signalling forms an element of the rheostatic program of seasonal body mass regulation. Leptin concentrations decrease in SD Siberian hamsters, and it has been suggested that this decrease in leptin is necessary for the initiation of seasonal torpor in Siberian hamsters (Freeman et al., 2004). In Syrian hamsters, treatment with high fat diet drives a reversible increase in body weight. When high fat diet is removed from Syrian hamster they revert to, and maintain, a seasonally appropriate body weight, this occurs without any major changes in food intake (Wade and Bartness, 1984). Studies such as this suggest that adiposity and seasonality have some degree of shared regulation by peripheral signalling.

However, there exist major differences between rheostat driven seasonal gain in body mass which occur seasonally in refractory Siberian hamsters and dietary driven obesity. First, while obesity primarily results from an increase in adiposity, seasonal changes in mass are far more widespread, affecting multiple tissues and systems (See chapter 2). Second, seasonal change in body mass occurs as a result of rheostatic changes in the ‘set point’ of body mass (Steinlechner et al., 1983). These two differences are key in discussing the mechanisms underlying seasonal changes in body mass. It is notable that the hypothalamic regulation of neuropeptides such as POMC appears to paradoxically increase under short photoperiod conditions in Siberian hamsters (Bao et al., 2019). Highlighting the key differences in body weight regulation under seasonal and obese conditions.

High fat diets can drive alterations in neuropeptide expression associated with energy balance. Short term high fat dietary treatment does not significantly affect expression of homeostatic expression of NPY, AgRP, POMC or CART in the rat hypothalamus (Heijboer et al., 2005). However, a more prolonged high fat

diet drives an increase in POMC and CART expression in the murine hypothalamus (Chaar et al., 2016). It does, however, drive alterations in peripheral insulin sensitivity and triglycerides accumulation (Heijboer et al., 2005). *Cart* expression has been found to increase in short photoperiod exposed Siberian hamsters (Adam et al., 2000). This change in Cart expression is consistent with the observed changes which occur in obese mouse models, where increased Cart expression is associated with decreasing body mass (Robson et al., 2002). Notably, somatostatin, which in chapter 2 and 3 was identified as a key regulator of rheostatic changes in body mass, appears protective against some of the metabolic changes which occur due to high fat diet, such as increased triglycerides and low density lipoprotein (LDL) in plasma (Li et al., 2010). Activation of somatostatin receptors by an artificial agonist of somatostatin appears to inhibit body mass by lowering food intake through an increase in satiety (Stengel et al., 2010).

Male rodents appear to be at significantly higher risk of deleterious health effets due to high fat diets, such as obesity, and metabolic and mental disruptions (Hwang et al., 2010). Female rodents display higher expression of POMC under HFD than male rodents, and this may serve to mitigate the higher caloric intake in females (Freire-Regatillo et al., 2020). However, male and female Siberian hamsters display similar physiological response ton short photoperiods, though do display some sex-specific changes in immune function (Bilbo and Nelson, 2003). HFD represents a major paradigm by which to differentiate seasonal and obese change sin body mass in male and female Siberian hamsters.

Molecular changes which occur during the photorefractory phase of the seasonal waveform are distinct from the changes that occur in long photoperiod animals. As Siberian hamsters become refractory, some transcripts, which were downregulated during the initial photoperiod response are upregulated again, such as the GnRH receptor (B. J. Prendergast et al., 2002). However, there are also unique changes in expression associated with photorefractoriness such as an upregulation of Solute carrier, family 1, member (*Slc1a2*) (B. J. Prendergast et al., 2002). In the arcuate nucleus, transcripts such as VGF (non-acronymic), Cellular retinoic acid binding protein 2 (*Crabp2*) and histamine H3 receptor (*H3r*) show a photorefractory switch back to long photoperiod like expression levels (Ross et al., 2005). Other transcripts such as *crbp1* and *rar*a show

downregulation upon exposure to short photoperiods but do not recover when refractory. It is notable that these changes precede refractory gains in body mass (Ross et al., 2005). The suppressor of cytokine signalling-3 (*Socs3*) is a transcript which is involved in the development of leptin insensitivity. *Socs3* deficient mice are resistant to diet induced weight gain and are protected from leptin insensitivity (Mori et al., 2004). Socs3 is downregulated by exposure to short photoperiods in Siberian hamsters and recovers as they become photorefractory (A. Tups et al., 2006). This presents some evidence of a seasonally programmed rheostatic mechanism regulating hypothalamic response to adiposity.

4.2 Hypothesis

Blood chemistry will remain stable despite large rheostatic changes in physiology. Altered dietary composition will disrupt the homeostatic defence of blood chemistry and body mass. Treatment of an obesogenic diet may reverse seasonal anorexia and induce metabolic disruption in blood chemistry. Similarly, treatment with a low-fat diet may lead to reductions in circulating triglycerides and cholesterol.

4.3 Methods

4.3.1 Ethics

All procedures carried out were conducted under home office license (PP5701950) and in accordance with ARRIVE guidelines at the veterinary research facility at the University of Glasgow. Male (n = 44) and female (n = 43) Siberian hamsters (*Phodopus Sungorus*) were used in this study.

4.3.2 Experimental Design

Animals were individually housed in polypropylene cages in either 16h light (LD) or 8h light (SD) for 8 weeks. Rodent chow (SDS [BK001]) and tap water were provided ad libitum. Body weight and food intake were measured weekly. Animals were held at a room temperature of 21°C, and a humidity of 50%. In the final week of the experiment animals in SD were transferred to treatment diets containing High Fat High Sugar (HFHS) (Special Diets Service [RM SY AFE 30% Fat 33% Sucrose 827140]) (female n = 4, male n = 4), Low Fat High Sugar (LFHS) (Special Diets Service [RM SY AFE 12% Fat 33% Sucrose 827139]) (female n = 5, male n = 5), Low Fat Low Sugar (LFLS) (Special Diets Service [RM SY AFE 12% Fat 5% Sucrose 827141]) (female n = 4, male n = 4), or remained on chow (female n = 5, male n = 5). Nutritional information of the diets is provided in table 3.2. During the final week, body mass and food intake were measured daily. At the end of the 8th week body mass, sweat gland temperature and pelage score were recorded. Animals were sacrificed by cervical dislocation followed by exsanguination. Interscapular brown adipose tissue and epididymal white adipose tissue were dissected, weighed and frozen on dry ice. Terminal trunk blood sample was collected and heparinised with 50ul heparin (Workhardt, 1,000 I.U./ml, PL 29831/0109). Gonad mass was recorded to confirm seasonal photoregression of reproduction. Tissues were stored at -80°C.

4.3.3 Blood Chemistry Analysis

Blood glucose, total triglycerides (TG), HDL cholesterol and total cholesterol (TC) was measured from truck blood. Measurements were carried out using a Standard LipidoCare Analyser (02LA10G) (SD Biosensor). This instrument is validated for medical diagnosis in humans and has the following testing limits (TG = 45 – 650 mg/DL, TC = 100 – 450 mg/dL, HDL = 25 – 95 mg/dL). Standard

Lipid Check Strip (02LCH10) (SD Biosensor) were used to characterise blood triglycerides and HDL. Standard Lipid Check Strip – Total Cholesterol (02LS20) (SD Biosensor) was used to characterise total cholesterol. Codefree Blood Glucose Test Strip (01GS11) (SD Biosensor) was used to measure blood glucose. Following measurements, plasma was separated and stored at -80°C.

4.3.4 Statistical Analysis

Food intake data was converted to total caloric intake using manufacturers indications of calorie content. Data was tested for normality using the Shapiro-Wilk test. When data violated normality, it was log transformed for analysis. Pre dietary treatment significance was determined using one-way repeated measures ANOVA. Changes in body mass were transformed to a percentage from starting body mass. Two-way ANOVAs were conducted to test for significance (Treatment and Sex). Post-hoc analyses were carried out using one sample t-test, using the SD chow fed group as a reference. Post hoc testing data was Bonferroni adjusted to minimise type 1 error rate. All data was analysed using the R package Rstatix and plotted using the r package GGPUBR. Data was considered significant when $P < 0.05$.

4.4 Results

4.4.1 Body Mass and Food Intake Confirm the Seasonal Response Prior to Dietary Treatment

In male hamsters there was a significant effect of photoperiod on body mass ($F = 20.945_{4, 224}$; $p < 0.001$). Post-hoc analysis revealed that significance occurred between the pre-treatment group and the 6 weeks ($P = 0.0024$) and 8 weeks ($P < 0.000001$) groups (fig 4-1a). In male hamsters there was a significant effect of photoperiod on food intake ($F = 12.402_{4, 178}$; $p < 0.001$). In female hamsters there was a significant effect of photoperiod on body mass ($F = 4.52_{4, 213}$; $p < 0.05$). Post-hoc analysis revealed that significance occurred between the pre-treatment group and the 6 weeks ($P = 0.016$) and 8 weeks ($P = 0.0017$) groups (fig 4-1c). In female hamsters there was a significant effect of photoperiod on food intake ($F = 8.148_{4, 178}$; $p < 0.05$). Post-hoc analysis revealed that significance occurred between the pre-treatment group and the 2 weeks ($P = 0.012$), 4 weeks ($P = 0.006$) and 6 weeks ($P = 0.024$) groups (fig 4-1d).

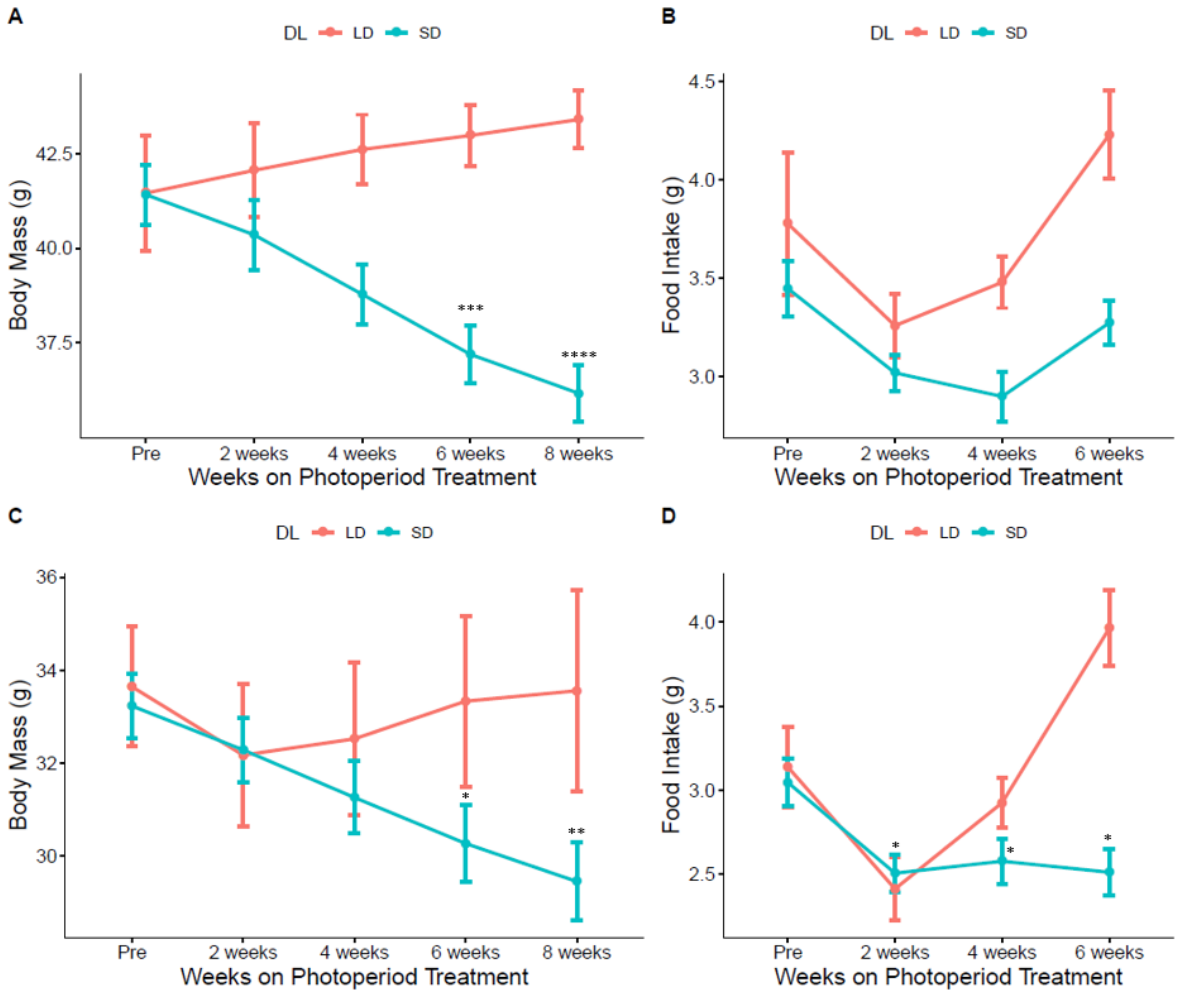

Figure 4-1: Photoperiod driven changes in body mass in male (n = 44) and female (n = 42) Siberian hamsters maintained on Long (male n = 10, female n = 8) or short (male n = 36, female n = 35) photoperiods. (A) Body mass of male Siberian hamsters. (B) Food intake of male Siberian hamsters under long and short photoperiods. (C) Body mass of female Siberian hamsters under long and short photoperiods. (D) Food intake of female Siberian hamsters under long and short photoperiods. Values are mean ± SEM. (* = P < 0.05, ** = P < 0.01, *** = P < 0.001, **** = P <0.0001 vs. control animals)

4.4.2 Dietary intake drives body mass changes in a sex dependant-manner

To test the effectiveness of different diets in SD hamsters, HF HS, LF HS and LF LS diets were given to male and female Siberian hamsters after 8 weeks SD exposure. Two-way ANOVA revealed that diet drove a significant effect on body mass change ($F = 24.221_{4, 529}$; $p < 0.001$). Sex did not drive a significant effect on body mass change ($F = 0.058_{1, 529}$; $p = 0.81$). There was an interaction effect of diet and sex on body mass change ($F = 9.667_{4, 529}$; $p < 0.001$). Post hoc testing revealed that male animals possessed a significant decrease in body mass after 1 day of dietary treatment with the LF LS diet (P = 0.012) (fig. 4-2a). On the second day of treatment male animals possessed significantly reduced body mass when treated with both HF HS (P = 0.02) and with LF LS (P = 0.028) diets. By the third day of treatment male animals showed significantly reduced body mass when treated with both HF HS (P = 0.0016) and with LF LS (P = 0.028) diets. No male animals showed significantly reduced body mass on day 4 of treatment. On day 5, male animals showed significantly reduced body mass when treated with LF LS diet (P = 0.044). By the third day of treatment female animals showed significantly reduced body mass when treated with HF HS (P = 0.04) diet. On the sixth day of treatment male animals showed decreased body mass when treated with HF HS diet (P = 0.0013). Female animals did not possess a significant decrease in body mass after one day of treatment (fig. 4-2b). On the sixth day of treatment female animals showed decreased body mass when treated with LF HS diet (P = 0.028).

Food intake was measured and converted to kilocalories (kcal) based on manufacturers specifications. Two-way ANOVA revealed that diet drove a significant effect on food intake ($F = 30.987_{4, 450}$; $p < 0.0001$). Sex did not drive a significant effect on food intake change ($F = 0.005_{1, 450}$; $p = 0.945$). There was an interaction of diet and sex on total food intake ($F = 5.92_{4, 450}$; $p < 0.001$). Post-hoc analyses revealed that male animals possessed decreased intake after one day of treatment with HF HS (P = 0.000792) and LF LS (P = 0.0000488) diets (fig. 4-2c). On the second day of treatment male animals possessed decreased intake with HF HS (P = 0.012) and LF LS (P = 0.056) diets. On the third, fourth and fifth days of treatment male animals did not show decreased intake on any treatment. On the sixth day of treatment male animals displayed decreased

intake when treated with HF HS diet (P = 0.0018). Post-hoc analyses revealed that female animals possessed decreased intake after one day of treatment with LD Chow (P = 0.004) and LF HS (P = 0.008) diets (fig. 4-2d). On the second day of treatment female animals possessed decreased intake with LD Chow (P = 0.0028) and HF HS (P = 0.0039) diets. On the third, fourth and fifth and sixth days of treatment male animals did not show decreased intake on any treatment.

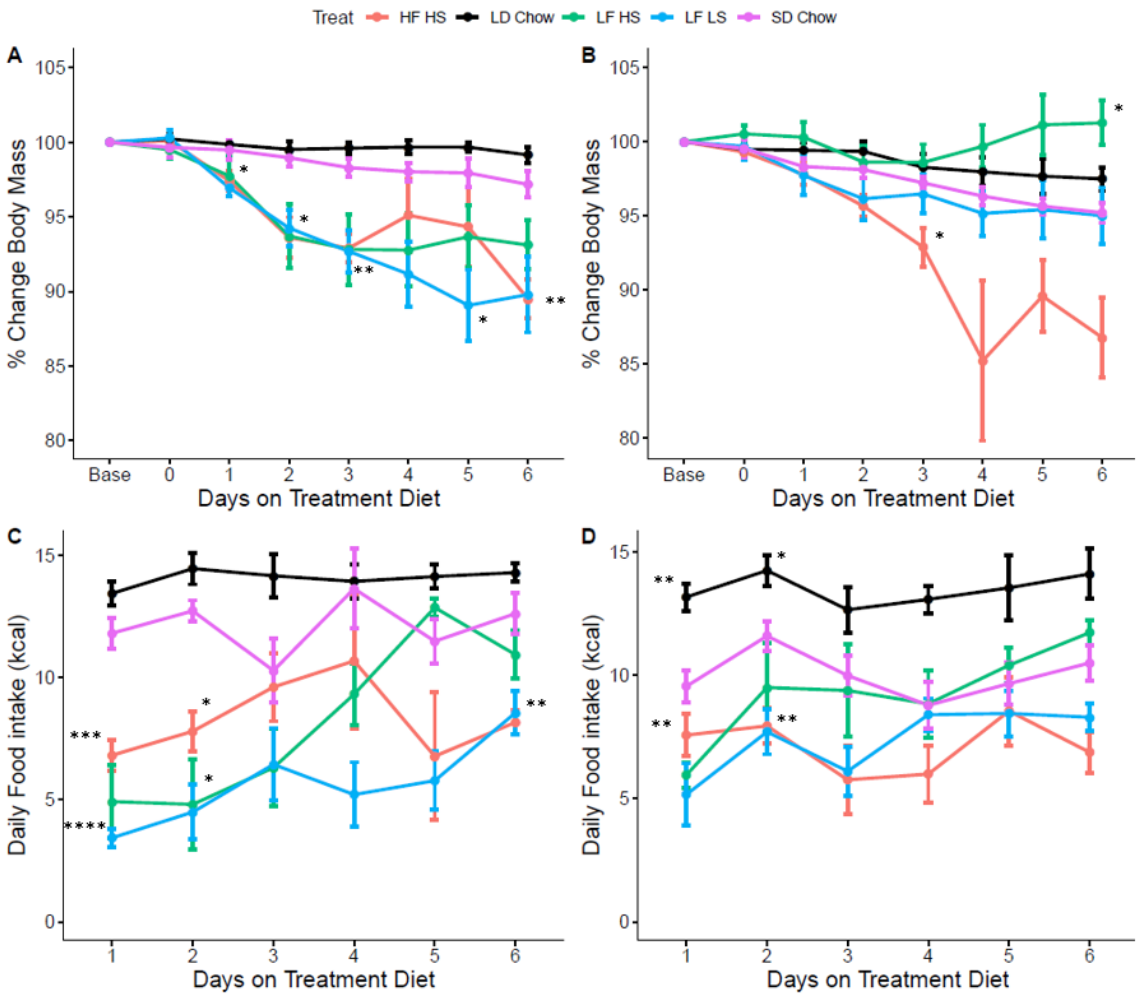

Figure 4-2: Percentage change in body mass and daily food intake in male (n = 44) and female (n = 42) short photoperiod exposed Siberian hamsters maintained on high fat high sugar diets (male n = 9, female n = 9), low fat high sugar diets (male n = 7, female n = 9), low fast low sugar diets (male n = 9, female n = 8), maintained on chow (male n = 9, female n = 9) or maintained on long photoperiod with chow (male n = 9, female n = 7). Body weight in male (A) and female (B) Siberian Hamsters measured over the treatment period. Food intake in kcal/day in male (C) and female (D) Siberian hamsters measured over the treatment period. Values are mean ± SEM. (* = P < 0.05, ** = P < 0.01, *** = P < 0.001, **** = P <0.0001 vs. control animals)

4.4.3 Diet Drives Limited Changes in Rheostatic Energy Regulation

To confirm seasonal responsiveness and investigate if dietary conditions affected the degree of seasonal responsiveness gonad mass (fig. 4-3a) was recorded immediately after animals had been sacrificed. Diet drove a significant effect on gonad mass ($F = 156.741_{4, 76}$; $p < 0.001$). Sex did drive a significant effect on body mass change ($F = 48.08_{1, 76}$; $p < 0.001$). There was an interaction effect of treatment and sex on body mass change ($F = 31.171_{4, 76}$; $p < 0.001$). Male animals display significantly increased gonad mass when fed with chow diet on LD ($p = 2.59E-07$) (fig. 4-3a). Male animals did not show any significant differences under different dietary treatments. Treatment drove a significant effect on sweat gland temperature in Siberian hamsters ($F = 4.026_{1, 76}$; $p < 0.001$). There was no effect of sex on sweat gland temperature ($F =0.353_{1,76}$; $p < 0.001$). There was no interactions of sex and treatment on sweat gland temperature ($F =0.178_{4, 76}$; $p < 0.001$). Female animals possessed significantly higher sweat gland temperature under the LD Chow treatment than the SD Chow treatment ($P = 0.00677$). There was a significant effect of treatment on BAT mass ($F = 20.918_{4, 76}$; $p < 0.001$). There was a significant effect of sex on BAT mass ($F = 8.876_{1, 76}$; $p < 0.01$). There was no interaction of treatment and sex on BAT mass ($F = 1.731_{4, 76}$; $p > 0.05$). There was a significant effect of treatment on WAT mass ($F = 22.223_{4, 76}$; $p < 0.001$). There was a significant effect of sex on WAT mass ($F = 320.161_{1, 76}$; $p < 0.001$). There was an interaction of treatment and sex on WAT mass ($F = 6.688_{4, 76}$; $p < 0.0001$) (fig. 4-3d).

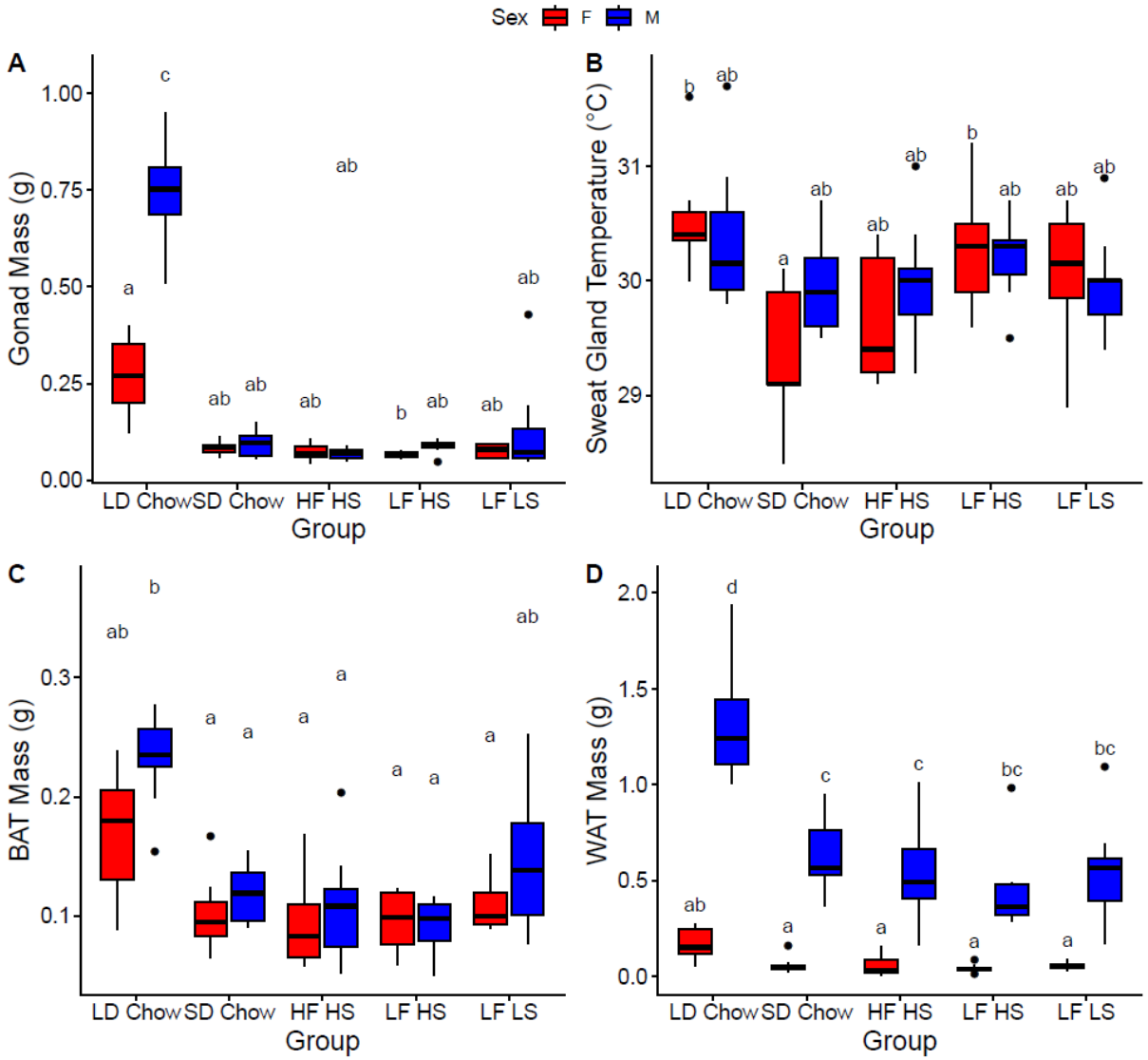

Figure 4-3: Physiology of male (n = 44) and female (n = 42) short photoperiod exposed Siberian hamsters maintained on high fat high sugar diets (male n = 9, female n = 9), low fat high sugar diets (male n = 7, female n = 9), low fat low sugar diets (male n = 9, female n = 8), maintained on chow (male n = 9, female n = 9) or maintained on long photoperiod with chow (male n = 9, female n = 7). Gonad mass (A), sweat gland temperature (B), BAT mass (C) and WAT mass (D) of short photoperiod exposed Siberian hamster fed treatment diets. Data shown is mean ± SEM. Lettering indicates significance groups ($P < 0.05$).

4.4.4 Internal Milieu Remains Relatively Constant Under Different Dietary Conditions

The blood chemistry profile of animals was assessed using the Standard LipidoCare Analyser (SD Biosensor). There was no significant effect of treatment on blood glucose levels mass ($F = 2.149_{4, 76}$; $p > 0.05$). There was no significant effect of sex on blood glucose levels ($F = 0.019_{1, 76}$; $p > 0.05$). There was no interaction of treatment and sex on blood glucose levels ($F = 0.97_{4, 76}$; $p > 0.05$) (fig. 4-4a). There was no significant effect of treatment on total cholesterol ($F = 1.341_{4, 76}$; $p > 0.05$). There was no significant effect of sex on total cholesterol ($F = 0.236_{1, 76}$; $p > 0.05$). There was a significant interaction of treatment and sex on total cholesterol ($F = 4.007_{4, 76}$; $p < 0.05$). There was a significant effect of treatment on triglycerides ($F = 2.698_{4, 76}$; $p < 0.05$). There was a significant effect of sex on triglycerides ($F = 7.481_{1, 76}$; $p < 0.05$). There was no significant interaction between treatment and sex on triglycerides ($F = 2.539_{4, 76}$; $p > 0.05$). Post hoc analysis of this data revealed that significance occurred between the female LD Chow fed group and the female LF HS ($P = 0.020475$) and LF LS ($P = 0.040815$) groups. The female LD Chow was also significantly different from the male LD chow fed group ($P = 0.0243$) (fig. 4-4c). The LipidoCare Analyser used for this analysis has testing limits, for HDL cholesterol these are 25 – 95 mg/dL. In this experiment a majority of animals in many groups were above this limit and for this reason the data has been excluded from analysis.

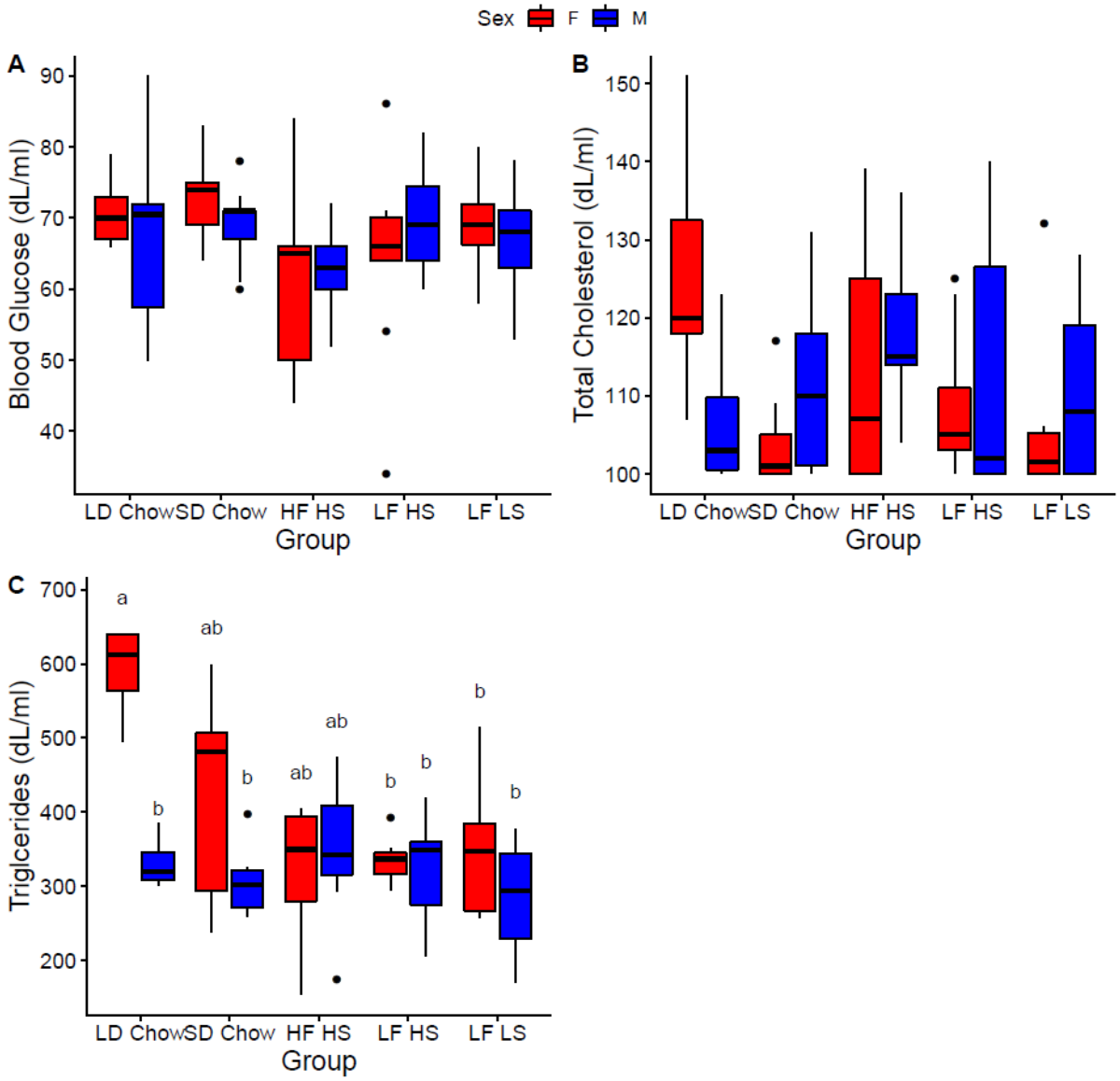

Figure 4-4: Blood chemistry of male (n = 44) and female (n = 42) short photoperiod exposed Siberian hamsters maintained on high fat high sugar diets (male n = 9, female n = 9), low fat high sugar diets (male n = 7, female n = 9), low fast low sugar diets (male n = 9, female n = 8), maintained on chow (male n = 9, female n = 9) or maintained on long photoperiod with chow (male n = 9, female n = 7). Blood glucose (A), total cholesterol (B) and triglycerides (C) of male and female Siberian hamsters in different treatment diets. Data shown is mean ± SEM. Lettering indicates significance grouping ($P < 0.05$).

4.5 Discussion

This chapter identified minimal changes in body mass of Siberian hamsters under most experimental conditions. Sex-specific response to high fat and high sugar diets in Siberian hamsters when presented with novel diets were identified. Both male and female hamsters showed large decreases in food intake upon exposure to new dietary conditions, followed by gradual acclimatisation and increase in food intake. Male hamsters showed significantly larger decreases in food intake than females, and additionally generally required a longer period to recover food intake (fig. 4-2). Sex specific response to altered diets, such as a high fat diet (HFD) have previously been well reported in rodents. Female rodents have demonstrated considerable resistance to the obesogenic effects of HFD, primarily driven by sex specific differences in hypothalamic regulation rather than differences in food intake. Female mice exposed to brief periods of HFD show reduced hypothalamic *npy* expression, while the major hypothalamic change in males is a reduction in *pomc* expression (Oraha et al., 2022). In female, but not male mice, HFD appears to drive a significant increase in median eminence neurogenesis and female weight gain in response to HFD seems to depend on this neurogenesis (Lee et al., 2014). Expression of ciliary neurotrophic factor (CNTF) in murine tanycytes is significantly increased under HFD conditions, but not in *ob*/*ob* animals, suggesting that tanycytes play a key role in regulating energy status in response to dietary changes via a mechanism independent of leptin signalling (Severi et al., 2013). In male mice, ablation of the median eminence drives increases in adiposity without a total increase in body mass, while also driving an increase in light phase energy expenditure (Yoo et al., 2020). Tanycytes are also thought to be critical to seasonal regulation (see introduction), these studies, taken in a seasonal context imply tanycytes as important integrators of seasonal and energetic conditions of an organism.

4.5.1 Stable Blood Chemistry under Rheostat Driven Reductions in Body Mass

Hamsters did not show significant changes in blood chemistry when treated with an obesogenic diet. Total cholesterol was protected across photoperiod and dietary treatments (fig 4-4b). Seasonal changes in total triglycerides are notable in that they only show significant seasonal change in male Siberian hamsters (fig.

4-4c). Male animals display far greater changes in adiposity than females (fig. 4-3d) and this likely leads to larger changes in blood triglycerides. Male Siberian hamsters only showed significantly reduced triglycerides when treated with one of the two low fat diets, implying that this change represents homeostatic disequilibrium rather than genuine rheostatic change. In support of this idea, Syrian hamsters melatonin injection to long photoperiod animals has no impact on plasma cholesterol levels despite large changes in circulating thyroid hormone (Vaughan et al., 1983). Changes in blood triglycerides are not well studied from a seasonal perspective in model organisms. However, seasonal changes in human triglyceride levels have been noted. In middle-aged humans, triglyceride levels are mildly higher in spring in women, but drastically higher during winter in men (Letellier and Desjarlais, 1982). Though curiously, the data presented here shows photoperiod driven changes occurring only in female hamsters (fig. 4-4). This chapter has demonstrated that seasonal changes in body mass are not ameliorated by exposure to an obesogenic diet, in fact most diets appear to increase the rate of weight loss. Sex-specific effects are also clear as female animals were the only group to gain weight on any treatment diet, with SD female animals fed LF HS diet showing a gradual increase. Overall, this data indicates a relatively stable blood chemistry exists in animals which are undergoing rheostat driven changes in body mass. Despite large seasonal reductions in body mass, blood chemistry remains homeostatically protected at physiological levels to maintain the health of the organism.

4.5.2 Sex-specific Response to High-Fat and High-Sugar Diets in Siberian Hamsters

Most groups in this study displayed reduced food intake and reduced body mass for the majority of the experimental period (fig. 4-2). Curiously, female mice were the only group to demonstrate an increase in body mass on any of the treatment conditions, with an increase in body mass when fed the LF HS diet (fig. 4-2b). Sex specific responses to high fat and high sugar diets have previously been reported in rodents. Both high fat and high sugar diets drive widespread changes in gut- and neuroinflammation. However female rodents appear to show more widespread changes in cytokine expression, which may lead to altered gut-brain axis signalling and subsequently response to altered diets (Church et al., 2022). This is especially worth noting as female hamsters do

not show higher food intake under LF HS diets, so the increase in weight may only be occurring from altered processing of food intake.

Dietary composition does not appear to significantly affect the physiology of the animals exposed to short photoperiods (fig. 4-3). Obesity is known to drive disruptions of reproductive fitness and to do so in a sex dependant manner. Short term exposure to high fat diets drives structural changes in both male and female rodent gonads. In males these changes include decreased diameter of seminiferous tubules and decreased number of Sertoli cells (Matuszewska et al., 2020). These changes bear some similarity to histological changes which occur in the testes of seasonal hamsters. In photo regressed Siberian hamsters, diameter of seminiferous tubules decreases drastically, however the number of Sertoli cells remains constant under short photoperiod (Sinha Hikim et al., 1988). In female animals, obesity driven reproductive changes include decrease in the diameters of corpora lutea and decrease in the diameter of ovarian follicles (Matuszewska et al., 2020). While obesity, drives changes in the diameter of follicles, short photoperiod drastically decreases their numbers. Large increases in the rate of follicular apoptosis leads to the seasonal development of follicular atresia and the loss of ovarian function (Moffatt-Blue et al., 2006). It could be expected that if obesity and photoperiod differentially drive gonad changes then there could be interacting effects of obesity and photoperiod on gonad mass. However, this is not apparent in this data, it is possible that photoperiod changes may mask any changes in gonad mass driven by obesity due to the extreme nature of seasonal changes.

4.5.3 Limitations

It should be noted that this experiment focuses only on one time point in the seasonal cycle. This may limit the interpretation of these results as changes occurring in blood chemistry, as with changes in neuropeptides seasonal blood chemistry may change dynamically across the seasonal waveform. Further analyses could involve multiple time-points in the seasonal waveform, most crucially the inclusion of a photorefractory group could allow for greater insight into the distinction between rheostatic recrudescence of body mass and seasonally inappropriate gain in body mass. Another limitation is the time scale during which animals were maintained on treatment diets, which may not have

been sufficient for significant physiological effects to arise. Rats maintained on high-fat diets can show significance increase in body mass after just one week of dietary treatment (Gauthier et al., 2006). It is notable that high fat diet did not induce a dyslipidaemia in these animals, which would be expected to develop as a result of high dietary fat regardless of changes in body mass. This may indicate that rheostatic alterations in food intake may eliminate the increase preference of rodents for high fat and high sugar diets.

4.6 Conclusions

The data presented within this chapter implies that an inappropriate obese phenotype generated by altered dietary conditions may be distinct from seasonal obesity. This is inline with findings from previous chapters. In chapter 3 it was demonstrated that seasonal rheostatic changes in neuropeptide expression which control body mass were distinct from the homeostatic mechanisms which defend body mass. In this chapter, it was demonstrated that blood chemistry remains stable under rheostatic changes in body mass. This is a critical element of allowing animals to survive the large changes in physiology. It indicates that blood chemistry continues to be protected homeostatically during the seasonal waveform and is unaffected by large rheostatic changes in energy balance.

Chapter 5 – General Conclusions

This thesis has aimed to characterise the molecular mechanisms underlying seasonally programmed energy rheostasis. By using a strategy of nuclei-specific transcriptome sequencing, several novel seasonal transcripts were identified. Many seasonal transcripts showed a pattern of expression in which there was an increase during the early photoreactive phase of the seasonal cycle. Of transcripts related to energy balance, the only major transcript which tracked rheostatic change in body mass was somatostatin. In chapter 3, the distinction between molecular regulation of homeostasis and rheostasis was investigated. Somatostatin was found to be non-responsive to an acute negative energetic challenge in the homeostatic regulation of body mass. In chapter 4, the seasonal energy balance rheostat was examined by altering dietary composition and caloric intake to increase positive energy balance. Under rheostatic change in body mass, blood chemistry remains homeostatically defended. However, alteration of dietary conditions can disrupt the homeostatic mechanisms defending blood chemistry. No dependent variable observed in short photoperiod hamsters was found to revert to long photoperiod conditions. This shows that under large changes in energy balance, homeostatic mechanisms continue to maintain seasonal programs in energy rheostasis. Overall, the data presented in this thesis support a clear distinction between rheostasis and homeostasis, and that rheostatic changes may leave homeostatic mechanisms relatively unperturbed.

5.1 – The role of hypothalamic neuropeptides programmed seasonal rheostasis

This thesis set out to characterise the molecular mechanisms underpinning the rheostatic changes associated with seasonal changes in physiology in the Siberian hamster. Recent developments in next generation sequencing technologies have allowed for new investigations into the molecular characteristics of seasonal changes in physiology. Recently, Illumina sequencing was used to characterise seasonal transcripts in the Siberian hamster (Bao et al., 2019).

In chapter 2, a study design in which Siberian hamsters were held in short photoperiods for up to 32 weeks and individual hypothalamic nuclei were sequenced at 4-week intervals. Rheostatic seasonal change are known to be

dynamic over time. For example, *dio3*, a critical enzyme involved in the regulation of photoperiodic signalling, expression begins to decline after 8 weeks in short photoperiod conditions (Milesi et al., 2017). These changes in *dio3* expression are driven by reversible DNA methylation within the promoter region of the gene (Stevenson and Prendergast, 2013). This thesis applied next generation sequencing technologies to Siberian hamster hypothalamic nuclei at distinct points in the seasonal waveform to identify unknown seasonal transcripts which may play a role in regulating the rheostatic set-point. This sequencing approach focused on the hypothalamus, at a nuclei-scale resolution, in order to determine the relative cycling of transcripts within individual hypothalamic nuclei. Additionally, this strategy allowed for distinct phases of the seasonal interval timer to be investigated.

Pituitary sequencing included the PD. A total of 250 transcripts were detected as seasonal rhythmic, with a large of number of these representing transcripts which were novel in a seasonal setting within the pars distalis. The well-known seasonal cycle of prolactin (Stewart and Marshall, 2022) was recapitulated during this sequencing. Some transcripts, such as *Mcoln1* (fig 2-7), have a pattern of expression which suggest a general decrease in exocytotic release during the photoreactive phase of the seasonal waveform. This implies that the pars distalis of the pituitary is reducing its total output during rheostatic and may implicate the tissue as a driver of physiological change.

5.1.1 TSH Signalling is the Photoperiod Responder in the Seasonal Rheostat

The MBH sequencing revealed 290 seasonal transcripts. The MBH was sectioned in such a way that several distinct regions were included in sequencing analyses. These included the PT of the pituitary, the ependymal layer of the third ventricle and the arcuate nucleus (ARC). The Arcuate nucleus is a major centre for the homeostatic regulation of energy balance, containing key neuron populations including POMC/CART neurons and NPY/AGrP neurons (Hill, 2010; Morton and Schwartz, 2001). These homeostatic neurons are responsive to circulating hormones, it is important to consider the external signals which may drive rheostasis. Thyroid hormone signalling is critical for the timing of seasonality. Previous work which has investigated *tshb* expression has identified

it as a major photo responsive gene within the pars tuberalis (Dardente et al., 2010). However, several studies have identified that TSH signalling is not recovered as animals become photorefractory (Milesi et al., 2017). This was replicated by data presented in this these (fig. 2-10). Loss of TSH signalling in short photoperiods drives an increase in *dio3* expression in Siberian hamsters (Hanon et al., 2008). From the perspective of rheostasis, TSH signalling represents a key responder to environmental conditions (photoperiod). It likely does not play a role in any timing mechanism necessarily, apart from potentially acting as an initiator, or in some species an entrainer, of endogenous rhythmicity. This suggests that the timing of rheostatic seasonal change occurs downstream of TSH signalling.

5.1.2 Somatostatin as the MBH rheostatic driver

Despite large changes in body mass and food intake, there were no observed changes in these classic energy regulating transcripts. Instead, somatostatin appears to be the primary transcript associated with energy balance which showed seasonal cycling. *Sst* showed a pattern of expression inverse to the seasonal cycle in body mass. This is in line with the expected role of this hormone as a regulator of growth hormone excretion from the pars distalis of the pituitary (Ferland et al., 1976). *Sst* expression is downregulated by TSH administration to short photoperiod Siberian hamsters (Klosen et al., 2013). Further, treatment of artificial somatostatin agonists drives short photoperiod like response in body mass and testicular regression in male Siberian hamsters (Dumbell et al., 2015). Somatostatin also regulates prolactin synthesis via receptor subtype Sstr2 (Shimon et al., 1997). This shows that somatostatin may act as a key output which effects rheostat driven changes in physiology. In chapter 2, it was shown that *tshb* expression within the PT was not necessary for a photorefractory increase in MBH somatostatin expression, as *sst* shows a strong photorefractory response while both *tshb* and *cga* do not. This suggests that somatostatin responds both to an initial photoperiod responder (TSH) but also to the endogenous timer. Sst therefore represents a key candidate for a rheostatic output. However, the exact nature of the timing mechanism underlying this change in rheostatic output remains to be elucidated.

5.1.3 A Rheostatic Timing Program is Switch-Like Within the Medio-basal Hypothalamus

Within the MBH sequencing several transcripts possessed a pattern of expression markedly like that of *dio3*. This implies a set of transcripts which are directly under the control of thyroid hormone signalling. Potentially, representing an immediate program within the hypothalamus which subsequently drives rheostatic changes in set-point of physiology. *Mef2c* is a transcription factor involved in neurogenesis and potentially plays a role in thyroid hormone signalling (Lee et al., 1997). *Mef2c* is interesting from the perspective of an interval timer, as it has been shown to upregulate the microRNA miR-92b which can, on turn, down regulate *mef2c* expression (Chen et al., 2012). *Mef2c* has been linked to the development of SST positive neurons (Allaway et al., 2021). Further, silencing of thyroid and retinoic acid receptors inhibits *mef2c* and leads to changes in histone deacetylase activity, providing further links to seasonal changes (Wu et al., 2001). Transcripts such as *mef2c* may be critical in the interval timing of the seasonal rheostatic control of energy balance in the Siberian hamster. If transcripts such as *mef2c* are involved in rheostatic changes then the downstream targets of *mef2c* within the hypothalamus should be investigated.

Many other novel transcripts may be involved in neurogenesis, such as *sugct* (*Busskamp* et al., 2014). A recent study proposed that seasonal changes in body mass are driven by neurodegeneration, arising from the loss of thyroid and retinoic acid signalling (Helfer et al., 2019). They proposed that compensatory neurogenesis from the tanycyte population counteract this and leads to the generation of seasonal rhythms (Helfer et al., 2019). Sequence evidence presented here provides evidence of seasonal neurogenesis occurring exclusively within the photoreactive phase of the seasonal waveform. *Mef2c* and associated transcripts may be acting to drive neurogenesis during the photoreactive phase. However, it is unclear if changes in expression are occurring within a stem cell niche, such as tanycytes, or if they represent changes in expression in adult neurons.

Evidence of remodelling of the tanycytes in Siberian hamsters exists both in literature (Kameda et al., 2003) and in data presented in chapter 2. Vimentin,

an intermediate filament component of the cytoskeleton, is expressed in tanycytes and has previously been demonstrated to be downregulated by short photoperiods in Siberian hamsters (Bolborea et al., 2011). Interestingly, tanycytes play an important role in the control of the timing of the oestrus cycle. Tanycyte end feet remodelling across the oestrus cycle facilitates changes in GnRH release (Prevot et al., 1999). Similarly, tanycyte process remodelling is significantly altered by exposure to short photoperiod (Kameda et al., 2003). In chapter 2, vimentin was shown to be downregulated by exposure to short photoperiod and to remain so as the animals become photorefractory (fig. 2-10f). This is in line with previous findings of vimentin (Herwig et al., 2013) and implies that tanycyte remodelling is not a core component of the timing element of rheostatic changes. Therefore, tanycytes represent a key candidate cellular population for the control of rheostatic changes in physiology. Further, it suggests that changes within tanycytes, e.g. *dio3*, occur within individual cells. If tanycytes are maturing into neurons within the hypothalamus, as some reports suggest (Moore et al., 2022), then expression of vimentin may remain low. Thus, it remains possible that tanycytes may act as a neurogenic niche across seasons and that this may play a role in rheostatic changes.

In future studies, the resolution of this sequencing could be substantially improved on a cellular level. This could be achieved by several approaches such as single cell RNA sequencing, or potentially via techniques such as FISH targeted against novel transcripts or proteins of interest. It will be critical to investigate the temporal relationship between transcripts in one hypothalamic nuclei and others. Potentially via administration of or inhibition of identified transcripts potentially responsible for driving the timing of the seasonal interval timer.

5.2 – Homeostatic Mechanisms Defend the Rheostatic "Set-point" of Body Mass

One of the major proposed models of seasonal change to body mass, is the change in a rheostatic set-point (Mercer et al., 2000a). However, much of the molecular basis driving changes in set-point are poorly understood. Chapter 3 and 4 investigated the distinction between rheostatic and homeostatic changes in energy balance. In the chapter 2 somatostatin had been identified as the key neuroendocrine signal of seasonal body mass. With other neuropeptides showing

no seasonal cycling. Chapter 3 utilised a food restriction protocol to differentiate between neural markers of homeostatic and rheostatic changes in energy balance regulation. Hamsters showed a typical body mass loss of approximately 1 gram after a 24-hour food restriction (fig. 3-8a). This loss in body mass demonstrates that both LD and SD exposed animals remain responsive to food restriction and a protocol to separate the neural control of homeostasis and rheostasis.

Neuropeptide expression within the hypothalamus was investigated to differentiate the homeostatic and rheostatic molecular programs. Neuropeptide-y is a key neuropeptide involved in the control of energy balance. In chapter 3, *npy* did not show any significant seasonal change, but showed significant upregulation after food restriction (fig 3-9). This suggests that *npy* acts only as a homeostatic regulator of energy balance. *Npy* has previously been reported to play a homeostatic role regardless of seasonal condition (Ebling and Barrett, 2008). Overexpression of *agrp,* which is co-expressed with *npy*, in short photoperiod exposed Siberian hamster, drives an increase in food intake but does not prevent seasonal body mass loss (Jethwa et al., 2010). Ablation of the arcuate nucleus using monosodium glutamate treatment, destroys the vast majority of POMC/CART and NPY/AgRP neurons but leaves seasonal cyclicity in body weight intact (Ebling et al., 1998). Some studies have identified slight photoperiod driven reductions in *npy* and *pomc* (Reddy et al., 1999). However, in this study the response of these neuropeptides to food restriction was far larger than to photoperiod. These results indicate that the neuroendocrine systems governing rheostasis and homeostasis are distinct at a molecular level. Rheostatic changes involve alterations to the set-point of body mass (Mrosovsky, 1990). This data implies that, under seasonal conditions, homeostatic mechanisms continue to defend the set-point without playing a role in the establishment of this set-point. This shows that homeostatic mechanisms and neuron populations responsible for homeostasis remain functional and are unaltered by rheostatic change in body mass. For example, an animal which lost upwards of 30% of it's body mass, as Siberian hamster do, would be classically under extreme homeostatic stress. Changes in the expression within POMC/CART and NPY/AgRP neurons would be large to ameliorate the energetic challenge. That this does not happen demonstrates the key role of homeostatic

neuropeptides in defending a set-point established by rheostasis. Results from chapter 2 indicated that individual hypothalamic nuclei follow unique patterns of expression. Chapter 2 identified *Sst* as the primary neuroendocrine marker of seasonal energy balance. In chapter 3, *Sst* expression was significantly increased under SD exposure (fig. 2-10), supporting data collected in chapter 2. *Sst* is expressed within the periventricular nucleus of the hypothalamus, which lies adjacent to the third ventricle, as well as the arcuate nucleus (Farhy and Veldhuis, 2004).

Conversely, classic arcuate transcripts associated with energy intake appear to act in a primarily homeostatic manner. Taken together, this could suggest that the arcuate nucleus and associated neuropeptides act to defend the rheostatic set-point of body mass in a homeostatic manner. The set-point does not instantly change, rather a progressive decrease in the defended set point of physiology occurs over a period of time. Periods of food restriction have previously been shown to not affect the set-point of body mass change (Steinlechner et al., 1983). In Soay sheep, *dio3* expression is increased in response to short photoperiod, but decreases as the animals become refractory to short photoperiod, without (Sáenz de Miera et al., 2013). This shows that the dissociation of TSH signalling and the endogenous timing of photorefractoriness persist across taxa and may represent an evolutionarily conserved rheostatic timing mechanism. The gradual change in the set-point may be an adaptation which allows animals to avoid homeostatic stresses as seasons change. In chapter 2, several transcripts were found to be upregulated exclusively within the photoreactive phase of the seasonal cycle and may represent a molecular program which decreases the set-point gradually. This rheostat may act as an on-off switch which controls the drift of the set-point, however more work is necessary on the effects of these neuropeptides on any rheostatic change in set-point. An example of this possible model of seasonal rheostatic change can be seen in figure 5-1.

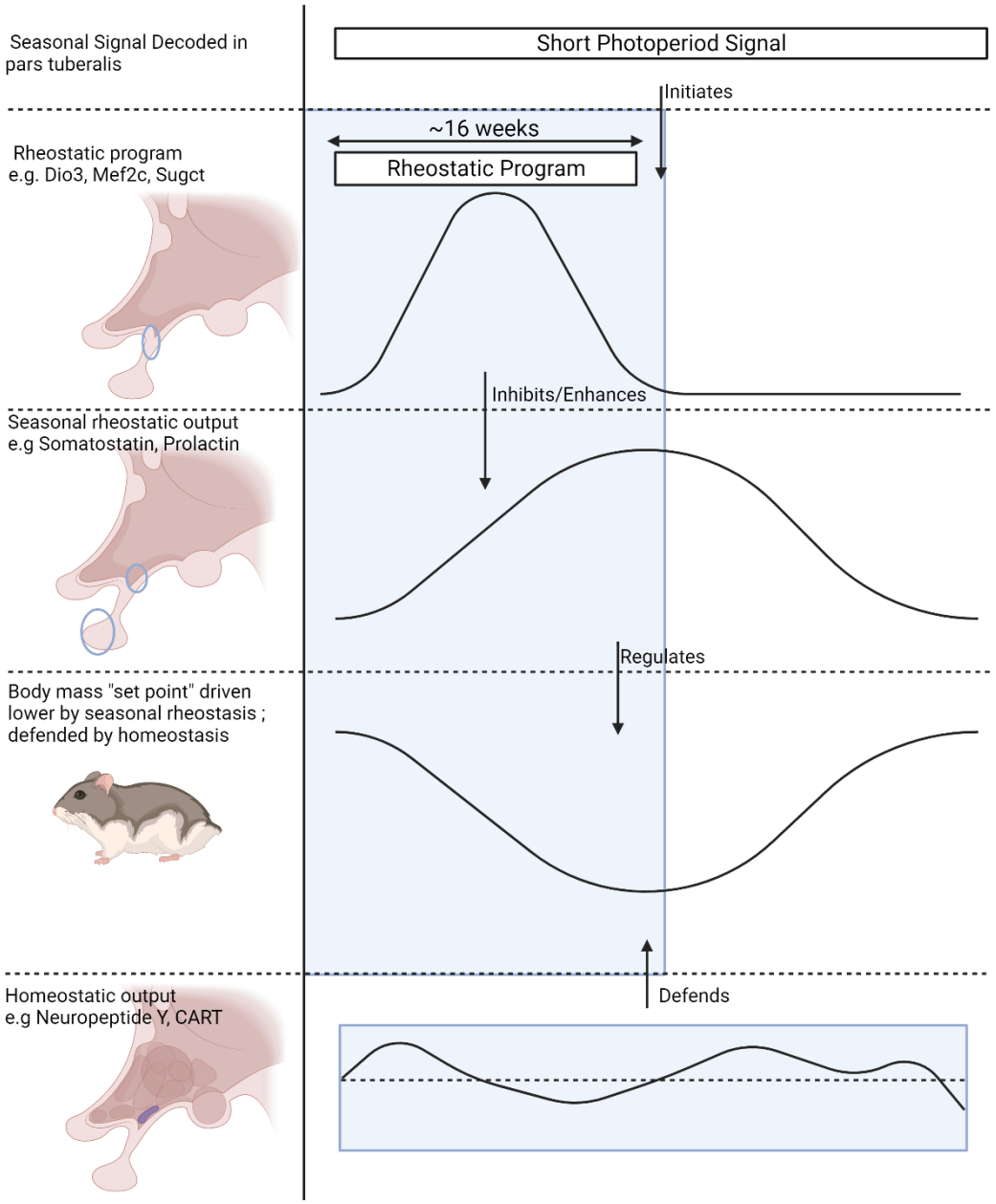

Figure 5-1: The proposed model of rheostasis mediated seasonal change in body mass. An interval timing mechanism active in the photoreactive phase of the seasonal cycle drive body mass down. After 16 weeks this mechanism is no longer active and body mass increases. Meanwhile, homeostatic mechanisms act to defend the new set-point of body mass. Figure made with Biorender.com.

5.3 – Internal Milieu Defence Demonstrates Homeostasis Despite Rheostatic Change in Body Mass

In chapter 4 the homeostatic mechanisms defending the body mass and blood chemistry were disrupted by introducing high fat, low fat, and high sugar diets. It was identified that short term introductions of an obesogenic diet does not ameliorate the seasonal loss in body mass. Seasonal changes in food intake may arise from reduced body mass rather than driving the reduction in body mass. Blood chemistry remains well defended in seasonal animals despite large rheostatic changes in body mass. Further, ability to defend blood chemistry from dietary challenge does not appear impaired in short photoperiod Siberian hamsters. Seasonal animals must defend blood chemistry to avoid adverse health implications from large changes in body mass.

5.4 - Defining a Model of Seasonal Programs in Energy Rheostasis

The data presented in this thesis has reinforced a clear distinction between homeostasis and rheostasis. Homeostatic mechanisms are unaffected by seasonal rheostasis. Melatonin signalling, entrained by external photoperiod acts as an initial signal to initiate a rheostatic program. This is decoded within the pars tuberalis, which acts as a responder to melatonin signalling. TSH signalling then communicates the decoded photoperiod signal to the hypothalamus. In the hypothalamus TSH signalling controls *dio3* expression. Dio3 drives the de-activation of thyroid hormone signalling from third ventricle tanycytes. A timing mechanism controls the expression of *dio3*, potentially involving transcripts such as *mef2c*. Within the hypothalamus the photoperiod signal, TSH, and the endogenous interval timer, *dio3*, are integrated in order to control the rheostat. The result of the integration of rheostatic signals for body mass is somatostatin signalling, which acts as an output to control a rheostatic effector. Somatostatin therefore acts as a rheostatic output which effects changes in the set-point of body mass. Somatostatin drives changes in growth hormone release which affects multiple physiological systems to regulate the set-point of body mass. Homeostatic mechanisms, which respond to energetic challenge remain unaffected by a gradual systematic decrease in body mass. Previously, seasonal changes in body mass have been linked to hypothalamic neuropeptides associated with homeostatic changes, such as POMC (Helfer and Stevenson,

2020). The work presented in this thesis proposes a distinct separation of the homeostatic and rheostatic regulation of body mass.

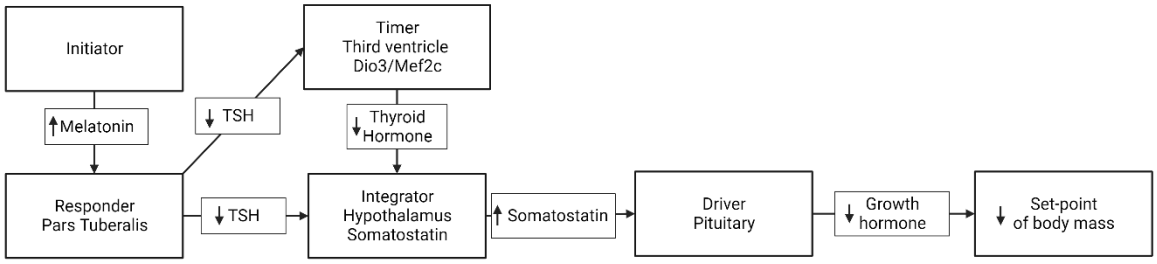

Figure 5-2: A model of a seasonal rheostatic interval timer. An initiator (melatonin) drives a photoperiod response within the pars tuberalis. The pars tuberalis responds to a short photoperiod signal by reducing TSH signalling. The tanycytes of the third ventricle respond by increasing *dio3* expression, which increases thyroid hormone deactivation. This thyroid hormone signal acts as a timer for neuroendocrine changes in the hypothalamus. Within the hypothalamus, photoperiod signalling, and photoperiodic history are integrated to determine the phasing of the seasonal waveform. Somatostatin is increased throughput the responsive phase of the seasonal waveform in response to thyroid hormone signalling. This drives a decrease in pituitary growth hormone release, which acts to lower the rheostatic set-point in body mass. Figure made with Biorender.com.

5.5 Summary and Future Work

The work described in this thesis aimed to characterise the molecular mechanism underpinning seasonal rheostatic changes in the Siberian hamster. Overall, these studies suggest that a host of genes upregulated during the photoreactive phase, drive the set-point of body mass downwards. Homeostatic mechanisms remain functional and act to defend the set-point in body mass. It was demonstrated that dynamic changes in expression occur throughout the seasonal waveform. Such transcripts may represent a distinct seasonal program acting within the photoreactive phase of the seasonal cycle in Siberian hamsters. Further, in chapter 2 and 3, it was demonstrated that homeostatic mechanisms remain functional under rheostat driven changes in body mass. However, the role of some novel transcripts remains unknown in seasonal contexts. Future research should investigate the functional links between transcripts identified and the set

point of body mass. Multiple approaches may be utilised to achieve this, such as the targeted knockout of identified transcripts which may be involve in seasonal rheostasis.

Appendix 1 – Full Results of Sequencing analysis (Rhythmicity)

Data Id	Data Label	tau	emp p	emp p BH Corrected	Pattern Shape
143	Atad2	0.552052	1.00E-05	0.001017	SPIKE
195	Casp8	0.534137	1.00E-05	0.001017	SPIKE
295	Chst3	0.679366	1.00E-05	0.001017	SPIKE
455	Epha3	0.679366	1.00E-05	0.001017	SPIKE
489	Fam214a	0.532093	1.00E-05	0.001017	ACOS
576	Gm12976	0.560647	1.00E-05	0.001017	SPIKE
583	Gm14340	0.578881	1.00E-05	0.001017	SPIKE
591	Gm16010	0.602464	1.00E-05	0.001017	SPIKE
669	Gm41036	0.552052	1.00E-05	0.001017	SPIKE
699	Gm9866	0.674142	1.00E-05	0.001017	SPIKE
813	Itgal	0.552052	1.00E-05	0.001017	SPIKE
840	Kcp	0.578881	1.00E-05	0.001017	SPIKE
951	Mbd6	0.535582	1.00E-05	0.001017	SPIKE
980	Mir684-1	0.598255	1.00E-05	0.001017	SPIKE
1190	Plekhg2	0.582086	1.00E-05	0.001017	SPIKE
1427	Slc30a2	0.552052	1.00E-05	0.001017	SPIKE
1602	Tmem253	0.609333	1.00E-05	0.001017	SPIKE
1634	Trim30a	0.552052	1.00E-05	0.001017	SPIKE
880	Ldlrap1	0.526576	2.00E-05	0.001926	SPIKE
57	Acp6	0.519659	4.00E-05	0.003486	SPIKE
401	Dhfr	0.519659	4.00E-05	0.003486	SPIKE
87	Akap10	0.513943	6.00E-05	0.00366	SPIKE
482	F830045P16Rik	0.501848	7.00E-05	0.00366	SPIKE
544	Gata3	0.503708	7.00E-05	0.00366	SPIKE
627	Gm31734	0.510349	6.00E-05	0.00366	SPIKE
784	Il15	0.509229	6.00E-05	0.00366	SPIKE

866	Ky	0.503979	7.00E-05	0.00366	SPIKE
897	LOC118567340	0.508016	6.00E-05	0.00366	SPIKE
907	LOC118568482	0.510324	6.00E-05	0.00366	SPIKE
927	Lsp1	0.510149	6.00E-05	0.00366	SPIKE
929	Ly6l	0.513911	6.00E-05	0.00366	SPIKE
1052	Neurod6	0.501848	7.00E-05	0.00366	SPIKE
1061	Nhlrc3	0.501069	7.00E-05	0.00366	SPIKE
1072	Nox4	0.501848	7.00E-05	0.00366	SPIKE
1565	Tgif2	0.511743	6.00E-05	0.00366	SPIKE
505	Fbxw10	0.496924	9.00E-05	0.004451	SPIKE
981	Mkx	0.499464	9.00E-05	0.004451	SPIKE
364	Cyp2u1	0.494468	1.40E-04	0.005693	SPIKE
467	Esr2	0.494468	1.40E-04	0.005693	SPIKE
638	Gm33046	0.494468	1.40E-04	0.005693	SPIKE
640	Gm33856	0.494468	1.40E-04	0.005693	SPIKE
1319	Robo3	0.494468	1.40E-04	0.005693	SPIKE
1631	Trex2	0.494468	1.40E-04	0.005693	SPIKE
1723	Wtip	0.494468	1.40E-04	0.005693	SPIKE
1769	Zfp444	0.494468	1.40E-04	0.005693	SPIKE
940	Man2b1	0.491997	1.50E-04	0.005967	SPIKE
827	Kcna3	0.490039	1.70E-04	0.006619	SPIKE
48	Acacb	0.48824	1.90E-04	0.007096	SPIKE
436	Eaf1	0.487454	1.90E-04	0.007096	SPIKE
643	Gm34299	0.487088	2.00E-04	0.007176	SPIKE
1239	Pros1	0.487088	2.00E-04	0.007176	SPIKE
28	4932438H23Rik	0.480478	2.40E-04	0.007572	SPIKE
234	Cd36	0.478905	2.40E-04	0.007572	SPIKE
271	Cfap100	0.479708	2.40E-04	0.007572	SPIKE

552	Gemin7	0.482357	2.30E-04	0.007572	SPIKE
595	Gm19412	0.482122	2.30E-04	0.007572	SPIKE
949	Marchf9	0.481999	2.30E-04	0.007572	SPIKE
1553	Tex21	0.478995	2.40E-04	0.007572	SPIKE
606	Gm25848	0.478053	2.50E-04	0.007754	SPIKE
130	Arid3a	0.473453	3.20E-04	0.009445	SPIKE
911	Lpcat2	0.473453	3.20E-04	0.009445	SPIKE
1478	Spc24	0.473935	3.20E-04	0.009445	SPIKE
1204	Poc1b	0.4705	4.30E-04	0.01249	SPIKE
1086	Nt5c1b	0.469266	4.40E-04	0.012581	SPIKE
1477	Spata6	0.468025	4.80E-04	0.013309	SPIKE
1737	Zbtb2	0.468222	4.80E-04	0.013309	SPIKE
221	Ccdc77	0.467217	5.00E-04	0.013456	SPIKE
618	Gm29941	0.467239	5.00E-04	0.013456	SPIKE
281	Cfap99	0.464948	5.70E-04	0.014901	SPIKE
370	Dach2	0.465168	5.70E-04	0.014901	SPIKE
335	Crhr2	0.461685	6.70E-04	0.01552	SPIKE
342	Cryba2	0.461685	6.70E-04	0.01552	SPIKE
390	Decr1	0.462636	6.30E-04	0.01552	NSPIKE
615	Gm29808	0.463013	6.30E-04	0.01552	SPIKE
1017	Myh7b	0.461685	6.70E-04	0.01552	SPIKE
1068	Nnmt	0.461685	6.70E-04	0.01552	SPIKE
1101	Olfr1418	0.461685	6.70E-04	0.01552	SPIKE
1379	Sft2d3	0.461685	6.70E-04	0.01552	SPIKE
1824	Zpld1	0.461685	6.70E-04	0.01552	SPIKE
656	Gm36684	0.460181	7.00E-04	0.016012	SPIKE
42	Abcc1	0.458162	7.20E-04	0.016095	SPIKE
1045	Neat1	0.457368	7.30E-04	0.016095	SPIKE

1770	Zfp446	0.457425	7.30E-04	0.016095	SPIKE
692	Gm52709	0.457	7.80E-04	0.016993	SPIKE
730	Gtf3c3	0.456037	8.00E-04	0.017223	NSPIKE
31	9030025P20Rik	0.454794	9.00E-04	0.01771	SPIKE
623	Gm31159	0.454794	9.00E-04	0.01771	SPIKE
644	Gm3435	0.454794	9.00E-04	0.01771	SPIKE
854	Kifc1	0.454794	9.00E-04	0.01771	SPIKE
891	Lmln	0.455085	8.80E-04	0.01771	SPIKE
1299	Rec8	0.455443	8.50E-04	0.01771	SPIKE
1397	Sim2	0.454794	9.00E-04	0.01771	SPIKE
1537	Tas1r1	0.454794	9.00E-04	0.01771	SPIKE
61	Actr5	0.449359	0.00103	0.0183	SPIKE
347	Crybg2	0.449359	0.00103	0.0183	SPIKE
433	E2f2	0.451306	9.70E-04	0.0183	SPIKE
662	Gm39646	0.449359	0.00103	0.0183	SPIKE
691	Gm52702	0.449021	0.00104	0.0183	SPIKE
1033	Nabp1	0.448879	0.00104	0.0183	SPIKE
1410	Slc15a4	0.449476	0.00103	0.0183	SPIKE
1558	Tfpi	0.45023	1.00E-03	0.0183	SPIKE
1560	Tgds	0.452489	9.60E-04	0.0183	SPIKE
1705	Wdhd1	0.45023	1.00E-03	0.0183	SPIKE
1819	Zkscan2	0.450348	1.00E-03	0.0183	SPIKE
1814	Zfp992	0.447867	0.00108	0.018823	SPIKE
796	Inf2	0.446162	0.00112	0.019155	SPIKE
1496	St18	0.447241	0.00112	0.019155	SPIKE
1648	Trpc7	0.445729	0.00122	0.020672	SPIKE
236	Cd5	0.443459	0.00136	0.021091	SPIKE
530	Frzb	0.443964	0.00135	0.021091	SPIKE
571	Glyat	0.443135	0.00136	0.021091	SPIKE
598	Gm20554	0.442857	0.00136	0.021091	SPIKE
637	Gm32896	0.443459	0.00136	0.021091	SPIKE
705	Gpalpp1	0.444173	0.00134	0.021091	SPIKE
1152	Pdpn	0.443964	0.00135	0.021091	SPIKE
1292	Rbm12b2	0.443459	0.00136	0.021091	SPIKE
1407	Slc12a7	0.444676	0.00128	0.021091	SPIKE
1615	Tnfsf13b	0.443459	0.00136	0.021091	SPIKE
102	Ankrd27	0.442004	0.00143	0.021991	SPIKE

373	Dapk2	0.440729	0.00152	0.022614	SPIKE
818	Itprip	0.440729	0.00152	0.022614	SPIKE
1113	Otulin	0.440729	0.00152	0.022614	SPIKE
1765	Zfp385c	0.441193	0.0015	0.022614	SPIKE
1125	Pan2	0.439445	0.00161	0.02357	SPIKE
1250	Pskh1	0.440203	0.00161	0.02357	SPIKE
4	1700003F12Rik	0.438754	0.00173	0.024353	SPIKE
553	Gfap	0.43849	0.00173	0.024353	NSPIKE
807	Irgm1	0.43881	0.00173	0.024353	SPIKE
811	Itga1	0.43881	0.00173	0.024353	SPIKE
1110	Osgin2	0.438832	0.00172	0.024353	SPIKE
2	0610038B21Rik	0.436681	0.00183	0.024444	SPIKE
39	Abca17	0.436564	0.00183	0.024444	SPIKE
410	Dleu7	0.436908	0.00177	0.024444	SPIKE
572	Gm11335	0.436689	0.00183	0.024444	SPIKE
1159	Pgbd1	0.436807	0.00182	0.024444	SPIKE
1596	Tmem190	0.436689	0.00183	0.024444	SPIKE
1694	Vmn2r42	0.436689	0.00183	0.024444	SPIKE
1220	Ppp4r1	0.436384	0.00191	0.025146	SPIKE
1791	Zfp759	0.436479	0.00191	0.025146	SPIKE
297	Chst5	0.433796	0.00206	0.025645	SPIKE
312	Cntnap5c	0.43435	0.00206	0.025645	SPIKE
359	Cyp19a1	0.43404	0.00206	0.025645	SPIKE
641	Gm34069	0.43404	0.00206	0.025645	SPIKE
677	Gm46603	0.43404	0.00206	0.025645	SPIKE
1374	Serping1	0.434081	0.00206	0.025645	ACOS
1451	Smagp	0.433865	0.00206	0.025645	SPIKE
1662	Ttll6	0.43404	0.00206	0.025645	SPIKE
1211	Pomt2	0.433343	0.00211	0.02609	SPIKE
916	Lrp3	0.433028	0.00213	0.02616	NSPIKE
138	Asgr1	0.430234	0.00239	0.027172	SPIKE
159	BC055324	0.429919	0.00244	0.027172	SPIKE
241	Cdc25b	0.429919	0.00244	0.027172	SPIKE
265	Cep162	0.430706	0.00237	0.027172	SPIKE
351	Csmd1	0.429521	0.00245	0.027172	SPIKE
555	Ggcx	0.4312	0.00231	0.027172	SPIKE
609	Gm26908	0.430982	0.00231	0.027172	SPIKE
724	Grin2a	0.429195	0.00245	0.027172	NSPIKE
890	Lmf1	0.431466	0.00231	0.027172	SPIKE
996	Mro	0.431174	0.00231	0.027172	SPIKE
1146	Pde6g	0.429571	0.00244	0.027172	SPIKE
1228	Prelid2	0.429919	0.00244	0.027172	SPIKE
1236	Prkd2	0.429919	0.00244	0.027172	SPIKE
1324	Rpp25	0.429721	0.00244	0.027172	ACOS
1485	Spon2	0.429571	0.00244	0.027172	SPIKE
1757	Zfp276	0.429888	0.00244	0.027172	SPIKE
394	Dennd3	0.428795	0.00252	0.02778	SPIKE
918	Lrrc18	0.428108	0.00255	0.027943	SPIKE

409	Dkk2	0.426012	0.00272	0.029628	SPIKE
1621	Tomt	0.425785	0.00274	0.02967	SPIKE
366	Cytip	0.424604	0.00293	0.031026	SPIKE
497	Fanci	0.424439	0.00294	0.031026	SPIKE
743	Hbp1	0.424603	0.00293	0.031026	NSPIKE
1446	Slco1a6	0.424604	0.00293	0.031026	SPIKE
1646	Trp73	0.424187	0.00295	0.031026	SPIKE
300	Clasrp	0.42381	0.00301	0.031476	SPIKE
675	Gm46526	0.423148	0.00318	0.032878	SPIKE
1173	Pkmyt1	0.423148	0.00318	0.032878	SPIKE
1177	Pla2g5	0.422293	0.00323	0.033021	SPIKE
1272	Rab37	0.422935	0.00323	0.033021	SPIKE
904	LOC118568224	0.4215	0.00338	0.034363	SPIKE
889	Llgl2	0.420395	0.00366	0.0366	SPIKE
1167	Pik3cg	0.420395	0.00366	0.0366	SPIKE
1459	Snord118	0.420503	0.00366	0.0366	SPIKE
947	Marchf11	0.418819	0.004	0.039567	SPIKE
1525	Syk	0.41864	0.004	0.039567	SPIKE
105	Ankrd35	0.418489	0.00411	0.04022	SPIKE
235	Cd3eap	0.418415	0.00411	0.04022	SPIKE
655	Gm36539	0.417654	0.00418	0.040688	SPIKE
944	Mapk11	0.41713	0.00434	0.042022	SPIKE
717	Gpr68	0.416665	0.00442	0.042348	NSPIKE
1269	Pyroxd2	0.416378	0.00442	0.042348	SPIKE
226	Ccn2	0.416355	0.00451	0.042986	SPIKE
233	Cd27	0.415005	0.00477	0.043213	SPIKE
353	Csnk1g1	0.415815	0.00457	0.043213	NSPIKE
584	Gm14393	0.415168	0.00477	0.043213	SPIKE
600	Gm20642	0.415168	0.00477	0.043213	SPIKE
719	Gpt2	0.415088	0.00477	0.043213	NSPIKE
735	Gys2	0.415168	0.00477	0.043213	SPIKE
920	Lrrc32	0.415168	0.00477	0.043213	SPIKE
1095	Nup210	0.415434	0.0047	0.043213	SPIKE
1175	Pla1a	0.41469	0.00477	0.043213	SPIKE
1469	Sowaha	0.415503	0.0047	0.043213	SPIKE
1803	Zfp873	0.414125	0.00486	0.043811	ACOS
586	Gm14846	0.413755	0.00501	0.044942	SPIKE
244	Cdiptos	0.412886	0.00518	0.045662	SPIKE
858	Klhl42	0.412393	0.00524	0.045662	SPIKE
1078	Npy1r	0.412481	0.00524	0.045662	NSPIKE
1126	Papolg	0.413306	0.00517	0.045662	SPIKE
1143	Pde1c	0.412305	0.00524	0.045662	SPIKE
1826	Zscan12	0.412436	0.00524	0.045662	SPIKE
90	Alas2	0.410264	0.00584	0.050411	SPIKE
517	Fignl1	0.410258	0.00584	0.050411	SPIKE
11	1700024G13Rik	0.409627	0.00602	0.051239	SPIKE
596	Gm19950	0.409627	0.00602	0.051239	SPIKE
847	Kif14	0.409607	0.00602	0.051239	SPIKE

124	Arhgap27	0.408393	0.00635	0.053061	SPIKE
899	LOC118567558	0.409462	0.00633	0.053061	SPIKE
1722	Wscd1	0.409225	0.00633	0.053061	NSPIKE
1743	Zbtb8b	0.409462	0.00633	0.053061	SPIKE
1020	Mynn	0.407947	0.0065	0.053581	NSPIKE
1415	Slc22a18	0.407973	0.0065	0.053581	SPIKE
1611	Tmppe	0.407973	0.0065	0.053581	SPIKE
117	Aph1c	0.407666	0.00658	0.053997	SPIKE
444	Egflam	0.40625	0.00695	0.056028	SPIKE
744	Hccs	0.406405	0.00695	0.056028	NSPIKE
1314	Rnf122	0.406393	0.00695	0.056028	SPIKE
1653	Tsks	0.406292	0.00695	0.056028	SPIKE
877	Lcp2	0.405974	0.00699	0.056103	SPIKE
91	Alox5	0.405065	0.0073	0.056846	SPIKE
453	Entpd1	0.405662	0.0072	0.056846	SPIKE
616	Gm29811	0.405262	0.00728	0.056846	SPIKE
819	Itpripl1	0.40515	0.00728	0.056846	SPIKE
978	Mir124-2hg	0.405258	0.00728	0.056846	SPIKE
991	Morn3	0.405176	0.00728	0.056846	SPIKE
1136	Pbld2	0.405468	0.0072	0.056846	SPIKE
1289	Rassf8	0.404033	0.00768	0.058316	SPIKE
1345	Satb2	0.40452	0.00765	0.058316	SPIKE
1404	Skor1	0.404387	0.00765	0.058316	SPIKE
1439	Slc66a1	0.404846	0.00764	0.058316	SPIKE
1449	Slx4	0.40395	0.00768	0.058316	SPIKE
1595	Tmem19	0.404977	0.00764	0.058316	SPIKE
1610	Tmem87b	0.403891	0.00776	0.05868	SPIKE
144	Atp2a3	0.403162	0.00795	0.058958	SPIKE
332	Cr2	0.402905	0.00799	0.058958	SPIKE
824	Jsrp1	0.403162	0.00795	0.058958	SPIKE
1073	Noxa1	0.402905	0.00799	0.058958	SPIKE
1291	Rbm12b1	0.403162	0.00795	0.058958	SPIKE
1520	Stxbp4	0.402933	0.00795	0.058958	SPIKE
1383	Sgta	0.402309	0.00827	0.060779	ACOS
184	Cand2	0.401414	0.00869	0.063357	SPIKE
945	Mapk7	0.401284	0.00869	0.063357	SPIKE
473	Etv6	0.400886	0.00874	0.063362	SPIKE
701	Gna15	0.400548	0.00876	0.063362	SPIKE
153	Bard1	0.400062	0.00911	0.065122	SPIKE
974	Micall2	0.400062	0.00911	0.065122	SPIKE
1708	Wdr59	0.400225	0.00911	0.065122	SPIKE
1575	Tiam2	0.399835	0.0094	0.066933	SPIKE
192	Card6	0.3993	0.00948	0.066982	SPIKE
1043	Ndst2	0.399398	0.00947	0.066982	SPIKE
114	Ano8	0.398623	0.00965	0.067285	SPIKE
729	Gtdc1	0.398276	0.00967	0.067285	SPIKE
734	Gys1	0.398729	0.00965	0.067285	SPIKE
1484	Spint1	0.398334	0.00965	0.067285	SPIKE

1185	Plch2	0.398057	0.00991	0.068694	SPIKE
1183	Plcd1	0.397029	0.01044	0.071022	SPIKE
1214	Ppef2	0.396863	0.01044	0.071022	SPIKE
1479	Spdl1	0.397837	0.01036	0.071022	SPIKE
1616	Tnks1bp1	0.397641	0.01036	0.071022	NSPIKE
1745	Zdhhc15	0.396863	0.01044	0.071022	SPIKE
1821	Zmynd12	0.396214	0.01055	0.071505	SPIKE
524	Foxn4	0.396067	0.01074	0.072257	SPIKE
1119	P3h1	0.396067	0.01074	0.072257	SPIKE
37	Aanat	0.395737	0.0111	0.074134	SPIKE
1798	Zfp819	0.395737	0.0111	0.074134	SPIKE
248	Cdkn2c	0.394899	0.01134	0.075042	SPIKE
871	Lama5	0.394324	0.0114	0.075042	SPIKE
1276	Rad21l	0.394586	0.01139	0.075042	SPIKE
1715	Wipf3	0.395456	0.01128	0.075042	SPIKE
770	Ifi47	0.394132	0.01159	0.075748	SPIKE
952	Mbnl3	0.394114	0.01159	0.075748	SPIKE
547	Gcfc2	0.392769	0.01214	0.076733	SPIKE
557	Ghdc	0.392769	0.01214	0.076733	SPIKE
791	Il18r1	0.392769	0.01214	0.076733	SPIKE
979	Mir125b-1	0.392769	0.01214	0.076733	SPIKE
1091	Nudt15	0.392568	0.01216	0.076733	SPIKE
1103	Opn3	0.39292	0.01213	0.076733	SPIKE
1234	Prkcd	0.393368	0.01204	0.076733	SPIKE
1347	Sbk2	0.392622	0.01216	0.076733	ACOS
1542	Tbxas1	0.392761	0.01214	0.076733	SPIKE
1823	Znhit2	0.393628	0.01182	0.076733	NSPIKE
1746	Zdhhc18	0.392531	0.01224	0.076972	SPIKE
7	1700016K19Rik	0.391293	0.01278	0.077132	SPIKE
12	1700030J22Rik	0.390563	0.01293	0.077132	SPIKE
14	2210408F21Rik	0.390948	0.01278	0.077132	SPIKE
41	Abcb1b	0.388514	0.01412	0.077132	SPIKE
79	Adgrv1	0.388514	0.01412	0.077132	SPIKE
95	Alx4	0.391719	0.01255	0.077132	SPIKE
132	Arih2	0.389999	0.0134	0.077132	SPIKE
177	C6	0.388514	0.01412	0.077132	SPIKE
199	Catsperd	0.388514	0.01412	0.077132	SPIKE
203	Cbx2	0.391412	0.01255	0.077132	SPIKE
284	Chaf1a	0.388687	0.01399	0.077132	NSPIKE
288	Chrdl2	0.388514	0.01412	0.077132	SPIKE
296	Chst4	0.388514	0.01412	0.077132	SPIKE
310	Cntn5	0.388453	0.01412	0.077132	SPIKE
348	Cryge	0.388514	0.01412	0.077132	SPIKE
376	Dcaf13	0.389176	0.01359	0.077132	NSPIKE
412	Dmrtc2	0.388514	0.01412	0.077132	SPIKE
477	Exoc6	0.392123	0.01242	0.077132	NSPIKE
502	Fbxl8	0.389313	0.01355	0.077132	SPIKE
631	Gm32313	0.388514	0.01412	0.077132	SPIKE

648	Gm35002	0.389605	0.01343	0.077132	SPIKE
660	Gm39307	0.388514	0.01412	0.077132	SPIKE
685	Gm51785	0.388514	0.01412	0.077132	SPIKE
694	Gm7072	0.388514	0.01412	0.077132	SPIKE
886	Lin28b	0.390244	0.01315	0.077132	SPIKE
931	Lzts1	0.391412	0.01255	0.077132	SPIKE
936	Mamdc4	0.390563	0.01293	0.077132	SPIKE
960	Mei4	0.391412	0.01255	0.077132	SPIKE
1013	Mybl2	0.388514	0.01412	0.077132	SPIKE
1135	Pbld1	0.388514	0.01412	0.077132	SPIKE
1241	Prox2	0.388514	0.01412	0.077132	SPIKE
1300	Reep4	0.389166	0.01359	0.077132	ACOS
1321	Rp1	0.389834	0.01342	0.077132	NSPIKE
1338	S100a5	0.388514	0.01412	0.077132	SPIKE
1429	Slc35b3	0.388614	0.01399	0.077132	SPIKE
1536	Tap2	0.39186	0.01254	0.077132	SPIKE
1538	Tbc1d13	0.389392	0.01355	0.077132	NSPIKE
1580	Timp1	0.389551	0.01343	0.077132	SPIKE
1593	Tmem159	0.388508	0.01412	0.077132	SPIKE
1633	Trim12c	0.388962	0.01392	0.077132	SPIKE
1704	Wdfy4	0.388514	0.01412	0.077132	SPIKE
1710	Wdr72	0.388514	0.01412	0.077132	SPIKE
1729	Xlr4b	0.390563	0.01293	0.077132	SPIKE
1758	Zfp28	0.389605	0.01343	0.077132	SPIKE
564	Gjc2	0.387665	0.01464	0.078958	SPIKE
688	Gm52229	0.387217	0.01466	0.078958	SPIKE
727	Gsc	0.387992	0.01453	0.078958	SPIKE
748	Hdac7	0.386955	0.01467	0.078958	SPIKE
1635	Trim30d	0.387665	0.01464	0.078958	SPIKE
163	Bhlhe22	0.38651	0.01502	0.080369	SPIKE
354	Csnk1g2	0.386715	0.01501	0.080369	NSPIKE
908	LOC118568718	0.386488	0.01532	0.081736	SPIKE
659	Gm39112	0.385027	0.01591	0.083477	SPIKE
798	Insm1	0.38582	0.01584	0.083477	NSPIKE
1231	Prim2	0.385027	0.01591	0.083477	SPIKE
1350	Scd3	0.38498	0.01592	0.083477	NSPIKE
1642	Trip13	0.385496	0.01585	0.083477	SPIKE
1760	Zfp282	0.385402	0.01585	0.083477	SPIKE
1035	Naip2	0.384264	0.01654	0.085988	SPIKE
1184	Plcd3	0.384264	0.01654	0.085988	SPIKE
1223	Prdm11	0.384432	0.01652	0.085988	NSPIKE
154	BB287469	0.383844	0.01686	0.087078	SPIKE
243	Cdhr4	0.38379	0.01689	0.087078	SPIKE
599	Gm20560	0.383293	0.01694	0.087078	SPIKE
1452	Smc4	0.383349	0.01692	0.087078	SPIKE
1007	Mthfr	0.382762	0.01709	0.087115	SPIKE
1154	Pdzk1ip1	0.382762	0.01709	0.087115	SPIKE
1355	Scube1	0.382762	0.01709	0.087115	SPIKE

608	Gm26871	0.382363	0.01745	0.088703	SPIKE
855	Kirrel	0.382047	0.01798	0.090892	SPIKE
977	Mir100hg	0.382141	0.01798	0.090892	NSPIKE
695	Gm7102	0.381185	0.01835	0.09125	SPIKE
969	Mfsd4b1	0.38142	0.01832	0.09125	SPIKE
983	Mlph	0.381186	0.01835	0.09125	SPIKE
1238	Prokr2	0.381151	0.01835	0.09125	SPIKE
1317	Rnpc3	0.381477	0.01832	0.09125	NSPIKE
1776	Zfp507	0.380926	0.01835	0.09125	SPIKE
1540	Tbc1d4	0.379532	0.01969	0.097649	SPIKE
333	Crb1	0.379065	0.01991	0.097943	SPIKE
1266	Pxmp4	0.379148	0.01991	0.097943	ACOS
1744	Zdhhc13	0.379111	0.01991	0.097943	SPIKE
520	Flnc	0.378726	0.02033	0.099475	SPIKE
537	Gabrq	0.378602	0.02033	0.099475	NSPIKE

References

Abrahamson, E.E., Moore, R.Y., 2001. Suprachiasmatic nucleus in the mouse: retinal innervation, intrinsic organization and efferent projections. Brain Research 916, 172–191. https://doi.org/10.1016/S0006-8993(01)02890-6

Abramicheva, P.A., Smirnova, O.V., 2019. Prolactin Receptor Isoforms as the Basis of Tissue-Specific Action of Prolactin in the Norm and Pathology. Biochemistry Moscow 84, 329–345. https://doi.org/10.1134/S0006297919040011

Acuña-Castroviejo, D., Martín, M., Macías, M., Escames, G., León, J., Khaldy, H., Reiter, R.J., 2001. Melatonin, mitochondria, and cellular bioenergetics. Journal of Pineal Research 30, 65–74. https://doi.org/10.1034/j.1600-079X.2001.300201.x

Adam, C.L., Moar, K.M., Logie, T.J., Ross, A.W., Barrett, P., Morgan, P.J., Mercer, J.G., 2000. Photoperiod Regulates Growth, Puberty and Hypothalamic Neuropeptide and Receptor Gene Expression in Female Siberian Hamsters1. Endocrinology 141, 4349–4356. https://doi.org/10.1210/endo.141.12.7807

Adams, J.M., Jeppesen, P.G.N., Sanger, F., Barrell, B.G., 1969. Nucleotide Sequence from the Coat Protein Cistron of R17 Bacteriophage RNA. Nature 223, 1009–1014. https://doi.org/10.1038/2231009a0

Ahima, R.S., Osei, S.Y., 2004. Leptin signaling. Physiology & Behavior, Reviews on Ingestive Science 81, 223–241. https://doi.org/10.1016/j.physbeh.2004.02.014

Åkerblom, A., Helmersson-Karlqvist, J., Weitoft, T., Larsson, A., 2017. Seasonal variations of urate in a Swedish adult population. Clin Rheumatol 36, 1595–1598. https://doi.org/10.1007/s10067-017-3591-z

Akeson, M., Branton, D., Kasianowicz, J.J., Brandin, E., Deamer, D.W., 1999. Microsecond Time-Scale Discrimination Among Polycytidylic Acid, Polyadenylic Acid, and Polyuridylic Acid as Homopolymers or as Segments Within Single RNA Molecules. Biophysical Journal 77, 3227–3233. https://doi.org/10.1016/S0006-3495(99)77153-5

Alberti, K.G.M.M., Juel Christensen, N., Engkjær Christensen, S., Prange Hansen, AA., Iversen, J., Lundbæk, K., Seyer-Hansen, K., Ørskov, H.,

1973. INHIBITION OF INSULIN SECRETION BY SOMATOSTATIN. The Lancet, Originally published as Volume 2, Issue 7841 302, 1299–1301. https://doi.org/10.1016/S0140-6736(73)92873-0

Allaway, K.C., Gabitto, M.I., Wapinski, O., Saldi, G., Wang, C.-Y., Bandler, R.C., Wu, S.J., Bonneau, R., Fishell, G., 2021. Genetic and epigenetic coordination of cortical interneuron development. Nature 597, 693–697. https://doi.org/10.1038/s41586-021-03933-1

Al-Qassab, H., Smith, M.A., Irvine, E.E., Guillermet-Guibert, J., Claret, M., Choudhury, A.I., Selman, C., Piipari, K., Clements, M., Lingard, S., Chandarana, K., Bell, J.D., Barsh, G.S., Smith, A.J.H., Batterham, R.L., Ashford, M.L.J., Vanhaesebroeck, B., Withers, D.J., 2009. Dominant Role of the p110ß Isoform of PI3K over p110α in Energy Homeostasis Regulation by POMC and AgRP Neurons. Cell Metab 10, 343–354. https://doi.org/10.1016/j.cmet.2009.09.008

Andersen, D.M., Keafer, B.A., 1987. An endogenous annual clock in the toxic marine dinoflagellate Gonyaulax tamarensis. Nature 325, 616–617. https://doi.org/10.1038/325616a0

Angelopoulou, E., Inquimbert, P., Klosen, P., Anderson, G., Kalsbeek, A., Simonneaux, V., 2021. Daily and Estral Regulation of RFRP-3 Neurons in the Female Mice. Journal of Circadian Rhythms 19, 4. https://doi.org/10.5334/jcr.212

Angelopoulou, E., Quignon, C., Kriegsfeld, L.J., Simonneaux, V., 2019. Functional Implications of RFRP-3 in the Central Control of Daily and Seasonal Rhythms in Reproduction. Front. Endocrinol. 10, 183. https://doi.org/10.3389/fendo.2019.00183

Anjum, S., Khattak, M.N.K., Tsutsui, K., Krishna, A., 2021. RF-amide related peptide-3 (RFRP-3): a novel neuroendocrine regulator of energy homeostasis, metabolism, and reproduction. Mol Biol Rep 48, 1837–1852. https://doi.org/10.1007/s11033-021-06198-z

Arancibia, S., Rage, F., Astier, H., Tapia-Arancibia, L., 2008. Neuroendocrine and Autonomous Mechanisms Underlying Thermoregulation in Cold Environment. Neuroendocrinology 64, 257–267. https://doi.org/10.1159/000127126

Ashkenasy, N., Sánchez-Quesada, J., Bayley, H., Ghadiri, M.R., 2005. Recognizing a Single Base in an Individual DNA Strand: A Step Toward DNA

Sequencing in Nanopores. Angewandte Chemie International Edition 44, 1401–1404. https://doi.org/10.1002/anie.200462114

Au-Yong, I.T.H., Thorn, N., Ganatra, R., Perkins, A.C., Symonds, M.E., 2009. Brown Adipose Tissue and Seasonal Variation in Humans. Diabetes 58, 2583–2587. https://doi.org/10.2337/db09-0833

Bachelot, A., Beaufaron, J., Servel, N., Kedzia, C., Monget, P., Kelly, P.A., Gibori, G., Binart, N., 2009. Prolactin independent rescue of mouse corpus luteum life span: identification of prolactin and luteinizing hormone target genes. American Journal of Physiology-Endocrinology and Metabolism 297, E676–E684. https://doi.org/10.1152/ajpendo.91020.2008

Bae, H.H., Larkin, J.E., Zucker, I., 2003. Juvenile Siberian Hamsters Display Torpor and Modified Locomotor Activity and Body Temperature Rhythms in Response to Reduced Food Availability. Physiological and Biochemical Zoology 76, 858–867. https://doi.org/10.1086/381462

Balthasar, N., Coppari, R., McMinn, J., Liu, S.M., Lee, C.E., Tang, V., Kenny, C.D., McGovern, R.A., Chua, S.C., Elmquist, J.K., Lowell, B.B., 2004. Leptin Receptor Signaling in POMC Neurons Is Required for Normal Body Weight Homeostasis. Neuron 42, 983–991. https://doi.org/10.1016/j.neuron.2004.06.004

Bao, R., Onishi, K.G., Tolla, E., Ebling, F.J.P., Lewis, J.E., Anderson, R.L., Barrett, P., Prendergast, B.J., Stevenson, T.J., 2019. Genome sequencing and transcriptome analyses of the Siberian hamster hypothalamus identify mechanisms for seasonal energy balance. Proc Natl Acad Sci USA 116, 13116–13121. https://doi.org/10.1073/pnas.1902896116

Barker-Gibb, M.L., Scott, C.J., Boublik, J.H., Clarke, I.J., 1995. The role of neuropeptide Y (NPY) in the control of LH secretion in the ewe with respect to season, NPY receptor subtype and the site of action in the hypothalamus. Journal of Endocrinology 147, 565–579. https://doi.org/10.1677/joe.0.1470565

Barrett, P., Bolborea, M., 2012. Molecular pathways involved in seasonal body weight and reproductive responses governed by melatonin: *Melatonin action for physiological adaptation*. Journal of Pineal Research 52, 376–388. https://doi.org/10.1111/j.1600-079X.2011.00963.x

Barrett, P., Ebling, F.J.P., Schuhler, S., Wilson, D., Ross, A.W., Warner, A., Jethwa, P., Boelen, A., Visser, T.J., Ozanne, D.M., Archer, Z.A., Mercer,

J.G., Morgan, P.J., 2007. Hypothalamic Thyroid Hormone Catabolism Acts as a Gatekeeper for the Seasonal Control of Body Weight and Reproduction. Endocrinology 148, 3608–3617. https://doi.org/10.1210/en.2007-0316

Barrett, P., Ivanova, E., Graham, E.S., Ross, A.W., Wilson, D., Plé, H., Mercer, J.G., Ebling, F.J., Schuhler, S., Dupré, S.M., Loudon, A., Morgan, P.J., 2006. Photoperiodic regulation of cellular retinoic acid-binding protein 1, GPR50 and nestin in tanycytes of the third ventricle ependymal layer of the Siberian hamster. Journal of Endocrinology 191, 687–698. https://doi.org/10.1677/joe.1.06929

Barrett, P., Ross, A.W., Balik, A., Littlewood, P.A., Mercer, J.G., Moar, K.M., Sallmen, T., Kaslin, J., Panula, P., Schuhler, S., Ebling, F.J., Ubeaud, C., Morgan, P.J., 2005. Photoperiodic Regulation of Histamine H3 Receptor and VGF Messenger Ribonucleic Acid in the Arcuate Nucleus of the Siberian Hamster. Endocrinology 146, 1930–1939. https://doi.org/10.1210/en.2004-1452

Bartness, T.J., McGriff, W.R., Maharaj, M.P., 1991. Effects of diabetes and insulin on photoperiodic responses in Siberian hamsters. Physiology & Behavior 49, 613–620. https://doi.org/10.1016/0031-9384(91)90287-X

Bartness, T.J., Song, C.K., 2007. Thematic review series: Adipocyte Biology. Sympathetic and sensory innervation of white adipose tissue. Journal of Lipid Research 48, 1655–1672. https://doi.org/10.1194/jlr.R700006-JLR200

Bechtold, D.A., Sidibe, A., Saer, B.R.C., Li, J., Hand, L.E., Ivanova, E.A., Darras, V.M., Dam, J., Jockers, R., Luckman, S.M., Loudon, A.S.I., 2012. A Role for the Melatonin-Related Receptor GPR50 in Leptin Signaling, Adaptive Thermogenesis, and Torpor. Current Biology 22, 70–77. https://doi.org/10.1016/j.cub.2011.11.043

Beck, B., 2006. Neuropeptide Y in normal eating and in genetic and dietary-induced obesity. Phil. Trans. R. Soc. B 361, 1159–1185. https://doi.org/10.1098/rstb.2006.1855

Benford, H., Bolborea, M., Pollatzek, E., Lossow, K., Hermans-Borgmeyer, I., Liu, B., Meyerhof, W., Kasparov, S., Dale, N., 2017. A sweet taste receptor-dependent mechanism of glucosensing in hypothalamic

tanycytes: Sweet Taste Receptors in Tanycytes. Glia 65, 773–789. https://doi.org/10.1002/glia.23125

Benjamini, Y., Hochberg, Y., 1995. Controlling the False Discovery Rate: A Practical and Powerful Approach to Multiple Testing. Journal of the Royal Statistical Society: Series B (Methodological) 57, 289–300. https://doi.org/10.1111/j.2517-6161.1995.tb02031.x

Bernard, C., 1865. An Introduction to the Study of Experimental Medicine. Courier Corporation.

Bernard, V., Young, J., Binart, N., 2019. Prolactin — a pleiotropic factor in health and disease. Nat Rev Endocrinol 15, 356–365. https://doi.org/10.1038/s41574-019-0194-6

Bernard, V., Young, J., Chanson, P., Binart, N., 2015. New insights in prolactin: pathological implications. Nat Rev Endocrinol 11, 265–275. https://doi.org/10.1038/nrendo.2015.36

Bernichtein, S., Touraine, P., Goffin, V., 2010. New concepts in prolactin biology. Journal of Endocrinology 206, 1–11. https://doi.org/10.1677/JOE-10-0069

Berson, D.M., 2002. Phototransduction by Retinal Ganglion Cells That Set the Circadian Clock. Science 295, 1070–1073. https://doi.org/10.1126/science.1067262

Betley, J.N., Cao, Z.F.H., Ritola, K.D., Sternson, S.M., 2013. Parallel, Redundant Circuit Organization for Homeostatic Control of Feeding Behavior. Cell 155, 1337–1350. https://doi.org/10.1016/j.cell.2013.11.002

Bi, S., Robinson, B.M., Moran, T.H., 2003. Acute food deprivation and chronic food restriction differentially affect hypothalamic NPY mRNA expression. American Journal of Physiology-Regulatory, Integrative and Comparative Physiology 285, R1030–R1036. https://doi.org/10.1152/ajpregu.00734.2002

Bilbo, S.D., Nelson, R.J., 2003. Sex differences in photoperiodic and stress-induced enhancement of immune function in Siberian hamsters. Brain, Behavior, and Immunity 17, 462–472. https://doi.org/10.1016/S0889-1591(03)00063-1

Bittman, E.L., Tubbiola, M.L., Foltz, G., Hegarty, C.M., 1999. Effects of Photoperiod and Androgen on Proopiomelanocortin Gene Expression in the Arcuate Nucleus of Golden Hamsters**This work was supported by NIH

Grants MH-44132 and K02-MH-00914 (to E.L.B.). Endocrinology 140, 197–206. https://doi.org/10.1210/endo.140.1.6458

Bittman, E.L., Weaver, D.R., 1990. The Distribution of Melatonin Binding Sites in Neuroendocrine Tissues of the Ewe1. Biology of Reproduction 43, 986–993. https://doi.org/10.1095/biolreprod43.6.986

Blackshaw, S., Snyder, S.H., 1999. Encephalopsin: A Novel Mammalian Extraretinal Opsin Discretely Localized in the Brain. J. Neurosci. 19, 3681–3690. https://doi.org/10.1523/JNEUROSCI.19-10-03681.1999

Bolborea, M., Dale, N., 2013. Hypothalamic tanycytes: potential roles in the control of feeding and energy balance. Trends in Neurosciences 36, 91–100. https://doi.org/10.1016/j.tins.2012.12.008

Bolborea, M., Laran-Chich, M.-P., Rasri, K., Hildebrandt, H., Govitrapong, P., Simonneaux, V., Pévet, P., Steinlechner, S., Klosen, P., 2011. Melatonin Controls Photoperiodic Changes in Tanycyte Vimentin and Neural Cell Adhesion Molecule Expression in the Djungarian Hamster (Phodopus sungorus). Endocrinology 152, 3871–3883. https://doi.org/10.1210/en.2011-1039

Bole-Feysot, C., Goffin, V., Edery, M., Binart, N., Kelly, P.A., 1998. Prolactin (PRL) and Its Receptor: Actions, Signal Transduction Pathways and Phenotypes Observed in PRL Receptor Knockout Mice. Endocrine Reviews 19, 225–268. https://doi.org/10.1210/edrv.19.3.0334

Borlongan, C.V., Yamamoto, M., Takei, N., Kumazaki, M., Ungsuparkorn, C., Hida, H., Sanberg, P.R., Nishino, H., 2000. Glial cell survival is enhanced during melatonin-induced neuroprotection against cerebral ischemia. The FASEB Journal 14, 1307–1317. https://doi.org/10.1096/fasebj14101307

Bourin, M., Hascoët, M., 2003. The mouse light/dark box test. Eur J Pharmacol 463, 55–65. https://doi.org/10.1016/s0014-2999(03)01274-3

Brandebourg, T., Hugo, E., Ben-Jonathan, N., 2007. Adipocyte prolactin: regulation of release and putative functions. Diabetes Obes Metab 9, 464–476. https://doi.org/10.1111/j.1463-1326.2006.00671.x

Brazeau, P., Vale, W., Burgus, R., Ling, N., Butcher, M., Rivier, J., Guillemin, R., 1973. Hypothalamic polypeptide that inhibits the secretion of immunoreactive pituitary growth hormone. Science 179, 77–79.

Buenning, E., 1940. Studies of photo-periodism in the tropics. Forschungsdienst 10, 550–3.

Buning, E., 1936. Die endogene Tagesrhythmik als Grundlage der photoperiodischen Reaktion. Berichte der deutschen botanischen Gesellschaft 54, 590–607.

Busskamp, V., Lewis, N.E., Guye, P., Ng, A.H., Shipman, S.L., Byrne, S.M., Sanjana, N.E., Murn, J., Li, Y., Li, S., Stadler, M., Weiss, R., Church, G.M., 2014. Rapid neurogenesis through transcriptional activation in human stem cells. Mol Syst Biol 10, 760. https://doi.org/10.15252/msb.20145508

Butler, A.A., Kesterson, R.A., Khong, K., Cullen, M.J., Pelleymounter, M.A., Dekoning, J., Baetscher, M., Cone, R.D., 2000. A unique metabolic syndrome causes obesity in the melanocortin-3 receptor-deficient mouse. Endocrinology 141, 3518–3521. https://doi.org/10.1210/endo.141.9.7791

Butler, M.P., Turner, K.W., Park, J.H., Schoomer, E.E., Zucker, I., Gorman, M.R., 2010. Seasonal regulation of reproduction: altered role of melatonin under naturalistic conditions in hamsters. Proc. R. Soc. B. 277, 2867–2874. https://doi.org/10.1098/rspb.2010.0396

Butler, T.Z., Pavlenok, M., Derrington, I.M., Niederweis, M., Gundlach, J.H., 2008. Single-molecule DNA detection with an engineered MspA protein nanopore. Proc. Natl. Acad. Sci. U.S.A. 105, 20647–20652. https://doi.org/10.1073/pnas.0807514106

Cameron, J.L., Nosbisch, C., 1991. Suppression of Pulsatile Luteinizing Hormone and Testosterone Secretion during Short Term Food Restriction in the Adult Male Rhesus Monkey (Macaca mulatta)*. Endocrinology 128, 1532–1540. https://doi.org/10.1210/endo-128-3-1532

Cannon, W.B., 1939. The wisdom of the body, 2nd ed, The wisdom of the body, 2nd ed. Norton & Co., Oxford, England.

Cannon, W.B., 1929. Organization for physiological homeostasis. Physiological Reviews 9, 399–431. https://doi.org/10.1152/physrev.1929.9.3.399

Cardoso, R.C., Alves, B.R.C., Sharpton, S.M., Williams, G.L., Amstalden, M., 2015. Nutritional Programming of Accelerated Puberty in Heifers: Involvement of Pro-Opiomelanocortin Neurones in the Arcuate Nucleus. Journal of Neuroendocrinology 27, 647–657. https://doi.org/10.1111/jne.12291

Carrillo-Vico, A., Lardone, P.J., Alvarez-Sánchez, N., Rodríguez-Rodríguez, A., Guerrero, J.M., 2013. Melatonin: buffering the immune system. Int J Mol Sci 14, 8638–8683. https://doi.org/10.3390/ijms14048638

Carter, D. S., Goldman, B.D., 1983. Progonadal role of the pineal in the Djungarian hamster (Phodopus sungorus sungorus): mediation by melatonin. Endocrinology 113, 1268–1273. https://doi.org/10.1210/endo-113-4-1268

Carter, Dennis S., Goldman, B.D., 1983. Antigonadal Effects of Timed Melatonin Infusion in Pinealectomized Male Djungarian Hamsters (*Phodopus sungorus sungorus*): Duration is the Critical Parameter*. Endocrinology 113, 1261–1267. https://doi.org/10.1210/endo-113-4-1261

Chaar, L.J., Coelho, A., Silva, N.M., Festuccia, W.L., Antunes, V.R., 2016. High-fat diet-induced hypertension and autonomic imbalance are associated with an upregulation of CART in the dorsomedial hypothalamus of mice. Physiological Reports 4, e12811. https://doi.org/10.14814/phy2.12811

Chaker, Z., George, C., Petrovska, M., Caron, J.-B., Lacube, P., Caillé, I., Holzenberger, M., 2016. Hypothalamic neurogenesis persists in the aging brain and is controlled by energy-sensing IGF-I pathway. Neurobiology of Aging 41, 64–72. https://doi.org/10.1016/j.neurobiolaging.2016.02.008

Chan, S.F., Huang, X., McKercher, S.R., Zaidi, R., Okamoto, S., Nakanishi, N., Lipton, S.A., 2015. Transcriptional profiling of MEF2-regulated genes in human neural progenitor cells derived from embryonic stem cells. Genomics Data 3, 24–27. https://doi.org/10.1016/j.gdata.2014.10.022

Chen, A.S., Marsh, D.J., Trumbauer, M.E., Frazier, E.G., Guan, X.-M., Yu, H., Rosenblum, C.I., Vongs, A., Feng, Y., Cao, L., Metzger, J.M., Strack, A.M., Camacho, R.E., Mellin, T.N., Nunes, C.N., Min, W., Fisher, J., Gopal-Truter, S., MacIntyre, D.E., Chen, H.Y., Van der Ploeg, L.H.T., 2000. Inactivation of the mouse melanocortin-3 receptor results in increased fat mass and reduced lean body mass. Nat Genet 26, 97–102. https://doi.org/10.1038/79254

Chen, P., Smith, M.S., 2004. Regulation of Hypothalamic Neuropeptide Y Messenger Ribonucleic Acid Expression during Lactation: Role of Prolactin. Endocrinology 145, 823–829. https://doi.org/10.1210/en.2003-1255

Chen, Z., Liang, S., Zhao, Y., Han, Z., 2012. miR-92b regulates Mef2 levels through a negative-feedback circuit during *Drosophila* muscle

development. Development 139, 3543–3552. https://doi.org/10.1242/dev.082719

Chiu, S., Wise, P.M., 1994. Prolactin Receptor mRNA Localization in the Hypothalamus by in situ Hybridization. J Neuroendocrinol 6, 191–199. https://doi.org/10.1111/j.1365-2826.1994.tb00572.x

Chou, T.C., Scammell, T.E., Gooley, J.J., Gaus, S.E., Saper, C.B., Lu, J., 2003. Critical Role of Dorsomedial Hypothalamic Nucleus in a Wide Range of Behavioral Circadian Rhythms. J. Neurosci. 23, 10691–10702. https://doi.org/10.1523/JNEUROSCI.23-33-10691.2003

Church, J.S., Renzelman, M.L., Schwartzer, J.J., 2022. Ten-week high fat and high sugar diets in mice alter gut-brain axis cytokines in a sex-dependent manner. The Journal of Nutritional Biochemistry 100, 108903. https://doi.org/10.1016/j.jnutbio.2021.108903

Cicchetti, D.V., n.d. Guidelines, Criteria, and Rules of Thumb for Evaluating Normed and Standardized Assessment Instruments in Psychology.

Cipolla-Neto, J., Amaral, F.G., Afeche, S.C., Tan, D.X., Reiter, R.J., 2014. Melatonin, energy metabolism, and obesity: a review. Journal of Pineal Research 56, 371–381. https://doi.org/10.1111/jpi.12137

Collins, F.S., Morgan, M., Patrinos, A., 2003. The Human Genome Project: Lessons from Large-Scale Biology. Science 300, 286–290. https://doi.org/10.1126/science.1084564

Condon, C.H., Chenoweth, S.F., Wilson, R.S., 2010. Zebrafish take their cue from temperature but not photoperiod for the seasonal plasticity of thermal performance. Journal of Experimental Biology 213, 3705–3709. https://doi.org/10.1242/jeb.046979

Considine, R.V., Sinha, M.K., Heiman, M.L., Kriauciunas, A., Stephens, T.W., Nyce, M.R., Ohannesian, J.P., Marco, C.C., McKee, L.J., Bauer, T.L., 1996. Serum immunoreactive-leptin concentrations in normal-weight and obese humans. N Engl J Med 334, 292–295. https://doi.org/10.1056/NEJM199602013340503

Cornelissen, G., 2014. Cosinor-based rhythmometry. Theoretical Biology and Medical Modelling 11, 16. https://doi.org/10.1186/1742-4682-11-16

Cornier, M.-A., Dabelea, D., Hernandez, T.L., Lindstrom, R.C., Steig, A.J., Stob, N.R., Van Pelt, R.E., Wang, H., Eckel, R.H., 2008. The Metabolic

Syndrome. Endocrine Reviews 29, 777–822. https://doi.org/10.1210/er.2008-0024

Cowley, M.A., Smart, J.L., Rubinstein, M., Cerdán, M.G., Diano, S., Horvath, T.L., Cone, R.D., Low, M.J., 2001. Leptin activates anorexigenic POMC neurons through a neural network in the arcuate nucleus. Nature 411, 480–484. https://doi.org/10.1038/35078085

Crawford, J.L., Thomson, B.P., Beaumont, M.F., Eckery, D.C., 2006. Plasma concentrations of prolactin in brushtail possums (Trichosurus vulpecula) in different physiological states. Journal of Endocrinology 190, 295–305. https://doi.org/10.1677/joe.1.06882

Curlewis, J.D., 1991. Seasonal changes in the reproductive organs and plasma and pituitary hormone content of the male Bennett's wallaby *(Macropus rufogriseus vufogriseus)*. Journal of Zoology 223, 223–231. https://doi.org/10.1111/j.1469-7998.1991.tb04762.x

Cushing, H., Goetsch, E., 1915. HIBERNATION AND THE PITUITARY BODY. Journal of Experimental Medicine 22, 25–47. https://doi.org/10.1084/jem.22.1.25

Dardente, H., 2012. Melatonin-Dependent Timing of Seasonal Reproduction by the Pars Tuberalis: Pivotal Roles for Long Daylengths and Thyroid Hormones: Melatonin-dependent timing of seasonal reproduction by the pars tuberalis. Journal of Neuroendocrinology 24, 249–266. https://doi.org/10.1111/j.1365-2826.2011.02250.x

Dardente, H., Menet, J.S., Poirel, V.-J., Streicher, D., Gauer, F., Vivien-Roels, B., Klosen, P., Pévet, P., Masson-Pévet, M., 2003. Melatonin induces Cry1 expression in the pars tuberalis of the rat. Molecular Brain Research 114, 101–106. https://doi.org/10.1016/S0169-328X(03)00134-7

Dardente, H., Wyse, C.A., Birnie, M.J., Dupré, S.M., Loudon, A.S.I., Lincoln, G.A., Hazlerigg, D.G., 2010. A Molecular Switch for Photoperiod Responsiveness in Mammals. Current Biology 20, 2193–2198. https://doi.org/10.1016/j.cub.2010.10.048

Davies, K.J.A., 2016. Adaptive homeostasis. Molecular Aspects of Medicine, Hormetic and regulatory effects of lipid oxidation products 49, 1–7. https://doi.org/10.1016/j.mam.2016.04.007

Day, T.A., 2005. Defining stress as a prelude to mapping its neurocircuitry: no help from allostasis. Prog Neuropsychopharmacol Biol Psychiatry 29, 1195–1200. https://doi.org/10.1016/j.pnpbp.2005.08.005

de Castro, J.M., 1991. Seasonal rhythms of human nutrient intake and meal pattern. Physiology & Behavior 50, 243–248. https://doi.org/10.1016/0031-9384(91)90527-U

DiMicco, J.A., Zaretsky, D.V., 2007. The dorsomedial hypothalamus: a new player in thermoregulation. American Journal of Physiology-Regulatory, Integrative and Comparative Physiology 292, R47–R63. https://doi.org/10.1152/ajpregu.00498.2006

Dobolyi, A., Oláh, S., Keller, D., Kumari, R., Fazekas, E.A., Csikós, V., Renner, É., Cservenák, M., 2020. Secretion and Function of Pituitary Prolactin in Evolutionary Perspective. Front. Neurosci. 14, 621. https://doi.org/10.3389/fnins.2020.00621

Duckett, K., Williamson, A., Kincaid, J.W.R., Rainbow, K., Corbin, L.J., Martin, H.C., Eberhardt, R.Y., Huang, Q.Q., Hurles, M.E., He, W., Brauner, R., Delaney, A., Dunkel, L., Grinspon, R.P., Hall, J.E., Hirschhorn, J.N., Howard, S.R., Latronico, A.C., Jorge, A.A.L., McElreavey, K., Mericq, V., Merino, P.M., Palmert, M.R., Plummer, L., Rey, R.A., Rezende, R.C., Seminara, S.B., Salnikov, K., Banerjee, I., Lam, B.Y.H., Perry, J.R.B., Timpson, N.J., Clayton, P., Chan, Y.-M., Ong, K.K., O'Rahilly, S., 2023. Prevalence of Deleterious Variants in MC3R in Patients With Constitutional Delay of Growth and Puberty. The Journal of Clinical Endocrinology & Metabolism dgad373. https://doi.org/10.1210/clinem/dgad373

Dumbell, R., Petri, I., Scherbarth, F., Diedrich, V., Schmid, H.A., Steinlechner, S., Barrett, P., 2017. Somatostatin Agonist Pasireotide Inhibits Exercise-Stimulated Growth in the Male Siberian Hamster (Phodopus sungorus). Journal of Neuroendocrinology 29. https://doi.org/10.1111/jne.12448

Dumbell, R.A., Scherbarth, F., Diedrich, V., Schmid, H.A., Steinlechner, S., Barrett, P., 2015. Somatostatin Agonist Pasireotide Promotes a Physiological State Resembling Short-Day Acclimation in the Photoperiodic Male Siberian Hamster (Phodopus sungorus). Journal of Neuroendocrinology 27, 588–599. https://doi.org/10.1111/jne.12289

Dupré, S.M., Miedzinska, K., Duval, C.V., Yu, L., Goodman, R.L., Lincoln, G.A., Davis, J.R.E., McNeilly, A.S., Burt, D.D., Loudon, A.S.I., 2010. Identification of Eya3 and TAC1 as Long-Day Signals in the Sheep Pituitary. Current Biology 20, 829–835. https://doi.org/10.1016/j.cub.2010.02.066

Duquenne, M., Folgueira, C., Bourouh, C., Millet, M., Silva, A., Clasadonte, J., Imbernon, M., Fernandois, D., Martinez-Corral, I., Kusumakshi, S., Caron, E., Rasika, S., Deliglia, E., Jouy, N., Oishi, A., Mazzone, M., Trinquet, E., Tavernier, J., Kim, Y.-B., Ory, S., Jockers, R., Schwaninger, M., Boehm, U., Nogueiras, R., Annicotte, J.-S., Gasman, S., Dam, J., Prévot, V., 2021. Leptin brain entry via a tanycytic LepR–EGFR shuttle controls lipid metabolism and pancreas function. Nat Metab 3, 1071–1090. https://doi.org/10.1038/s42255-021-00432-5

Duston, J., Bromage, N., 1991. Circannual Rhythms of Gonadal Maturation in Female Rainbow Trout (Oncorhynchus mykiss). J Biol Rhythms 6, 49–53. https://doi.org/10.1177/074873049100600106

Ebling, F.J.P., Barrett, P., 2008. The Regulation of Seasonal Changes in Food Intake and Body Weight. Journal of Neuroendocrinology 20, 827–833. https://doi.org/10.1111/j.1365-2826.2008.01721.x

Ebling, F.J.P., Lincoln, G.A., 1987. ß-Endorphin Secretion in Rams Related to Season and Photoperiod. Endocrinology 120, 809–818. https://doi.org/10.1210/endo-120-2-809

Ebling, F.P., Arthurs, O.J., Turney, B.W., Cronin, A.S., 1998. Seasonal Neuroendocrine Rhythms in the Male Siberian Hamster Persist After Monosodium Glutamate-Induced Lesions of the Arcuate Nucleus in the Neonatal Period. Journal of Neuroendocrinology 10, 701–712. https://doi.org/10.1046/j.1365-2826.1998.00253.x

Ellis, C., Moar, K.M., Logie, T.J., Ross, A.W., Morgan, P.J., Mercer, J.G., 2008. Diurnal profiles of hypothalamic energy balance gene expression with photoperiod manipulation in the Siberian hamster, Phodopus sungorus. American Journal of Physiology-Regulatory, Integrative and Comparative Physiology 294, R1148–R1153. https://doi.org/10.1152/ajpregu.00825.2007

Engeli, S., Janke, J., Gorzelniak, K., Böhnke, J., Ghose, N., Lindschau, C., Luft, F.C., Sharma, A.M., 2004. Regulation of the nitric oxide system in human adipose tissue. Journal of Lipid Research 45, 1640–1648. https://doi.org/10.1194/jlr.M300322-JLR200

Enriori, P.J., Evans, A.E., Sinnayah, P., Cowley, M.A., 2006. Leptin Resistance and Obesity. Obesity 14, 254S-258S. https://doi.org/10.1038/oby.2006.319

Ernst, W., Trummer, E., Mead, J., Bessant, C., Strelec, H., Katinger, H., Hesse, F., 2006. Evaluation of a genomics platform for cross-species transcriptome analysis of recombinant CHO cells. Biotechnol. J. 1, 639–650. https://doi.org/10.1002/biot.200600010

Farhy, L.S., Veldhuis, J.D., 2004. Putative GH pulse renewal: periventricular somatostatinergic control of an arcuate-nuclear somatostatin and GH-releasing hormone oscillator. American Journal of Physiology-Regulatory, Integrative and Comparative Physiology 286, R1030–R1042. https://doi.org/10.1152/ajpregu.00473.2003

Ferguson, M., Sohal, B.H., Forster, M.J., Sohal, R.S., 2007. Effect of long-term caloric restriction on oxygen consumption and body temperature in two different strains of mice. Mechanisms of Ageing and Development 128, 539–545. https://doi.org/10.1016/j.mad.2007.07.005

Ferland, L., Labrie, F., Jobin, M., Arimura, A., Schally, A.V., 1976. Physiological role of somatostatin in the control of growth hormone and thyrotropin secretion. Biochemical and Biophysical Research Communications 68, 149–156. https://doi.org/10.1016/0006-291X(76)90022-X

Fine, J.B., Bartness, T.J., 1996. Day length and body mass affect diet self-selection by siberian hamsters. Physiology & Behavior 59, 1039–1050. https://doi.org/10.1016/0031-9384(95)02240-6

Finley, C.M., Gorman, M.R., Tuthill, C.R., Zucker, I., 1995. Long-Term Reproductive Effects of a Single Long Day in the Siberian Hamster (Phodopus sungorus. J Biol Rhythms 10, 33–41. https://doi.org/10.1177/074873049501000103

Fitzgerald, P., Dinan, T.G., 2008. Prolactin and dopamine: What is the connection? A Review Article. J Psychopharmacol 22, 12–19. https://doi.org/10.1177/0269216307087148

Fleischmann, R.D., Adams, M.D., White, O., Clayton, R.A., Kirkness, E.F., Kerlavage, A.R., Bult, C.J., Tomb, J.-F., Dougherty, B.A., Merrick, J.M., McKenney, K., Sutton, G., FitzHugh, W., Fields, C., Gocayne, J.D., Scott, J., Shirley, R., Liu, L., Glodek, A., Kelley, J.M., Weidman, J.F., Phillips, C.A., Spriggs, T., Hedblom, E., Cotton, M.D., Utterback, T.R., Hanna, M.C., Nguyen, D.T., Saudek, D.M., Brandon, R.C., Fine, L.D., Fritchman, J.L., Fuhrmann, J.L., Geoghagen, N.S.M., Gnehm, C.L., McDonald, L.A., Small, K.V., Fraser, C.M., Smith, H.O., Venter, J.C., 1995. Whole-Genome

Random Sequencing and Assembly of *Haemophilus influenzae* Rd. Science 269, 496–512. https://doi.org/10.1126/science.7542800

Forbes, S., Li, X.F., Kinsey-Jones, J., O'Byrne, K., 2009. Effects of ghrelin on Kisspeptin mRNA expression in the hypothalamic medial preoptic area and pulsatile luteinising hormone secretion in the female rat. Neuroscience Letters 460, 143–147. https://doi.org/10.1016/j.neulet.2009.05.060

Freeman, D.A., Lewis, D.A., Kauffman, A.S., Blum, R.M., Dark, J., 2004. Reduced leptin concentrations are permissive for display of torpor in Siberian hamsters. American Journal of Physiology-Regulatory, Integrative and Comparative Physiology 287, R97–R103. https://doi.org/10.1152/ajpregu.00716.2003

Freeman, D.A., Zucker, I., 2001. Refractoriness to melatonin occurs independently at multiple brain sites in Siberian hamsters. Proceedings of the National Academy of Sciences 98, 6447–6452. https://doi.org/10.1073/pnas.111140398

Freire-Regatillo, A., Fernández-Gómez, M.J., Díaz, F., Barrios, V., Sánchez-Jabonero, I., Frago, L.M., Argente, J., García-Segura, L.M., Chowen, J.A., 2020. Sex differences in the peripubertal response to a short-term, high-fat diet intake. J Neuroendocrinology 32, e12756. https://doi.org/10.1111/jne.12756

Gantz, I., Fong, T.M., 2003. The melanocortin system. American Journal of Physiology-Endocrinology and Metabolism 284, E468–E474. https://doi.org/10.1152/ajpendo.00434.2002

Garner, W.W., Allard, H.A., 1920. EFFECT OF THE RELATIVE LENGTH OF DAY AND NIGHT AND OTHER FACTORS OF THE ENVIRONMENT ON GROWTH AND REPRODUCTION IN PLANTS. Monthly Weather Review 48, 415–415. https://doi.org/10.1175/1520-0493(1920)48<415b:EOTRLO>2.0.CO;2

Gauthier, M.-S., Favier, R., Lavoie, J.-M., 2006. Time course of the development of non-alcoholic hepatic steatosis in response to high-fat diet-induced obesity in rats. British Journal of Nutrition 95, 273–281. https://doi.org/10.1079/BJN20051635

Ge, S.X., Jung, D., Yao, R., 2020. ShinyGO: a graphical gene-set enrichment tool for animals and plants. Bioinformatics 36, 2628–2629. https://doi.org/10.1093/bioinformatics/btz931

Gerardo-Gettens, T., Moore, B.J., Stern, J.S., Horwitz, B.A., 1989. Prolactin stimulates food intake in a dose-dependent manner. American Journal of Physiology-Regulatory, Integrative and Comparative Physiology 256, R276–R280. https://doi.org/10.1152/ajpregu.1989.256.1.R276

Ghamari-Langroudi, M., Cakir, I., Lippert, R.N., Sweeney, P., Litt, M.J., Ellacott, K.L.J., Cone, R.D., 2018. Regulation of energy rheostasis by the melanocortin-3 receptor. Science Advances 4, eaat0866. https://doi.org/10.1126/sciadv.aat0866

Giordano, M., 2013. Homeostasis: An underestimated focal point of ecology and evolution. Plant Science 211, 92–101. https://doi.org/10.1016/j.plantsci.2013.07.008

Goldman, B.D., 2001. Mammalian photoperiodic system: formal properties and neuroendocrine mechanisms of photoperiodic time measurement. J Biol Rhythms 16, 283–301. https://doi.org/10.1177/074873001129001980

Goodman, T., Hajihosseini, M.K., 2015. Hypothalamic tanycytes—masters and servants of metabolic, neuroendocrine, and neurogenic functions. Front. Neurosci. 9. https://doi.org/10.3389/fnins.2015.00387

Gorman, M.R., Zucker, I., 1995. Testicular regression and recrudescence without subsequent photorefractoriness in Siberian hamsters. American Journal of Physiology-Regulatory, Integrative and Comparative Physiology 269, R800–R806. https://doi.org/10.1152/ajpregu.1995.269.4.R800

Greenman, Y., Tordjman, K., Stern, N., 1998. Increased body weight associated with prolactin secreting pituitary adenomas: weight loss with normalization of prolactin levels: Prolactin and increased body weight. Clinical Endocrinology 48, 547–553. https://doi.org/10.1046/j.1365-2265.1998.00403.x

Greggor, A.L., Jolles, J.W., Thornton, A., Clayton, N.S., 2016. Seasonal changes in neophobia and its consistency in rooks: the effect of novelty type and dominance position. Animal Behaviour 121, 11–20. https://doi.org/10.1016/j.anbehav.2016.08.010

Gross, C.G., 1998. Claude Bernard and the Constancy of the Internal Environment. Neuroscientist 4, 380–385. https://doi.org/10.1177/107385849800400520

Gu, Z., Eils, R., Schlesner, M., 2016. Complex heatmaps reveal patterns and correlations in multidimensional genomic data. Bioinformatics 32, 2847–2849. https://doi.org/10.1093/bioinformatics/btw313

Hadley, M.E., Haskell-Luevano, C., 1999. The Proopiomelanocortin System. Annals of the New York Academy of Sciences 885, 1–21. https://doi.org/10.1111/j.1749-6632.1999.tb08662.x

Hannedouche, S., Beck, V., Leighton-Davies, J., Beibel, M., Roma, G., Oakeley, E.J., Lannoy, V., Bernard, J., Hamon, J., Barbieri, S., Preuss, I., Lasbennes, M.-C., Sailer, A.W., Suply, T., Seuwen, K., Parker, C.N., Bassilana, F., 2013. Identification of the C3a Receptor (C3AR1) as the Target of the VGF-derived Peptide TLQP-21 in Rodent Cells. Journal of Biological Chemistry 288, 27434–27443. https://doi.org/10.1074/jbc.M113.497214

Hanon, E.A., Lincoln, G.A., Fustin, J.-M., Dardente, H., Masson-Pévet, M., Morgan, P.J., Hazlerigg, D.G., 2008. Ancestral TSH Mechanism Signals Summer in a Photoperiodic Mammal. Current Biology 18, 1147–1152. https://doi.org/10.1016/j.cub.2008.06.076

Hanson, E.S., Dallman, M.F., 1995. Neuropeptide Y (NPY) May Integrate Responses of Hypothalamic Feeding Systems and the Hypothalamo-Pituitary-Adrenal Axis. Journal of Neuroendocrinology 7, 273–279. https://doi.org/10.1111/j.1365-2826.1995.tb00757.x

Hastings, M.H., Herzog, E.D., 2004. Clock Genes, Oscillators, and Cellular Networks in the Suprachiasmatic Nuclei. J Biol Rhythms 19, 400–413. https://doi.org/10.1177/0748730404268786

Hazlerigg, D., Lomet, D., Lincoln, G., Dardente, H., 2018. Neuroendocrine correlates of the critical day length response in the Soay sheep. Journal of Neuroendocrinology 30, e12631. https://doi.org/10.1111/jne.12631

Hazlerigg, D.G., Andersson, H., Johnston, J.D., Lincoln, G., 2004. Molecular Characterization of the Long-Day Response in the Soay Sheep, a Seasonal Mammal. Current Biology 14, 334–339. https://doi.org/10.1016/j.cub.2004.01.057

Hazlerigg, D.G., Gonzalez-Brito, A., Lawson, W., Hastings, M.H., Morgan, P.J., 1993. Prolonged exposure to melatonin leads to time-dependent sensitization of adenylate cyclase and down-regulates melatonin

receptors in pars tuberalis cells from ovine pituitary. Endocrinology 132, 285–292. https://doi.org/10.1210/en.132.1.285

Hazlerigg, D.G., Lincoln, G.A., 2011. Hypothesis: Cyclical Histogenesis Is the Basis of Circannual Timing. J Biol Rhythms 26, 471–485. https://doi.org/10.1177/0748730411420812

Hazlerigg, D.G., Wagner, G.C., 2006. Seasonal photoperiodism in vertebrates: from coincidence to amplitude. Trends in Endocrinology & Metabolism 17, 83–91. https://doi.org/10.1016/j.tem.2006.02.004

Heijboer, A.C., Voshol, P.J., Donga, E., van Eden, C.G., Havekes, L.M., Romijn, J.A., Pijl, H., Corssmit, E.P.M., 2005. High fat diet induced hepatic insulin resistance is not related to changes in hypothalamic mRNA expression of NPY, AgRP, POMC and CART in mice. Peptides 26, 2554–2558. https://doi.org/10.1016/j.peptides.2005.05.013

Heldmaier, G., Steinlechner, S., 1981. Seasonal control of energy requirements for thermoregulation in the djungarian hamster (Phodopus sungorus), living in natural photoperiod. J Comp Physiol B 142, 429–437. https://doi.org/10.1007/BF00688972

Helfer, G., Barrett, P., Morgan, P.J., 2019. A unifying hypothesis for control of body weight and reproduction in seasonally breeding mammals. Journal of Neuroendocrinology 31, e12680. https://doi.org/10.1111/jne.12680

Helfer, G., Stevenson, T.J., 2020. Pleiotropic effects of proopiomelanocortin and VGF nerve growth factor inducible neuropeptides for the long-term regulation of energy balance. Molecular and Cellular Endocrinology 514, 110876. https://doi.org/10.1016/j.mce.2020.110876

Helwig, M., Khorooshi, R.M.H., Tups, A., Barrett, P., Archer, Z.A., Exner, C., Rozman, J., Braulke, L.J., Mercer, J.G., Klingenspor, M., 2006. PC1/3 and PC2 Gene Expression and Post-Translational Endoproteolytic Pro-Opiomelanocortin Processing is Regulated by Photoperiod in the Seasonal Siberian Hamster (Phodopus sungorus). J Neuroendocrinol 18, 413–425. https://doi.org/10.1111/j.1365-2826.2006.01431.x

Henry, Ba, Goding, J., Tilbrook, A., Dunshea, F., Clarke, I., 2001. Intracerebroventricular infusion of leptin elevates the secretion of luteinising hormone without affecting food intake in long-term food-restricted sheep, but increases growth hormone irrespective of

bodyweight. Journal of Endocrinology 168, 67–77. https://doi.org/10.1677/joe.0.1680067

Henry, Belinda, Rao, A., Tilbrook, A.J., Clarke, I., 2001. Chronic food-restriction alters the expression of somatostatin and growth hormone-relasing hormone in the ovariectomized ewe. The Journal of endocrinology 170, R1-5. https://doi.org/10.1677/joe.0.170R001

Hentges, S.T., Otero-Corchon, V., Pennock, R.L., King, C.M., Low, M.J., 2009. Proopiomelanocortin Expression in both GABA and Glutamate Neurons. J. Neurosci. 29, 13684–13690. https://doi.org/10.1523/JNEUROSCI.3770-09.2009

Herwig, A., Vries, E.M. de, Bolborea, M., Wilson, D., Mercer, J.G., Ebling, F.J.P., Morgan, P.J., Barrett, P., 2013. Hypothalamic Ventricular Ependymal Thyroid Hormone Deiodinases Are an Important Element of Circannual Timing in the Siberian Hamster (Phodopus sungorus). PLOS ONE 8, e62003. https://doi.org/10.1371/journal.pone.0062003

Hill, J.W., 2010. Gene Expression and the Control of Food Intake by Hypothalamic POMC/CART Neurons. Open Neuroendocrinol J 3, 21–27.

Hill, S.M., Belancio, V.P., Dauchy, R.T., Xiang, S., Brimer, S., Mao, L., Hauch, A., Lundberg, P.W., Summers, W., Yuan, L., Frasch, T., Blask, D.E., 2015. Melatonin: an inhibitor of breast cancer. Endocrine-Related Cancer 22, R183–R204. https://doi.org/10.1530/ERC-15-0030

Hilsabeck, T.A.U., Liu-Bryan, R., Guo, T., Wilson, K.A., Bose, N., Raftery, D., Beck, J.N., Lang, S., Jin, K., Nelson, C.S., Oron, T., Stoller, M., Promislow, D., Brem, R.B., Terkeltaub, R., Kapahi, P., 2022. A fly GWAS for purine metabolites identifies human FAM214 homolog medusa, which acts in a conserved manner to enhance hyperuricemia-driven pathologies by modulating purine metabolism and the inflammatory response. GeroScience 44, 2195–2211. https://doi.org/10.1007/s11357-022-00557-9

Ho, J.M., Smith, N.S., Adams, S.A., Bradshaw, H.B., Demas, G.E., 2012. Photoperiodic Changes in Endocannabinoid Levels and Energetic Responses to Altered Signalling at CB $_1$ Receptors in Siberian Hamsters: Endocannabinoids across sex and season. Journal of Neuroendocrinology 24, 1030–1039. https://doi.org/10.1111/j.1365-2826.2012.02312.x

Holekamp, K.E., Nunes, S., Talamantes, F., 1988. Circulating prolactin in free-living California ground squirrels (Spermophilus beecheyi). General and

Comparative Endocrinology 71, 484–492. https://doi.org/10.1016/0016-6480(88)90278-X

Horton, T.H., Yellon, S.M., 2001. Aging, Reproduction, and the Melatonin Rhythm in the Siberian Hamster. J Biol Rhythms 16, 243–253. https://doi.org/10.1177/074873001129001953

Houseknecht, K.L., Baile, C.A., Matteri, R.L., Spurlock, M.E., 1998. The biology of leptin: a review. Journal of Animal Science 76, 1405. https://doi.org/10.2527/1998.7651405x

Howell-Skalla, L., Cattet, M., Ramsay, M., Bahr, J., 2002. Seasonal changes in testicular size and serum LH, prolactin and testosterone concentrations in male polar bears (Ursus maritimus). Reproduction 729–733. https://doi.org/10.1530/rep.0.1230729

Huang, W., Ramsey, K.M., Marcheva, B., Bass, J., 2011. Circadian rhythms, sleep, and metabolism. J Clin Invest 121, 2133–2141. https://doi.org/10.1172/JCI46043

Hughes, M.E., Hogenesch, J.B., Kornacker, K., 2010. JTK_CYCLE: An Efficient Nonparametric Algorithm for Detecting Rhythmic Components in Genome-Scale Data Sets. J Biol Rhythms 25, 372–380. https://doi.org/10.1177/0748730410379711

Huszar, D., Lynch, C.A., Fairchild-Huntress, V., Dunmore, J.H., Fang, Q., Berkemeier, L.R., Gu, W., Kesterson, R.A., Boston, B.A., Cone, R.D., Smith, F.J., Campfield, L.A., Burn, P., Lee, F., 1997. Targeted disruption of the melanocortin-4 receptor results in obesity in mice. Cell 88, 131–141. https://doi.org/10.1016/s0092-8674(00)81865-6

Hutchison, A.L., Maienschein-Cline, M., Chiang, A.H., Tabei, S.M.A., Gudjonson, H., Bahroos, N., Allada, R., Dinner, A.R., 2015. Improved Statistical Methods Enable Greater Sensitivity in Rhythm Detection for Genome-Wide Data. PLoS Comput Biol 11, e1004094. https://doi.org/10.1371/journal.pcbi.1004094

Hwang, L., Wang, C., Li, T., Chang, S., Lin, L., Chen, Ching-Ping, Chen, Chiung-Tong, Liang, K., Ho, I., Yang, W., Chiou, L., 2010. Sex Differences in High-fat Diet-induced Obesity, Metabolic Alterations and Learning, and Synaptic Plasticity Deficits in Mice. Obesity 18, 463–469. https://doi.org/10.1038/oby.2009.273

Isovich, E., del Carmen Diaz, M., Lasaga, M., Pisera, D., Zambruno, C., Theas, M.S., Seilicovich, A., Duvilanski, B.H., 1994. Involvement of hypothalamic substance P in the effect of prolactin on dopamine release: NeuroReport 5, 1752–1754. https://doi.org/10.1097/00001756-199409080-00016

Izquierdo, A.G., Crujeiras, A.B., Casanueva, F.F., Carreira, M.C., 2019. Leptin, Obesity, and Leptin Resistance: Where Are We 25 Years Later? Nutrients 11, 2704. https://doi.org/10.3390/nu11112704

Jarjisian, S.G., Piekarski, D.J., Place, N.J., Driscoll, J.R., Paxton, E.G., Kriegsfeld, L.J., Zucker, I., 2013. Dorsomedial Hypothalamic Lesions Block Syrian Hamster Testicular Regression in Short Day Lengths Without Diminishing Increased Testosterone Negative-Feedback Sensitivity1. Biology of Reproduction 89. https://doi.org/10.1095/biolreprod.113.109587

Jefimow, M., Przybylska-Piech, A.S., 2022. Housing conditions modify seasonal changes in basal metabolism and body mass of the Siberian hamster, Phodopus sungorus. J Comp Physiol B 192, 513–526. https://doi.org/10.1007/s00360-022-01434-9

Jeppesen, J., Hein, H.O., Suadicani, P., Gyntelberg, F., 2000. High Triglycerides and Low HDL Cholesterol and Blood Pressure and Risk of Ischemic Heart Disease. Hypertension 36, 226–232. https://doi.org/10.1161/01.HYP.36.2.226

Jethwa, P.H., Warner, A., Fowler, M.J., Murphy, M., De Backer, M.W., Adan, R. a. H., Barrett, P., Brameld, J.M., Ebling, F.J.P., 2010. Short-Days Induce Weight Loss in Siberian Hamsters Despite Overexpression of the Agouti-Related Peptide Gene. Journal of Neuroendocrinology 22, 564–575. https://doi.org/10.1111/j.1365-2826.2010.02001.x

Jethwa, P.H., Warner, A., Nilaweera, K.N., Brameld, J.M., Keyte, J.W., Carter, W.G., Bolton, N., Bruggraber, M., Morgan, P.J., Barrett, P., Ebling, F.J.P., 2007. VGF-Derived Peptide, TLQP-21, Regulates Food Intake and Body Weight in Siberian Hamsters. Endocrinology 148, 4044–4055. https://doi.org/10.1210/en.2007-0038

Jilg, A., Moek, J., Weaver, D.R., Korf, H.-W., Stehle, J.H., Von Gall, C., 2005. Rhythms in clock proteins in the mouse pars tuberalis depend on MT1 melatonin receptor signalling. European Journal of Neuroscience 22, 2845–2854. https://doi.org/10.1111/j.1460-9568.2005.04485.x

Johnston, J.D., Cagampang, F.R.A., Stirland, J.A., Carr, A.-J.F., White, M.R.H., Davis, J.R.E., Loudon, A.S.I., 2003. Evidence for an endogenous *per1* - and *ICER* -independent seasonal timer in the hamster pituitary gland. FASEB j. 17, 810–815. https://doi.org/10.1096/fj.02-0837com

Jou, W.M., Haegeman, G., Ysebaert, M., Fiers, W., 1972. Nucleotide Sequence of the Gene Coding for the Bacteriophage MS2 Coat Protein. Nature 237, 82–88. https://doi.org/10.1038/237082a0

Kalsbeek, A., Garidou, M.-L., Palm, I.F., Van Der Vliet, J., Simonneaux, V., Pévet, P., Buijs, R.M., 2000. Melatonin sees the light: blocking GABA-ergic transmission in the paraventricular nucleus induces daytime secretion of melatonin: GABA release in control of the daily melatonin rhythm. European Journal of Neuroscience 12, 3146–3154. https://doi.org/10.1046/j.1460-9568.2000.00202.x

Kameda, Y., Arai, Y., Nishimaki, T., 2003. Ultrastructural localization of vimentin immunoreactivity and gene expression in tanycytes and their alterations in hamsters kept under different photoperiods. Cell and Tissue Research 314, 251–262. https://doi.org/10.1007/s00441-003-0789-y

Kauffman, A.S., Freeman, D.A., Zucker, I., 2003. Termination of Neuroendocrine Refractoriness to Melatonin in Siberian Hamsters (Phodopus sungorus): Reversing refractoriness to melatonin. Journal of Neuroendocrinology 15, 191–196. https://doi.org/10.1046/j.1365-2826.2003.00966.x

Keenan, A.B., Torre, D., Lachmann, A., Leong, A.K., Wojciechowicz, M.L., Utti, V., Jagodnik, K.M., Kropiwnicki, E., Wang, Z., Ma'ayan, A., 2019. ChEA3: transcription factor enrichment analysis by orthogonal omics integration. Nucleic Acids Research 47, W212–W224. https://doi.org/10.1093/nar/gkz446

Kim, Mi Seong, Muallem, S., Kim, S.H., Kwon, K.B., Kim, Min Seuk, 2019. Exosomal release through TRPML1-mediated lysosomal exocytosis is required for adipogenesis. Biochemical and Biophysical Research Communications 510, 409–415. https://doi.org/10.1016/j.bbrc.2019.01.115

Klein, D.C., Moore, R.Y., 1979. Pineal N-acetyltransferase and hydroxyindole-O-methyl-transferase: control by the retinohypothalamic tract and the suprachiasmatic nucleus. Brain Research 174, 245–262. https://doi.org/10.1016/0006-8993(79)90848-5

Klosen, P., Bienvenu, C., Demarteau, O., Dardente, H., Guerrero, H., Pévet, P., Masson-Pévet, M., 2002. The mt1 Melatonin Receptor and RORß Receptor Are Co-localized in Specific TSH-immunoreactive Cells in the Pars Tuberalis of the Rat Pituitary. J Histochem Cytochem. 50, 1647–1657. https://doi.org/10.1177/002215540205001209

Klosen, P., Sébert, M.-E., Rasri, K., Laran-Chich, M.-P., Simonneaux, V., 2013. TSH restores a summer phenotype in photoinhibited mammals via the RF-amides RFRP3 and kisspeptin. The FASEB Journal 27, 2677–2686. https://doi.org/10.1096/fj.13-229559

Kneis, P., Siegmund, R., 1976. Heart rate and locomotor activity in fish: Correlation and circadian and circannual differences inCyprinus carpio L. Experientia 32, 474–476. https://doi.org/10.1007/BF01920805

Kobayashi, Masako, Kobayashi, Maiko, 2006. The relationship between obesity and seasonal variation in body weight among elementary school children in Tokyo. Economics & Human Biology 4, 253–261. https://doi.org/10.1016/j.ehb.2005.08.002

Koch, T.L., Ramiro, I.B.L., Flórez Salcedo, P., Engholm, E., Jensen, K.J., Chase, K., Olivera, B.M., Bjørn-Yoshimoto, W.E., Safavi-Hemami, H., 2022. Reconstructing the Origins of the Somatostatin and Allatostatin-C Signaling Systems Using the Accelerated Evolution of Biodiverse Cone Snail Toxins. Molecular Biology and Evolution 39, msac075. https://doi.org/10.1093/molbev/msac075

Kolaczynski, J.W., Ohannesian, J.P., Considine, R.V., Marco, C.C., Caro, J.F., 1996. Response of leptin to short-term and prolonged overfeeding in humans. The Journal of Clinical Endocrinology & Metabolism 81, 4162–4165. https://doi.org/10.1210/jcem.81.11.8923877

Koo, T.K., Li, M.Y., 2016. A Guideline of Selecting and Reporting Intraclass Correlation Coefficients for Reliability Research. J Chiropr Med 15, 155–163. https://doi.org/10.1016/j.jcm.2016.02.012

Koob, G., 2001. Drug Addiction, Dysregulation of Reward, and Allostasis. Neuropsychopharmacology 24, 97–129. https://doi.org/10.1016/S0893-133X(00)00195-0

Koronowski, K.B., Kinouchi, K., Welz, P.-S., Smith, J.G., Zinna, V.M., Shi, J., Samad, M., Chen, S., Magnan, C.N., Kinchen, J.M., Li, W., Baldi, P., Benitah, S.A., Sassone-Corsi, P., 2019. Defining the Independence of the

Liver Circadian Clock. Cell 177, 1448-1462.e14. https://doi.org/10.1016/j.cell.2019.04.025

Kouidhi, S., Clerget-Froidevaux, M.-S., 2018. Integrating Thyroid Hormone Signaling in Hypothalamic Control of Metabolism: Crosstalk Between Nuclear Receptors. IJMS 19, 2017. https://doi.org/10.3390/ijms19072017

Krude, H., Biebermann, H., Luck, W., Horn, R., Brabant, G., Grüters, A., 1998. Severe early-onset obesity, adrenal insufficiency and red hair pigmentation caused by POMC mutations in humans. Nat Genet 19, 155–157. https://doi.org/10.1038/509

Krulich, L., Dhariwal, A.P., McCann, S.M., 1968. Stimulatory and inhibitory effects of purified hypothalamic extracts on growth hormone release from rat pituitary in vitro. Endocrinology 83, 783–790. https://doi.org/10.1210/endo-83-4-783

Kumar, V., Singh, S., Misra, M., Malik, S., 2001. Effects of duration and time of food availability on photoperiodic responses in the migratory male blackheaded bunting (Emberiza melanocephala). J Exp Biol 204, 2843–2848. https://doi.org/10.1242/jeb.204.16.2843

Kyne, R.F., Barrett, A.R., Brown, L.M., Paul, M.J., 2019. Prepubertal ovarian inhibition of Light/Dark Box exploration and novel object investigation in juvenile Siberian hamsters. Hormones and Behavior 115, 104559. https://doi.org/10.1016/j.yhbeh.2019.07.007

Lam, B.Y.H., Cimino, I., Polex-Wolf, J., Nicole Kohnke, S., Rimmington, D., Iyemere, V., Heeley, N., Cossetti, C., Schulte, R., Saraiva, L.R., Logan, D.W., Blouet, C., O'Rahilly, S., Coll, A.P., Yeo, G.S.H., 2017. Heterogeneity of hypothalamic pro-opiomelanocortin-expressing neurons revealed by single-cell RNA sequencing. Molecular Metabolism 6, 383–392. https://doi.org/10.1016/j.molmet.2017.02.007

Lam, B.Y.H., Williamson, A., Finer, S., Day, F.R., Tadross, J.A., Gonçalves Soares, A., Wade, K., Sweeney, P., Bedenbaugh, M.N., Porter, D.T., Melvin, A., Ellacott, K.L.J., Lippert, R.N., Buller, S., Rosmaninho-Salgado, J., Dowsett, G.K.C., Ridley, K.E., Xu, Z., Cimino, I., Rimmington, D., Rainbow, K., Duckett, K., Holmqvist, S., Khan, A., Dai, X., Bochukova, E.G., Trembath, R.C., Martin, H.C., Coll, A.P., Rowitch, D.H., Wareham, N.J., van Heel, D.A., Timpson, N., Simerly, R.B., Ong, K.K., Cone, R.D., Langenberg, C., Perry, J.R.B., Yeo, G.S., O'Rahilly, S., 2021. MC3R links

nutritional state to childhood growth and the timing of puberty. Nature 599, 436–441. https://doi.org/10.1038/s41586-021-04088-9

Langlet, F., Levin, B.E., Luquet, S., Mazzone, M., Messina, A., Dunn-Meynell, A.A., Balland, E., Lacombe, A., Mazur, D., Carmeliet, P., Bouret, S.G., Prevot, V., Dehouck, B., 2013. Tanycytic VEGF-A Boosts Blood-Hypothalamus Barrier Plasticity and Access of Metabolic Signals to the Arcuate Nucleus in Response to Fasting. Cell Metabolism 17, 607–617. https://doi.org/10.1016/j.cmet.2013.03.004

Laperrousaz, E., Denis, R.G., Kassis, N., Contreras, C., López, M., Luquet, S., Cruciani-Guglielmacci, C., Magnan, C., 2018. Lipoprotein Lipase Expression in Hypothalamus Is Involved in the Central Regulation of Thermogenesis and the Response to Cold Exposure. Front. Endocrinol. 9, 103. https://doi.org/10.3389/fendo.2018.00103

Laperrousaz, E., Moullé, V.S., Denis, R.G., Kassis, N., Berland, C., Colsch, B., Fioramonti, X., Philippe, E., Lacombe, A., Vanacker, C., Butin, N., Bruce, K.D., Wang, H., Wang, Y., Gao, Y., Garcia-Caceres, C., Prévot, V., Tschöp, M.H., Eckel, R.H., Le Stunff, H., Luquet, S., Magnan, C., Cruciani-Guglielmacci, C., 2017. Lipoprotein lipase in hypothalamus is a key regulator of body weight gain and glucose homeostasis in mice. Diabetologia 60, 1314–1324. https://doi.org/10.1007/s00125-017-4282-7

Lavie, P., 1997. Melatonin: Role in Gating Nocturnal Rise in Sleep Propensity. J Biol Rhythms 12, 657–665. https://doi.org/10.1177/074873049701200622

Leak, R.K., Card, J.P., Moore, R.Y., 1999. Suprachiasmatic pacemaker organization analyzed by viral transynaptic transport. Brain Research 819, 23–32. https://doi.org/10.1016/S0006-8993(98)01317-1

Lechan, R.M., Fekete, C., 2005. Role of Thyroid Hormone Deiodination in the Hypothalamus. Thyroid 15, 883–897. https://doi.org/10.1089/thy.2005.15.883

Lee, D.A., Bedont, J.L., Pak, T., Wang, H., Song, J., Miranda-Angulo, A., Takiar, V., Charubhumi, V., Balordi, F., Takebayashi, H., Aja, S., Ford, E., Fishell, G., Blackshaw, S., 2012. Tanycytes of the hypothalamic median eminence form a diet-responsive neurogenic niche. Nat Neurosci 15, 700–702. https://doi.org/10.1038/nn.3079

Lee, D.A., Yoo, S., Pak, T., Salvatierra, J., Velarde, E., Aja, S., Blackshaw, S., 2014. Dietary and sex-specific factors regulate hypothalamic neurogenesis

in young adult mice. Front. Neurosci. 8. https://doi.org/10.3389/fnins.2014.00157

Lee, Y., Nadal-Ginard, B., Mahdavi, V., Izumo, S., 1997. Myocyte-specific enhancer factor 2 and thyroid hormone receptor associate and synergistically activate the alpha-cardiac myosin heavy-chain gene. Mol Cell Biol 17, 2745–2755. https://doi.org/10.1128/MCB.17.5.2745

Lehnert, T., Sonntag, D., Konnopka, A., Riedel-Heller, S., König, H.-H., 2013. Economic costs of overweight and obesity. Best Practice & Research Clinical Endocrinology & Metabolism 27, 105–115. https://doi.org/10.1016/j.beem.2013.01.002

Leitner, C., Bartness, T.J., 2011. An Intact Dorsomedial Hypothalamic Nucleus, but Not the Subzona Incerta or Reuniens Nucleus, Is Necessary for Short-Day Melatonin Signal-Induced Responses in Siberian Hamsters. Neuroendocrinology 93, 29–39. https://doi.org/10.1159/000320474

Lerner, A.B., Case, J.D., Takahashi, Y., Lee, T.H., Mori, W., 1958. ISOLATION OF MELATONIN, THE PINEAL GLAND FACTOR THAT LIGHTENS MELANOCYTES [1]. J. Am. Chem. Soc. 80, 2587–2587. https://doi.org/10.1021/ja01543a060

Letellier, G., Desjarlais, F., 1982. Study of seasonal variations for eighteen biochemical parameters over a four-year period. Clinical Biochemistry 15, 206–211. https://doi.org/10.1016/S0009-9120(82)90112-6

Lewis, J.E., Ebling, F.J.P., 2018. Hamsters as Model Species for Neuroendocrine Studies, in: Model Animals in Neuroendocrinology. John Wiley & Sons, Ltd, pp. 161–179. https://doi.org/10.1002/9781119391128.ch7

Lewy, A.J., Wehr, T.A., Goodwin, F.K., Newsome, D.A., Markey, S.P., 1980. Light Suppresses Melatonin Secretion in Humans. Science 210, 1267–1269. https://doi.org/10.1126/science.7434030

Li, W., Shi, Y.-H., Yang, R., Cui, J., Xiao, Y., Wang, B., Le, G.-W., 2010. Effect of somatostatin analog on high-fat diet-induced metabolic syndrome: Involvement of reactive oxygen species. Peptides 31, 625–629. https://doi.org/10.1016/j.peptides.2009.11.008

Lin, Q., Schwarz, J., Bucana, C., N. Olson, E., 1997. Control of Mouse Cardiac Morphogenesis and Myogenesis by Transcription Factor MEF2C. Science 276, 1404–1407. https://doi.org/10.1126/science.276.5317.1404

Lincoln, G., 2019. A brief history of circannual time. J Neuroendocrinol 31, e12694. https://doi.org/10.1111/jne.12694

Lincoln, G., Messager, S., Andersson, H., Hazlerigg, D., 2002. Temporal expression of seven clock genes in the suprachiasmatic nucleus and the pars tuberalis of the sheep: evidence for an internal coincidence timer. Proc Natl Acad Sci U S A 99, 13890–13895. https://doi.org/10.1073/pnas.212517599

Lincoln, G.A., Baker, B.I., 1995. Seasonal and photoperiod-induced changes in the secretion of α-melanocyte-stimulating hormone in Soay sheep: temporal relationships with changes in ß-endorphin, prolactin, follicle-stimulating hormone, activity of the gonads and growth of wool and horns. Journal of Endocrinology 144, 471–481. https://doi.org/10.1677/joe.0.1440471

Lincoln, G.A., Clarke, I.J., 1994. Photoperiodically-lnduced Cycles in the Secretion of Prolactin in Hypothalamo-Pituitary Disconnected Rams: Evidence for Translation of the Melatonin Signal in the Pituitary Gland. J Neuroendocrinol 6, 251–260. https://doi.org/10.1111/j.1365-2826.1994.tb00580.x

Lincoln, G.A., Clarke, I.J., Sweeney, T., 1996. 'Hamster-like' Cycles in Testicular Size in the Absence of Gonadotrophin Secretion in HPD Rams Exposed to Long-term Changes in Photoperiod and Treatment with Melatonin. Journal of Neuroendocrinology 8, 855–866. https://doi.org/10.1046/j.1365-2826.1996.05397.x

Lincoln, G.A., Ebling, F.J.P., Almeida, O.F.X., 2008. Generation of Melatonin Rhythms, in: Evered, D., Clark, S. (Eds.), Novartis Foundation Symposia. John Wiley & Sons, Ltd., Chichester, UK, pp. 129–148. https://doi.org/10.1002/9780470720981.ch9

Lisci, C., Lewis, J.E., Daniel, Z.C.T.R., Stevenson, T.J., Monnier, C., Marshall, H.J., Fowler, M., Ebling, F.J.P., Ferri, G.-L., Cocco, C., Jethwa, P.H., 2019. Photoperiodic changes in adiposity increase sensitivity of female Siberian hamsters to systemic VGF derived peptide TLQP-21. PLoS ONE 14, e0221517. https://doi.org/10.1371/journal.pone.0221517

Liu, X., Sha, Y., Lv, W., Cao, G., Guo, X., Pu, X., Wang, J., Li, S., Hu, J., Luo, Y., 2022. Multi-Omics Reveals That the Rumen Transcriptome, Microbiome, and Its Metabolome Co-regulate Cold Season Adaptability of Tibetan Sheep. Front. Microbiol. 13, 859601. https://doi.org/10.3389/fmicb.2022.859601

Lopez-Vicchi, F., Ladyman, S.R., Ornstein, A.M., Gustafson, P., Knowles, P., Luque, G.M., Grattan, D.R., Becu-Villalobos, D., 2020. Chronic high prolactin levels impact on gene expression at discrete hypothalamic nuclei involved in food intake. FASEB j. 34, 3902–3914. https://doi.org/10.1096/fj.201902357R

Lotter, E.C., Krinsky, R., McKay, J.M., Treneer, C.M., Porte Jr., D., Woods, S.C., 1981. Somatostatin decreases food intake of rats and baboons. Journal of Comparative and Physiological Psychology 95, 278–287. https://doi.org/10.1037/h0077777

Ma, Y., Olendzki, B.C., Li, W., Hafner, A.R., Chiriboga, D., Hebert, J.R., Campbell, M., Sarnie, M., Ockene, I.S., 2006. Seasonal variation in food intake, physical activity, and body weight in a predominantly overweight population. Eur J Clin Nutr 60, 519–528. https://doi.org/10.1038/sj.ejcn.1602346

MacGregor, D.J., Lincoln, G.A., 2008. A Physiological Model of a Circannual Oscillator. J Biol Rhythms 23, 252–264. https://doi.org/10.1177/0748730408316796

Maechler, M., 2019. Finding groups in data": Cluster analysis extended Rousseeuw et al. R package version 2.

Manchester, L.C., Coto-Montes, A., Boga, J.A., Andersen, L.P.H., Zhou, Z., Galano, A., Vriend, J., Tan, D.-X., Reiter, R.J., 2015. Melatonin: an ancient molecule that makes oxygen metabolically tolerable. Journal of Pineal Research 59, 403–419. https://doi.org/10.1111/jpi.12267

Manfredi-Lozano, M., Roa, J., Ruiz-Pino, F., Piet, R., Garcia-Galiano, D., Pineda, R., Zamora, A., Leon, S., Sanchez-Garrido, M.A., Romero-Ruiz, A., Dieguez, C., Vazquez, M.J., Herbison, A.E., Pinilla, L., Tena-Sempere, M., 2016. Defining a novel leptin–melanocortin–kisspeptin pathway involved in the metabolic control of puberty. Molecular Metabolism 5, 844–857. https://doi.org/10.1016/j.molmet.2016.08.003

Marcovitch, S., 1923. Plant Lice and Light Exposure. Science 58, 537–538. https://doi.org/10.1126/science.58.1513.537.b

Marczynski, T.J., Yamaguchi, N., Ling, G.M., Grodzinska, L., 1964. Sleep induced by the administration of melatonin (5-methoxy-N-acetyltryptamine) to the hypothalamus in unrestrained cats. Experientia 20, 435–437. https://doi.org/10.1007/BF02152134

Martinez-Bakker, M., Bakker, K.M., King, A.A., Rohani, P., 2014. Human birth seasonality: latitudinal gradient and interplay with childhood disease dynamics. Proc. R. Soc. B. 281, 20132438. https://doi.org/10.1098/rspb.2013.2438

Matuszewska, J., Ziarniak, K., Dudek, M., Kołodziejski, P., Pruszyńska-Oszmałek, E., Śliwowska, J.H., 2020. Effects of short-term exposure to high-fat diet on histology of male and female gonads in rats. Acta Histochemica 122, 151558. https://doi.org/10.1016/j.acthis.2020.151558

Mayo Fiske, V., 1941. EFFECT OF LIGHT ON SEXUAL MATURATION, ESTROUS CYCLES, AND ANTERIOR PITUITARY OF THE RAT [1]. Endocrinology 29, 187–196. https://doi.org/10.1210/endo-29-2-187

Maywood, E.S., Bittman, E.L., Hastings, M.H., 1996. Lesions of the Melatonin- and Androgen-Responsive Tissue of the Dorsomedial Nucleus of the Hypothalamus Block the Gonadal Response of Male Syrian Hamsters to Programmed Infusions of Melatonin1. Biology of Reproduction 54, 470–477. https://doi.org/10.1095/biolreprod54.2.470

Maywood, E.S., Buttery, R.C., Vance, G.H.S., Herbert, J., Hastings, M.H., 1990. Gonadal Responses of the Male Syrian Hamster to Programmed Infusions of Melatonin are Sensitive to Signal Duration and Frequency but Not to Signal Phase Nor to Lesions of The Suprachiasmatic Nuclei1. Biology of Reproduction 43, 174–182. https://doi.org/10.1095/biolreprod43.2.174

McEwen, B.S., Wingfield, J.C., 2003. The concept of allostasis in biology and biomedicine. Hormones and Behavior 43, 2–15. https://doi.org/10.1016/S0018-506X(02)00024-7

McLaren, M., Kennedy, G., Bolton-Smith, C., Belch, J., 2000. Seasonal variation in plasma levels of endothelin-1 and nitric oxide. International angiology : a journal of the International Union of Angiology 19, 351–3.

Menestrina, G., 1986. Ionic channels formed byStaphylococcus aureus alpha-toxin: Voltage-dependent inhibition by divalent and trivalent cations. J. Membrain Biol. 90, 177–190. https://doi.org/10.1007/BF01869935

Meng, Q.-Y., Chen, X.-N., Zhao, J., Swaab, D.F., Zhou, J.-N., 2011. Distribution of retinoic acid receptor-α immunoreactivity in the human hypothalamus. Neuroscience 174, 132–142. https://doi.org/10.1016/j.neuroscience.2010.11.058

Mercer, J.G., Adam, C.L., Morgan, P.J., 2000a. Towards an Understanding of Physiological Body Mass Regulation: Seasonal Animal Models. Nutritional Neuroscience 3, 307–320. https://doi.org/10.1080/1028415X.2000.11747328

Mercer, J.G., Lawrence, C.B., Beck, B., Burlet, A., Atkinson, T., Barrett, P., 1995. Hypothalamic NPY and prepro-NPY mRNA in Djungarian hamsters: effects of food deprivation and photoperiod. Am J Physiol 269, R1099-1106. https://doi.org/10.1152/ajpregu.1995.269.5.R1099

Mercer, J.G., Moar, K.M., Logie, T.J., Findlay, P.A., Adam, C.L., Morgan, P.J., 2001. Seasonally Inappropriate Body Weight Induced by Food Restriction: Effect on Hypothalamic Gene Expression in Male Siberian Hamsters. Endocrinology 142, 4173–4181. https://doi.org/10.1210/endo.142.10.8454

Mercer, J.G., Moar, K.M., Ross, A.W., Hoggard, N., Morgan, P.J., 2000b. Photoperiod regulates arcuate nucleus POMC, AGRP, and leptin receptor mRNA in Siberian hamster hypothalamus. American Journal of Physiology-Regulatory, Integrative and Comparative Physiology 278, R271–R281. https://doi.org/10.1152/ajpregu.2000.278.1.R271

Merkley, C.M., Shuping, S.L., Nestor, C.C., 2020. Neuronal networks that regulate gonadotropin-releasing hormone/luteinizing hormone secretion during undernutrition: evidence from sheep. Domestic Animal Endocrinology 73, 106469. https://doi.org/10.1016/j.domaniend.2020.106469

Mettke-Hofmann, C., 2007. Object Exploration of Garden and Sardinian Warblers Peaks in Spring. Ethology 113, 174–182. https://doi.org/10.1111/j.1439-0310.2006.01307.x

Milesi, S., Simonneaux, V., Klosen, P., 2017. Downregulation of Deiodinase 3 is the earliest event in photoperiodic and photorefractory activation of the gonadotropic axis in seasonal hamsters. Scientific reports 7, 1–10.

Millington, G.W., 2007. The role of proopiomelanocortin (POMC) neurones in feeding behaviour. Nutrition & Metabolism 4, 18. https://doi.org/10.1186/1743-7075-4-18

Modell, H., Cliff, W., Michael, J., McFarland, J., Wenderoth, M.P., Wright, A., 2015. A physiologist's view of homeostasis. Adv Physiol Educ 39, 259–266. https://doi.org/10.1152/advan.00107.2015

Moffatt-Blue, C.S., Sury, J.J., Young, K.A., 2006. Short photoperiod-induced ovarian regression is mediated by apoptosis in Siberian hamsters (Phodopus sungorus). Reproduction 131, 771–782. https://doi.org/10.1530/rep.1.00870

Mohawk, J.A., Takahashi, J.S., 2011. Cell autonomy and synchrony of suprachiasmatic nucleus circadian oscillators. Trends in Neurosciences 34, 349–358. https://doi.org/10.1016/j.tins.2011.05.003

Moore, A., Chinnaiya, K., Kim, D.W., Brown, S., Stewart, I., Robins, S., Dowsett, G.K.C., Muir, C., Travaglio, M., Lewis, J.E., Ebling, F., Blackshaw, S., Furley, A., Placzek, M., 2022. Loss of Function of the Neural Cell Adhesion Molecule NrCAM Regulates Differentiation, Proliferation and Neurogenesis in Early Postnatal Hypothalamic Tanycytes. Front. Neurosci. 16, 832961. https://doi.org/10.3389/fnins.2022.832961

Moore, K.E., 1987. Interactions between Prolactin and Dopaminergic Neurons1. Biology of Reproduction 36, 47–58. https://doi.org/10.1095/biolreprod36.1.47

Moore, R.Y., 1995. Neural control of the pineal gland. Behavioural Brain Research 73, 125–130. https://doi.org/10.1016/0166-4328(96)00083-6

Moore, R.Y., Speh, J.C., Leak, R.K., 2002. Suprachiasmatic nucleus organization. Cell Tissue Res 309, 89–98. https://doi.org/10.1007/s00441-002-0575-2

Morgan, C., Thompson, R.C., Watson, S.J., Akil, H., 2003. Syrian hamster proopiomelanocortin cDNA cloning and early seasonal changes in testicular expression. General and Comparative Endocrinology 133, 353–357. https://doi.org/10.1016/S0016-6480(03)00189-8

Morgan, P.J., Webster, C.A., Mercer, J.G., Ross, A.W., Hazlerigg, D.G., MacLean, A., Barrett, P., 1996. The ovine pars tuberalis secretes a factor(s) that regulates gene expression in both lactotropic and nonlactotropic pituitary cells. Endocrinology 137, 4018–4026. https://doi.org/10.1210/endo.137.9.8756579

Mori, H., Hanada, R., Hanada, T., Aki, D., Mashima, R., Nishinakamura, H., Torisu, T., Chien, K.R., Yasukawa, H., Yoshimura, A., 2004. Socs3 deficiency in the brain elevates leptin sensitivity and confers resistance to diet-induced obesity. Nat Med 10, 739–743. https://doi.org/10.1038/nm1071

Morishige, W.K., Rothchild, I., 1974. Temporal aspects of the regulation of corpus luteum function by luteinizing hormone, prolactin and placental luteotrophin during the first half of pregnancy in the rat. Endocrinology 95, 260–274. https://doi.org/10.1210/endo-95-1-260

Morton, G.J., Schwartz, M.W., 2001. The NPY/AgRP neuron and energy homeostasis. Int J Obes 25, S56–S62. https://doi.org/10.1038/sj.ijo.0801915

Mrosovsky, N., 1990. Rheostasis: The physiology of change, Rheostasis: The physiology of change. Oxford University Press, New York, NY, US.

Mullis, K., Faloona, F., Scharf, S., Saiki, R., Horn, G., Erlich, H., 1986. Specific Enzymatic Amplification of DNA In Vitro: The Polymerase Chain Reaction. Cold Spring Harbor Symposia on Quantitative Biology 51, 263–273. https://doi.org/10.1101/SQB.1986.051.01.032

Munley, K.M., Deyoe, J.E., Ren, C.C., Demas, G.E., 2020. Melatonin mediates seasonal transitions in aggressive behavior and circulating androgen profiles in male Siberian hamsters. Hormones and Behavior 117, 104608. https://doi.org/10.1016/j.yhbeh.2019.104608

Munley, K.M., Rendon, N.M., Demas, G.E., 2018. Neural Androgen Synthesis and Aggression: Insights From a Seasonally Breeding Rodent. Frontiers in Endocrinology 9.

Murphy, M., Ebling, F.J.P., 2011. The Role of Hypothalamic Tri-Iodothyronine Availability in Seasonal Regulation of Energy Balance and Body Weight. Journal of Thyroid Research 2011, e387562. https://doi.org/10.4061/2011/387562

Murphy, M., Samms, R., Warner, A., Bolborea, M., Barrett, P., Fowler, M.J., Brameld, J.M., Tsintzas, K., Kharitonenkov, A., Adams, A.C., Coskun, T., Ebling, F.J.P., 2013. Increased Responses to the Actions of Fibroblast Growth Factor 21 on Energy Balance and Body Weight in a Seasonal Model of Adiposity. Journal of Neuroendocrinology 25, 180–189. https://doi.org/10.1111/j.1365-2826.2012.02383.x

Myers, M.G., Cowley, M.A., Münzberg, H., 2008. Mechanisms of Leptin Action and Leptin Resistance. Annu. Rev. Physiol. 70, 537–556. https://doi.org/10.1146/annurev.physiol.70.113006.100707

Nagano, M., Kelly, P.A., 1994. Tissue distribution and regulation of rat prolactin receptor gene expression. Quantitative analysis by polymerase chain

reaction. Journal of Biological Chemistry 269, 13337–13345. https://doi.org/10.1016/S0021-9258(17)36838-2

Nakamura, W., Yamazaki, S., Takasu, N.N., Mishima, K., Block, G.D., 2005. Differential response of Period 1 expression within the suprachiasmatic nucleus. J Neurosci 25, 5481–5487. https://doi.org/10.1523/JNEUROSCI.0889-05.2005

Nakao, N., Ono, H., Yamamura, T., Anraku, T., Takagi, T., Higashi, K., Yasuo, S., Katou, Y., Kageyama, S., Uno, Y., Kasukawa, T., Iigo, M., Sharp, P.J., Iwasawa, A., Suzuki, Y., Sugano, S., Niimi, T., Mizutani, M., Namikawa, T., Ebihara, S., Ueda, H.R., Yoshimura, T., 2008. Thyrotrophin in the pars tuberalis triggers photoperiodic response. Nature 452, 317–322. https://doi.org/10.1038/nature06738

Nassar, Z.D., Mah, C.Y., Dehairs, J., Burvenich, I.J., Irani, S., Centenera, M.M., Helm, M., Shrestha, R.K., Moldovan, M., Don, A.S., Holst, J., Scott, A.M., Horvath, L.G., Lynn, D.J., Selth, L.A., Hoy, A.J., Swinnen, J.V., Butler, L.M., 2020. Human DECR1 is an androgen-repressed survival factor that regulates PUFA oxidation to protect prostate tumor cells from ferroptosis. eLife 9, e54166. https://doi.org/10.7554/eLife.54166

Nayak, G., Zhang, K.X., Vemaraju, S., Odaka, Y., Buhr, E.D., Holt-Jones, A., Kernodle, S., Smith, A.N., Upton, B.A., D'Souza, S., Zhan, J.J., Diaz, N., Nguyen, M.-T., Mukherjee, R., Gordon, S.A., Wu, G., Schmidt, R., Mei, X., Petts, N.T., Batie, M., Rao, S., Hogenesch, J.B., Nakamura, T., Sweeney, A., Seeley, R.J., Van Gelder, R.N., Sanchez-Gurmaches, J., Lang, R.A., 2020. Adaptive Thermogenesis in Mice Is Enhanced by Opsin 3-Dependent Adipocyte Light Sensing. Cell Reports 30, 672-686.e8. https://doi.org/10.1016/j.celrep.2019.12.043

Nelson, R.J., 2004. Seasonal immune function and sickness responses. Trends in Immunology 25, 187–192. https://doi.org/10.1016/j.it.2004.02.001

Nelson, R.J., Demas, G.E., 1996. Seasonal Changes in Immune Function. The Quarterly Review of Biology 71, 511–548. https://doi.org/10.1086/419555

Nicholls, T.J., Follett, B.K., Robinson, J.E., 1983. A photoperiodic response in gonadectomized Japanese quail exposed to a single long day. Journal of Endocrinology 97, 121–126. https://doi.org/10.1677/joe.0.0970121

Nikitin, D.A., Chernov, T.V., Zhelezova, A.D., Tkhakakhova, A.K., Nikitina, S.A., Semenov, M.V., Xenofontova, N.A., Kutovaya, O.V., 2019. Seasonal

Dynamics of Microbial Biomass in Soddy-Podzolic Soil. Eurasian Soil Sc. 52, 1414–1421. https://doi.org/10.1134/S1064229319110073

Niska-Blakie, J., Gopinathan, L., Low, K.N., Kien, Y.L., Goh, C.M.F., Caldez, M.J., Pfeiffenberger, E., Jones, O.S., Ong, C.B., Kurochkin, I.V., Coppola, V., Tessarollo, L., Choi, H., Kanagasundaram, Y., Eisenhaber, F., Maurer-Stroh, S., Kaldis, P., 2020. Knockout of the non-essential gene SUGCT creates diet-linked, age-related microbiome disbalance with a diabetes-like metabolic syndrome phenotype. Cell. Mol. Life Sci. 77, 3423–3439. https://doi.org/10.1007/s00018-019-03359-z

Olias, G., Viollet, C., Kusserow, H., Epelbaum, J., Meyerhof, W., 2004. Regulation and function of somatostatin receptors. Journal of Neurochemistry 89, 1057–1091. https://doi.org/10.1111/j.1471-4159.2004.02402.x

Ollmann, M.M., Wilson, B.D., Yang, Y.-K., Kerns, J.A., Chen, Y., Gantz, I., Barsh, G.S., 1997. Antagonism of Central Melanocortin Receptors in Vitro and in Vivo by Agouti-Related Protein. Science 278, 135–138. https://doi.org/10.1126/science.278.5335.135

Oraha, J., Enriquez, R.F., Herzog, H., Lee, N.J., 2022. Sex-specific changes in metabolism during the transition from chow to high-fat diet feeding are abolished in response to dieting in C57BL/6J mice. Int J Obes 46, 1749–1758. https://doi.org/10.1038/s41366-022-01174-4

Ostrom, K.M., 1990. A review of the hormone prolactin during lactation. Prog Food Nutr Sci 14, 1–43.

Ozdeslik, R.N., Olinski, L.E., Trieu, M.M., Oprian, D.D., Oancea, E., 2019. Human nonvisual opsin 3 regulates pigmentation of epidermal melanocytes through functional interaction with melanocortin 1 receptor. Proc. Natl. Acad. Sci. U.S.A. 116, 11508–11517. https://doi.org/10.1073/pnas.1902825116

Pandi-Perumal, S.R., Trakht, I., Srinivasan, V., Spence, D.W., Maestroni, G.J.M., Zisapel, N., Cardinali, D.P., 2008. Physiological effects of melatonin: Role of melatonin receptors and signal transduction pathways. Progress in Neurobiology 85, 335–353. https://doi.org/10.1016/j.pneurobio.2008.04.001

Peragine, D.E., Pokarowski, M., Mendoza-Viveros, L., Swift-Gallant, A., Cheng, H.-Y.M., Bentley, G.E., Holmes, M.M., 2017. RFamide-related peptide-3

(RFRP-3) suppresses sexual maturation in a eusocial mammal. Proc. Natl. Acad. Sci. U.S.A. 114, 1207–1212. https://doi.org/10.1073/pnas.1616913114

Perez-Leon, J.A., Warren, E.J., Allen, C.N., Robinson, D.W., Lane Brown, R., 2006. Synaptic inputs to retinal ganglion cells that set the circadian clock. European Journal of Neuroscience 24, 1117–1123. https://doi.org/10.1111/j.1460-9568.2006.04999.x

Pinto, S., Roseberry, A.G., Liu, H., Diano, S., Shanabrough, M., Cai, X., Friedman, J.M., Horvath, T.L., 2004. Rapid Rewiring of Arcuate Nucleus Feeding Circuits by Leptin. Science 304, 110–115. https://doi.org/10.1126/science.1089459

Poole, E.I., Rust, V.A., Crosby, K.M., 2020. Nitric Oxide Acts in the Rat Dorsomedial Hypothalamus to Increase High Fat Food Intake and Glutamate Transmission. Neuroscience 440, 277–289. https://doi.org/10.1016/j.neuroscience.2020.05.039

Porniece Kumar, M., Cremer, A.L., Klemm, P., Steuernagel, L., Sundaram, S., Jais, A., Hausen, A.C., Tao, J., Secher, A., Pedersen, T.Å., Schwaninger, M., Wunderlich, F.T., Lowell, B.B., Backes, H., Brüning, J.C., 2021. Insulin signalling in tanycytes gates hypothalamic insulin uptake and regulation of AgRP neuron activity. Nat Metab 3, 1662–1679. https://doi.org/10.1038/s42255-021-00499-0

Prasad, B.M., Conover, C.D., Sarkar, D.K., Rabii, J., Advis, J.-P., 2008. Feed Restriction in Prepubertal Lambs: Effect on Puberty Onset and on in vivo Release of Luteinizing-Hormone-Releasing Hormone, Neuropeptide Y and Beta-Endorphin from the Posterior-Lateral Median Eminence. Neuroendocrinology 57, 1171–1181. https://doi.org/10.1159/000126484

Prendergast, B.J., Gorman, M.R., Zucker, I., 2000. Establishment and persistence of photoperiodic memory in hamsters. Proc Natl Acad Sci U S A 97, 5586–5591.

Prendergast, B. J., Mosinger, B., Kolattukudy, P.E., Nelson, R.J., 2002. Hypothalamic gene expression in reproductively photoresponsive and photorefractory Siberian hamsters. Proceedings of the National Academy of Sciences 99, 16291–16296. https://doi.org/10.1073/pnas.232490799

Prendergast, B.J., Nelson, R.J., 2005. Affective responses to changes in day length in Siberian hamsters (Phodopus sungorus).

Psychoneuroendocrinology 30, 438–452. https://doi.org/10.1016/j.psyneuen.2004.08.008

Prendergast, Brian J., Nelson, R.J., Zucker, I., 2002. 19 - Mammalian Seasonal Rhythms: Behavior and Neuroendocrine Substrates, in: Pfaff, D.W., Arnold, A.P., Fahrbach, S.E., Etgen, A.M., Rubin, R.T. (Eds.), Hormones, Brain and Behavior. Academic Press, San Diego, pp. 93–156. https://doi.org/10.1016/B978-012532104-4/50021-4

Prevot, V., Croix, D., Bouret, S., Dutoit, S., Tramu, G., Stefano, G.B., Beauvillain, J.C., 1999. Definitive evidence for the existence of morphological plasticity in the external zone of the median eminence during the rat estrous cycle: implication of neuro-glio-endothelial interactions in gonadotropin-releasing hormone release. Neuroscience 94, 809–819. https://doi.org/10.1016/S0306-4522(99)00383-8

Purvis, K., Clausen, O.P.F., Olsen, A., Haug, E., Hansson, V., 1979. Prolactin and Leydig Cell Responsiveness to LH/hCG in the Rat. Archives of Andrology 3, 219–230. https://doi.org/10.3109/01485017908988408

Pyter, L.M., Nelson, R.J., 2006. Enduring effects of photoperiod on affective behaviors in Siberian hamsters (Phodopus sungorus). Behavioral Neuroscience 120, 125–134. https://doi.org/10.1037/0735-7044.120.1.125

Quarta, C., Claret, M., Zeltser, L.M., Williams, K.W., Yeo, G.S.H., Tschöp, M.H., Diano, S., Brüning, J.C., Cota, D., 2021. POMC neuronal heterogeneity in energy balance and beyond: an integrated view. Nat Metab 3, 299–308. https://doi.org/10.1038/s42255-021-00345-3

Ralph, M., Foster, R., Davis, F., Menaker, M., 1990. Transplanted suprachiasmatic nucleus determines circadian period. Science 247, 975–978. https://doi.org/10.1126/science.2305266

Reddy, A.B., Cronin, A.S., Ford, H., Ebling, F.J.P., 1999. Seasonal regulation of food intake and body weight in the male Siberian hamster: studies of hypothalamic orexin (hypocretin), neuropeptide Y (NPY) andpro-opiomelanocortin (POMC): Orexin and seasonal rhythms. European Journal of Neuroscience 11, 3255–3264. https://doi.org/10.1046/j.1460-9568.1999.00746.x

Reiter, R., Tan, D.-X., Terrón, M., Alvarado, L., Czarnocki, Z., 2007. Melatonin and its metabolites: New findings regarding their production and their

radical scavenging actions. Acta biochimica Polonica 54, 1–9. https://doi.org/10.18388/abp.2007_3264

Reiter, R.J., Tan, D., Osuna, C., Gitto, E., 2000. Actions of melatonin in the reduction of oxidative stress: A review. J Biomed Sci 7, 444–458. https://doi.org/10.1007/BF02253360

Revel, F.G., Saboureau, M., Pévet, P., Mikkelsen, J.D., Simonneaux, V., 2006. Melatonin Regulates Type 2 Deiodinase Gene Expression in the Syrian Hamster. Endocrinology 147, 4680–4687. https://doi.org/10.1210/en.2006-0606

Revel, F.G., Saboureau, M., Pévet, P., Simonneaux, V., Mikkelsen, J.D., 2008. RFamide-Related Peptide Gene Is a Melatonin-Driven Photoperiodic Gene. Endocrinology 149, 902–912. https://doi.org/10.1210/en.2007-0848

Rezai-Zadeh, K., Münzberg, H., 2013. Integration of sensory information via central thermoregulatory leptin targets. Physiology & Behavior, Society for the Study of Ingestive Behavior (SSIB) 2012 121, 49–55. https://doi.org/10.1016/j.physbeh.2013.02.014

Riddle, O., Bates, R.W., Dykshorn, S.W., 1933. The preparation, IDENTIFICATION AND ASSAY OF PROLACTIN—A HORMONE OF THE ANTERIOR PITUITARY. American Journal of Physiology-Legacy Content 105, 191–216. https://doi.org/10.1152/ajplegacy.1933.105.1.191

Robson, A.J., Rousseau, K., Loudon, A.S.I., Ebling, F.J.P., 2002. Cocaine and Amphetamine-Regulated Transcript mRNA Regulation in the Hypothalamus in Lean and Obese Rodents. Journal of Neuroendocrinology 14, 697–709. https://doi.org/10.1046/j.1365-2826.2002.00830.x

Roenneberg, T., Aschof, J., 1990. Annual Rhythm of Human Reproduction: I. Biology, Sociology, or Both? J Biol Rhythms 5, 195–216. https://doi.org/10.1177/074873049000500303

Roenneberg, T., Radic, T., Gödel, M., Merrow, M., 2009. Seasonality and Photoperiodism in Fungi, in: Nelson, R.J., Denlinger, D.L., Somers, D.E. (Eds.), Photoperiodism. Oxford University PressNew York, pp. 134–163. https://doi.org/10.1093/acprof:oso/9780195335903.003.0007

Rojansky, N., Brzezinski, A., Schenker, J.G., 1992. Seasonality in human reproduction: an update. Human Reproduction 7, 735–745. https://doi.org/10.1093/oxfordjournals.humrep.a137729

Ross, A.W., Bell, L.M., Littlewood, P.A., Mercer, J.G., Barrett, P., Morgan, P.J., 2005. Temporal Changes in Gene Expression in the Arcuate Nucleus Precede Seasonal Responses in Adiposity and Reproduction. Endocrinology 146, 1940–1947. https://doi.org/10.1210/en.2004-1538

Rousseau, K., Atcha, Z., Cagampang, F.R.A., Le Rouzic, P., Stirland, J.A., Ivanov, T.R., Ebling, F.J.P., Klingenspor, M., Loudon, A.S.I., 2002. Photoperiodic Regulation of Leptin Resistance in the Seasonally Breeding Siberian Hamster (*Phodopus sungorus*). Endocrinology 143, 3083–3095. https://doi.org/10.1210/endo.143.8.8967

Ruby, N.F., 1995. Paraventricular nucleus ablation disrupts daily torpor in Siberian hamsters. Brain Research Bulletin 37, 193–198. https://doi.org/10.1016/0361-9230(94)00279-A

Rudic, R.D., McNamara, P., Curtis, A.-M., Boston, R.C., Panda, S., Hogenesch, J.B., FitzGerald, G.A., 2004. BMAL1 and CLOCK, Two Essential Components of the Circadian Clock, Are Involved in Glucose Homeostasis. PLoS Biol 2, e377. https://doi.org/10.1371/journal.pbio.0020377

Ruf, T., Stieglitz, A., Steinlechner, S., Blank, J.L., Heldmaier, G., 1993. Cold exposure and food restriction facilitate physiological responses to short photoperiod in Djungarian hamsters (Phodopus sungorus). Journal of Experimental Zoology 267, 104–112. https://doi.org/10.1002/jez.1402670203

Sáenz de Miera, C., Hanon, E.A., Dardente, H., Birnie, M., Simonneaux, V., Lincoln, G.A., Hazlerigg, D.G., 2013. Circannual Variation in Thyroid Hormone Deiodinases in a Short-Day Breeder. Journal of Neuroendocrinology 25, 412–421. https://doi.org/10.1111/jne.12013

Saffari, B., Ong, J., Kern, P., 1992. Regulation of adipose tissue lipoprotein lipase gene expression by thyroid hormone in rats. Journal of Lipid Research 33, 241–249. https://doi.org/10.1016/S0022-2275(20)41544-5

Sakai, Y., Ohkubo, K., Matsushita, Y., Akamine, S., Ishizaki, Y., Torisu, H., Ihara, K., Sanefuji, M., Kim, M.-S., Lee, K.-U., Shaw, C.A., Lim, J., Nakabeppu, Y., Hara, T., 2013. Neuroendocrine phenotypes in a boy with 5q14 deletion syndrome implicate the regulatory roles of myocyte-specific enhancer factor 2C in the postnatal hypothalamus. European Journal of Medical Genetics 56, 475–483. https://doi.org/10.1016/j.ejmg.2013.06.009

Sanger, F., Nicklen, S., Coulson, A.R., 1977. DNA sequencing with chain-terminating inhibitors. Proc. Natl. Acad. Sci. U.S.A. 74, 5463–5467. https://doi.org/10.1073/pnas.74.12.5463

Saucisse, N., Mazier, W., Simon, V., Binder, E., Catania, C., Bellocchio, L., Romanov, R.A., Léon, S., Matias, I., Zizzari, P., Quarta, C., Cannich, A., Meece, K., Gonzales, D., Clark, S., Becker, J.M., Yeo, G.S.H., Fioramonti, X., Merkle, F.T., Wardlaw, S.L., Harkany, T., Massa, F., Marsicano, G., Cota, D., 2021. Functional heterogeneity of POMC neurons relies on mTORC1 signaling. Cell Reports 37, 109800. https://doi.org/10.1016/j.celrep.2021.109800

Scacchi, M., Pincelli, A., Cavagnini, F., 1999. Growth hormone in obesity. Int J Obes 23, 260–271. https://doi.org/10.1038/sj.ijo.0800807

Scherbarth, F., Diedrich, V., Dumbell, R.A., Schmid, H.A., Steinlechner, S., Barrett, P., 2015. Somatostatin receptor activation is involved in the control of daily torpor in a seasonal mammal. American Journal of Physiology-Regulatory, Integrative and Comparative Physiology 309, R668–R674. https://doi.org/10.1152/ajpregu.00191.2015

Schmidt, T.M., Chen, S.-K., Hattar, S., 2011. Intrinsically photosensitive retinal ganglion cells: many subtypes, diverse functions. Trends in Neurosciences 34, 572–580. https://doi.org/10.1016/j.tins.2011.07.001

Schuhler, S., Ebling, F.J.P., 2006. Role of melanocortin in the long-term regulation of energy balance: Lessons from a seasonal model. Peptides, The Melanocortin Pathway 2005 Part II 27, 301–309. https://doi.org/10.1016/j.peptides.2005.03.060

Schwartz, M.W., Seeley, R.J., Woods, S.C., Weigle, D.S., Campfield, L.A., Burn, P., Baskin, D.G., 1997. Leptin Increases Hypothalamic Pro-opiomelanocortin mRNA Expression in the Rostral Arcuate Nucleus. Diabetes 46, 2119–2123. https://doi.org/10.2337/diab.46.12.2119

Seidah, N.G., Benjannet, S., Hamelin, J., Mamarbachi, A.M., Basak, A., Marcinkiewicz, J., Mbikay, M., Chrétien, M., Marcinkiewicz, M., 1999. The subtilisin/kexin family of precursor convertases. Emphasis on PC1, PC2/7B2, POMC and the novel enzyme SKI-1. Ann. N. Y. Acad. Sci. 885, 57–74. https://doi.org/10.1111/j.1749-6632.1999.tb08665.x

Sethi, S., Tsutsui, K., Chaturvedi, C.M., 2010. Age-dependent variation in the RFRP-3 neurons is inversely correlated with gonadal activity of mice.

General and Comparative Endocrinology 168, 326–332. https://doi.org/10.1016/j.ygcen.2010.04.011

Severi, I., Perugini, J., Mondini, E., Smorlesi, A., Frontini, A., Cinti, S., Giordano, A., 2013. Opposite effects of a high-fat diet and calorie restriction on ciliary neurotrophic factor signaling in the mouse hypothalamus. Front. Neurosci. 7. https://doi.org/10.3389/fnins.2013.00263

Shimon, I., Taylor, J.E., Dong, J.Z., Bitonte, R.A., Kim, S., Morgan, B., Coy, D.H., Culler, M.D., Melmed, S., 1997. Somatostatin receptor subtype specificity in human fetal pituitary cultures. Differential role of SSTR2 and SSTR5 for growth hormone, thyroid-stimulating hormone, and prolactin regulation. J Clin Invest 99, 789–798. https://doi.org/10.1172/JCI119225

Shor, E.K., Brown, S.P., Freeman, D.A., 2022. Bacteria and Bellicosity: Photoperiodic Shifts in Gut Microbiota Drive Seasonal Aggressive Behavior in Male Siberian Hamsters. J Biol Rhythms 37, 296–309. https://doi.org/10.1177/07487304221092105

Siler, T.M., VandenBerg, G., Yen, S.S.C., Brazeau, P., Vale, W., Guillemin, R., 1973. INHIBITION OF GROWTH HORMONE RELEASE IN HUMANS BY SOMATOSTATIN. The Journal of Clinical Endocrinology & Metabolism 37, 632–634. https://doi.org/10.1210/jcem-37-4-632

Sinha Hikim, A.P., Bartke, A., Russell, L.D., 1988. Morphometric Studies on Hamster Testes in Gonadally Active and Inactive States: Light Microscope Findings1. Biology of Reproduction 39, 1225–1237. https://doi.org/10.1095/biolreprod39.5.1225

Slominski, R.M., Reiter, R.J., Schlabritz-Loutsevitch, N., Ostrom, R.S., Slominski, A.T., 2012. Melatonin membrane receptors in peripheral tissues: Distribution and functions. Molecular and Cellular Endocrinology 351, 152–166. https://doi.org/10.1016/j.mce.2012.01.004

Sonntag, W.E., Gottschall, P.E., Meites, J., 1986. Increased secretion of somatostatin-28 from hypothalamic neurons of aged rats in vitro. Brain Research 380, 229–234. https://doi.org/10.1016/0006-8993(86)90217-9

Speakman, J.R., Mitchell, S.E., 2011. Caloric restriction. Molecular Aspects of Medicine, Caloric Restriction 32, 159–221. https://doi.org/10.1016/j.mam.2011.07.001

Spears, N., Finley, C.M., Whaling, C.S., Tuthill, C.R., Zucker, I., 1990. Sustained reproductive responses in Djungarian hamsters (Phodopus sungorus) exposed to a single long day. Reproduction 88, 635–643. https://doi.org/10.1530/jrf.0.0880635

Spiegelman, B.M., Flier, J.S., 2001. Obesity and the Regulation of Energy Balance. Cell 104, 531–543. https://doi.org/10.1016/S0092-8674(01)00240-9

Steinlechner, St., Heldmaier, G., Becker, H., 1983. The seasonal cycle of body weight in the Djungarian hamster: photoperiodic control and the influence of starvation and melatonin. Oecologia 60, 401–405. https://doi.org/10.1007/BF00376859

Stengel, A., Goebel, M., Wang, L., Rivier, J., Kobelt, P., Mönnikes, H., Taché, Y., 2010. Activation of brain somatostatin 2 receptors stimulates feeding in mice: Analysis of food intake microstructure. Physiology & Behavior 101, 614–622. https://doi.org/10.1016/j.physbeh.2010.09.009

Sterling, P., Eyer, J., 1988. Allostasis: A New Paradigm to Explain Arousal Pathology. Handbook of of Life Stress, Cognition and Health.

Stevenson, T.J., 2023. On Rheostasis; the Hierarchical Organization of Physiological Stabillity. Oxford University Press, Oxford, England.

Stevenson, T.J., Onishi, K.G., Bradley, S.P., Prendergast, B.J., 2014. Cell-autonomous iodothyronine deiodinase expression mediates seasonal plasticity in immune function. Brain, Behavior, and Immunity 36, 61–70. https://doi.org/10.1016/j.bbi.2013.10.008

Stevenson, T.J., Prendergast, B.J., 2013. Reversible DNA methylation regulates seasonal photoperiodic time measurement. Proceedings of the National Academy of Sciences 110, 16651–16656. https://doi.org/10.1073/pnas.1310643110

Stevenson, T.J., Visser, M.E., Arnold, W., Barrett, P., Biello, S., Dawson, A., Denlinger, D.L., Dominoni, D., Ebling, F.J., Elton, S., Evans, N., Ferguson, H.M., Foster, R.G., Hau, M., Haydon, D.T., Hazlerigg, D.G., Heideman, P., Hopcraft, J.G.C., Jonsson, N.N., Kronfeld-Schor, N., Kumar, V., Lincoln, G.A., MacLeod, R., Martin, S. a. M., Martinez-Bakker, M., Nelson, R.J., Reed, T., Robinson, J.E., Rock, D., Schwartz, W.J., Steffan-Dewenter, I., Tauber, E., Thackeray, S.J., Umstatter, C., Yoshimura, T., Helm, B., 2015. Disrupted seasonal biology impacts health, food security and

ecosystems. Proceedings of the Royal Society B: Biological Sciences 282, 20151453. https://doi.org/10.1098/rspb.2015.1453

Stewart, C., Hamilton, G., Marshall, C.J., Stevenson, T.J., 2022. Transcriptome analyses of nine endocrine tissues identifies organism-wide transcript distribution and structure in the Siberian hamster. Sci Rep 12, 13552. https://doi.org/10.1038/s41598-022-16731-0

Stewart, C., Marshall, C.J., 2022. Seasonality of prolactin in birds and mammals. Journal of Experimental Zoology Part A: Ecological and Integrative Physiology 337, 919–938. https://doi.org/10.1002/jez.2634

Stoddart, D., Heron, A.J., Mikhailova, E., Maglia, G., Bayley, H., 2009. Single-nucleotide discrimination in immobilized DNA oligonucleotides with a biological nanopore. Proc. Natl. Acad. Sci. U.S.A. 106, 7702–7707. https://doi.org/10.1073/pnas.0901054106

Takahashi, K.A., Cone, R.D., 2005. Fasting Induces a Large, Leptin-Dependent Increase in the Intrinsic Action Potential Frequency of Orexigenic Arcuate Nucleus Neuropeptide Y/Agouti-Related Protein Neurons. Endocrinology 146, 1043–1047. https://doi.org/10.1210/en.2004-1397

Tan, D.-X., Hardeland, R., Manchester, L.C., Paredes, S.D., Korkmaz, A., Sainz, R.M., Mayo, J.C., Fuentes-Broto, L., Reiter, R.J., 2010. The changing biological roles of melatonin during evolution: from an antioxidant to signals of darkness, sexual selection and fitness. Biological Reviews 85, 607–623.

Tan, D.-X., Manchester, L.C., Liu, X., Rosales-Corral, S.A., Acuna-Castroviejo, D., Reiter, R.J., 2013. Mitochondria and chloroplasts as the original sites of melatonin synthesis: a hypothesis related to melatonin's primary function and evolution in eukaryotes. Journal of Pineal Research 54, 127–138. https://doi.org/10.1111/jpi.12026

Tannenbaum, G.S., Zhang, W.-H., Lapointe, M., Zeitler, P., Beaudet, A., 1998. Growth Hormone-Releasing Hormone Neurons in the Arcuate Nucleus Express Both Sst1 and Sst2 Somatostatin Receptor Genes. Endocrinology 139, 1450–1453. https://doi.org/10.1210/endo.139.3.5977

Tendler, A., Bar, A., Mendelsohn-Cohen, N., Karin, O., Kohanim, Y.K., Maimon, L., Milo, T., Raz, M., Mayo, A., Tanay, A., others, 2021. Hormone seasonality in medical records suggests circannual endocrine circuits. Proceedings of the National Academy of Sciences 118.

The C. elegans Sequencing Consortium*, 1998. Genome Sequence of the Nematode *C. elegans* : A Platform for Investigating Biology. Science 282, 2012–2018. https://doi.org/10.1126/science.282.5396.2012

Thompson, D.L., Oberhaus, E.L., 2015. Prolactin in the Horse: Historical Perspective, Actions and Reactions, and Its Role in Reproduction. Journal of Equine Veterinary Science 35, 343–353. https://doi.org/10.1016/j.jevs.2015.03.199

Tong, Y., Pelletier, G., 2008. Prolactin Regulation of Pro-Opiomelanocortin Gene Expression in the Arcuate Nucleus of the Rat Hypothalamus. Neuroendocrinology 56, 561–565. https://doi.org/10.1159/000126274

Tóth, B.B., Arianti, R., Shaw, A., Vámos, A., Veréb, Z., Póliska, S., Győry, F., Bacso, Z., Fésüs, L., Kristóf, E., 2020. FTO Intronic SNP Strongly Influences Human Neck Adipocyte Browning Determined by Tissue and PPARγ Specific Regulation: A Transcriptome Analysis. Cells 9, 987. https://doi.org/10.3390/cells9040987

True, C., Kirigiti, M.A., Kievit, P., Grove, K.L., Smith, M.S., 2011. Leptin is not the Critical Signal for Kisspeptin or Luteinising Hormone Restoration During Exit from Negative Energy Balance: Hypoleptinaemia and negative energy balance. Journal of Neuroendocrinology 23, 1099–1112. https://doi.org/10.1111/j.1365-2826.2011.02144.x

Tups, A., Barrett, P., Ross, A.W., Morgan, P.J., Klingenspor, M., Mercer, J.G., 2006. The Suppressor of Cytokine Signalling 3, SOCS3, may be One Critical Modulator of Seasonal Body Weight Changes in the Siberian Hamster, Phodopus sungorus. Journal of Neuroendocrinology 18, 139–145. https://doi.org/10.1111/j.1365-2826.2005.01394.x

Tups, Alexander, Helwig, M., Stöhr, S., Barrett, P., Mercer, J.G., Klingenspor, M., 2006. Photoperiodic regulation of insulin receptor mRNA and intracellular insulin signaling in the arcuate nucleus of the Siberian hamster, Phodopus sungorus. American Journal of Physiology-Regulatory, Integrative and Comparative Physiology 291, R643–R650. https://doi.org/10.1152/ajpregu.00807.2005

Ubuka, T., Morgan, K., Pawson, A.J., Osugi, T., Chowdhury, V.S., Minakata, H., Tsutsui, K., Millar, R.P., Bentley, G.E., 2009. Identification of Human GnIH Homologs, RFRP-1 and RFRP-3, and the Cognate Receptor, GPR147 in

the Human Hypothalamic Pituitary Axis. PLoS ONE 4, e8400. https://doi.org/10.1371/journal.pone.0008400

Vale, W., Rivier, C., Brazeau, P., Guillemin, R., 1974. Effects of somatostatin on the secretion of thyrotropin and prolactin. Endocrinology 95, 968–977. https://doi.org/10.1210/endo-95-4-968

Varela, L., Horvath, T.L., 2012. Leptin and insulin pathways in POMC and AgRP neurons that modulate energy balance and glucose homeostasis. EMBO Rep 13, 1079–1086. https://doi.org/10.1038/embor.2012.174

Vaughan, M.K., Richardson, B.A., Johnson, L.Y., Petterborg, L.J., Powanda, M.C., Reiter, R.J., Smith, I., 1983. Natural and synthetic analogues of melatonin and related compounds II. Effects on plasma thyroid hormones and cholesterol levels in male Syrian hamsters. J. Neural Transmission 56, 279–291. https://doi.org/10.1007/BF01243496

Venter, J.C., Adams, M.D., Sutton, G.G., Kerlavage, A.R., Smith, H.O., Hunkapiller, M., 1998. Shotgun Sequencing of the Human Genome. Science 280, 1540–1542. https://doi.org/10.1126/science.280.5369.1540

Vijayan, E., McCann, S.M., 1979. In Vivo and in Vitro Effects of Substance P and Neurotensin on Gonadotropin and Prolactin Release*. Endocrinology 105, 64–68. https://doi.org/10.1210/endo-105-1-64

Vohra, M.S., Benchoula, K., Serpell, C.J., Hwa, W.E., 2022. AgRP/NPY and POMC neurons in the arcuate nucleus and their potential role in treatment of obesity. European Journal of Pharmacology 915, 174611. https://doi.org/10.1016/j.ejphar.2021.174611

Wade, G.N., Bartness, T.J., 1984. Seasonal obesity in Syrian hamsters: effects of age, diet, photoperiod, and melatonin. American Journal of Physiology-Regulatory, Integrative and Comparative Physiology 247, R328–R334. https://doi.org/10.1152/ajpregu.1984.247.2.R328

Wakatsuki, A., Okatani, Y., Ikenoue, N., Kaneda, C., Fukaya, T., 2001. Effects of short-term melatonin administration on lipoprotein metabolism in normolipidemic postmenopausal women. Maturitas 38, 171–177. https://doi.org/10.1016/S0378-5122(00)00221-8

Wang, X., Gu, J., Miyoshi, E., Honke, K., Taniguchi, N., 2006. Phenotype Changes of Fut8 Knockout Mouse: Core Fucosylation Is Crucial for the Function of Growth Factor Receptor(s), in: Methods in Enzymology. Elsevier, pp. 11–22. https://doi.org/10.1016/S0076-6879(06)17002-0

Warde-Farley, D., Donaldson, S.L., Comes, O., Zuberi, K., Badrawi, R., Chao, P., Franz, M., Grouios, C., Kazi, F., Lopes, C.T., Maitland, A., Mostafavi, S., Montojo, J., Shao, Q., Wright, G., Bader, G.D., Morris, Q., 2010. The GeneMANIA prediction server: biological network integration for gene prioritization and predicting gene function. Nucleic Acids Research 38, W214–W220. https://doi.org/10.1093/nar/gkq537

Warner, A., Jethwa, P.H., Wyse, C.A., I'Anson, H., Brameld, J.M., Ebling, F.J.P., 2010. Effects of photoperiod on daily locomotor activity, energy expenditure, and feeding behavior in a seasonal mammal. American Journal of Physiology-Regulatory, Integrative and Comparative Physiology 298, R1409–R1416. https://doi.org/10.1152/ajpregu.00279.2009

Warren, E.J., Allen, C.N., Brown, R.L., Robinson, D.W., 2006. The light-activated signaling pathway in SCN-projecting rat retinal ganglion cells. European Journal of Neuroscience 23, 2477–2487. https://doi.org/10.1111/j.1460-9568.2006.04777.x

Watson, J.D., Crick, F.H.C., 1953. Molecular Structure of Nucleic Acids: A Structure for Deoxyribose Nucleic Acid. Nature 171, 737–738. https://doi.org/10.1038/171737a0

Wehr, T.A., 1992. In short photoperiods, human sleep is biphasic. Journal of Sleep Research 1, 103–107. https://doi.org/10.1111/j.1365-2869.1992.tb00019.x

Welsh, D.K., Logothetis, D.E., Meister, M., Reppert, S.M., 1995. Individual neurons dissociated from rat suprachiasmatic nucleus express independently phased circadian firing rhythms. Neuron 14, 697–706. https://doi.org/10.1016/0896-6273(95)90214-7

Williams, K.W., Margatho, L.O., Lee, C.E., Choi, M., Lee, S., Scott, M.M., Elias, C.F., Elmquist, J.K., 2010. Segregation of Acute Leptin and Insulin Effects in Distinct Populations of Arcuate Proopiomelanocortin Neurons. J Neurosci 30, 2472–2479. https://doi.org/10.1523/JNEUROSCI.3118-09.2010

Wollnik, F., Breit, A., Reinke, D., 1991. Seasonal change in the temporal organization of wheel-running activity of the European hamster, Cricetus cricetus. The Science of Nature 78, 419–422.

Wood, S.H., Hindle, M.M., Mizoro, Y., Cheng, Y., Saer, B.R.C., Miedzinska, K., Christian, H.C., Begley, N., McNeilly, J., McNeilly, A.S., Meddle, S.L.,

Burt, D.W., Loudon, A.S.I., 2020. Circadian clock mechanism driving mammalian photoperiodism. Nat Commun 11, 4291. https://doi.org/10.1038/s41467-020-18061-z

Woods, H.A., Wilson, J.K., 2013. An information hypothesis for the evolution of homeostasis. Trends in Ecology & Evolution 28, 283–289. https://doi.org/10.1016/j.tree.2012.10.021

Woods, S.C., Lotter, E.C., McKay, L.D., Porte, D., 1979. Chronic intracerebroventricular infusion of insulin reduces food intake and body weight of baboons. Nature 282, 503–505. https://doi.org/10.1038/282503a0

Wu, X., Li, H., Park, E.-J., Chen, J.D., 2001. SMRTe Inhibits MEF2C Transcriptional Activation by Targeting HDAC4 and 5 to Nuclear Domains *. Journal of Biological Chemistry 276, 24177–24185. https://doi.org/10.1074/jbc.M100412200

Wurtman, R.J., Axelrod, J., Chu, E.W., 1963. Melatonin, a Pineal Substance: Effect on the Rat Ovary. Science 141, 277–278. https://doi.org/10.1126/science.141.3577.277

Yanovsky, M.J., Kay, S.A., 2002. Molecular basis of seasonal time measurement in Arabidopsis. Nature 419, 308–312. https://doi.org/10.1038/nature00996

Yasuo, S., Fischer, C., Bojunga, J., Iigo, M., Korf, H.-W., 2014. 2-Arachidonoyl glycerol sensitizes the pars distalis and enhances forskolin-stimulated prolactin secretion in Syrian hamsters. Chronobiology International 31, 337–342. https://doi.org/10.3109/07420528.2013.852104

Yasuo, S., Koch, M., Schmidt, H., Ziebell, S., Bojunga, J., Geisslinger, G., Korf, H.-W., 2010. An endocannabinoid system is localized to the hypophysial pars tuberalis of Syrian hamsters and responds to photoperiodic changes. Cell Tissue Res 340, 127–136. https://doi.org/10.1007/s00441-010-0930-7

Yasuo, S., Korf, H.-W., 2011. The hypophysial pars tuberalis transduces photoperiodic signals via multiple pathways and messenger molecules. General and Comparative Endocrinology 172, 15–22. https://doi.org/10.1016/j.ygcen.2010.11.006

Yasuo, S., Watanabe, M., Nakao, N., Takagi, T., Follett, B.K., Ebihara, S., Yoshimura, T., 2005. The Reciprocal Switching of Two Thyroid Hormone-Activating and -Inactivating Enzyme Genes Is Involved in the Photoperiodic

Gonadal Response of Japanese Quail. Endocrinology 146, 2551–2554. https://doi.org/10.1210/en.2005-0057

Yellon, S.M., Fagoaga, O.R., Nehlsen-Cannarella, S.L., 1999. Influence of photoperiod on immune cell functions in the male Siberian hamster. American Journal of Physiology-Regulatory, Integrative and Comparative Physiology 276, R97–R102. https://doi.org/10.1152/ajpregu.1999.276.1.R97

Yoo, S., Cha, D., Kim, S., Jiang, L., Cooke, P., Adebesin, M., Wolfe, A., Riddle, R., Aja, S., Blackshaw, S., 2020. Tanycyte ablation in the arcuate nucleus and median eminence increases obesity susceptibility by increasing body fat content in male mice. Glia 68, 1987–2000. https://doi.org/10.1002/glia.23817

Yoshimura, E., Tajiri, E., Hatamoto, Y., Tanaka, S., 2020. Changes in Season Affect Body Weight, Physical Activity, Food Intake, and Sleep in Female College Students: A Preliminary Study. IJERPH 17, 8713. https://doi.org/10.3390/ijerph17238713

Yoshimura, T., Yasuo, S., Watanabe, M., Iigo, M., Yamamura, T., Hirunagi, K., Ebihara, S., 2003. Light-induced hormone conversion of T4 to T3 regulates photoperiodic response of gonads in birds. Nature 426, 178–181. https://doi.org/10.1038/nature02117

Yu, Y., Deng, C., Huang, X.-F., 2009. Obese reversal by a chronic energy restricted diet leaves an increased Arc NPY/AgRP, but no alteration in POMC/CART, mRNA expression in diet-induced obese mice. Behavioural Brain Research 205, 50–56. https://doi.org/10.1016/j.bbr.2009.07.003

Zang, L.-Y., Cosma, G., Gardner, H., Vallyathan, V., 1998. Scavenging of reactive oxygen species by melatonin. Biochimica et Biophysica Acta (BBA) - General Subjects 1425, 469–477. https://doi.org/10.1016/S0304-4165(98)00099-3

Zhao, S., Fernald, R.D., 2005. Comprehensive Algorithm for Quantitative Real-Time Polymerase Chain Reaction. Journal of Computational Biology 12, 1047–1064. https://doi.org/10.1089/cmb.2005.12.1047

Zielinski, T., Moore, A.M., Troup, E., Halliday, K.J., Millar, A.J., 2014. Strengths and Limitations of Period Estimation Methods for Circadian Data. PLoS ONE 9, e96462. https://doi.org/10.1371/journal.pone.0096462